Gold-Tellurium Clusters and Tetrachloridoaurates with Divalent Cations

Dissertation

zur Erlangung des Doktorgrades (Dr. rer. nat.)

der

Mathematisch–Naturwissenschaftlichen Fakultät

der

Rheinischen Friedrich–Wilhelms–Universität Bonn

vorgelegt von

Christian Rudolf Landvogt

aus

Mayen

Bonn, 2016

Angefertigt mit Genehmigung der Mathematisch-Naturwissenschaftlichen Fakultät der Rheinischen Friedrich-Wilhelms-Universität Bonn

1. Gutachter: Prof. Dr. Johannes Beck
2. Gutachter: Prof. Dr. Robert Glaum

Tag der Promotion: 20. Februar 2017
Erscheinungsjahr: 2017

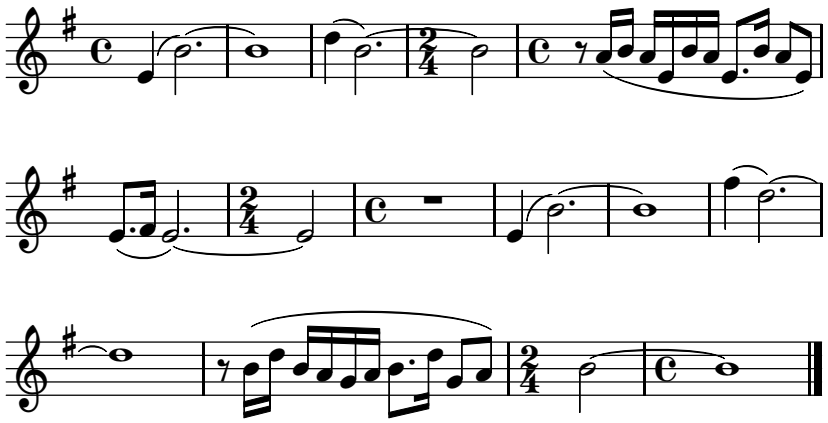

"The Ecstasy of Gold" composed by Ennio Morricone in 1966
for the film score of *"The Good, the Bad and the Ugly"*.

Contents

Abstract

The solid state reaction of AuX_3, Te and a Lewis-acidic metal halide results in a series of compounds containing the new cationic gold-tellurium cluster $(Au_6Te_{18}X_n)^{(6-n)+}$. $AuTe_2X$ can be used instead of AuX_3, but depending on the kind of Lewis-acidic metal halide the product can be different. The Lewis acids AlX_3, $GaCl_3$, $ZrCl_4$, $MoOCl_3$, $BiCl_3$, $NbCl_5$ and $TaCl_5$ have all been used to successfully obtain $(Au_6Te_{18})[ZrCl_6]_3$, $(Au_6Te_{18})[AlX_4]_6$, $(Au_6Te_{18}X)[MCl_4]_5$, $(Au_6Te_{18}Cl)[MoOCl_4]_5$, $(Au_6Te_{18}Cl_2)[Mo_2O_2Cl_8]_2$, $(Au_6Te_{18}Cl_2)[Bi_4Cl_{16}]$and $(Au_6Te_{18}Cl_2)[MCl_6]_4$.
With two exceptions the crystal structures of all target compounds were solved, even though the x-ray diffraction data for some compounds give ambiguous results, because of disordered sites within the cation. The structure of the cation itself can be derived from a cube. Taking a $3 \times 3 \times 3$ cube, analogous to the Rubik's cube, all 27 blocks represent a possible atom position. The central block of each face is occupied by a gold atom. The cube's centre and two corner positions are unoccupied and the remaining 18 positions are occupied by tellurium. For compounds with halide atoms X attached to the cation, these atoms occupy one or both of the empty corner positions.
Further investigation towards the physical properties of this new class of compounds reveals a high diamagnetic moment for the cation itself ($\chi_{\mathrm{mol}} = -8.2 \cdot 10^{-4} \frac{\mathrm{cm}^3}{\mathrm{mol}}$). Both compounds containing isolated Mo^{V} atoms show the expected paramagnetism corresponding to their d^1 configuration (1.67 μ_{B} and 1.83 μ_{B}). Semi-conducting behaviour is observed for three of the compounds and is expected for the untested compounds, too, because all samples are of black-metallic appearance. Additionally, the electronic structure of three representatives is investigated by theoretical calculations, which reveal band gaps between 0.4 eV to 2.0 eV. These calculations also provide valuable help for the interpretation of the ambiguous x-ray diffraction data sets.

As a second central result achieved in this work, the first salts of divalent metal cations with $[AuCl_4]^-$ anions are reported. The compounds $Cd[AuCl_4]_2$ and $Zn[AuCl_4]_2 \cdot (AuCl_3)_{1.115}$ are obtained from reactions of MCl_2 and elemental gold in liquid chlorine and subsequent annealing. The crystal structures of both compounds are reported herein. The latter compound possesses an incommensurately modulated composite crystal structure. The first subsystem contains polymeric chains of zinc(II) tetrachloroaurate(III), while the second subsystem consists of Au_2Cl_6 dimers, which are located in channels built up by the first subsystem. The structural parameters of these dimers show only small deviations from neat $AuCl_3$. It is revealed from a detailed analysis of the crystal structure that the 4+2 coordination sphere, usually found for Au^{3+}, is only achieved for both subsystems through interaction with each other.

Zusammenfassung

Die Festkörperreaktion zwischen AuX_3, Te und einem Lewis-saurem Metallhalogenid ergibt eine Reihe von Verbindungen, die den neuen kationischen Gold-Tellur-Cluster $(Au_6Te_{18}X_n)^{(6-n)+}$ enthalten. An Stelle von AuX_3 kann auch $AuTe_2X$ eingesetzt werden, allerdings kann dies je nach eingesetztem Metallhalogenid zu unterschiedlichen Produkten führen. Aus Umsetzungen mit den Lewis-Säuren AlX_3, $GaCl_3$, $ZrCl_4$, $MoOCl_3$, $BiCl_3$, $NbCl_5$ und $TaCl_5$ wurden erfolgreich die Verbindungen $(Au_6Te_{18})[ZrCl_6]_3$, $(Au_6Te_{18})[AlX_4]_6$, $(Au_6Te_{18}X)[MCl_4]_5$, $(Au_6Te_{18}Cl)[MoOCl_4]_5$, $(Au_6Te_{18}Cl_2)[Mo_2O_2Cl_8]_2$, $(Au_6Te_{18}Cl_2)[Bi_4Cl_{16}]$und $(Au_6Te_{18}Cl_2)[MCl_6]_4$ synthetisiert.
Mit Ausnahme zweier Verbindungen konnten die Einkristallstrukturen von allen Zielverbindungen gelöst und verfeinert werden, obwohl die Beugungsdaten für einige Verbindungen aufgrund von fehlgeordneten Lagen innerhalb des Kations nicht eindeutig sind. Die Struktur des Kations kann von einem Würfel abgeleitet werden. Ausgehend von einem $3 \times 3 \times 3$ Würfel, etwa einem Zauberwürfel, können alle 27 Blöcke als mögliche Atompositionen aufgefasst werden. Der mittlere Block jeder der sechs Flächen ist mit einem Gold-Atom besetzt. Die zentrale Position im Inneren des Würfels und zwei diagonal gegenüberliegende Ecken bleiben frei. Die übrigen 18 Positionen werden mit Tellur-Atomen besetzt. In Verbindungen, in denen am Kation zusätzlich ein oder zwei Halogenatome X gebunden sind, besetzen diese eine oder beide der bisher unbesetzten Ecken.
Die Untersuchung der physikalischen Eigenschaften dieser neuen Substanzklasse, ergibt ein hohes diamagnetisches Moment ($\chi_{\mathrm{mol}} = -8.2 \cdot 10^{-4} \frac{\mathrm{cm}^3}{\mathrm{mol}}$) für das Kation. Die beiden Verbindungen, die isolierte Mo^{V} Atome enthalten, zeigen, wie zu erwarten, Paramagnetismus in Übereinstimmung mit den d^1 konfigurierten Mo-Atomen (1.67 μ_{B} und 1.83 μ_{B}). Halbleiter-Eigenschaften werden für drei Verbindungen experimentell belegt und aufgrund des schwarz-metallischen Aussehens für alle synthetisierten Verbindungen vermutet. Zusätzlich ergeben theoretische Rechnungen an drei Vertretern Bandlücken zwischen 0.4 eV und 2.0 eV. Mit Hilfe dieser Rechnungen wird ebenfalls die Lösung der Einkristallstrukturen der mehrdeutigen Datensätzen unterstützt.

Als zweites wichtiges Ergebnis dieser Arbeit, wird über die ersten Salze eines zweiwertigen Metallkations mit $[AuCl_4]^-$ als Gegenion berichtet. Die Verbindungen $Cd[AuCl_4]_2$ und $Zn[AuCl_4]_2 \cdot (AuCl_3)_{1.115}$ können aus der Reaktion von elementarem Gold mit MCl_2 in flüssigem Chlor mit anschließendem Tempern erhalten werden. Die Einkristallstrukturen beider Verbindungen wurden bestimmt. Die letztgenannte Verbindung besitzt eine inkommensurabel modulierte Kompositstruktur. Das erste Subsystem besteht aus Ketten von Zink(II)-tetrachloroaurat(III). Das zweite Subsystem enthält Au_2Cl_6 Dimere, die sich in Kanälen, die vom ersten Subsystem aufgespannt werden, befinden. Die Struktur der Dimere unterscheidet sich kaum von reinem $AuCl_3$. Eine eingehende Analyse der Einkristallstruktur zeigt, dass die 4+2 Koordinationssphäre, wie sie überlicherweise für Au^{3+} beobachtet wird, wechselseitig durch die beiden Subsysteme vervollständigt wird.

Chapter 1

Introduction

1.1 Gold

Gold, atomic number 79, is one of the longest known and consciously used elements. Historians estimate its earliest use to before 6,000 BCE. The oldest gold sample was found in a burial site in Bulgaria known as Varna Necropolis and is dated between 4,600 BCE and 4,200 BCE [1]. There are other findings which are dated further back to the copper ages, but these estimations are disputed [2].

Pure gold is a soft, malleable and ductile metal. It is very stable against most chemicals, but gets easily dissolved by *aqua regia* or alkaline solutions of cyanide. The latter is used for mining and electroplating. Industrial-scale, high purity gold is obtained electrochemically by the Wohlwill process, which yields 99.999 % pure gold. There are other, more convenient processes, like the Miller process, which are used if a lesser purity is acceptable.

Gold has been used throughout human history as part of alloys for jewellery and ritual purposes. Additionally, gold was a world-wide used currency for indirect exchange, because of its chemical stability and its rare occurrence. A less quantifiable reason is probably its "golden" appearance, which makes it stand out and draws the human eye and interest to it. This attraction, together with its role as a currency, dominated the alchemy's desire to create gold out of more common elements.

In the recent past gold has been applied to many industrial applications, mostly as corrosion-free electrical connectors. This is a trade-off between its price, a very high chemical stability and a high electronic conductivity, which is only surpassed by copper and silver.

Naturally gold occurs – besides in native deposits – in telluride minerals (see Figure 1.1), such as krennerite/sylvanite ($(Au, Ag)Te_2$), nagyagite ($Pb_5Au(Te, Sb)_4S_{5-8}$), petzite (Ag_3AuTe_2) and calaverite ($AuTe_2$). The latter is rather uncommon. However, the mineral held the interest of mineralogists and crystallographers for a long time. It was the first mineral which seemed to violate Haüy's Law of rational indices for face indexing. Goldschmidt *et al.* indexed 105 different calaverite specimen, which resulted in 92 forms, but this indexing was only possible

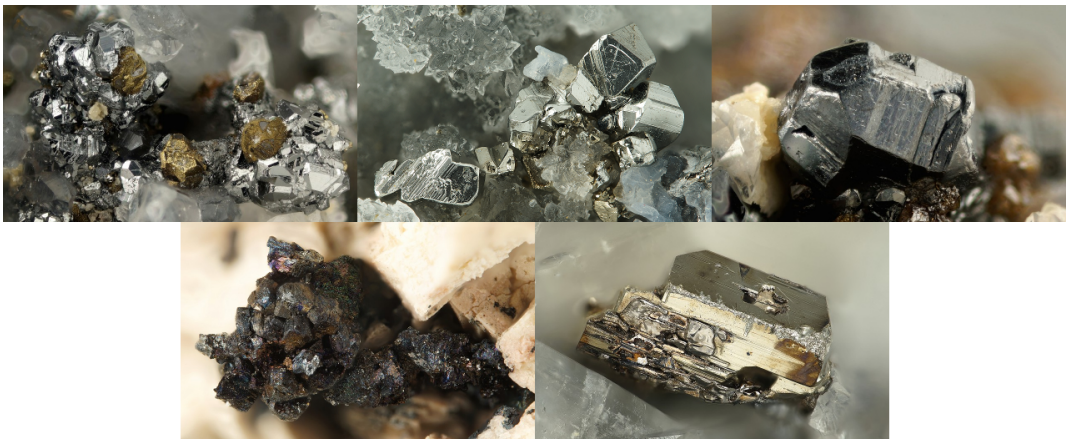

Figure 1.1: The gold tellurium minerals krennerite, sylvanite, nagyagite, petzite and calaverite (from top left to bottom right). Pictures taken from [3].

by using five different lattices [4, 5]. With the advent of x-ray crystallography a basic structure could be solved in 1935 [6], but still additional diffraction spots – not covered by the used unit cell – remained unexplained. Many years later, in 1988, Schutte and DeBoer solved the structure using the superspace approach [7] as an incommensurately modulated structure. The tellurium atoms showed a displacement modulation, which was interpreted as valence fluctuation between gold(I) and gold(III). This compound is still not fully understood, which can be seen by the fairly recent publication by Bindi *et al.* in 2009, which investigates the effect of the silver dopant concentration in $Au_{1-x}Ag_xTe_2$ on the incommensurate modulation [8].

The oxidation state of gold in its compounds ranges from -1 to +5. The most important ones are Au(I) and Au(III). With the exception of AuI_3 all gold(I) and gold(III) halides are known, although AuF has only been observed in gas phase [9]. The monovalent gold halides form zig-zag chains of linearly coordinated gold atoms, while gold(III) is usually coordinated in a square-planar fashion. In AuF_3 adjacent $[AuF_4]$ units are connected via *cis* aligned corners into an infinite spiral, while the other trihalides form molecular planar Au_2X_6 dimers. AuX_3 is a Lewis acid and is able to receive an additional halide from a Lewis base to form square-planar tetrahaloaurates $[AuX_4]^-$. Numerous salts consisting of this anion and a monovalent metal cation are found in literature: $M[AuF_4]$ with M = Li – Cs, Ag [10–14]; $M[AuCl_4]$ with M = Na – Cs, Ag, Tl [15–20]; $M[AuBr_4]$ with M = K – Cs [17, 21, 22]; $M[AuI_4]$ with M = Li, K [23].

Switching to divalent metal cations dramatically changes the number of known compounds. The tetraflouroaurates are still numerous ($M[AuF_4]_2$ with M = Mg, Ba, Ni, Pd, Ag, Au, Zn – Hg [24–28]), but for the heavier homologues of flourine there are only a few exceptions, of which none strictly fits to the sum formula $M[AuX_4]_2$. The two closest examples are found for chlorine: In 1988 P. G. Jones reported a zinc(II) tetrachloroaurate disolvate [29] and relatively recently a tetraamminepalladium salt was reported by Plyusnin *et al.* [30]. The divalent metal cation in both compounds, however, have additional ligands alongside the tetrachloroaurate. Additionally, there are a few compounds which contain a higher charged metal cation and tetrachloroaurate, but "free" halide anions as well. A single exception is again found for the fluorine containing compounds: 1996 Graudejus *et al.* reported the synthesis of $La[AuF_4]_3$ [31].

Seventeen years ago Stefan Wagner tried to fill this gap while working on his PhD thesis [32]. Despite many attempts under various reaction conditions, his success on this issue was very limited. He obtained two isotypic tetrahaloaurates with a complex, but still only singly charged cation: $[BiX_2][AuX_4]$ with X = Cl, Br [33]. The results concerning divalent metal cations included $Hg[AuX_4]$ X = Cl, Br, but the crystal system of the tetrachloroaurate could not be determined unambiguously. Powder diffraction indicated the successful synthesis of a cadmium compound, but even the cell determination was doubtful. Wagner successfully synthesized salts of tetrahaloaurates with a higher charged cation, but in these compounds additional halide anions were present (i. e. $Pb_3[AuCl_4]_2Cl_2$).

1.2 Tellurium

Tellurium, element no. 52, was first discovered in 1782 in gold tellurium minerals by the Austrian chemist and mineralogist Franz-Joseph Müller von Reichenstein. He investigated the reason for a lower gold yield than expected from gold ores in Faczebaja, Romania. He was able to determine some properties of tellurium, but never identified the metal itself and thus called it *metallum problematicum* [34]. Some years later, in 1798, Martin Heinrich Klaproth examined von Reichenstein's samples and concluded, that they must contain a new element, which he named tellurium after "*tellus*", the Latin word for earth [35].

In the earth's crust tellurium is roughly as rare as platinum. It is seldom found natively. Usually it occurs in minerals together with noble metals, especially with gold, to whom it has the highest affinity of all elements. Additionally lead and bismuth minerals are common. Commercial production of tellurium does not rely on minerals, as they are too uncommon, but extracts it from anode sludges from copper and nickel electrolytes.

There are a few commercial applications for tellurium. It is used as an additive in alloys to make them more machinable. Cadmium telluride is used in solar panels and doped with zinc it can be used for x-ray detection. Germanium antimony tellurium (GeSbTe), a "phase change material", is used for rewritable DVD media whereas bismuth telluride and lead telluride are used in thermoelectric devices.

Tellurium does not posses as many allotropes as its lighter homologues. Besides the gas phase species Te_2, there is the stable *catena*-polytellurium $^1_\infty[Te]$, which consists of twisted chains and the high pressure modification $^3_\infty[Te]$, which corresponds to β-Po. Additionally *cyclo*-octatellurium is found as a guest molecule in $[Cs_3Te_6][Te_8]$ and a two dimensional slab of tellurium is known only as an intercalate with iodine [9].

All group 16 elements form polycations. Selenium and tellurium polycations have been known for a long time. In qualitative inorganic analysis selenium and tellurium polycations are formed by dissolving the elements in concentrated sulphuric acid. The detection is based on the specific colour of the resulting polycations: Se_8^{2+}: *green* and Te_4^{2+}: *red*. This behaviour was already discovered by M. Klaproth in 1798, when he investigated the newly discovered element

tellurium [35]. The reason behind the coloured solution, or rather the structure of the cation, could only be solved with the determination of the crystal structure of $(Se_4)[HS_2O_7]_2$ carried out by Gillespie *et al.* in 1971 [36]. A year later the analogous tetratellurium polycation in the compounds $(Te_4)[AlCl_4]_2$ and $(Te_4)[Al_2Cl_7]_2$ were examined by x-ray diffraction by Corbett *et al.* [37]. There are many tellurium polycations known today: ${Te_n}^{2+}$ n = 4, 6, 7, 8, 10; ${Te_6}^{4+}$ and ${Te_8}^{4+}$ [38, 39]. The individual structures of these cations are very versatile. ${Te_7}^{2+}$, ${Te_8}^{2+}$ and ${Te_{10}}^{2+}$ are polymeric chains, however, ${Te_8}^{2+}$ is also found as a bicyclic cation in other compounds. ${Te_4}^{2+}$ is an aromatic, square-planar cation. ${Te_6}^{4+}$ crystallises as a prism, while in ${Te_6}^{2+}$ one edge is elongated and the cation is better described as a chair conformation than a prism. These polycations are usually obtained from reactions of elemental tellurium with oxidizing reagents or by comproportionation reactions of Te(IV) halides with elemental tellurium.

Tellurium also readily forms polytelluride anions. Many alkali metal salts are accessible by the reaction of tellurium with the respective metal, dissolved in liquid ammonia. This was also the starting point of the chemical investigation of these anions by Hugot in 1900 [40]. The most versatile anions are the ${Te_n}^{2-}$ dianions, which range from monoatomic to oligomers (n = 1 - 13) [41]. Additionally the blue coloured radical anion ${Te_2}^{-}$ is known, as are ${Te_6}^{-}$ and ${Te_6}^{3-}$ [9]. Classification of the dianions proves difficult. The short-chain dianions (n = 2 – 4) mimic parts of the twisted chain as found in the structure of elemental tellurium. ${Te_5}^{2-}$ and ${Te_6}^{2-}$ have also been observed as isolated entities, but compounds with complicated chains also exist. ${Te_7}^{2-}$ and ${Te_8}^{2-}$ on the other hand are both bicyclic molecules, while ${Te_{12}}^{2-}$ and ${Te_{13}}^{2-}$ are isolated, unbranched chains. Smith and Ibers gave an overview over the solid state structures of polytelluride anions [41] and came to the conclusion that trying to summarize their structural features proves to be very difficult. In addition to the diversity already presented, the telluride anions – in at first glance similar compounds – tend to differ slightly but definitely from one another. One reason for this, especially compared to selenium or sulphur, is the high affinity of tellurium towards intermolecular interaction, usually referred to as secondary interaction. Dividing the tellurium part of a structure into discrete entities is sometimes very challenging because of these intermolecular contacts. Taking all this into account, the only viable summary for the polytelluride anions is, that they are very flexible and seem to posses many different degrees of freedom to tailor themselves for the respective cation.

1.3 Gold tellurium compounds

The number of compounds with both discussed elements, gold and tellurium, is rather small. The ICSD currently holds 81 datasets of crystal structure determinations of compounds containing both elements [42]. Roughly half of these datasets contain minerals with varying – mostly Au/Ag – element substitutions. This group however already contains two unusual compounds from a crystallographic point of view. One is the already discussed calaverite, the other remarkable mineral is montbrayite Au_2Te_3, which crystallises in the rarely found space

group $P1$ (no. 1) [43]. The remaining structures consist of a few individual compounds and four larger groups of compounds: There are four alkali gold tellurides which were synthesized by Bronger *et al.*, namely MAuTe with M = Na – Cs [44]. The sodium and potassium compounds consist of hexagonal AuTe layers, the other two compounds build chains of gold and tellurium. In both structures the gold-tellurium part is separated by the alkali cations. If $AgAuTe_4$ [45] and Ag_3AuTe_2 [46] are discounted, these two compounds are actually the minerals sylvanite and petzite, there is only one known transition-metal gold telluride (CrAuTe) [47], even though heavy element tellurides have been in the focus of interest for different applications for a long time. In the case of the chromium compound, its thermoelectrical properties were investigated, but yielded unsatisfactory results. Finally there are a few compounds known, that crystallize with rare-earth metals instead of transition-metals: $RE_5Au_2Te_2$ with RE = Y, Dy, Ho, Lu; RE_6AuTe_2 with RE = Sc, Y, Dy, Ho, Lu; and $RE_7Au_2Te_2$ with M = Tb, Dy, Ho [48, 49]. These compounds usually contain gold centred polyhedra of the rare-earth metal as building units, which are separated by tellurium atoms. Thus no direct gold tellurium interaction is observed in this compounds in contrast to the discussed compounds above. Samples of these compounds display metallic behaviour.

The last group consists of the gold telluride halides. There are – in total – four compounds deposited in the database: $AuTe_2X$ with X = Cl, Br, I and AuTeI. These compounds were first published in 1970 by Rabenau *et al.* [50]. The gold ditelluride halides display an interesting discrepancy: They show metallic conductivity in contrast to their possibly ionic sum formula: Au^{3+} Te_2^{2-} X^-. Additionally crystals of $AuTe_2X$ are not transparent but of a silvery-white appearance. However, the lighter homologues ($AuSe_2X$) are transparent and their properties – they are isolators – agree with a salt-like interpretation of the sum formula. This is not unexpected as gold tellurium compounds often show deviating behaviour, which is commonly attributed to the imprecise formulation of tellurium's high affinity to gold. This is an empirical observation and is not based on kinetics or thermodynamics, but for example on the fact that gold tellurium minerals are the only naturally found gold compounds. The crystal structure of $AuTe_2Br$ consists of corrugated cationic layers of gold ditelluride which are separated by the bromide anions. Another publication by Zhou *et. al* from 1981 studied the electronic structure of this compound and revealed a high anisotropy in its electronic properties, which corresponds to its layered structure [51].

The wide range of properties of heavy metal tellurides already published and particulary the metallic conductivity of the gold telluride halides, together with the surprisingly low number of known gold tellurium compounds, were the movitation for this work. Since the electronic properties of $AuTe_2X$ were linked to its layer structure, a possible starting point to obtain new compounds with still intact metallic conductivity, was to exchange the separating halide anions. Similar, but larger anions, like tetrabromoaluminate, should prove the electronic properties to be independent of the layer stacking. By introducing less innocent anions, it might be possible to induce new properties. This thesis deals with the experimental results of reactions of chlorides of divalent metals with $AuCl_3$ and reactions of $AuTe_2X$ or AuX_3 with Lewis-acidic metal halides. The found novel $M[AuCl_4]_2$ and gold-tellurium cluster compounds open up new chapters in the crystal chemistry of the noble metal.

Chapter 2

Experimental Part

2.1 Analytical Methods

2.1.1 X-Ray Powder Diffraction

Samples for x-ray powder diffraction were prepared in two different ways depending on the sensitivity of the sample. Air sensitive compounds were filled into glass capillaries (wall thickness 0.01 mm, diameter 0.02 mm – sometimes 0.03 mm) inside the glove box. The capillaries were sealed inside the box using an electrically heated tantalum wire. Air stable compounds were prepared as a flatmount between two thin Mylar foils.
Two different powder diffractometers were used. One (STADI P, STOE, Darmstadt) was equipped with a cobalt x-ray source (PANalytical, Almelo, NL) and a germanium (111) monochromator (CoK_{α_1} wavelength of $\lambda = 1.78896$ Å). The diffractometer had two independent sets of circles equipped, with a smaller (opening angle of $2\Theta = 4°$) and a larger (opening angle of $2\Theta = 35°$) position sensitive detector (PSD, STOE, Darmstadt). The software suite "Win XPOW" [52] was used to control the diffractometer and to examine and process the collected data.
The other diffractometer (D8 Advance, Bruker, Karlsruhe) provided CuK_{α_1} radiation ($\lambda = 1.540598$ Å) monochromatized with a germanium (111) monochromator from a copper x-ray source (Siemens, Munich). The detector was a position sensitive detector (MBraun, Garching) with an opening angle of $2\Theta = 4°$. The programm "XRD Commander" from the software suite "DIFFRACplus" [53] was used to control the diffractor. After converting the file format with "XRD Files Exchange", data analysis was also done with "Win XPOW" .

2.1.2 X-Ray Single Crystal Diffraction

All samples for single crystal x-ray diffraction were transferred from either argon filled ampoules or vessels into perfluorinated oil (FOMBLIN Y HVAC 140/13, Solvay, Brussels, BE) from which suitable crystals were selected. All crystals were glued to a glass fibre using the oil

which solidified on the diffractometer by inserting it into the the cold (usually 123 K) nitrogen gas flow.
The diffractometer was a κ-CCD four circle diffractometer (Bruker-Nonius, Delft, NL) equipped with a molybdenum x-ray source. The x-ray beam was monochromatized with a graphite single crystal resulting in $MoK_{\overline{\alpha}}$ radiation with a wavelength of $\lambda = 0.71073$ Å. The detector was a CCD area detector with a diameter of 95 mm. The cooling device was a Cryostream 700 (Oxford Cryosystems, Oxford, UK).
Data collection was done using the program "Collect" [54]. The unit cell was determined by "HKL-Scalepack" [55] and the data integration and reduction was performed by "HKL-Denzo" [55]. Initial structure solutions were achieved by charge-flipping implemented in "Superflip" [56]. Structure refinement was done using "SHELXL-97" [57] and "SHELXL-2014" [58]. Semi-emperical absorption correction based on the large redundancy of the data set as proposed by Blessing [59] (implemented in "PLATON" [60, 61]) was applied. The program suite "WinGX" [62] was used for simplified access to these programs. "Diamond 3" [63] was used for structure visualization.
The data of the modulated crystal structure was processed with "APEX2" [64] and the absorption correction was done by "SADABS" [64]. The structure refinement was performed with JANA2006 [65].

2.1.3 Energy Dispersive X-Ray Spectroscopy (EDX)

For elemental analysis energy dispersive x-ray spectroscopy was used. Measurements were done on a scanning electron microscope (DSM 940, Zeiss, Jena) which reconstructs images of the sample from back scattered or secondary electrons. For quantitative analysis the microscope was equipped with a lithium-drifted silicon detector (PV 9800, EDAX Inc., Mahwah NJ, USA). Measurement samples were prepared onto a circular aluminium sample holder (12 mm diameter) which was fitted with conducting graphite foil to keep the sample from statically charging itself. In case the sample was not (semi-)conducting the sample was sputtered with carbon (Sputtermodul 11430, Fa. SPI Supplies). The accelerating voltage for all quantitative measurements was 25 kV.
For air sensitive samples, the preparation was performed inside the glove box and the samples could be transferred under argon within a special chamber, first to the sputter device and afterwards to the electron scanning microscope.

2.1.4 Conductivity Measurements

The samples for temperature dependent conductivity measurements were prepared inside the glove box in a small glass tube (inner diameter = 2 mm, height = 2 cm, sample thickness $\sim$ 2 mm) which was closed and contacted on both sides by gold plated electrodes. A SourceMeter 2400 (Keithley Instruments, Cleveland OH, USA) was used to supply an offset voltage and read back the resulting current, from which the resistance was calculated. The temperature was controlled by a custom built heating chamber surrounding the complete sample.

2.1.5 Magnetic Susceptibility Measurements

The samples for magnetic susceptibility measurements were filled into a polypropylene powder sample holder (Quantum Design) in the glove box. The sample quantity was usually in the range from 10 mg to 20 mg. The measurements were performed with a PPMS Vibrating Sample Magnetometer (VSM) (Quantum Design, San Diego CA, USA). The sample was measured in a magnetic field of 10 kOe in the temperature range of 1.9 K to 300 K. The collected data was corrected against a measurement of the empty sample holder, which was done beforehand. Additionally, an incremental diamagnetic correction [66] was applied to the data.

2.1.6 Raman Spectroscopy

The samples for vibrational Raman spectroscopy were prepared in melting point determination tubes (diameter = 1 mm), which were sealed afterwards. Measurements were performed with an FT-Raman spectrometer (MultiRAM, Bruker, Karlsruhe) equipped with a Nd:YAG-Laser ($\lambda = 1064$ nm) as excitation source and a liquid nitrogen cooled germanium detector. Bands occurring at 74 cm^{-1} and 78 cm^{-1} were assigned to the excitation laser itself. The laser output was set to 15 mW.

2.2 Quantum Chemical Calculations

All quantum chemical calculations were carried out by "CRYSTAL14" [67]. Since the investigated system involved heavy atoms and large unit cells, the compound $AuTe_2Br$ was used to test the basis sets and different exchange functionals. $AuTe_2Br$ presented a similar chemical environment to the studied gold tellurium cations. One of the best results for $AuTe_2Br$ was achieved with the PW1PW hybrid method [68]. Additionally, the PW1PW functional is known to yield better band gap estimates, which are of interest in this work, but requires more calculation time. As a compromise to cut down on CPU time, only PBE [69] with an additional dispersion correction (D3) [70–72] was used for the much more demanding relaxation of all structural parameters, followed by a single point PW1PW calculation to acquire the ground state wave function. The PW1PW exchange functional is a linear combination (20:80) of the Hartree-Fock expression and the Perdew-Wang exchange functional. [73, 74]
One electron properties – band structures and (projected) densities of states – were calculated by running "properties" from CRYSTAL software package. The Fourier-Legendre technique [75] with a Monkhorst-Pack net [76] and shrinking factor of $s = 12$ (for $(Au_6Te_{18}Cl_2)[Mo_2O_2Cl_8]_2$) and $s = 4$ (for $(Au_6Te_{18})[AlCl_4]_6$) was applied to calculate the PDOS. The calculated properties were plotted using gnuplot [77]. All axes representing energy were shifted relative to the fermi energy ($E_F = 0$).

2.3 Preparative Methods

Since most of the used compounds are sensitive to air – mostly due to hydrolysis – handling of these substances was done using either Schlenk techniques or inside a glove box.

2.3.1 Working under Inert Gas Atmosphere

Schlenk Line

The used Schlenk line enabled working under argon or reduced pressure. The used vacuum pump was a rotary vane pump (RD4, Vacuubrand, Wertheim) and supplied a reduced pressure of at least 10^{-3} mbar according to the pressure gauge (Combitron CM 300, Leybold, Cologne). The used inert gas was purified argon 4.6 (Ar $\geq$ 99.996 %, $O_2 \leq 6$ ppm, $N_2 \leq 20$ ppm, $H_2O \leq 5$ ppm; Praxair, Düsseldorf). The gas was routed through several drying towers, which were filled with silica gel (to remove moisture), potassium hydroxide pellets (to remove acidic impurities), 3 Å molecular sieve (to adsorb water) and finally phosphorus pentoxide (to remove basic impurities). As a final purification step the gas was routed through a furnace heated to 650 °C filled with titanium sponge to remove any traces of oxygen or nitrogen down to the equilibrium partial pressure of TiO or TiN, respectively.
The Schlenk line was completely built of borosilicate glass and was assembled using ground joints. The pumped gas was routed through a cold trap – cooled by liquid nitrogen – to protect the vacuum pump from volatile compounds and improve the achieved low pressure.
Further equipment was connected to the Schlenk line using ground joints. All glass vessels were heated at least two times under reduced pressure using a Teclu laboratory burner. Ampoules were charged inside the argon countercurrent flow. All of them were sealed while connected to the Schlenk line. Reaction and sublimation ampoules were sealed under reduced pressure while ampoules for storage and portioning were sealed under argon.

Glove Box

Further preparations were done inside a glove box. The used glove box (Labmaster 130, MBraun, Garching) contained a high precision balance (BP61S, Sartorius AG, Göttingen) and a microscope (MZ6, Leica Microsystems GmbH, Wetzlar) integrated in the front window. The inert gas was argon 4.6 (see above) which was purified using a molecular sieve (400 pm) and a BTS catalyst (molecular sieve with finely dispersed copper). The oxygen and water content inside the glove box was usually between 1 ppm and 10 ppm.

2.3.2 Working at the "Chlorination Schlenk Line"

The syntheses of compounds that required chlorine or hydrogen chloride was carried out at a special designed, permanently installed Schlenk line (see Figure 2.1). Additionally to

the Schlenk line described above it provided three additional inlets. The inlet for hydrogen chlorine only routed the gas flow from the pressurised gas cylinder through a sulfuric acid filled bubble counter, the other remaining inlets, one meant for chlorine and the other for hydrogen, additionally dried the gas over phosphorous pentoxide. For safety reasons the hydrogen gas cylinder was not permanently installed to prevent the forming of explosive mixtures of hydrogen and chlorine. Between this part and the normal Schlenk line there was an additional cold trap to condense the chlorine prior to its use. For this purpose the cold trap was cooled using a dry ice/ethanol mixture. The condensed chlorine was transported by an argon gas flow inside the reaction tube. The setup contained a programmable furnace (B70.3011, Linn High Therm GmbH, Eschenfelden), which was able to heat up to 1100 °C.

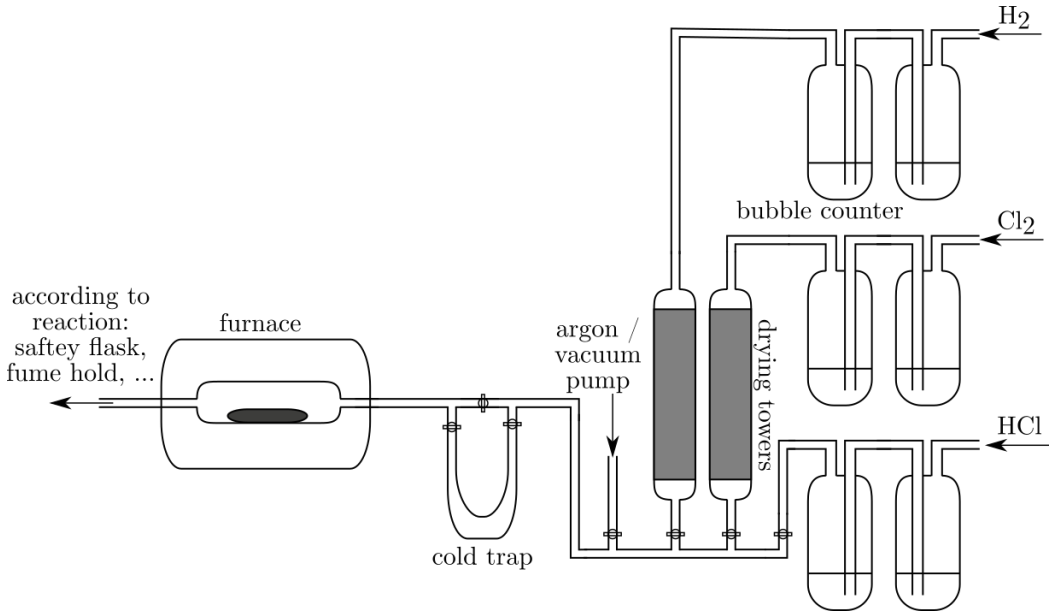

Figure 2.1: Schematic representation of the "chlorination Schlenk line".

2.4 Reactant Synthesis

2.4.1 Recycling of Collected Gold Scraps

First the collected residues were evaporated to dryness and dissolved in *aqua regia*. The resulting solution was filtered. The filtrate was concentrated and again diluted with concentrated hydrochloric acid multiple times until no more nitrous fumes were evolved. With ammonium chloride the acidity of the solution was adjusted to pH 4-5. Finally gold was reduced with gaseous SO_2. The precipitated gold was filtered off.

2.4.2 Purification of Tellurium

$$\mathrm{Te} + \mathrm{H_2} \rightleftharpoons \mathrm{H_2Te} \tag{2.1}$$

Tellurium powder was placed in a fused silica boat in a fused silica tube and was heated to roughly 600 °C under a flow of dry hydrogen [78]. Tellurium was transported as hydrogen telluride, which decomposes at lower temperatures. After removal of the fused silica boat the product was collected from the tube.

2.4.3 Gold(III) chloride, $AuCl_3$

$$2\,\mathrm{Au} + 3\,\mathrm{Cl_2} \xrightarrow{\text{RT, 7 d}} 2\,\mathrm{AuCl_3} \tag{2.2}$$

Gold(III) chloride was synthesized from the elements. An excess of liquid chlorine was condensed onto pre-filled gold powder in a thick-walled borosilicate ampoule. The chlorine was frozen with liquid nitrogen and the ampoule was sealed under reduced pressure and placed at room temperature for 7 days in a vertical position. The ampoule was opened and the remaining chlorine was evaporated to yield the product.

2.4.4 Gold(III) bromide, $AuBr_3$

$$2\,\mathrm{Au} + 3\,\mathrm{Br_2} \xrightarrow{\text{140 °C, 4 d}} 2\,\mathrm{AuBr_3} \tag{2.3}$$

An excess of freshly distilled bromine was condensed onto gold powder in a thick-walled borosilicate ampoule. The bromine was frozen with liquid nitrogen and the ampoule was sealed under reduced pressure and heated to 140 °C for 4 days. The remaining bromine was evaporated to yield the product [79].

2.4.5 Gold(III) telluride halide, $AuTe_2X$, X = Cl, Br

$$4\,\mathrm{Au} + 7\,\mathrm{Te} + \mathrm{TeX_4} \longrightarrow 4\,\mathrm{AuTe_2X} \tag{2.4}$$

Both compounds have been prepared from stoichiometric mixtures of gold, tellurium and the corresponding tellurium halide [50]. The reactants were sealed in an evacuated borosilicate glass ampoule and heated to 300 °C. The chloride was annealed for 21 days, the bromide for 15 days.

2.4.6 Aluminium(III) chloride, $AlCl_3$

Aluminium(III) chloride was sublimated two times at 125 °C [80]. To account for iron chloride impurities, 5 *wt*% elemental aluminium was added. The resulting product was colourless.

2.4.7 Aluminium(III) bromide, $AlBr_3$

$$2\,Al + 3\,Br_2 \longrightarrow 2\,AlBr_3 \tag{2.5}$$

Aluminium(III) bromide was synthesized from the elements [78]. Freshly distilled bromine was added dropwise to an excess of chopped pieces of aluminium cooled by ice water. After the bromine was completely added, the seemingly black product was sublimated and collected in glass ampoules. Finally the crude product was sublimated again at 90 °C to yield a colourless product.

2.4.8 Bismuth(III) chloride, $BiCl_3$

$$2\,Bi + 3\,Cl_2 \longrightarrow 2\,BiCl_3 \tag{2.6}$$

Bismuth(III) chloride was prepared from liquated bismuth and chlorine [78]. Bismuth was placed in a fused silica boat inside a fused silica tube and was slightly heated inside an argon atmosphere. The temperature was slowly raised further under a flow of dry chlorine until the reaction started and the product sublimated to the colder part of the silica tube. After removal of the silica boat the product was collected from the tube.

2.4.9 Cadmium(II) chlorid, $CdCl_2$

$$Cd + 2\,HCl \xrightarrow{450\ °C} CdCl_2 + H_2 \tag{2.7}$$

Cadmium(II) chloride was synthesized from sublimated cadmium powder and hydrogen chloride at 450 °C [78]. The cadmium powder was placed in a fused silica boat inside a fused silica tube. The sample was heated under a flow of dry hydrogen chloride resulting in sublimation of the product to the colder part of the silica tube. After removal of the silica boat the product was collected from the tube.

2.4.10 Niobium(V) chloride, $NbCl_5$ & Tantalum(V) chloride, $TaCl_5$

$$2\,Nb + 5\,Cl_2 \xrightarrow{250\ °C,\ 4\ h} 2\,NbCl_5 \tag{2.8}$$

$$2\,Ta + 5\,Cl_2 \xrightarrow{250\ °C,\ 4\ h} 2\,TaCl_5 \tag{2.9}$$

Niobium(V) chloride and tantalum(V) chloride were synthesized from the elements [78]. The metal was placed inside a fused silica boat inside a fused silica tube and was heated under argon atmosphere to remove traces of air and water. The sample was heated under a flow of dry chlorine to 250 °C for 4 hours. The product was sublimated to the colder part of the tube. After removal of the silica boat the product was collected from the tube.

2.4.11 Molybdenum(V) pentachloride, $MoCl_5$

$$2\,Mo + 5\,Cl_2 \xrightarrow{400\ °C} 2\,MoCl_5 \tag{2.10}$$

Molybdenum(V) chloride was prepared from the elements. Molybdenum powder was placed inside a fused silica tube and first reduced with dry hydrogen at 1000 °C for one hour. After thoroughly removing all traces of hydrogen the freshly reduced metal was chlorinated in an argon/chlorine gas flow at 400 °C. The reaction took 1.5 h.

2.4.12 Molybdenum(V) oxide trichloride, $MoOCl_3$

$$3\,MoCl_5 + Sb_2O_3 \longrightarrow 3\,MoOCl_3 + 2\,SbCl_3 \tag{2.11}$$

Molybdenum(V) oxide trichloride was prepared from $MoCl_5$ and Sb_2O_3 [81]. The reactants were sealed inside a borosilicate glass ampoule. The ampoule was divided in two halves by a constriction. It was placed inside a furnace with the empty half outside. First the ampoule was heated to 80 °C for four hours, then to 120 °C for three hours and finally to 150 °C for two hours. The unwanted liquid product antimony trichloride condensed in the cooler part of the ampoule, while the desired product $MoOCl_3$ formed in the hotter part. $MoOCl_3$ and $SbCl_3$ were separated by dividing the ampoule at the constriction. To further purify the raw product, it was sublimated at 240 °C.

2.4.13 Tellurium(IV) chloride, $TeCl_4$

$$Te + 2\,Cl_2 \longrightarrow TeCl_4 \tag{2.12}$$

Tellurium tetrachloride was prepared from the elements [78]. Tellurium was gently heated with a lab burner under a gas flow of dry chlorine to start the reaction. The reaction mixture liquidated and changed colour from black to dark red and finally yellow. After further heating the product changed its colour to light yellow. After a short cooling period, the product was heated again under a mixture of chlorine and hydrogen chlorine to remove any traces of oxide chlorides. Finally the colourless product was sublimated in a chlorine gas flow.

2.4.14 Tellurium(IV) bromide, $TeBr_4$

$$Te + 2\,Br_2 \longrightarrow TeBr_4 \tag{2.13}$$

Tellurium tetrabromide was prepared from the elements [78]. Roughly twice the amount of required bromine was condensed onto tellurium powder. The mixture stood over night. The excess of bromine was removed by slightly heating the mixture in an argon gas flow. The reaction tube was sealed under reduced pressure and placed horizontally in a furnace to

sublimate the crude product at 350 °C. The product partially disproportionated to tellurium subbromides and bromine. The ampoule was opened under argon and after evaporation of the bromine the bright yellow product could be isolated.

2.4.15 Zinc(II) chloride, $ZnCl_2$

$$Zn + 2\,HCl \xrightarrow{700\ °C} ZnCl_2 + H_2 \tag{2.14}$$

Zinc(II) chloride was synthesized from zinc powder and hydrogen chloride at 700 °C [78]. The zinc powder was placed in a fused silica boat inside a fused silica tube. The sample was heated under a flow of dry hydrogen chloride resulting in sublimation of the product to the colder part of the fused silica tube. After removal of the fused silica boat the product was collected from the tube.

2.4.16 Zirconium(IV) tetrachloride, $ZrCl_4$

$$ZrOCl_2 + SOCl_2 \longrightarrow ZrCl_4 + SO_2\uparrow \tag{2.15}$$

Commercial $ZrCl_4$ was purified because it is often contaminated with $ZrOCl_2$. Distilled thionyl chloride was placed in a round bottom flask. $ZrCl_4$ was slowly added to the mixture. Because of the exothermic reaction between $ZrOCl_2$ and $SOCl_2$ the mixture turned warm. It was shortly heated to reflux temperature (15 min). Afterwards the excess of thionyl chloride was evaporated and the product was sublimated under dynamic vacuum.

2.5 Other used Chemicals

Table 2.1: Used commercial chemicals.

Compound	Manufacturer	Purity / Note
Aluminium	Sigma Aldrich, St. Louis, MO, USA	99 %, -200 mesh
Antimony(III) oxide	Sigma Aldrich, St. Louis, MO, USA	99.999 %
Bismuth	Merck, Darmstadt	> 99 %
Bromine	Sigma Aldrich, St. Louis, MO, USA	99+%
Cadmium	Merck, Darmstadt, 99 %, powder	
Chlorine	Praxair, Düsseldorf	Cl_2 3.0
Gallium(III) chloride	Alfa Aesar, Lancashire, UK	ultra dry, 99.999%
Gold	*group stock, scraps*	

continued on next page

Compound	Manufacturer	Purity / Note
Hydrochloric acid	VWR, Radnor, PA, USA	37 %, AnalR
Hydrogen	Air Liquide, Düsseldorf	H_2 3.0
Hydrogen chloride	Praxair, Düsseldorf	HCl 2.5
Molybdenum	Acros Organics, Geel, Belgium	99.999 %, -200 mesh
Niobium	*group stock, scraps*	turnings
Tantalum	H. C. Stark, Newton, MA, USA	TaMP STA-40KD
Tellurium	Merck, Darmstadt	99 %, powder
Zinc	Grüssing GmbH Analytika, Filsum	powder
Zirconium(IV) chloride	Merck, Darmstadt	water-free, p.a.

2.6 Product Synthesis

2.6.1 General Synthesis Method for Compounds Containing the $(Au_6Te_{18}X_n)^{(6-n)+}$ Cation

$$6\,AuTe_2X + 6\,Te + (6{-}n)\,LA \xrightarrow{400\ ^\circ C,\ 7\ d} (Au_6Te_{18}X_n)[LB]_{(6-n)} \tag{2.16}$$

$$6\,AuX_3 + 18\,Te + (6{-}n)\,LA \xrightarrow{400\ ^\circ C,\ 7\ d} (Au_6Te_{18}X_n)[LB]_{(6-n)} \tag{2.17}$$

All compounds of this family were synthesized using the same general method. The reaction mixture consisted of a gold compound, either gold(III) telluride halide or gold(III) halide, elemental tellurium and a lewis-acidic metal halide. This mixture was sealed in a short borosilicate ampoule ($\sim$ 8 cm length, 9 mm diameter, 1.0 mm wall thickness), which was heated twice under reduced pressure beforehand, and was slowly heated (1 K/min) to 400 °C. After 7 days the ampoule was slowly cooled (0.2 K/min) to room temperature. Because transport reactions occurred as competing side reactions the ampoule was placed in a large furnace to minimize the experienced temperature gradient. For example, several compounds containing tellurium polycations or TeX_3^+ cations were identified by their lattice parameters on the single crystal diffractometer: $(Te_6)[ZrCl_6]$, $(Te_6)[HfCl_6]$, $(TeCl_3)[AuCl_4]$.
The compounds discussed in this work were prepared using the weighted samples listed in Table 2.2. Usually the gold compound was added in amounts around 0.2 mmol. The reactions given in equations 2.16 and 2.17 are not balanced properly. Depending on the actual reactants there were different side products. In most cases the corresponding gold(III) telluride halide and tellurium(IV) halide was found.

Table 2.2: Weighted samples for all discussed compounds containing a gold tellurium cation.

Compound	Gold Compound	Lewis Acid	Tellurium
$(Au_6Te_{18})[AlCl_4]_6$	87.8 mg $AuTe_2Cl$	20.1 mg $AlCl_3$	23.1 mg Te
$(Au_6Te_{18})[AlBr_4]_6$	95.2 mg $AuTe_2Br$	48.0 mg $AlBr_3$	23.2 mg Te
$(Au_6Te_{18})[ZrCl_4]_3$	93.1 mg $AuCl_3$	35.8 mg $ZrCl_4$	117.5 mg Te
$(Au_6Te_{18}Cl)[AlCl_4]_5$	61.9 mg $AuCl_3$	22.7 mg $AlCl_3$	78.1 mg Te
$(Au_6Te_{18}Cl)[GaCl_4]_5$	55.3 mg $AuCl_3$	26.8 mg $GaCl_3$	69.8 mg Te
$(Au_6Te_{18}Br)[AlCl_4]_5$	22.5 mg $AuCl_3$	16.5 mg $AlBr_3$	28.4 mg Te
$(Au_6Te_{18}Br)[AlCl_4]_5$	105.4 mg $AuBr_3$	26.8 mg $AlCl_3$	92.4 mg Te
$(Au_6Te_{18}Br)[AlBr_4]_5$	192.5 mg $AuBr_3$	98.0 mg $AlBr_3$	168.8 mg Te
$(Au_6Te_{18}Cl)[MoOCl_4]_5$	122.9 mg $AuTe_2Cl$	55.5 mg $MoOCl_3$	32.4 mg Te
$(Au_6Te_{18}Cl_2)[Mo_2O_2Cl_8]_2$	156.5 mg $AuCl_3$	93.9 mg $MoOCl_3$	197.5 mg Te
$(Au_6Te_{18}Cl_2)[Bi_4Cl_{16}]$	26.0 mg $AuCl_3$	22.5 mg $BiCl_3$	32.8 mg Te
$(Au_6Te_{18}Cl_2)[Bi_4Cl_{16}]$	98.4 mg $AuTe_2Cl$	63.6 mg $BiCl_3$	25.8 mg Te
$(Au_6Te_{18}Cl_2)[NbCl_6]_4$	36.1 mg $AuCl_3$	26.8 mg $NbCl_5$	45.6 mg Te
$(Au_6Te_{18}Cl_2)[TaCl_6]_4$	95.5 mg $AuCl_3$	112.8 mg $TaCl_5$	120.5 mg Te

Additional Observations

The synthesis conditions for these compounds were highly specific. From visual inspections the reactants seemed to form a melt at the applied reaction temperatures. This assumption was supported by the low cooling rate, which was needed to yield the product as a crystalline powder. A temperature gradient inside the reaction ampoule usually led to formation of side-products by transport reactions and in the worst case prevented the desired product from forming. The halide contents of the obtained cations in reactions with the same Lewis acid was different depending on the used gold compound. Using gold(III) chloride led to a higher chlorine content in the cation, while using gold(III) telluride halide led to a lower chlorine content. A reason for this outcome could be the Lewis acidity of the reaction melt. Following this argument, the melt, formed from $AuCl_3$ as a reactant, should contain gold halide or gold/tellurium halide species with a higher Lewis acidity compared to the melt formed by starting from $AuTe_2Cl$. From the anion's point of view this means that the Lewis acidic metal chloride, i. e. $AlCl_3$, abstracts a chloride from the former gold species more easily.

All this discussion is further complicated by the unbalanced reaction equations containing gold(III) halide as starting material. Until $(Au_6Te_{18})[ZrCl_6]_3$ was successfully synthesized from $AuCl_3$, halide-free cations seemed to be impossible to be obtained from this reaction mixture.

2.6.2 $Zn[AuCl_4]_2 \cdot (AuCl_3)_{1.115}$ and $Cd[AuCl_4]_2$

$$ZnCl_2 + 3.115\,Au \xrightarrow[2)\ 230\ °C,\ 7\ d]{1)\ Cl_2,\ RT,\ 28\ d} Zn[AuCl_4]_2 \cdot (AuCl_3)_{1.115} \tag{2.18}$$

$$CdCl_2 + 2\,Au \xrightarrow[2)\ 230\ °C,\ 7\ d]{1)\ Cl_2,\ RT,\ 28\ d} Cd[AuCl_4]_2 \tag{2.19}$$

A borosilicate ampoule ($\sim$ 10 cm length, 12 mm diameter, 2.2 mm wall thickness) was filled with a stoichiometric mixture of elemental gold (104 mg or 58.8 mg) and zinc(II) chloride (21.1 mg) or cadmium(II) chloride (27.4 mg) respectively. Chlorine was condensed onto the mixture, frozen with liquid nitrogen and the ampoule was sealed under reduced pressure and placed vertically for four weeks at ambient temperature. The ampoule was opened and the excess of chlorine was evaporated. The orange mixture was sealed in a long ($\sim$ 25 cm) glass ampoule having a constriction. The ampoule was placed asymmetrically in a furnace with the filled part placed in the hot central zone. The mixture was heated to 240 °C for 7 days to sublimate off the excess of gold(III) chloride to the colder part of the ampoule. The ampoule was divided at the constriction to isolate the product. The yield was low, but could be improved by longer reaction times (in the range of several months) for the first reaction step.

Chapter 3

Results and Discussion

3.1 General Description of the $(Au_6Te_{18}X_n)^{(6-n)+}$ Cation

Since (almost) all compounds discussed in this work contain the eponymous $(Au_6Te_{18}X_n)^{(6-n)+}$ cation (X = Cl, Br; n = 0 - 2), the general aspects of this molecular entity will be discussed first. To further simplify the discussion, the possible halide anions X coordinated to the gold-tellurium part of the cation will be disregarded for the moment. The central $(Au_6Te_{18})^{6+}$ entity (exemplarily taken from the crystal structure of $(Au_6Te_{18})[ZrCl_6]_3$), which is found in all compounds, is shown in Figure 3.1. The structure of the cation may be described by two different approaches.

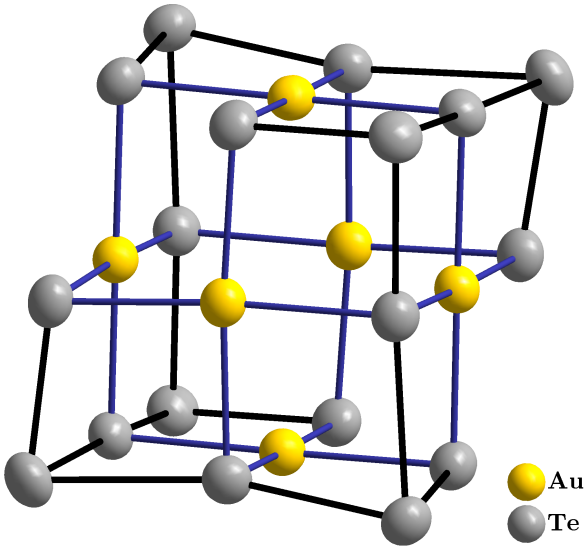

Figure 3.1: The $(Au_6Te_{18})^{6+}$ cation taken from the crystal structure of $(Au_6Te_{18})[ZrCl_6]_3$. The displacement ellipsoids represent a probability of 90 %.

The starting point for the first way of description is the arrangement of the gold atoms. Six gold atoms are arranged in form of an octahedron. The distances between the atoms, however, are way too large to be considered as bonding interactions (roughly 3.8 Å cf.

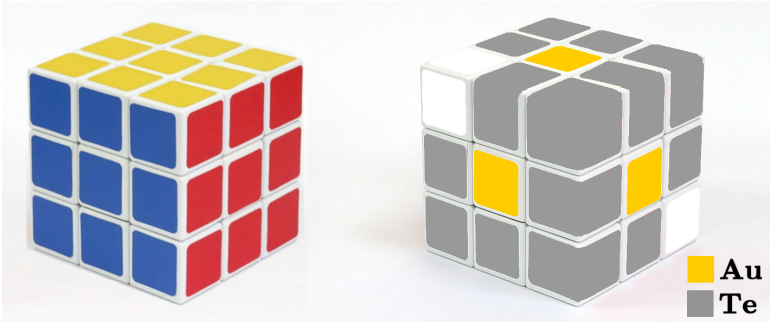

Figure 3.2: A Rubik's cube and a recoloured cube to emphasize the relation to the $(Au_6Te_{18})^{6+}$ cation.

$2r_{vdW}(Au) = 3.32$ Å [82]). All twelve edges of the Au_6 octahedron are capped by tellurium atoms. Six of the eight faces are capped by the remaining tellurium atoms. The remaining two unoccupied faces are located on opposite sides of the Au_6 octahedron, to form the $(Au_6Te_{18})^{6+}$ cation.

The second way of description, however, is preferred, because it omits the Au_6 octahedron as there is no indication of gold–gold interactions in the cation. Here, the starting point is derived from a $3 \times 3 \times 3$ cube – for example analogous to the famous Rubik's cube (see Figure 3.2). All 27 blocks of the cube represent a possible atom position. The cube's centre position is vacant, as are two corners across the space diagonal. The central block of all six faces represents a gold atom. The remaining 18 positions (six corners and twelve edges) represent the tellurium atoms. The resemblance of the cation to a cube will be used for nomination in all further discussion of structural features of the cation. The sum formula of the cation as described above is $(Au_6Te_{18})^{6+}$. The other two variants, which are discussed in this work are $(Au_6Te_{18}X)^{5+}$ and $(Au_6Te_{18}X_2)^{4+}$. The additional halide atoms occupy either one or both vacant corner positions.

Both aforementioned discussions omit the fact that the cation is not as symmetric as the descriptions might imply. The atoms on the cube corner positions are displaced outwards, away from the cube's centre (see Figure 3.3), regardless of whether it is a tellurium or a halide atom. This distortion together with the two vacant corner positions would still allow for an idealized D_{3d} point symmetry, but this has not been observed as a site symmetry for the cation in all compounds studied so far. In the crystal structure of $(Au_6Te_{18}Br)[AlBr_4]_5$, the local symmetry of the cation is C_3. In all other compounds the cation is only centrosymmetric, with the expection of $(Au_6Te_{18})[ZrCl_6]_3$, where the whole cation is on a general position. All observed cations, however, usually show only very small deviations from the idealized D_{3d} symmetry.

The discussion of the cation so far focused only on the structural arrangement, not on a chemical interpretation of valences and bonds. The most basic approach starts by breaking down the sum formula into (smaller) ions. The smallest entity thus consists only of a gold(III) cation and the well known angled tritellurium dianion: $(Au^{3+}(Te_3)^{2-})_6$ (see Figure 3.4). This would imply a purely ionic interaction within the cation which is most certainly an oversimplification. Nevertheless, the obvious merit of this idea is the perfectly matching ionic charge and the

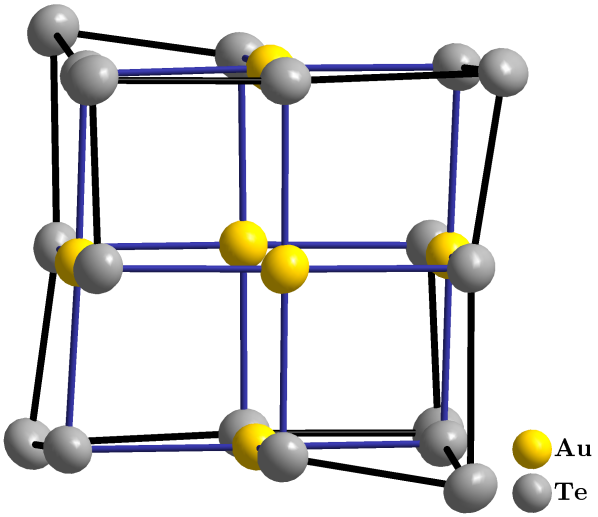

Figure 3.3: The $(Au_6Te_{18})^{6+}$ cation taken from the crystal structure of $(Au_6Te_{18})[ZrCl_6]_3$. The viewing direction along a cube edge is slightly tilted to emphasize the displaced tellurium atoms at the corner position. The displacement ellipsoids represent a probability of 90 %.

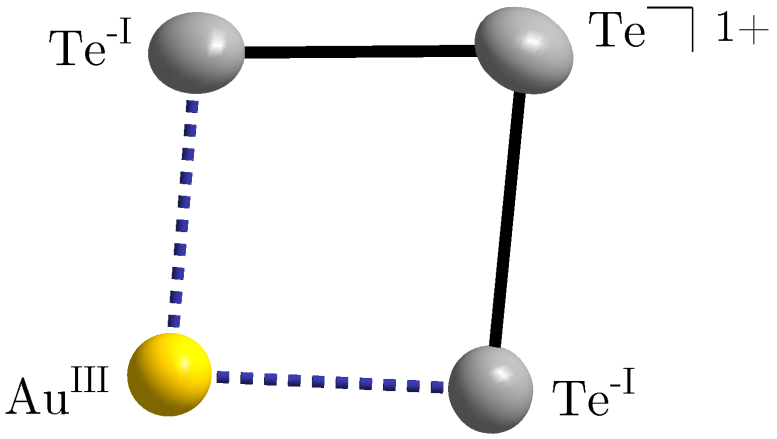

Figure 3.4: Ionic building parts $(Au^{3+} + (Te_3)^{2-})$ of the $(Au_6Te_{18})^{6+}$ cation taken from the crystal structure of $(Au_6Te_{18})[ZrCl_6]_3$. The displacement ellipsoids represent a probability of 90 %.

nearly perfect square-planar coordination of all gold atoms as expected for gold(III). On the other hand, the question arises why the constituents of the cation assemble in the observed way. Evenly distributing the actual anion of the respective compound between the gold cation and tellurium anion would result in a much better charge balance. This might even allow for a better space filling since the cation's centre is empty. Additionally, the gold tellurium distances (see Table 3.1) indicate at least a partial covalent nature of the interaction. Consequently the conclusion is that, although the interpretation of gold(III) and $(Te_3)^{2-}$ ions has some merit, there must be also a significant covalent interaction between gold and tellurium and the various tritellurium dianions. This will become even more apparent in the discussion of the actual crystal structures, as there are often close contacts present between two anions according to the above discussed ionic valence model.

Even though the exact interatomic distances differ between the individual compounds, it is possible to state a reasonably small range for the different types of interatomic distances.

Table 3.1: Average atom distances for the cation of all discussed compounds.

Atoms 1, 2	d(min)	d(max)	d(avg)
Au $\cdots$ Au	3.66 Å	3.97 Å	3.80 Å
Au — Te	2.66 Å	2.71 Å	2.69 Å
Te — Te	2.71 Å	3.17 Å	2.89 Å

Table 3.2: Average bond angles for the cation of all discussed compounds. The indices indicate the tellurium atom position on a cube edge (*ed*) or a cube corner (*co*).

Atoms 1, 2, 3	∠(min)	∠(max)	∠(avg)
Te_{ed} — Au — Te_{ed}	85°	97°	90°
Au — Te_{ed} — Au	85°	96°	90°
Te_{ed} — Te_{co} — Te_{ed}	76°	86°	82°
Te_{co} — Te_{ed} — Te_{co}	162°	174°	169°

Table 3.1 only lists the averaged values over all discussed compounds. A more detailed listing is available in the appendix (see Tables A.81 - A.83). The listing according to Table 3.1 is sufficient to see that all gold-tellurium bond lengths cover the very narrow range of only 2.69 Å ± 0.03 Å. The dispersion of the Au··Au range is only slightly wider: 3.80 Å ± 0.17 Å. Since the gold atoms do not interact directly with each other, this is one of the few degrees of freedom left for the cation for distortion and to gain the best fit with the crystal packing. Finally, the Te–Te bond lengths distribution is wider and covers a range of 2.89 Å ± 0.28 Å. There are two reasons for this. First, the cube corner is disordered in some compounds, and second, the underlying $(Te_3)^{2-}$ moiety is asymmetrically distorted. Te–Te bonding lengths together with their corresponding Te–X distances will be discussed individually for each compound. The distribution of the bonding angles inside the cation is analogous (see Table 3.2). The various bonding angles at the gold atoms and the tellurium atoms on cube edges – Te–Au–Te and Au–Te–Au – are all narrowly distributed around 90°, which substantiates both the geometrically description of the cation as a cube and the assignment of the Au^{3+} oxidation state. The angles which include a tellurium atom on a corner position on the other hand reflect the already mentioned displacement of atoms on corner positions. The distribution itself is still very narrow, but deviates from the ideal angle of 90° or 180° respectively. All in all, this overview suggests that the cation itself is on one hand versatile concerning the attachment of halide atoms on its corners, but on the other hand also barely affected and stable against the influence of its chemical neighbourhood.

3.2 Compounds Containing the $(Au_6Te_{18})^{6+}$ Cation

3.2.1 $(Au_6Te_{18})[ZrCl_6]_3$

The compound $(Au_6Te_{18})[ZrCl_6]_3$ crystallizes in the acentric space group *Cc* and is of black-metallic appearance. It consists of the $(Au_6Te_{18})^{6+}$ cation and three octahedral hexachlorozirconate(IV) anions. Because of the absence of inversion centres in the space group, the asymmetric unit contains the full sum formula. The crystal structure of this compound, together with both isotypic crystal structures as described in the next section, has the distinctive feature that the already discussed $(Te_3)^{2-}$ anions are present with discrete bond lengths (see Figure 3.5). The cation is located on a general position though all 18 Te–Te bond lengths are different. Still, there is for each $(Te_3)^{2-}$ moiety a shorter bond (roughly 2.71 Å; thick bonds in Figure 3.5) and a longer bond (roughly 2.85 Å; see Table 3.3). Usually $(Te_3)^{2-}$ is observed with two almost identical bond lengths [41]. In this case the reason for the asymmetry lies in additional interactions between various $(Te_3)^{2-}$ anions. The shorter bond always points towards an empty corner position while the longer bond is located along a cube edge towards an occupied cube corner position. This distance is about 3.10 Å (dashed lines in Figure 3.5), which is shorter than twice the van-der-Waals radius of Te, suggesting that the bond is elongated, because the middle tellurium atom of the neighbouring anion donates electron density into the anti-bonding orbitals of the parent $(Te_3)^{2-}$ anion.

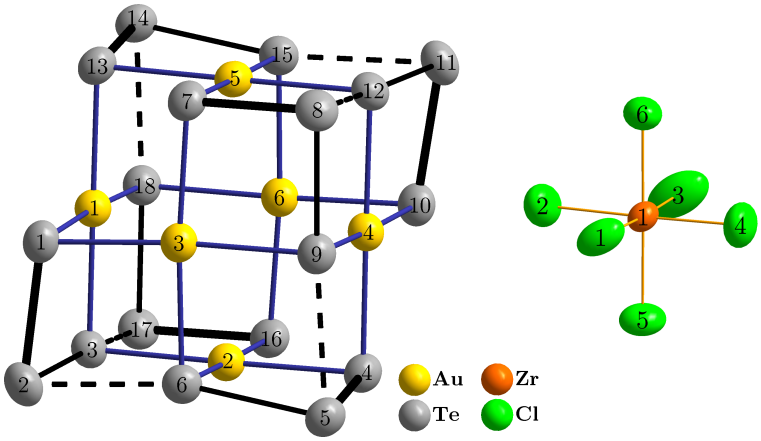

Figure 3.5: The $(Au_6Te_{18})^{6+}$ cation with distinct $(Te_3)^{2-}$ moieties *(left)* and exemplarily one of the three idenpendent $[ZrCl_6]^{2-}$ anions *(right)* taken from the crystal structure of $(Au_6Te_{18})[ZrCl_6]_3$. The element symbol has been omitted from the atom numbering to enhance readability. Short bonds are emphasized by thick lines. The displacement ellipsoids represent a probability of 90 %.

The Te(1)–Te(2)–Te(3) bond angle and the analogous angles lie between 83° and 86° (see Table 3.3). Compared to 100° to 115° found for less tightly coordinated tellurium anions [41] the bond angles here are more compressed to enable the square-planar coordination for the gold(III) ion. One of the few examples of compounds coordinating $(Te_3)^{2-}$ anions is the complex anion $[Cu_3Te_3(Te_3)_3]^{9-}$ [83], which has a Te-Te-Te bond angle of 88°, similar to this work. On the other hand the *ansa*-metallocene $[PhP(C_5Me_4)_2]Zr(Te_3)$ [84] exhibits a Te–Te–Te bond angle of 100°. This suggests that the Te_3^{2-} anion is able to bend itself to fit

Table 3.3: Overview of the tellurium bond lengths and angles in the crystal structure of $(Au_6Te_{18})[ZrCl_6]_3$. Because the cation has no crystallographic imposed symmetry, all Te–Te bonds are listed to show the high pseudo symmetry.

Atoms 1, 2	Distance / *Å*	Atoms 1, 2, 3	Angle / °
Te(1) — Te(2)	2.728(2)	Te(1) — Te(2) — Te(3)	83.93(6)
Te(2) — Te(3)	2.839(2)	Te(4) — Te(5) — Te(6)	85.20(6)
Te(4) — Te(5)	2.721(2)	Te(7) — Te(8) — Te(9)	84.11(6)
Te(5) — Te(6)	2.852(2)	Te(10) — Te(11) — Te(12)	85.72(6)
Te(7) — Te(8)	2.719(2)	Te(13) — Te(14) — Te(15)	85.59(6)
Te(8) — Te(9)	2.855(2)	Te(16) — Te(17) — Te(18)	83.38(6)
Te(10) — Te(11)	2.732(2)	Te(3) — Te(2) — Te(6)	79.63(6)
Te(11) — Te(12)	2.830(2)	Te(6) — Te(5) — Te(9)	77.50(5)
Te(13) — Te(14)	2.723(2)	Te(9) — Te(8) — Te(12)	76.79(5)
Te(14) — Te(15)	2.839(2)	Te(12) — Te(11) — Te(15)	78.77(6)
Te(16) — Te(17)	2.714(2)	Te(15) — Te(14) — Te(18)	78.42(5)
Te(17) — Te(18)	2.861(2)	Te(18) — Te(17) — Te(3)	77.48(5)
Te(2) — Te(6)	3.060(2)	Te(1) — Te(2) — Te(6)	80.31(5)
Te(5) — Te(9)	3.086(2)	Te(4) — Te(5) — Te(9)	82.04(5)
Te(8) — Te(12)	3.135(2)	Te(7) — Te(8) — Te(12)	80.85(5)
Te(11) — Te(15)	3.117(2)	Te(10) — Te(11) — Te(15)	80.43(6)
Te(14) — Te(18)	3.049(2)	Te(13) — Te(14) — Te(18)	81.68(5)
Te(17) — Te(3)	3.091(2)	Te(16) — Te(17) — Te(3)	81.15(5)

within the preferences of coordinated transition metal atoms, gold in this case. This fits within the behaviour of tellurium discussed for tellurium polyanions in Chapter 1. All Te–Te–Te bond angles are smaller than 90° (see Table 3.3) which shows again the distortion of the ideal cube geometry by the atoms on the cube corner positions.

As already mentioned, the counterion in this crystal structure is hexachlorozirconate(IV). The anion itself shows no deviation from its usual appearance (see Figure 3.5). The Zr–Cl bond lengths cover a range from 2.4 Å to 2.6 Å and there are three independent $[ZrCl_6]^{2-}$ moieties in the crystal structure.

The mutual coordination of cation and anion is best described by examining the Au··Cl distances. If only distances up to the sum of the respective van-der-Waals radii (3.41 Å) are considered, only the distance between atom pair Au(2) and Cl(1) (coordinated to Zr(1)) is short enough (3.10 Å, see Figure 3.6). If the investigated range is widened to 3.70 Å, the chlorine atoms Cl(8) and Cl(12) – both belong to the octahedron surrounding Zr(2) – have relevant distances to Au(1) and Au(6) respectively. This connectivity results in a chain running along the crystallographic *c* axis (see Figure 3.7). The cations located along

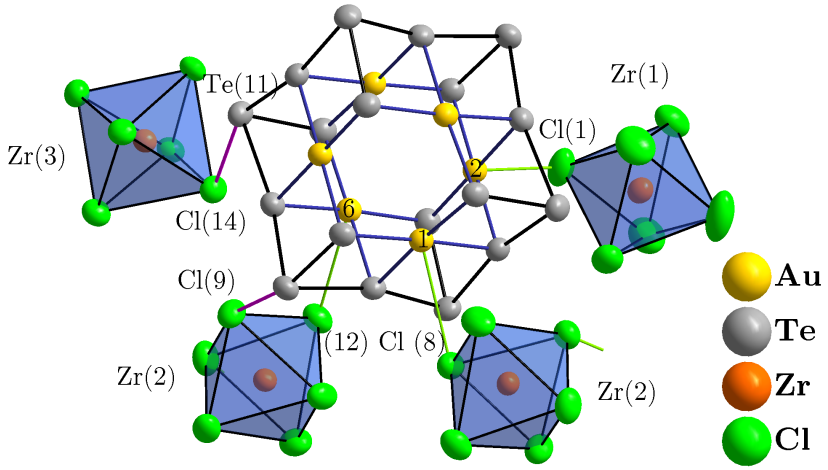

Figure 3.6: Detail of the crystal structure of $(Au_6Te_{18})[ZrCl_6]_3$. The green coloured bonds are the Cl··Au contacts, while the pink coloured once correspond to Cl··Te contacts. The displacement ellipsoids represent a probability of 90 %.

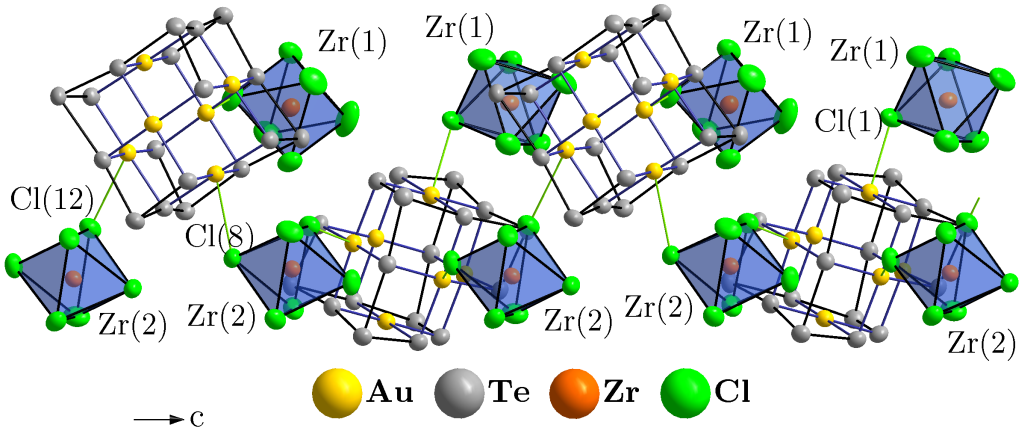

Figure 3.7: The $^1_\infty\left\{[(Au_6Te_{18})\,[ZrCl_6]_{1/1}\,[ZrCl_6]_{2/2}]^{2+}\right\}$ chain taken from the crystal structure of $(Au_6Te_{18})[ZrCl_6]_3$. The upper part of the figure contains only Zr(1) centred octahedra, while the lower part contains only Zr(2) centred octahedra. The displacement ellipsoids represent a probability of 90 %.

this chain are arranged in a zig-zag pattern, because the coordinating chlorine atoms of the $ZrCl_6$ octahedron are in *cis* configuration. This chain can be described by the Niggli formula $^1_\infty\left\{[(Au_6Te_{18})\,[ZrCl_6]_{1/1}\,[ZrCl_6]_{2/2}]^{2+}\right\}$. The remaining $ZrCl_6$ octahedron is located in the gaps inside the zig-zag chain with the shortest Au··Cl distance still being 4.51 Å. The shortest distance of a chlorine atom to a tellurium atom with only 3.37 Å on the other hand is present between Cl(14) and Te(11) (see Figure 3.6), which is well below the sum of the van-der-Waals radii (3.81 Å). While the positioning of the chlorine atoms straight above the gold atoms supported the purely ionic interpretation of the cation, this short contact between chlorine and tellurium shows once again, that the bonding situation is apparently more complicated. This is not only indicated by a single short Cl··Te contact, but by the numerous contacts in the range below the sum of the van-der-Waals radii. For a full distance histogram see Appendix A.3.

Since all molecular constituents by themselves may possess a centre of symmetry, the question arises why this compound crystallizes in an acentric space group. Almost all parts of the crystal structure have negligible deviations from an arrangement fitting the space group $C2/c$. Only the Zr(1) Cl_6 octahedron is arranged in a fashion which prohibits a two-fold axis along the crystallographic b axis to allow for a better crystal packing.

3.2.2 $(Au_6Te_{18})[AlX_4]_6$ with X = Cl, Br

Crystal Structure

The two compounds $(Au_6Te_{18})[AlCl_4]_6$ and $(Au_6Te_{18})[AlBr_4]_6$ are isotypic and crystallize in the orthorhombic space group *Pbca*. The crystals are of black-metallic appearance. They consist of the $(Au_6Te_{18})^{6+}$ cation and tetrahedral $[AlX_4]^-$ anions. The asymmetric unit of the unit cell contains half the sum formula: three independent $[AlX_4]^-$ anions and half of the centrosymmetric cation. Even though the cation possesses a higher site symmetry than the one found in the crystal structure of $(Au_6Te_{18})[ZrCl_6]_3$, the structure is basically unchanged since the cation displays a very high non-crystallographic local symmetry (see Figure 3.8). Within the $(Au_6Te_{18})^{6+}$ cation, it is again possible to identify three discrete $(Te_3)^{2-}$ anions, with three distinct distance ranges: a short Te–Te bond along the cube edge towards an unoccupied corner position, a longer Te–Te bond pointing to a neighboured $(Te_3)^{2-}$ anion and finally a long Te··Te contact between the tritellurium dianions (see Table 3.4).

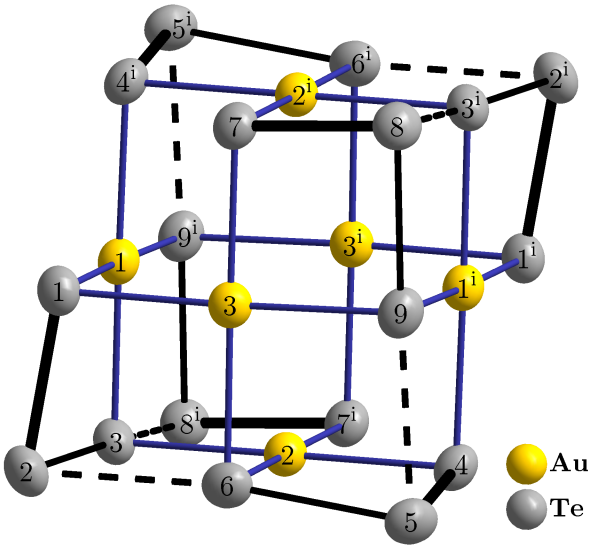

Figure 3.8: The $(Au_6Te_{18})^{6+}$ cation with distinct $(Te_3)^{2-}$ moieties exemplarily taken from the crystal structure of $(Au_6Te_{18})[AlCl_4]_6$. The element symbol has been omitted from the atom numbering to enhance readability. Short bonds are emphasized by thick lines. The displacement ellipsoids represent a probability of 90 %. The indices indicate the following symmetry operations: (i) $-x$, $-y$, $-z$.

The coordination of the cation by the tetrahaloaluminate anions can be described again by starting from the gold··halide interaction. All six gold atoms are coordinated by a chlorine or bromine atom respectively with a distance shorter than the sum of the respective van-der-Waals

Table 3.4: Overview of selected bond lengths in the crystal structure of $(Au_6Te_{18})[AlCl_4]_6$ and $(Au_6Te_{18})[AlBr_4]_6$.

$(Au_6Te_{18})[AlCl_4]_6$		$(Au_6Te_{18})[AlBr_4]_6$	
Atoms 1, 2	Distance / Å	Atoms 1, 2	Distance / Å
Te(1)—Te(2)	2.7319(6)	Te(1)—Te(2)	2.7416(6)
Te(2)—Te(3)	2.8666(6)	Te(2)—Te(3)	2.8407(6)
Te(2)—Te(6)	3.0939(6)	Te(2)—Te(6)	3.1482(6)
Au(2) ··· Cl(1)	3.152(2)	Au(2) — Br(1)	3.2155(8)
Au(1) ··· Cl(5)	3.225(2)	Au(1) — Br(5)	3.2318(8)
Au(3) ··· Cl(7)	3.273(2)	Au(3) — Br(7)	3.2113(8)

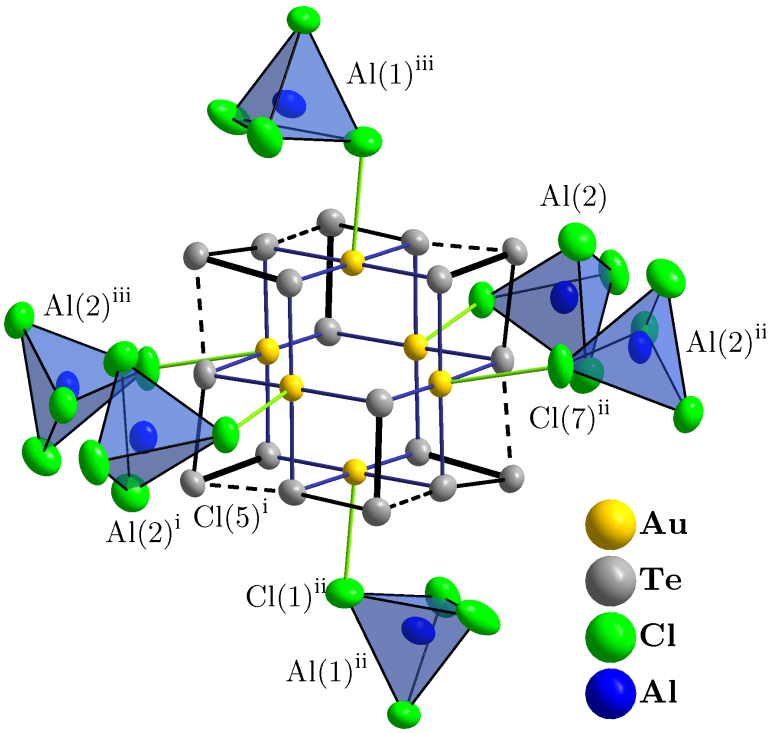

Figure 3.9: The $(Au_6Te_{18})^{6+}$ cation with its coordinating $[AlCl_4]^-$ anions exemplarily taken from the crystal structure of $(Au_6Te_{18})[AlCl_4]_6$. The displacement ellipsoids represent a probability of 90 %. The indices indicate the following symmetry operations: (i) $-x$, $-y$, $-z$; (ii) $-x$, $\frac{1}{2}+y$, $\frac{1}{2}-z$; (iii) x, $\frac{1}{2}-y$, $\frac{1}{2}+z$.

radii (see Table 3.4). Two of the six tetrahedra – the ones containing Al(1) – coordinate terminally to only one cation, while the other four tetrahedra – surrounding Al(2) – bridge two neighbouring cations. This connectivity results in layers perpendicular to the crystallographic a axis, which can be expressed by the Niggli formula ${}^2_\infty\left\{[(Au_6Te_{18})\,[AlX_4]_{2/1}\,[AlX_4]_{4/2}]^{2+}\right\}$ (see Figure 3.10). A small difference between the two isotypic compounds exists in the Au··X distances. The distance to the terminally coordinated $[AlCl_4]^-$ anions is slightly shorter than the distance to bridging anions. This separation is, however, not observed for $(Au_6Te_{18})[AlBr_4]_6$ (see Table 3.4). The last independent tetrahaloaluminate anion is located farther from the

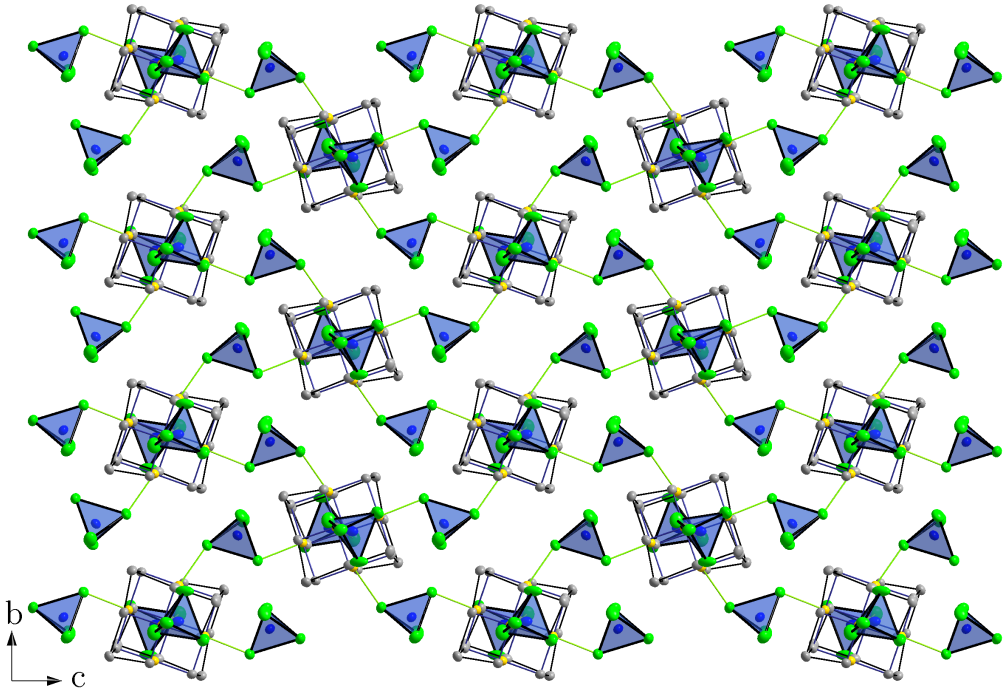

Figure 3.10: The ${}^{2}_{\infty}\left\{[(Au_6Te_{18})\,[AlX_4]_{2/1}\,[AlX_4]_{4/2}]^{2+}\right\}$ layer exemplarily taken from the crystal structure of $(Au_6Te_{18})[AlCl_4]_6$. The displacement ellipsoids represent a probability of 90 %.

gold atoms and has – similar to the crystal structure of $(Au_6Te_{18})[ZrCl_6]_3$ – short contacts to the tellurium atoms of the cation. For a full tellurium··halide distance histogram see Appendix A.3. These (pink coloured) tetrahedra interconnect the layers mentioned above (see Figure 3.11).

Theoretical Calculations

For the compound $(Au_6Te_{18})[AlCl_4]_6$ electronic structure calculations were performed. Figure 3.12 shows the projected density of states. It shows a fundamental band gap of about 1.95 eV above the fermi energy, therefore the compound is expected to exhibit semi-conducting behaviour and fits with the black-metallic appearance of the compound. The states below and above the band gap are mostly dominated by states derived from tellurium *p* orbitals with a small contribution to the states above the band gap from gold *d* assigned states. There seems to be no significant influence on the electronic states near the band gap by the anionic substructure.

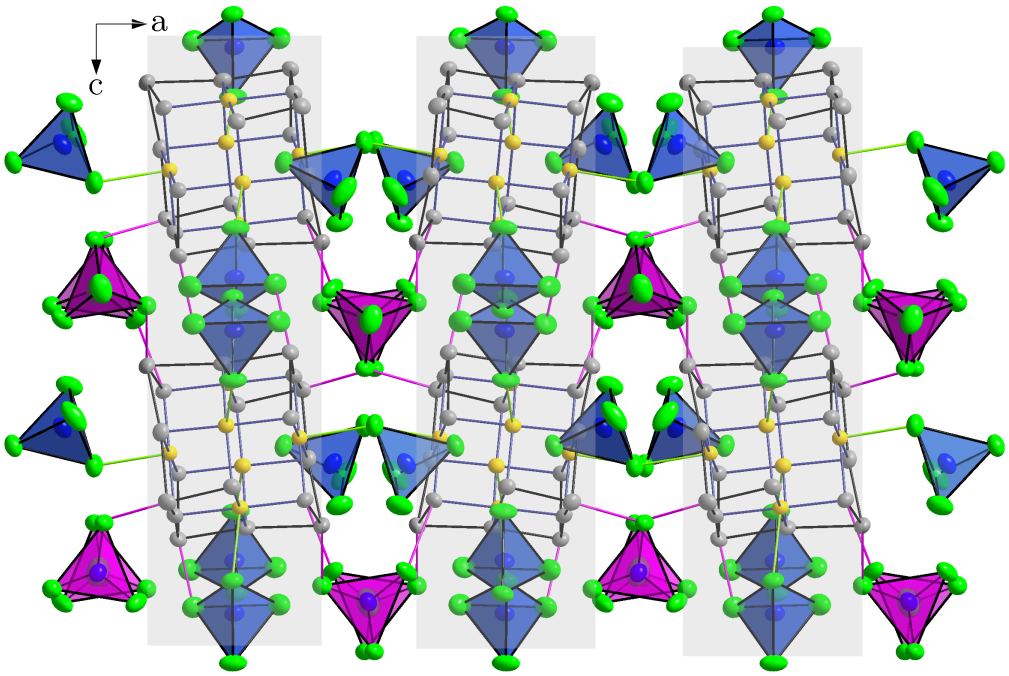

Figure 3.11: The connection between adjacent layers through the pink tetrahedra surrounding Al(3) exemplarily taken from the crystal structure of $(Au_6Te_{18})[AlCl_4]_6$. The viewing direction is along the layers (highlighted in grey) as seen in Figure 3.10. The displacement ellipsoids represent a probability of 90 %.

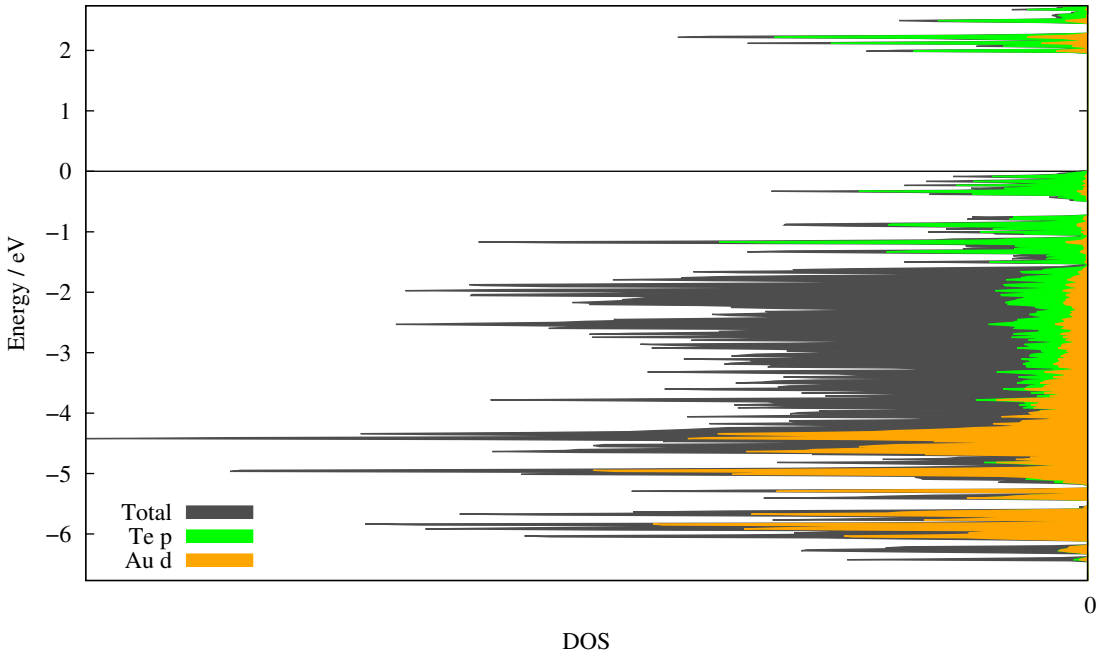

Figure 3.12: Projected density of states for $(Au_6Te_{18})[AlCl_4]_6$. The total DOS and the contributions corresponding to tellurium p and gold d orbitals are shown. The band gap is 1.95 eV wide. The energy axis is shifted relative to the fermi energy ($E_F = 0$).

3.3 Compounds Containing the $(Au_6Te_{18}X)^{5+}$ Cation

3.3.1 $(Au_6Te_{18}Cl)[MoOCl_4]_5$

Crystal Structure

The compound $(Au_6Te_{18}Cl)[MoOCl_4]_5$ crystallizes in the triclinic space group $P\bar{1}$ and is of black-metallic appearance. The compound consists of the $(Au_6Te_{18}Cl)^{5+}$ cation, one $[MoOCl_4]^-$ anion and two $[Mo_2O_2Cl_8]^{2-}$ anions. The asymmetric unit contains in principle the full sum formula, but there are two independent centrosymmetric $(Au_6Te_{18}Cl)^{5+}$ cations in the crystal structure, so only half of each cation belongs to the asymmetric unit. The difference between the two cations is for most parts negligible. Once again, both independent cations contain Te–Te bond lengths which make it possible to assign discrete $(Te_3)^{2-}$ fragments with a short and a long bond inside the $(Te_3)^{2-}$ anion (about 2.73 Å and 2.86 Å) and a long contact to the second tellurium atom of the next fragment (3.06 Å).

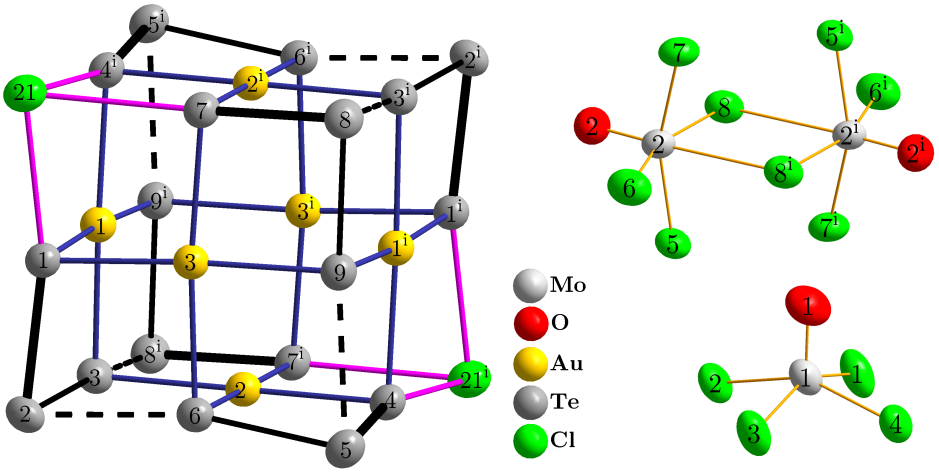

Figure 3.13: One of the two independent $(Au_6Te_{18}Cl_{2/2})^{5+}$ cations with distinct $(Te_3)^{2-}$ moieties *(left)* and the two different anions $[MoOCl_4]^-$ and $[Mo_2O_2Cl_8]^{2-}$ *(right)* taken from the crystal structure of $(Au_6Te_{18}Cl)[MoOCl_4]_5$. The element symbol has been omitted from the atom numbering to enhance readability. Short bonds are emphasized by thick lines. The displacement ellipsoids represent a probability of 90 %. The indices indicate the following symmetry operations: (i) $-x$, $-y$, $-z$.

The sum formula of the cation is better described as $(Au_6Te_{18}Cl_{2/2})^{5+}$, because both unoccupied corners of $(Au_6Te_{18})^{6+}$ are now occupied by a chlorine atom, which is shared with the next (but symmetrically equivalent) cation, thus forming a chain along the crystallographic a axis (Figure 3.14). The Te–Cl distances range from 2.99 Å to 3.15 Å and differ slightly between the two cations (see Table 3.5). The position of the chlorine atom with respect to only one cation is related to a section from the crystal structure of $TeCl_4$, wherein chlorine is also positioned on a cube corner with similar Te–Cl distances of 2.90 Å [85].

The Te–Cl–Te bond angles lie within the same range as Te–Te–Te bond angles centred on corner positions (see Table 3.5). In context of the chlorine atom's bridging role in this crystal structure, the anion Cl^- is coordinated by a distorted octahedron formed by six tellurium

Table 3.5: Overview of the Te–Cl bond lengths and angles in the crystal structure of $(Au_6Te_{18}Cl)[MoOCl_4]_5$. The upper half of the table corresponds to the first and the lower half to second symmetrically independent cation.

Atoms 1, 2	Distance / Å	Atoms 1, 2, 3	Angle / °
Te(1) — Cl(21)	2.9888(6)	Te(1) – Cl(21) – Te(4)	83.11(2)
Te(4) — Cl(21)	3.1199(7)	Te(1) – Cl(21) – Te(7)	81.78(2)
Te(7) — Cl(21)	3.1575(7)	Te(4) – Cl(21) – Te(7)	76.19(2)
Te(10) — Cl(22)	3.0799(7)	Te(10) – Cl(22) – Te(13)	81.93(2)
Te(13) — Cl(22)	3.0838(6)	Te(10) – Cl(22) – Te(16)	77.32(2)
Te(16) — Cl(22)	3.1297(7)	Te(13) – Cl(22) – Te(16)	79.53(2)

Table 3.6: Overview of the Au ·· Cl distances in the crystal structure of $(Au_6Te_{18}Cl)[MoOCl_4]_5$. The left half of the table corresponds to the first and the right half to second symmetrically independent cation.

Atoms 1, 2	Distance / Å	Atoms 1, 2	Distance / Å
Au(1) ··· Cl(1)	3.137(3)	Au(4) ··· Cl(3)	3.158(3)
Au(2) ··· Cl(8)	3.399(3)	Au(5) ··· Cl(18)	3.597(3)
Au(3) ··· Cl(14)	3.405(3)	Au(6) ··· Cl(12)	3.581(3)

atoms, which are negatively charged according to the interpretation as $(Te_3)^{2-}$ anions. This is again evidence that there are significant covalent interactions in contradiction to a purely ionic interpretation.

Additionally, there are Te··Te contacts between tellurium atoms on corner positions of adjacent cations, which are as short as 3.65 Å. Exploring these contacts builds up layers parallel to $(20\overline{3})$.

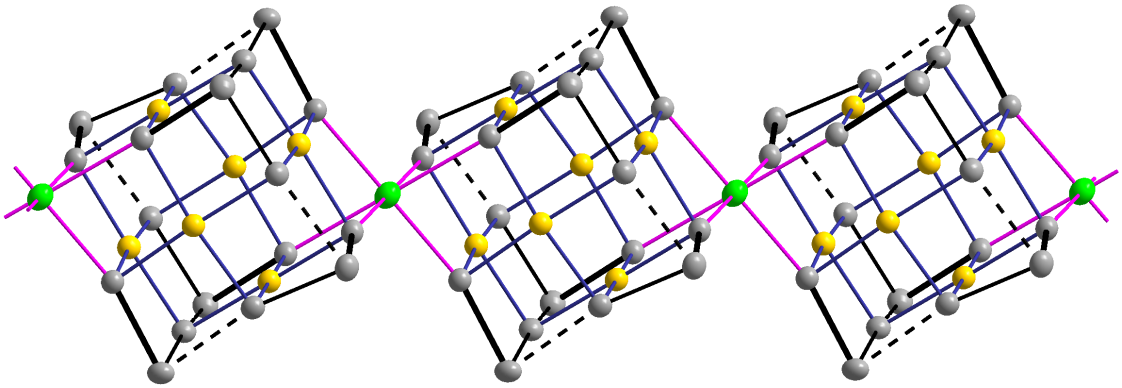

Figure 3.14: Cationic chain taken from the crystal structure of $(Au_6Te_{18}Cl)[MoOCl_4]_5$. The chain can be described by the Niggli formula $^1_\infty\{[(Au_6Te_{18})\,Cl_{2/2}]^{5+}\}$. The thicker bonds are shorter. The displacement ellipsoids represent a probability of 90 %.

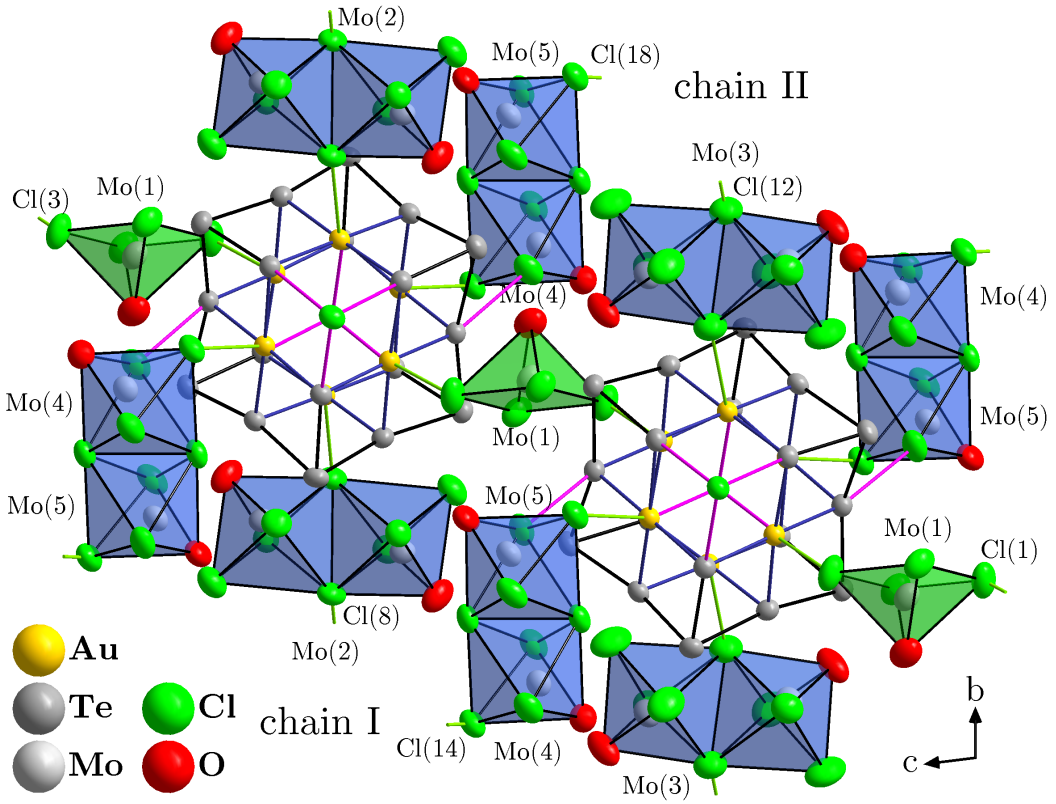

Figure 3.15: Structure detail taken from the crystal structure of $(Au_6Te_{18}Cl)[MoOCl_4]_5$. Chain I/II describe the two symmetrically independant chains formed by the cations and correspond to the chain depicted above/below. The atom numbering corresponds to both molybdenum atoms if not specified otherwise. Symmetrically equivalent chlorine atoms have only been labelled once. Green lines depict gold-chlorine contacts, pink lines depict tellurium-chlorine contacts or bonds. The displacement ellipsoids represent a probability of 90 %.

As mentioned earlier there are two different anions in the crystal structure. There is one square-pyramidal $[MoOCl_4]^-$ anion and two dinuclear $[Mo_2O_2Cl_8]^{2-}$ dianions. The dianion could be described as two edge-connected octahedra, but the bridging Mo–Cl bonds are asymmetric, which suggests the interpretation as two associated square-pyramidal moieties. The oxygen atom is always in the same plane as the bridging chlorine atoms, which again fits with the square-pyramidal description, where the oxygen is always the tip of the pyramid. The distance between the metal atoms in a double octahedron is about 4.20 Å showing the absence of a Mo–Mo bond.

The cationic chains are interconnected *via* the chlorine atoms of the anions. There are basically three different contacts. The chlorine atoms Cl(1) and Cl(3) – both part of the $[MoOCl_4]^-$ anion containing Mo(1) – have the shortest contacts to gold atoms of both independent cations, thus connecting the two symmetrically inequivalent chains (see Table 3.5 and Figure 3.15). Additionally, the chains are bridged by Cl(14) and Cl(18), belonging to the dianion containing the Mo(4) and Mo(5) atoms. The centrosymmetric dianions containing Mo(2) and Mo(3) bridge symmetrically equivalent chains *via* Cl(8) and Cl(12), respectively. This complex network is only achieved when distances up to 3.60 Å are considered, which is slightly longer than the sum of the respective van-der-Waals radii (see Table 3.6). There are also short

contacts between the chlorine atoms belonging to the molybdate anions and the tellurium atoms of the cation well below the sum of the van-der-Waals radii. The shortest contact is 3.18 Å, significantly shorter than the above discussed contacts between gold and chlorine, but the structure buildup is much better described through these longer contacts. A full distance histogram between Te and Cl atoms is available in the Appendix A.3.

Magnetic Measurements

The sum formula and the crystal structure of $(Au_6Te_{18}Cl)[MoOCl_4]_5$ suggest a paramagnetic behaviour originating from the magnetically isolated Mo^V ions with d^1 configuration. Therefore only a fifth of the molecular weight, i.e. $(Au_6Te_{18}Cl)_{0.2}[MoOCl_4]$, was used for the evaluation of the collected to data. Figure 3.16 shows the data after correction against the sample holder and diamagnetic increments [66]. Fitting according to the Curie-Weiss law gives a magnetic moment of 1.83 μ_B and a Weiss constant of -8 K. The Weiss constant points at an anti-ferromagnetic coupling between the molybdenum atoms inside a double octahedron at very low temperatures. The magnetic moment is slightly larger than expected from the magnetic moment calculated from the spin-only approximation (1.73 μ_B). The literature for a similar molybdenum compound reports a value slightly lower (1.64 μ_B [86]) than the approximation. However, comparisons to other Mo^V compounds might prove difficult, because of the unique coexistence of both isolated $[MoOCl_4]^-$ anions and dimerised $[Mo_2O_2Cl_8]^{2-}$ dianions, as found in this compound. Additionally, the exact value heavily depends on the applied diamagnetic correction, because of the large diamagnetic influence of the gold-tellurium cation. Finally, owed to the synthesis conditions, it can not be ruled out that the enhanced magnetic moment results from an impurity (i. e. $MoOCl_3$).

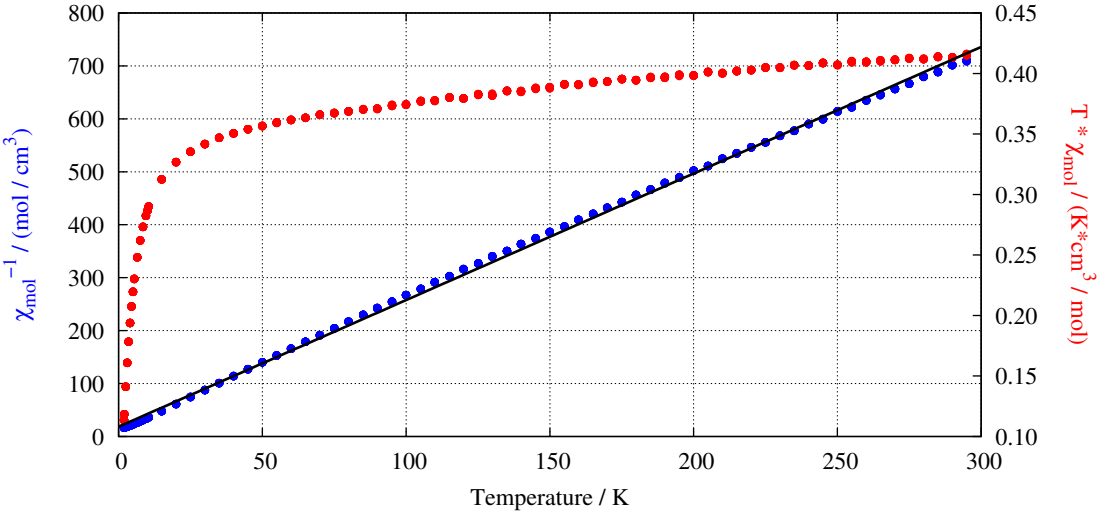

Figure 3.16: Plot of the temperature dependent reciprocal molar susceptibility (blue circles) and $T * \chi_{mol}$ (red circles) of $(Au_6Te_{18}Cl)_{0.2}[MoOCl_4]$. The black line shows the the linear regression according to the Curie-Weiss law, which gives a magnetic moment of 1.83 μ_B and a Weiss constant of -8 K.

3.3.2 $(Au_6Te_{18}X)[MCl_4]_5$ with X = Cl; M = Al, Ga or X = Br; M = Al

Crystal Structure

The compounds $(Au_6Te_{18}Cl)[AlCl_4]_5$, $(Au_6Te_{18}Cl)[GaCl_4]_5$ and $(Au_6Te_{18}Br)[AlCl_4]_5$ are all isotypic and crystallize in the monoclinic space group $P2_1/c$. The crystals are of black-metallic appearance. The compound consists of the $(Au_6Te_{18}X)^{5+}$ cation and five tetrachlorometallate anions. The asymmetric unit, however, contains five independent anions and two independent halves of the centrosymmetric cation.

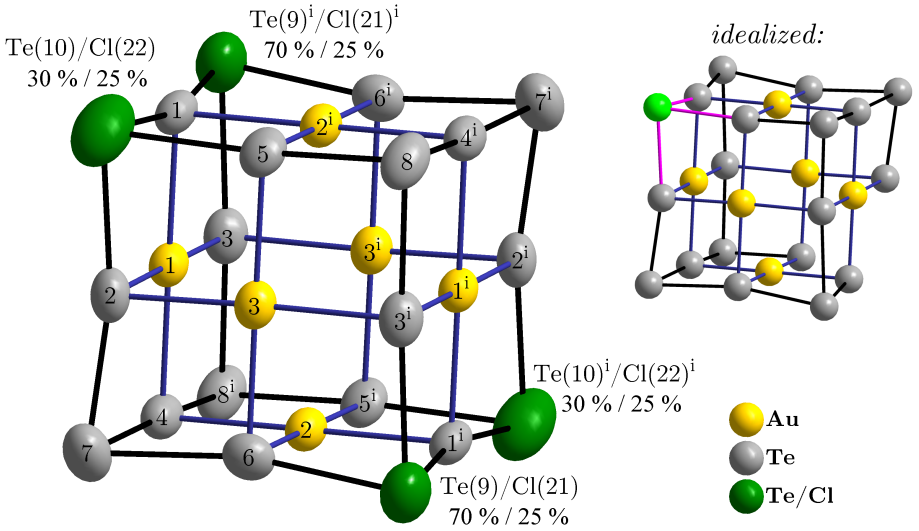

Figure 3.17: One of the two independent $(Au_6Te_{18}Cl)^{5+}$ cations exemplarily taken from the crystal structure of $(Au_6Te_{18}Cl)[AlCl_4]_5$. The element symbol has been omitted from the atom numbering to enhance readability. The displacement ellipsoids represent a probability of 90 %. The percentages correspond to the site occupancy factor. The indices indicate the following symmetry operations: (i) $-x, -y, -z$. The upper right corner shows an idealized, fully ordered cation.

In contrast to the crystal structures presented up until now, the cation in these crystal structures is disordered. Four of the eight cation corners are fully occupied by tellurium atoms, the remaining four corner positions are occupied in total by two tellurium and one halide atoms to fulfil the sum formula. Only two of these positions are symmetrically independent. All disordered corner positions are statistically occupied by either a fourth chlorine atom or by 70 % (or 30 %) tellurium. Overall both independent positions are only occupied to 95 % or 55 % (see Figure 3.17). The idealized $(Au_6Te_{18}X)^{5+}$ cation has only one unoccupied corner position and is therefore acentric. The "bulk" of the cation, however, is centrosymmetric and there seems to be too little interaction of the halide atom with its environment to significantly influence the energy for different orientations. So the crystal structure only shows the resulting disorder of the cation within the crystal packing.

Another consequence of the disorder is, that the formal $(Te_3)^{2-}$ anions cannot be found as building blocks of the cation by discriminating bond lengths any more. The bond lengths involving the tellurium atoms located on an edge to all corner positions varies between 2.73 Å and 3.05 Å (see Table 3.7). This is the same range that is observed for other fully ordered

Table 3.7: Overview of the Te–Te/X bond lengths and angles in the crystal structure of $(Au_6Te_{18}Cl)[AlCl_4]_5$ and $(Au_6Te_{18}Br)[AlCl_4]_5$. The largest deviation lies in the distance to Te(10)/X(22), which is plausible as this mixed site contains the most halide content compared to tellurium.

Atoms 1, 2	Distance / *Å*	
	$(Au_6Te_{18}Cl)[AlCl_4]_5$	$(Au_6Te_{18}Br)[AlCl_4]_5$
Te(2) — Te(7)	2.771(2)	2.780(2)
Te(4) — Te(7)	2.996(2)	2.982(2)
Te(6) — Te(7)	2.900(2)	2.919(2)
Te(3) — Te(8)	2.858(2)	2.859(2)
Te(4) — Te(8)	2.941(2)	2.949(2)
Te(5) — Te(8)	2.769(2)	2.775(2)
Te(1) — Te(9)	2.742(2)	2.738(2)
Te(3) — Te(9)	3.023(2)	3.048(2)
Te(6) — Te(9)	2.945(2)	2.944(2)
Te(1) — Te(10)	2.800(3)	2.934(2)
Te(2) — Te(10)	2.889(3)	2.991(2)
Te(5) — Te(10)	2.938(3)	3.049(2)

cations and also in accordance with the Te–X bond length found in the crystal structure of the corresponding tellurium(IV) halide [85]. Table 3.7 also displays the differences (or similarities) for the cations with either chlorine or bromine. The bonding distances are very similar. The largest deviation can be found in the distance from Te(1), Te(2) and Te(5) to Te(10)/X(22), which is expected, as this site contains the highest halide content in relation to tellurium. As can be seen in Figure 3.17, the displacement ellipsoids of the disordered positions are still very large. This is an artefact of the disorder, because the corner position of the tellurium or halide atom differs for every cation orientation and the single crystal structure only reflects the average electron density. A more elaborate disorder model with separate tellurium and halide atom positions might improve the large displacement ellipsoids but would not supply more reliable crystal chemical information, because of the limited resolution of the dataset.

The coordination between the cation and tetrachlorometallate anions is similar but not identical for each independent cation. The anions coordinate with their chlorine atoms to the gold atoms of the cations. If only distances up to the sum of the van-der-Waals radii are considered, only one of the two cations shows contacts to four tetrachlorometallate anions. If the search radius is enlarged up to 3.80 Å, the second cation is also coordinated by four terminal anions and the cations are bridged by an additional anion (containing M(3)). This builds up a chain, which contains the full sum formula and corresponds to the Niggli formula $^1_\infty\left\{(Au_6Te_{18}X)\,[MCl_4]_{4/1}\,[MCl_4]_{2/2}\right\}$ (see Figure 3.18). These chains run along the $(1\bar{1}0)$ direction. As usual for this class of compounds there are tellurium-chlorine contacts, which are

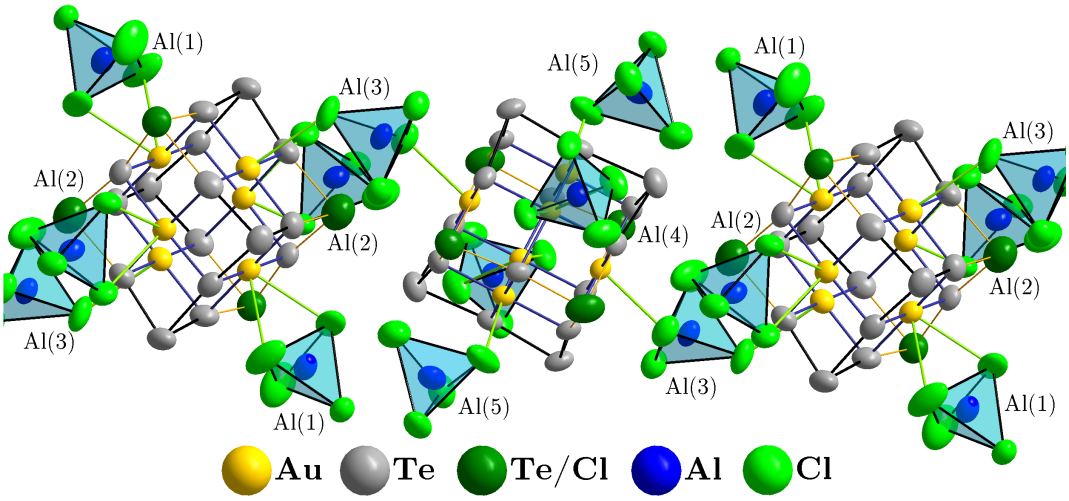

Figure 3.18: The $^{1}_{\infty}\left\{(Au_6Te_{18}X)\,[MCl_4]_{4/1}\,[MCl_4]_{2/2}\right\}$ chain exemplarily taken from the crystal structure of $(Au_6Te_{18}Cl)[AlCl_4]_5$. The anion disorder has been omitted for clarity. The displacement ellipsoids represent a probability of 90 %.

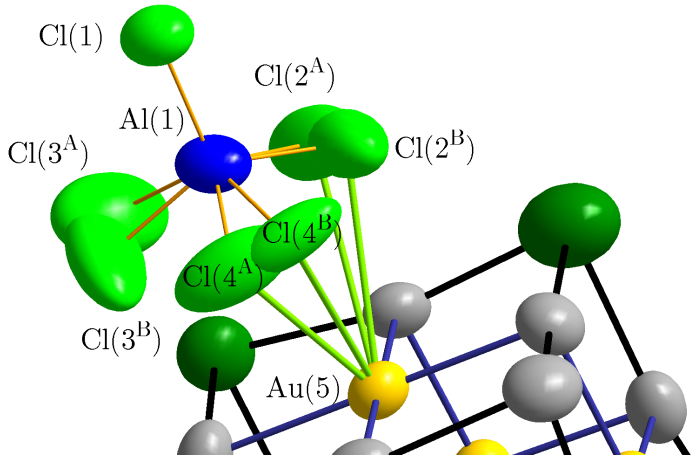

Figure 3.19: The disordered anion containing M(1) (here Al(1) taken from the crystal structure of $(Au_6Te_{18}Cl)[AlCl_4]_5$). The chlorine atoms Cl(2) and Cl(4) compete for a better interaction with Au(5) resulting in a slight disorder of three of the four chloride ligands. The displacement ellipsoids represent a probability of 90 %.

also below the sum of the van-der-Waals radii, starting from 3.32 Å, however these distances will not be discussed in detail. For the sake of completeness, Appendix A.3 holds halide tellurium distance histograms for all discussed compounds. The anionic substructure also shows a disorder. Three chlorine atoms bound to M(1) are slightly disordered since the chlorine atoms compete for a better coordination to the gold atom (see Figure 3.19).

Finally, there are some direct contacts among the cations themselves. The corner positions with the higher occupancy (Te(9) and Te(19)) are orientated towards each other with a distance of only 3.60 Å (or 3.70 Å for $(Au_6Te_{18}Br)[AlCl_4]_5$). This must be carefully evaluated because of the mixed occupancy. If the occupation on adjacent corners includes a halide atom, the distance is longer than the sum of the van-der-Waals radii. If both positions are occupied

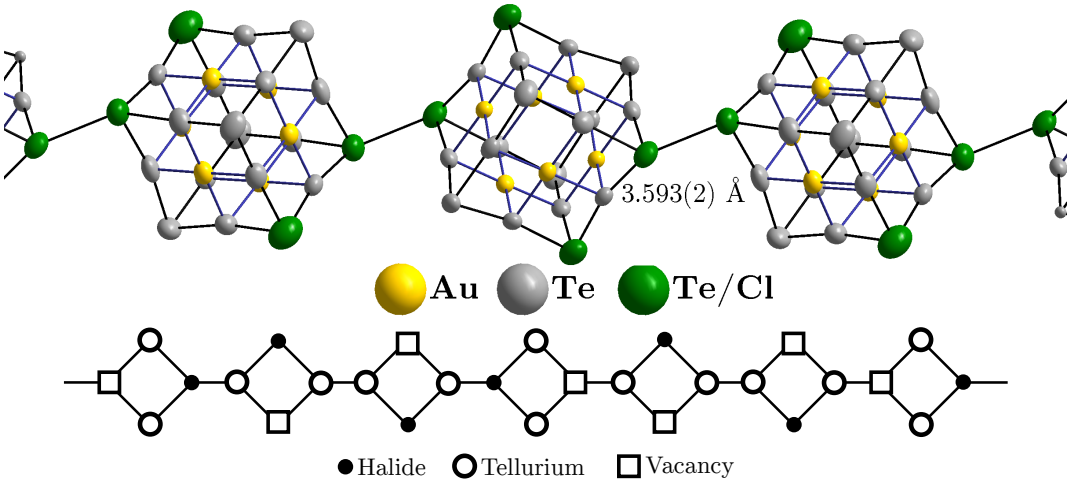

Figure 3.20: *Top:* The short contact between disordered atom sites exemplarily taken from the crystal structure of $(Au_6Te_{18}Cl)[AlCl_4]_5$. The displacement ellipsoids represent a probability of 90 %. *Bottom:* Schematic representation of a possible arrangement detail. The graphical representation of the cation is reduced to the four disordered corner positions.

by tellurium, however, the contact is shorter than the respective sum. Figure 3.20 shows the structure detail and a schematic of possible arrangements. The schematic representation reduces the cation to the four disordered corner positions, of which three are occupied in all cases. There are seven stylised cations with different orientations towards each other shown. However, this does not reflect a translation period, since the statistical distribution of the schematic differs slightly from the refined occupancies. Still, the conclusion from the schematic is that there must be situations, where both adjacent corners are occupied by a tellurium atom. So relatively short Te–Te contacts can be expected to exist within the crystal structure, just like in the fully ordered structure of $(Au_6Te_{18}Cl)[MoOCl_4]_5$.

Magnetic Measurements

A magnetic measurement was performed to verify the sum formula, which suggests a diamagnetic compound. Figure 3.21 shows the corrected data and confirms a relatively strong diamagnetic moment of roughly $\chi_{mol} = -1.376 \cdot 10^{-3} \frac{cm^3}{mol}$ (averaged from the data above 75 K). By subtracting diamagnetic increments [66] it is possible to calculate the diamagnetic influence of the $(Au_6Te_{18})^{6+}$ cation, the value of which is reused for the diamagnetic correction in other measurements performed in this work. It amounts to $\chi_{mol} = -8.198 \cdot 10^{-4} \frac{cm^3}{mol}$.

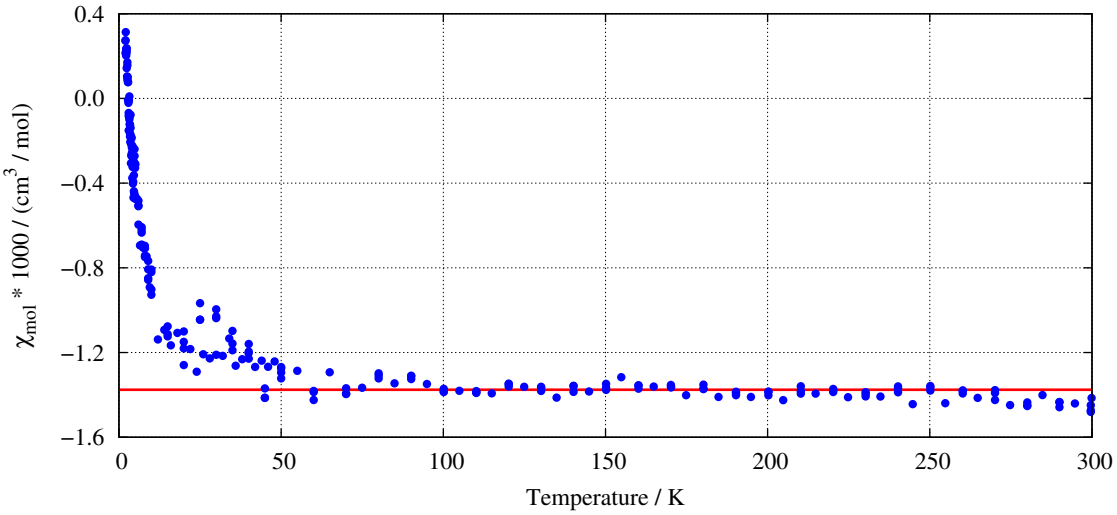

Figure 3.21: Plot of the temperature dependent molar susceptibility of $(Au_6Te_{18}Cl)[AlCl_4]_5$. Blue circles donate data points after correction against a blank sample. The red line is the extrapolated susceptibility of $\chi_{mol} = -1.376 \cdot 10^{-3} \frac{cm^3}{mol}$. The rising susceptibility for very low temperatures is attributed to paramagnetic impurities.

3.3.3 $(Au_6Te_{18}Br)[AlBr_4]_5$

Crystal Structure

The compound $(Au_6Te_{18}Br)[AlBr_4]_5$ crystallizes in the acentric space group $P31c$ and is of black-metallic appearance. Despite the analogous sum formula it is not isotypic to the compounds discussed in the previous section. The structure consists of the $(Au_6Te_{18}Br)^{5+}$ cation and five tetrahedral $[AlBr_4]^-$ anions. The cation has the point symmetry C_3, which is the closest to the idealized D_{3d} point symmetry for all observed cations until now. The cation is again heavily disordered (see Figure 3.22). The refinement suggests that only two of the eight corner positions are occupied exclusively be tellurium. The remaining six corners - generated from only two symmetrically independent sites - are statistically occupied by 4 tellurium and one bromine atom. No preference is recognizable from the refinement data. The high degree of disorder once again prevents the identification of $(Te_3)^{2-}$ fragments. The bond lengths from the tellurium atoms located on an edge to disordered corner positions spawns the expected range from 2.85 Å to 3.04 Å (see Table 3.8). This fits with the distances observed in other discussed compounds from this work and the Te–Br distance known from $TeBr_4$ (see Appendix A.1.15).

The reason for the polar space group is found within the anions. These are regular tetrabromoaluminate tetrahedra, which, of course, do not possess a centre of symmetry. Additionally, the anions are arranged in an acentric fashion, prohibiting any inversion centres.

The anion containing Al(2) (orange tetrahedra in Figure 3.23) has the shortest contacts to the cation's gold atoms. It is coordinated terminally with a bromine-gold distance of 3.75 Å, already beyond the sum of the van-der-Waals radii. Widening the examined distance to 3.85 Å connects

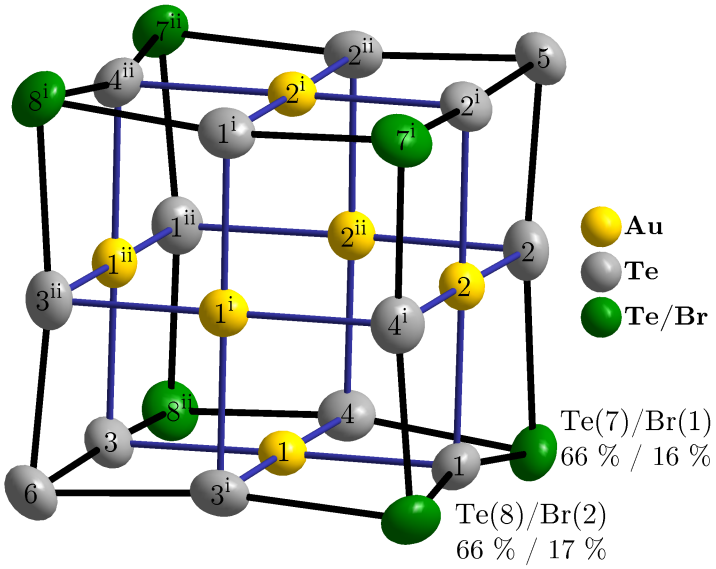

Figure 3.22: The disorded $(Au_6Te_{18}Br)^{5+}$ cation taken from the crystal structure of $(Au_6Te_{18}Br)[AlBr_4]_5$. The element symbol has been omitted from the atom numbering to enhance readability. The displacement ellipsoids represent a probability of 90 %. The percentages correspond to the site occupancy factor. The indices indicate the following symmetry operations: (i) $-y, x-y, z$; (ii) $y-x, -x, z$.

Table 3.8: Overview of the Te–Te bond lengths and Au ·· Br distances in the crystal structure of $(Au_6Te_{18}Br)[AlBr_4]_5$.

Atoms 1, 2	Distance / Å	Atoms 1, 2	Distance / Å
Te(1) — Te(7)	2.864(3)	Te(1) — Te(8)	2.873(3)
Te(2) — Te(7)	3.037(2)	Te(3) — Te(8)	3.025(3)
Te(4) — Te(7)	2.864(3)	Te(4) — Te(8)	2.872(3)
Te(2) — Te(5)	2.855(2)	Au(1) · · · Br(4)	3.847(3)
Te(3) — Te(6)	2.872(2)	Au(1) · · · Br(6)	3.998(3)
		Au(2) · · · Br(7)	3.745(3)
		Au(2) · · · Br(8)	3.883(3)

the cations via the Al(1) tetrahedron (blue) to a layer perpendicular to the c axis. One side of the layer accommodates the terminal anions, while the other side contains the bridging anions. This layer can be expressed as a Niggli formula: ${}^{2}_{\infty}\left\{[(Au_6Te_{18}Br)\,[AlBr_4]_{3/1}\,[AlBr_4]_{3/3}]^{+}\right\}$. The remaining anion (containing Al(3); green) is slightly farther away, with an Au··Br distance of 4.00 Å. This adds another anion shared by three cations to the aforementioned layer and expands the Niggli formula to reflect the full sum formula: ${}^{2}_{\infty}\left\{(Au_6Te_{18}Br)\,[AlBr_4]_{3/1}\,[AlBr_4]_{6/3}\right\}$ (see Figure 3.23).

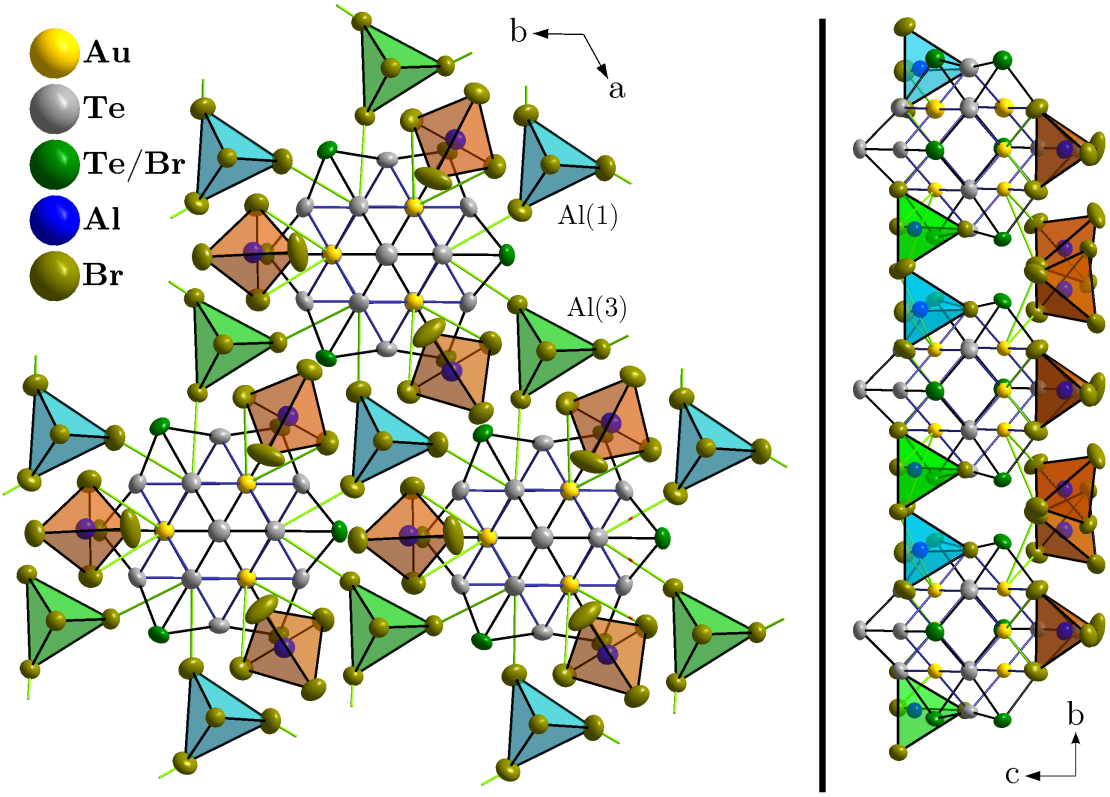

Figure 3.23: Structure detail taken from the crystal structure of $(Au_6Te_{18}Br)[AlBr_4]_5$. Terminally coordinated anions are depicted by orange tetrahedra, the bridging anions are depicted by blue and green tetrahedra, with the slightly tighter coordinated anions (containing Al(1)) coloured blue. The displacement ellipsoids represent a probability of 90 %. *Left:* The plane perpendicular to *c* formed by the cation anion interaction is shown. The plane can be expressed by the Niggli formula: ${}^{2}_{\infty}\left\{(Au_6Te_{18}Br)\,[AlBr_4]_{3/1}\,[AlBr_4]_{6/3}\right\}$. *Right:* View along the plane. The terminally coordinated anions are on the opposite face of the layer as the bridging anions.

Conductivity Measurements

Temperature dependent conductivity measurements of $(Au_6Te_{18}Br)[AlBr_4]_5$ were performed to investigate its properties. The compound shows typical semi-conducting behaviour with decreasing resistance at higher temperatures. Figure 3.24 shows an Arrhenius plot of a full heating-cooling-cycle with an offset voltage of 1 V. The activation energy for the charge transport is calculated from the slope of a linear regression for heating and cooling individually. The activation energy for the charge transport is averaged to roughly 830 meV. For low offset voltages no current can be measured. A reason for this could be a low carrier concentration at the fermi level. On the other hand, higher offset voltages initiate redox reactions.

Theoretical Calculations

Theoretical calculations were performed to investigate the elemental composition of the disorder. Early solutions of the single crystal x-ray diffraction data did not include bromine on the disordered sites, but an additional tellurium atom was assumed to yield the sum formula

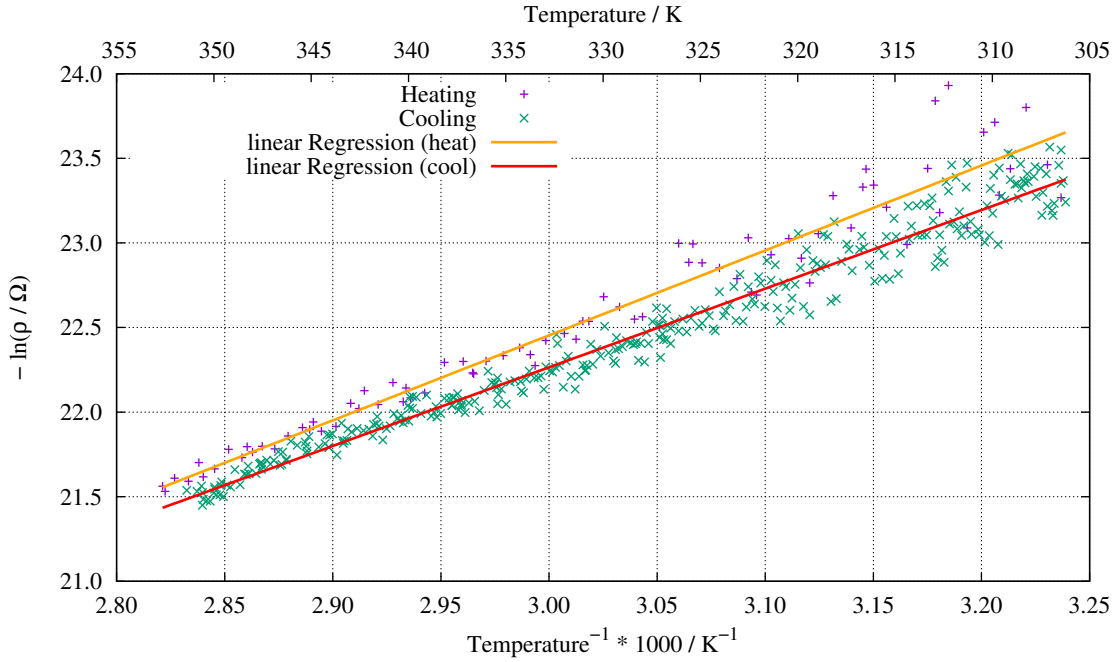

Figure 3.24: Arrhenius plot of the temperature dependent conductivity of $(Au_6Te_{18}Br)[AlBr_4]_5$. Data points from a full cycle of heating and cooling are shown. The slope of the linear regression for data points while cooling gives $E_A = 800$ meV and while heating gives $E_A = 860$ meV.

$(Au_6Te_{19})[AlBr_4]_5$. Since the crystal structure is disordered, it is necessary to resolve this disorder.

If only one cation is considered, the disorder can be described by nine different order variants. Six of these variants retain monoclinic Cc symmetry (this is a *translationengleich* subgroup of index 3 of $P31c$), the other three variants lose all symmetry operators, and only translation symmetry is left ($P1$). This still does not cover different orientations of adjacent cations. To account for this, a supercell would be necessary, which is impractical since the starting cell is already very large for the used computational method. This symmetry reduction is valid for both discussed sum formulas as for both models the atom opposite to the unoccupied corner must be either a tellurium atom or a bromine atom.

Since the initial structure model is disordered, relaxation of all structural parameters is essential, but very time consuming because of the already mentioned unit cell's size. Only one calculation of the Cc variants converged for each model. Figure 3.25 shows their density of states (DOS). Even though this is only a partial result, the difference is quite striking. For the assumed composition $(Au_6Te_{19})[AlBr_4]_5$ there are empty states above the fermi energy (red coloured DOS in Figure 3.25), which should result in metallic conductivity. The compound $(Au_6Te_{18}Br)[AlBr_4]_5$ with a bromine atom instead of a tellurium atom (green coloured DOS in Figure 3.25) on the other hand, exhibits a band gap of roughly 1 eV above the fermi energy, which indicates a semi-conductor.

As discussed in the previous paragraph, the experimental result of the temperature-dependent conductivity measurement proves the compound to be a semi-conductor. The determined

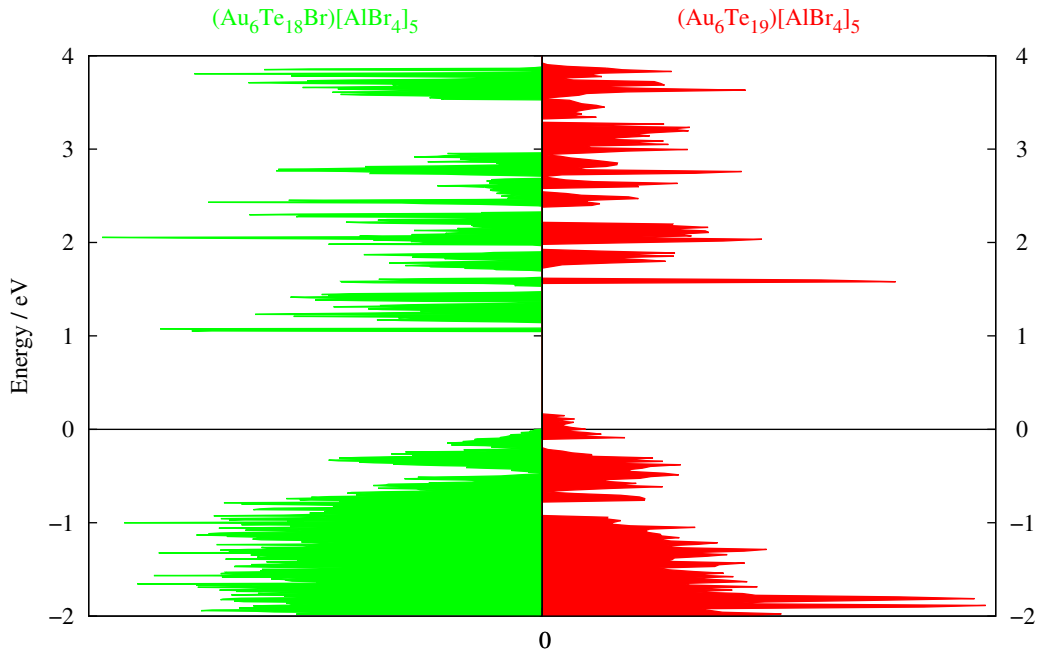

Figure 3.25: Comparison of the calculated density of states of both discussed structure models. The left half shows the DOS for the correct composition of $(Au_6Te_{18}Br)[AlBr_4]_5$, while the right half shows the DOS of the alternate structure model with an assumed composition of $(Au_6Te_{19})[AlBr_4]_5$. The first compound should be a semi-conductor with a fundamental band gap of roughly 1 eV. The second compound is expected to be a metallic conductor.

activation energy for the charge transport is slightly lower than the calculated fundamental band gap. The theoretical value is expected to be overestimated, because the calculation only applies to the ground state and does not consider the excited state of the charge transport. Even though this calculation is only a partial result, it provides a mutual confirmation between experimental and theoretical results for $(Au_6Te_{18}Br)[AlBr_4]_5$ and against $(Au_6Te_{19})[AlBr_4]_5$ as the correct composition for this compound.

3.4 Compounds Containing the $(Au_6Te_{18}Cl_2)^{4+}$ Cation

3.4.1 $(Au_6Te_{18}Cl_2)[Mo_2O_2Cl_8]_2$

Crystal Structure

The compound $(Au_6Te_{18}Cl_2)[Mo_2O_2Cl_8]_2$ crystallizes in the monoclinic space group $P2_1/n$ and is of black-metallic appearance. This is the only compound from this structure family to yield crystals with distinctive faces on applying the described synthesis protocol (see Figure 3.26). The compound consists of the $(Au_6Te_{18}Cl_2)^{4+}$ cation and two $[Mo_2O_2Cl_8]^{2-}$ anions. The asymmetric unit contains half of the centrosymmetric cation and one complex anion. Even though the cation shows no disorder, no discrete $(Te_3)^{2-}$ moieties can be identified by discriminating Te–Te bond lengths within the cation (see Figure 3.27).

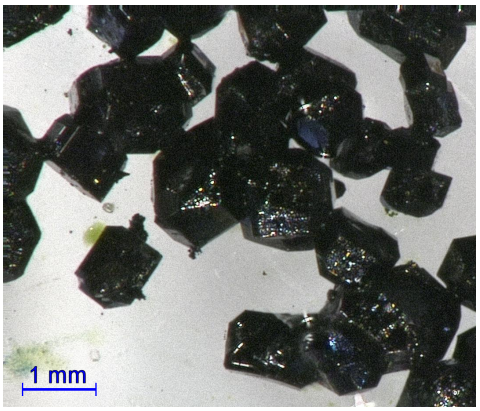

Figure 3.26: Microscopic image of crystals of $(Au_6Te_{18}Cl_2)[Mo_2O_2Cl_8]_2$. The scale is displayed in the lower left corner.

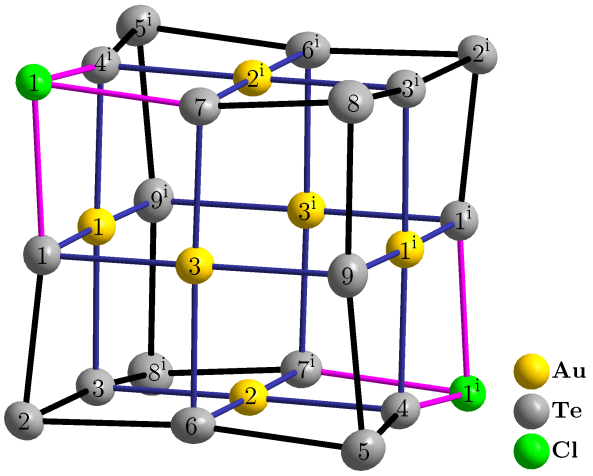

Figure 3.27: The $(Au_6Te_{18}Cl_2)^{4+}$ cation taken from the crystal structure of $(Au_6Te_{18}Cl_2)[Mo_2O_2Cl_8]_2$. The element symbol has been omitted from the atom numbering to enhance readability. The displacement ellipsoids represent a probability of 90 %. The indices indicate the following symmetry operations: (i) $-x$, $-y$, $-z$.

The range of the Te–Te bond lengths, however, is the same as observed for the other discussed compounds (see Table 3.9). This suggests that the individual character of the tritellurium fragments is even less pronounced in comparison to the other discussed cations. This seems plausible, since – in the purely ionic model – there would be a very unfavourable coulomb interaction, because the negative chlorine atoms are right next to three tellurium atoms (Te(1), Te(4) and Te(7)), which each carry a negative charge of a Te_3^{2-} fragment. The Te–Cl bond lengths are roughly 2.90 Å, which fits the Te–Cl bond lengths known for $TeCl_4$ [85], wherein chlorine is positioned on a corner position as well.

Table 3.9: Overview of the Te–Te/Cl bond lengths and Au ·· Cl distances in the crystal structure of $(Au_6Te_{18}Cl_2)[Mo_2O_2Cl_8]_2$.

Atoms 1, 2	Distance / *Å*	Atoms 1, 2	Distance / *Å*
Te(1) — Te(2)	2.7792(8)	Te(3) — Te(8)	2.9487(9)
Te(2) — Te(3)	2.9382(9)	Te(5) — Te(9)	2.9179(8)
Te(4) — Te(5)	2.7633(9)	Te(1) — Cl(1)	2.925(2)
Te(5) — Te(6)	3.0418(8)	Te(4) — Cl(1)	2.902(2)
Te(7) — Te(8)	2.7659(8)	Te(7) — Cl(1)	2.893(2)
Te(8) — Te(9)	2.9783(8)	Au(1) ··· Cl(6)	3.291(2)
Te(2) — Te(6)	2.9035(8)	Au(2) ··· Cl(2)	3.004(2)

The counterion in this compound is an edge connected double octahedron of $[Mo_2O_2Cl_8]^{2-}$. As in the structure of $(Au_6Te_{18}Cl)[MoOCl_4]_5$, the oxygen atoms are in the same plane as the connecting edge and the metal atoms are displaced away from each other resulting in a Mo–Mo distance of 4.08 Å. The chlorine atom Cl(2) has a short contact to Au(2) with only 3.00 Å, and the distance between Cl(6) and Au(1) is only 3.29 Å (see Table 3.9). This mutual coordination links the cations and anions to chains running along the *a* axis, which can be described by the Niggli formula $^1_\infty\left\{(Au_6Te_{18}Cl_2)\,[Mo_2O_2Cl_8]_{4/2}\right\}$ (see Figure 3.28). As observed for other compounds within this work, there are contacts below the sum of the van-der-Waals radii between tellurium atoms and chlorine atoms belonging to the anion. The shortest of these contacts is between Te(2) and Cl(4) with 3.32 Å, but does not add further linking among the already described chains.

Magnetic Measurements

The sum formula and the crystal structure of the compound of $(Au_6Te_{18}Cl_2)[Mo_2O_2Cl_8]_2$ suggest a paramagnetic behaviour originating from the magnetically isolated Mo^V ions with d^1 configuration. Therefore only a fourth of the molecular weight, i.e. $(Au_6Te_{18}Cl_2)_{0.25}[MoOCl_4]$, was used for the evaluation of the collected to data. Figure 3.29 shows the collected data after correction against the sample holder and diamagnetic increments [66]. Fitting according to the Curie-Weiss law gives a magnetic moment of 1.67 μ_B and a Weiss constant of -4 K. This is in accordance with the expected magnetic moment calculated from the spin-only

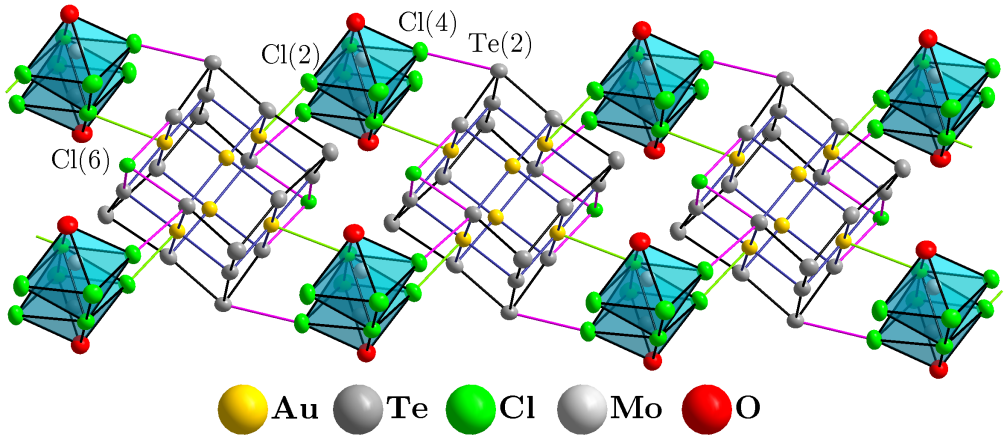

Figure 3.28: The $^{1}_{\infty}\left\{(Au_6Te_{18}Cl_2)\,[Mo_2O_2Cl_8]_{4/2}\right\}$ chain taken from the crystal structure of $(Au_6Te_{18}Cl_2)[Mo_2O_2Cl_8]_2$. The chain runs along the a axis. Gold tellurium contacts are depicted as green lines, chlorine tellurium contacts as pink coloured lines. The displacement ellipsoids represent a probability of 90 %.

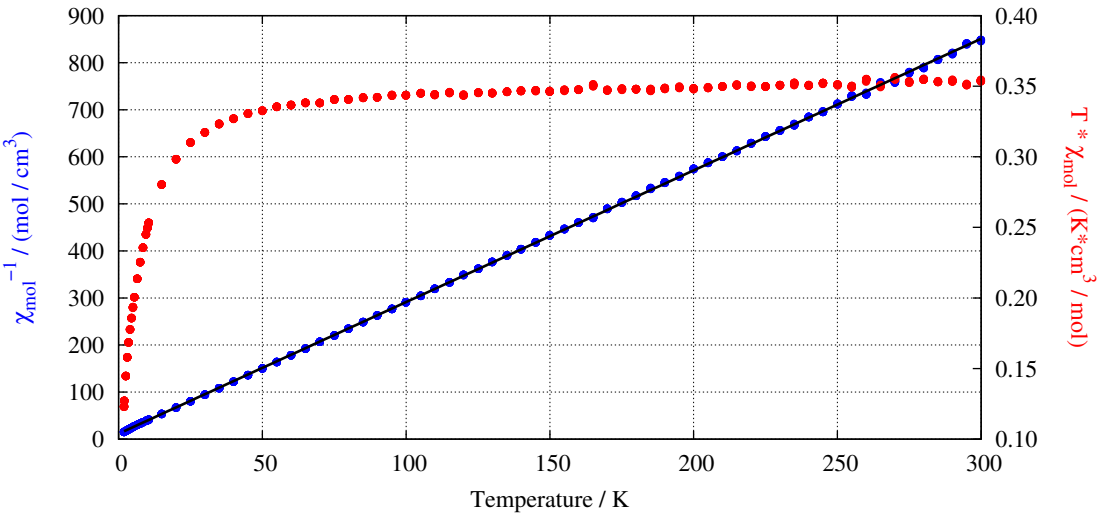

Figure 3.29: Plot of the temperature dependent reciprocal molar susceptibility (blue circles) and $T * \chi_{mol}$ (red circles) of $(Au_6Te_{18}Cl_2)_{0.25}[MoOCl_4]$. The black line shows the linear regression according to the Curie-Weiss law, which gives a magnetic moment of 1.67 μ_B and a Weiss constant of -4 K.

approximation (1.73 μ_B) and the literature [86] - opposed to the slightly higher value found for $(Au_6Te_{18}Cl)[MoOCl_4]_5$. The Weiss constant points at a weak anti-ferromagnetic coupling between the molybdenum atoms inside a double octahedron at very low temperatures.

Conductivity Measurements

Temperature dependent conductivity measurements were performed using an offset voltage of 0.1 V. The compound shows typical semi-conducting behaviour with decreasing resistance at higher temperatures. Figure 3.30 shows an Arrhenius plot of a full heating-cooling-cycle. The activation energy for the charge transport is calculated from the slope of a linear regression for heating and cooling individually, but gives the same activation energy of 780 meV for both.

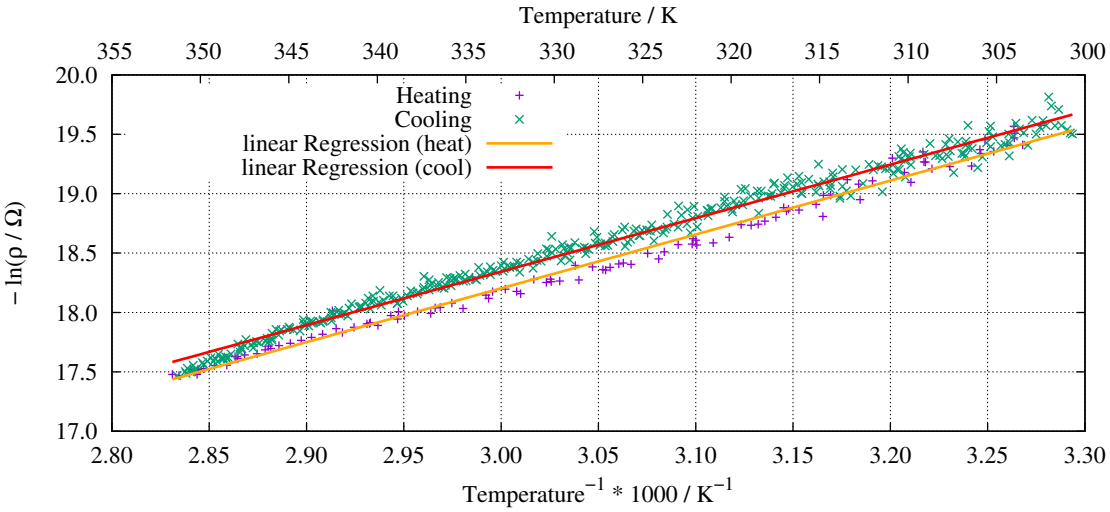

Figure 3.30: Arrhenius plot of the temperature dependent conductivity of $(Au_6Te_{18}Cl_2)[Mo_2O_2Cl_8]_2$. Data points from a full cycle of heating and cooling are shown. The slope of the linear regression for data points while cooling and heating gives $E_A = 780$ meV.

Theoretical Calculations

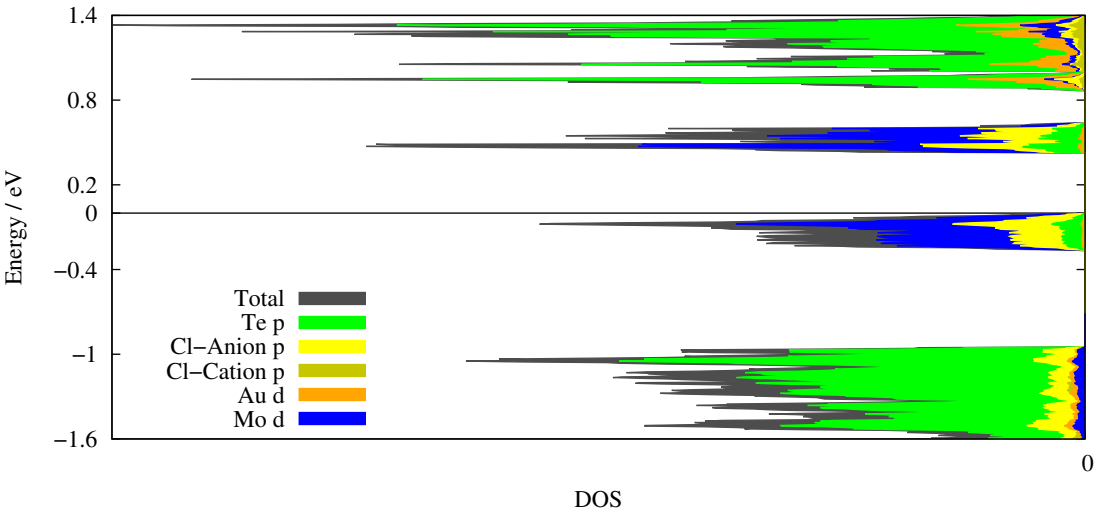

Figure 3.31: Projected density of states for $(Au_6Te_{18}Cl_2)[Mo_2O_2Cl_8]_2$. The total DOS and the contributions corresponding to certain orbitals of gold, tellurium, molybdenum and chlorine are shown. The band gap is 430 meV wide. The energy axis is shifted relative to the fermi energy ($E_F = 0$).

Electronic structure calculations for $(Au_6Te_{18}Cl_2)[Mo_2O_2Cl_8]_2$ were performed. Figure 3.31 shows the projected density of states, only orbitals with significant contributions are included. The contributions of the chlorine p orbitals are split for the atoms belonging to the cationic and the anionic part of the structure. According to the theoretical results, the compound is a semi-conductor with a band gap of about 430 meV. This value is lower than the experimentally determined activation energy of the charge transport (780 meV). Since the theoretical value is expected to be overestimated, this discrepancy may be explained by grain boundaries and other real effects. Additionally to the band gap, there is a core gap from -950 meV to -250 meV.

The electronic states above and below the fermi energy are mostly dominated by contributions from the anionic part of the structure in contrast to the PDOS of $(Au_6Te_{18})[AlCl_4]_6$, where these states are dominated by the cationic substructure (see Figure 3.12). If the states below and above the band gap are omitted for the moment a similar situation as observed for $(Au_6Te_{18})[AlCl_4]_6$ is found: Mostly Te p dominated states below and above a roughly 1.8 eV wide gap are found. This allows the conclusion that the mutual electronic influence between the anionic and the cationic substructures are small and that the electronic structure of the cation in $(Au_6Te_{18})[AlCl_4]_6$ and in $(Au_6Te_{18}Cl_2)[Mo_2O_2Cl_8]_2$ are very similar.

3.4.2 $(Au_6Te_{18}Cl_2)[Bi_4Cl_{16}]$

The compound $(Au_6Te_{18}Cl_2)[Bi_4Cl_{16}]$ crystallizes in the monoclinic space group $P2_1/c$ and is of black-metallic appearance. The crystal structure consists of the $(Au_6Te_{18}Cl_2)^{4+}$ cation the complex $[Bi_4Cl_{16}]^{4-}$ anion. The asymmetric unit contains in principle the full sum formula, but there are two symmetrically independent cations and anions each, so only half of each belongs to the asymmetric unit. Consequently, the cation and the anion are both centrosymmetric.

Six out of the eight corner positions in the two symmetrically independent cations are disordered. These three independent positions are occupied by either tellurium or chlorine (see Figure 3.32). The occupancy factors in the first cation are not much different from a pure statistical distribution, while the second cation clearly disfavours one position for chlorine (see Table 3.10). The reason for this unequal distribution is not apparent from the crystal structure and therefore might be an artefact of the dataset refinement. As expected, no tritellurium fragments are discernible from the Te–Te bond lengths distribution. This might originate from both, the disorder as in the crystal structures of $(Au_6Te_{18}X)[MCl_4]_5$ and from the two coordinated chlorine atoms as observed for $(Au_6Te_{18}Cl_2)[Mo_2O_2Cl_8]_2$. In any case, the range of the Te–Te/Cl bond lengths is the same as observed for the other discussed compounds (2.86 Å to 3.00 Å, see Table 3.11) and thus fits also with the Te–Cl distance for the chlorine atom on the corner position in tellurium(IV) chloride [85].

The counterion in this compound is the complex anion $[Bi_4Cl_{16}]^{4-}$. Basically it consists of four edge-connected octahedra (see Figure 3.33). The octahedra containing Bi(2) share an edge with all three remaining octahedra, while the other octahedra containing Bi(1) only share an edge with two of the former octahedra. Halobismuthate anions are very diverse in their

Table 3.10: The distribution of the mixed occupancy sites from the cations in $(Au_6Te_{18}Cl_2)[Bi_4Cl_{16}]$.

Cation I		Cation II	
Atoms 1/2 on site	Occupancy factor	Atoms 1/2 on site	Occupancy factor
Te(8) / Cl(17)	0.781 / 0.219	Te(18) / Cl(20)	0.749 / 0.251
Te(9) / Cl(18)	0.662 / 0.338	Te(19) / Cl(21)	0.955 / 0.045
Te(10) / Cl(19)	0.557 / 0.442	Te(20) / Cl(22)	0.296 / 0.704

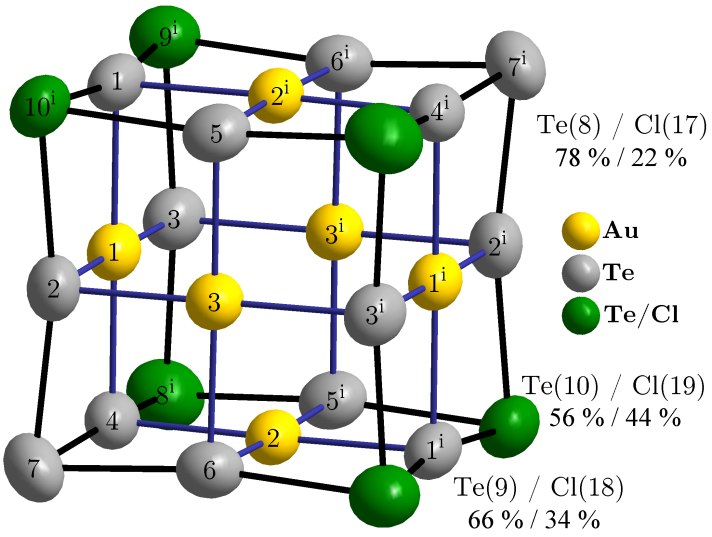

Figure 3.32: One of the two symmetrically independent disordered $(Au_6Te_{18}Cl_2)^{4+}$ cations taken from the crystal structure of $(Au_6Te_{18}Cl_2)[Bi_4Cl_{16}]$. The element symbol has been omitted from the atom numbering to enhance readability. The displacement ellipsoids represent a probability of 90 %. The percentages correspond to the site occupancy factor. The indices indicate the following symmetry operations: (i) $-x$, $-y$, $-z$.

Table 3.11: Overview of the Te–Te/Cl bond lengths and Au ·· Cl distances in the crystal structure of $(Au_6Te_{18}Cl_2)[Bi_4Cl_{16}]$.

Atoms 1, 2	Distance / Å	Atoms 1, 2	Distance / Å
Te(2) — Te(7)	2.868(2)	Te(6) — Te(9)	2.996(2)
Te(4) — Te(7)	2.902(2)	Te(1) — Te(10)	2.941(2)
Te(6) — Te(7)	2.871(2)	Te(2) — Te(10)	2.955(2)
Te(3) — Te(8)	2.893(2)	Te(5) — Te(10)	2.887(2)
Te(4) — Te(8)	2.933(2)	Au(2) ··· Cl(12)	3.275(5)
Te(5) — Te(8)	2.878(2)	Au(1) ··· Cl(1)	3.340(5)
Te(1) — Te(9)	2.874(2)	Au(6) ··· Cl(4)	3.353(5)
Te(3) — Te(9)	2.861(2)	Au(4) ··· Cl(3)	3.433(5)

connectivity. The usual explanation is that the cation influences the formation of the complex halobismuthate. This fits quite nicely in this case, since the faces of both, the cation and the anion, are roughly the same size. Beck *et. al* reported on the compound $(Te_4)(Te_{10})[Bi_4Cl_{16}]$, which contains a halobismuthate anion with the same sum formula, but the anion is not a discrete entity, but a polymeric chain [39]. The particular halobismuthate anion from this work has, so far, only been reported in few crystal structures, which all contain either organic cations or at least organic ligands (see [87–90]). The Bi–Cl bond distances vary between 2.46 Å and 3.07 Å, which is in the range usually reported for chlorobismuthate anions.

As already mentioned, the larger face of the anion is roughly the same size as a face of the cation, which allows to derive the mutual coordination between the cations and anions from

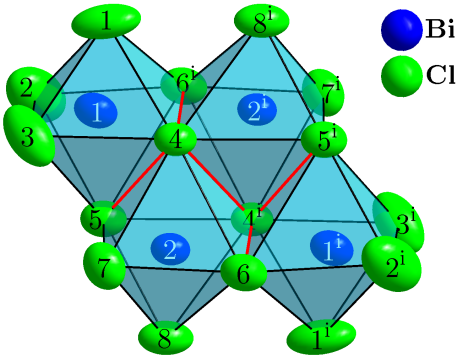

Figure 3.33: The complex anion $[Bi_4Cl_{16}]^{4-}$ taken from the crystal structure of $(Au_6Te_{18}Cl_2)[Bi_4Cl_{16}]$. Shared octahedron edges are highlighted in red. The displacement ellipsoids represent a probability of 90 %. The indices indicate the following symmetry operations: (i) $-x$, $-y$, $-z$.

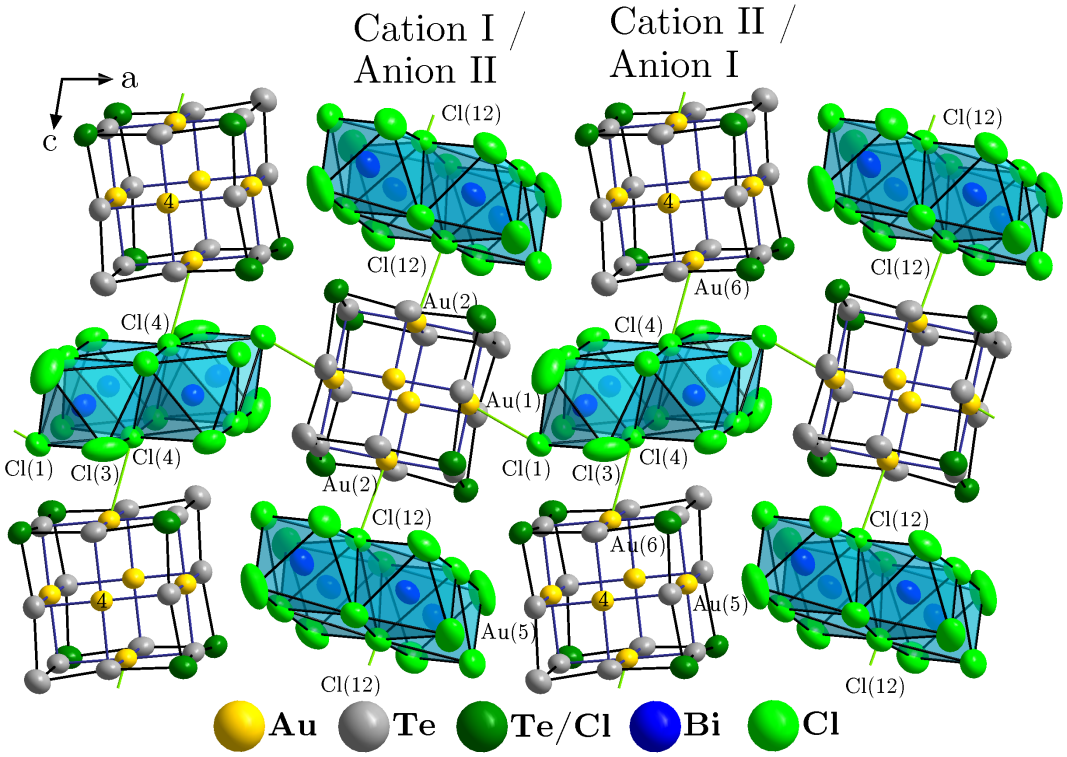

Figure 3.34: Layer taken from the crystal structure of $(Au_6Te_{18}Cl_2)[Bi_4Cl_{16}]$. The layer is perpendicular to the b axis. The green lines depict gold chlorine contacts. As can be seen, one anion has contacts to four cations, while the other anion is only connected to two cations. The displacement ellipsoids represent a probability of 90 %.

the rock salt structure type: all cations are surrounded by six anions and *vice versa*. However, the distances between cations and anions are not all equal. If only distances up to the sum of the respective van-der-Waals radii are considered, a plane tiled with both symmetrically independent cations and anions is constructed (see Figure 3.34). The atoms Au(1) and Au(2) from the first cation and Au(6) from the second cation have contacts between 3.27 Å and 3.36 Å to adjacent chlorine atoms (see Table 3.11). The shortest Au··Cl contact for Au(5) is much longer (3.81 Å), which results in a slightly wider cation-anion coordination for the second cation. Adjacent layers are symmetrically equivalent and are translated by half of the c

axis (as generated by the space group's *c* glide-plane). The shortest contact between layers is between Au(4), belonging to the second cation, and Cl(3) from the first anion (and *vice versa*). The Au(4)··Cl(3) distance, however, is slightly longer than the sum of the van-der-Waals radii (see Table 3.11).

3.4.3 $(Au_6Te_{18}Cl_2)[MCl_6]_4$ with M = Nb, Ta

Both isotypic compounds $(Au_6Te_{18}Cl_2)[NbCl_6]_4$ and $(Au_6Te_{18}Cl_2)[TaCl_6]_4$ are of black-metallic appearance. It was not possible to collect a reliable x-ray diffraction data set of neither of the two compounds. The data sets could be indexed by a triclinic unit cell. The attempted structure solution and refinement indicate that these compounds probably crystallize in the triclinic space group $P\bar{1}$, but it was not possible to refine a single crystal data set with satisfactory results. The cation seems to be disordered similar to the cation in the crystal structure of $(Au_6Te_{18}Cl_2)[Bi_4Cl_{16}]$. At first glance the counterions are regular hexachlorometallate anions, but some of the $[MCl_6]^-$ octahedra are particularly unstable in the refinement. Since the single crystal data is not reliable, these compounds will not be discussed further. Only the so far determined unit cell parameters are listed in the Appendix (see Table A.56 and A.57).

3.5 Classification of the Gold Tellurium Cluster

The cation itself consists of 24 metal atoms. In order to classify this novel species, the first possible class which comes to mind, might be metal clusters. The structure of the cationic cluster reminds of a mixture between the well known M_6X_8 and M_6X_{12} metal halide clusters: the gold atoms are arranged in form of an octahedron and all edges, as well as six faces, are capped by tellurium. Additional halide atoms can be present capping the remaining two faces. However, the gold atom itself is electronically satisfied and has no need for metal-metal interactions, as can be seen from the long gold-gold distances in all crystal structures.

The next potential class to classify the Au-Te cluster might be Zintl polycations. As mentioned several times throughout this work, many structural clues support the interpretation as regular Au^{3+}. The total cationic charge, however, is only 6+ (for the halide-free cation) which leaves a charge of 12– to be distributed among the tellurium fragments of the cation. A purely ionic model, using the quite common tritellurium dianion ($(Te_3)^{2-}$), however, fails when the crystal structure is examined in more detail. For example, many close contacts between seemingly anionic (tellurium) fragments can be found. Assuming an oxidation state of 1+ for gold would lead to a formal oxidation state of zero for tellurium. However, a linear coordination is usually found for Au^{+}. Instead, the gold coordination is actually almost perfect square-planar. Additionally, a longer contact between gold and a halide atom, belonging to the respective anion in the crystal structure, is found in all examined compounds. This extended gold coordination is observed for most gold(III) compounds, i.e. $AuCl_3$. The only possible conclusion is to accept the gold(III) oxidation state and to assign an anionic character to the tellurium part of the cation, but with a less strict charge distribution than $(Te_3)^{2-}$ implies.

A last attempt is to consider the cation itself as an aggregate of gold cations and tellurium polyanions. As mentioned before, a discrete charge distribution is not feasible, which renders the declaration of discrete tritellurium dianions void. The introduction already referred to Smith and Ibers' failed attempt to summarize the solid state structures of tellurium polyanions [41]. They did encounter many deviations from the expected behaviour of the polyanion in compounds, which were expected to behave analogous. This is basically reflected by the new compound family presented in this work. The only distinct change between the examined solid state structures seems to be an adjustment of the tellurium-tellurium interactions. While the cation with no halide atom attached seems to at least partially reflect the decomposition into six individual $(Te_3)^{2-}$ anions, this already imprecise distinction gets blurred more and more with the addition of the halide atoms.

3.6 Ambiguity of the Element Assignment for the Disordered Crystal Structures

A major problem during the discovery and exploration of this novel compound family was the element assignment for the disordered cations. The very first compound discovered was $(Au_6Te_{18})[AlCl_4]_6$, which showed no disorder and therefore provided no problems in the single crystal structure solution. The second compound being synthesized was $(Au_6Te_{18}Cl)[AlCl_4]_5$. The initial structure refinement for this compound simply assumed a split position for both unoccupied corner positions and the refinement against the sum formula $(Au_6Te_{18})[AlCl_4]_5$ yielded acceptable R values. According to this structure model the cation keeps its sum formula and instead its charge is changed from +6 to +5. Differently charged tellurium polyanions are known, which lent this model some credibility. With the on growing number of newly discovered compounds, not only the cation charge needed adjustment, but also the tellurium content varied, too. Table 3.12 shows the resulting sum formula for both structure models. All listed compounds can be refined with good and almost identical R values. As can be seen from this table, no sensible system to justify the varying charge and tellurium content is easily obvious for the alternate model.

Table 3.12: Comparison of the sum formulas for the herein supported model (halide containing cations) and the alternate model (tellurium contents and formal charge varying cation).

Halide model	Varying Te model
$(Au_6Te_{18}Cl)[AlCl_4]_5$	$(Au_6Te_{18})[AlCl_4]_5$
$(Au_6Te_{18}Cl)[GaCl_4]_5$	$(Au_6Te_{18})[GaCl_4]_5$
$(Au_6Te_{18}Br)[AlCl_4]_5$	$(Au_6Te_{19})[AlCl_4]_5$
$(Au_6Te_{18}Br)[AlBr_4]_5$	$(Au_6Te_{19})[AlBr_4]_5$
$(Au_6Te_{18}Cl_2)[Mo_2O_2Cl_8]_2$	$(Au_6Te_{18.63})[Mo_2O_2Cl_8]_2$

Additionally, experimentally determined physical properties also did not match up. The already mentioned compound $(Au_6Te_{18})[AlCl_4]_5$ (according to the alternate model) was revealed to be diamagnetic (see Figure 3.21, section 3.3.2), while the sum formula might hint at an unpaired electron. The correct sum formula $(Au_6Te_{18}Cl)[AlCl_4]_5$ on the other hand is expected to be diamagnetic.

The next problematic property was the electrical conductivity of $(Au_6Te_{19})[AlBr_4]_5$ or rather $(Au_6Te_{18}Br)[AlBr_4]_5$. Temperature dependent resistance measurements showed typical semi-conductor behaviour (see Figure 3.24, section 3.3.3). Parallel to the experiment, theoretical calculations were performed to verify this behaviour. For the alternate model ($(Au_6Te_{19})[AlBr_4]_5$), these calculations suggested a metal-like density of states. The calculations for $(Au_6Te_{18}Br)[AlBr_4]_5$, however, yielded a DOS with a band gap (see Figure 3.25, section 3.3.3), which matches the experimental result.

Simply using elemental analysis to determine the actual stoichiometric composition is a major challenge for this specific question. On one hand the preparation of these compounds does not yield pure phases, which lowers the significance of measurements performed on bulk samples (which is further hampered because tellurium and halides are usually determined in separate experiments). On the other hand local probes like EDX are too imprecise to reveal the necessary small differences between the discussed sum formulas.

Table 3.13: EDX measurements of $(Au_6Te_{18}Br)[AlCl_4]_5$ in atomic percent. The top shows individual measurements and their average values, the bottom the expected values for both discussed models.

	Au M	**Te L**	**Br L**	**Al K**	**Cl K**
	8.45	31.76	1.19	28.52	30.08
	7.03	32.17	1.90	31.48	27.42
	11.06	35.47	1.22	22.33	29.93
	8.45	31.76	1.19	28.52	30.08
	7.03	32.17	1.90	31.48	27.42
	11.06	35.47	1.22	22.32	29.93
average	10.09	32.03	1.44	25.00	31.44
expected values for					
$(Au_6Te_{18}Br)[AlCl_4]_5$	12.00	36.00	2.00	10.00	40.00
$(Au_6Te_{19})[AlCl_4]_5$	12.00	38.00	0.00	10.00	40.00

The compound $(Au_6Te_{18}Br)[AlCl_4]_5$ might prove an exception to this statement. The single crystal x-ray data refinement left little doubt that all anions exclusively contained chlorine and no bromine, although the reactants for this synthesis were $AlBr_3$, $AuCl_3$ and Te. EDX measurements, however, revealed small amounts of bromine (see Table 3.13). For this particular element combination, however, there is another drawback: The Al K line and the Br L line overlap almost perfectly, which lowers the accuracy for both elements. Still, accepting the single crystal result (concerning the anions) there are only two explanations: Either the bromine content originates from amorphous impurities sticking to the sample surface or the cation indeed contains bromide anions, verifying the presented model.

Finally, taking all these inconsistencies into consideration, the logical conclusion is to discard the alternate model. The herein supported model provides a sensible systematic hierarchy for the cation's sum formula and charge, is supported by the limited elemental analysis possible on the obtained phases, and reconciles experimental and theoretical results of physical properties.

3.7 Salts of Tetrachloroaurate(III) with Group 12 Cations

3.7.1 $Cd[AuCl_4]_2$

The compound $Cd[AuCl_4]_2$ forms transparent, orange crystals and crystallizes in the monoclinic space group $I2/a$. The constituents are divalent cadmium cations and tetrachloroaurate(III) anions. The asymmetric part of the unit cell contains only half of the sum formula. As

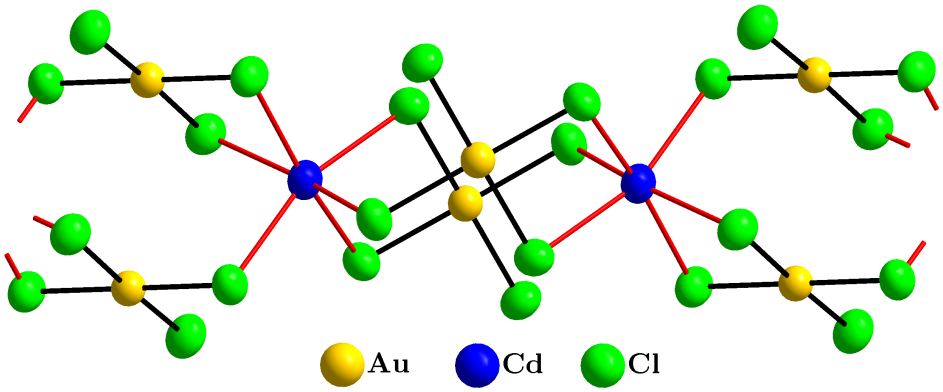

Figure 3.35: Chain running along the crystallographic c axis in the crystal structure of $Cd[AuCl_4]_2$. The tetrachloroaurate(III) anions are symmetry induced coplanar. The displacement ellipsoids represent a probability of 90 %.

usual, the tetrachloroaurate(III) anion shows very little deviation from a perfect square-planar coordination of the gold atom. The four independent Au–Cl bond lengths range from 2.26 to 2.32 Å and the Cl–Au–Cl angles are very close to 90° (see Table 3.14).

The divalent cadmium cation is coordinated by six chlorine atoms in form of a distorted octahedron. These chlorine atoms belong to four different tetrachloroaurate(III) anions, with two anions forming a bidentate coordination. The Cd–Cl distances are almost identical (2.62 Å), while the Cl–Cd–Cl angles, ranging from 77° to 100°, clearly reflect the distortion from an ideal octahedron (see Figure 3.36 and Table 3.14).

The connectivity discussed above results in chains with coplanar tetrachloroaurate(III) anions bridging two cations (see Figure 3.35). There is no indication of any interaction between the gold atoms of coplanar anions, as they are 4.04 Å apart. The chains run along the crystallographic c axis and can be described by the Niggli formula $^1_\infty\left\{Cd\,[Cl(AuCl)Cl_2]_{2/2}\,[Cl_2(AuCl)Cl]_{2/2}\right\}$. As the Niggli formula suggests, the chlorine atom Cl(1) of every anion is not participating in the cadmium coordination sphere. This chlorine atom, together with Cl(3), completes the common 4+2 coordination sphere around gold, as known from gold(III) chloride (see Figure 3.36). This fits perfectly with the Au–Cl bonding lengths inside the anion: Closest bound is the "non-coordinating" Cl(1), while the longest bond is found for Cl(3), which is additionally part of the extended coordination sphere of the next gold atom. This 4+2 coordination interlinks the chains (see Figure 3.37; blue bonds). The chains are arranged in a hexagonal rod packing. Overall the crystal structure shows no unexpected features.

Table 3.14: Overview of bond lengths and angles in the crystal structure of $Cd[AuCl_4]$. The indices correspond to the following symmetry operations: (i) $-x$, $-\frac{1}{2}+y$, $\frac{1}{2}-z$; (ii) x, $\frac{1}{2}-y$, $-\frac{1}{2}+z$; (iii) $\frac{1}{2}-x$, y, $-z$; (iv) $\frac{1}{2}-x$, $\frac{1}{2}-y$, $\frac{1}{2}-z$.

Atoms 1, 2	Distance / Å	Atoms 1, 2, 3	Angle / °
Au—Cl(1)	2.261(3)	Cl(1)—Au—Cl(2)	90.30(7)
Au—Cl(2)	2.293(1)	Cl(2)—Au—Cl(3)	89.87(7)
Au—Cl(3)	2.316(3)	Cl(3)—Au—Cl(4)	89.60(7)
Au—Cl(4)	2.286(2)	Cl(4)—Au—Cl(1)	90.24(7)
Au···Cl(1)^{i}	3.338(2)	Cl(1)···Au···Cl(1)^{i}	101.44(7)
Au···Cl(3)^{iv}	3.532(2)	Cl(1)···Au···Cl(3)^{iv}	82.17(7)
Cd—Cl(2)	2.623(2)	Cl(2)—Cd—Cl(2)^{iii}	77.64(8)
Cd—Cl(3)^{ii}	2.622(2)	Cl(2)—Cd—Cl(3)^{iv}	93.28(6)
Cd—Cl(4)^{ii}	2.630(3)	Cl(2)—Cd—Cl(4)^{ii}	90.11(6)
Au···Au^{ii}	4.0400(6)	Cl(2)—Cd—Cl(4)^{iv}	100.36(6)
		Cl(3)^{ii}—Cd—Cl(3)^{iv}	99.29(9)
		Cl(3)^{iv}—Cd—Cl(4)^{ii}	94.97(6)
		Cl(3)^{ii}—Cd—Cl(4)^{ii}	76.26(6)

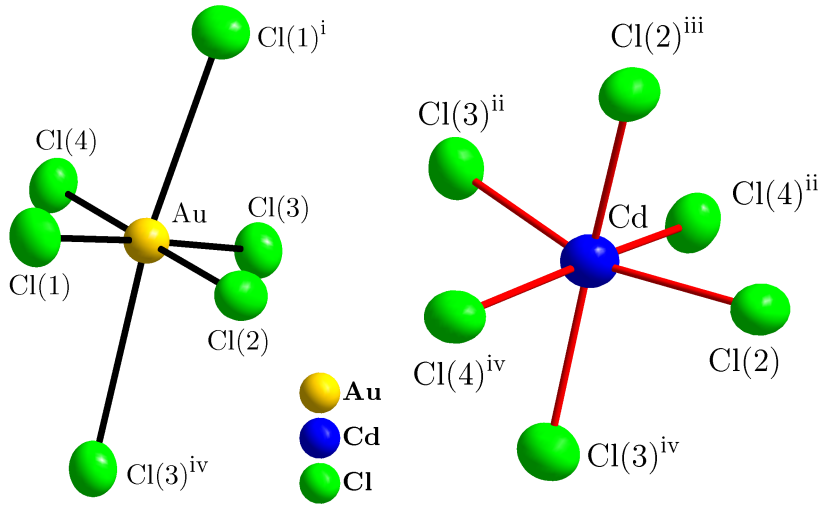

Figure 3.36: The distorted Cl_6-octahedra surrounding Au *(left)* and Cd *(right)* in the crystal structure of $Cd[AuCl_4]_2$. The atom numbering and indices correspond to the symmetry operations from Table 3.14. The displacement ellipsoids represent a probability of 90 %.

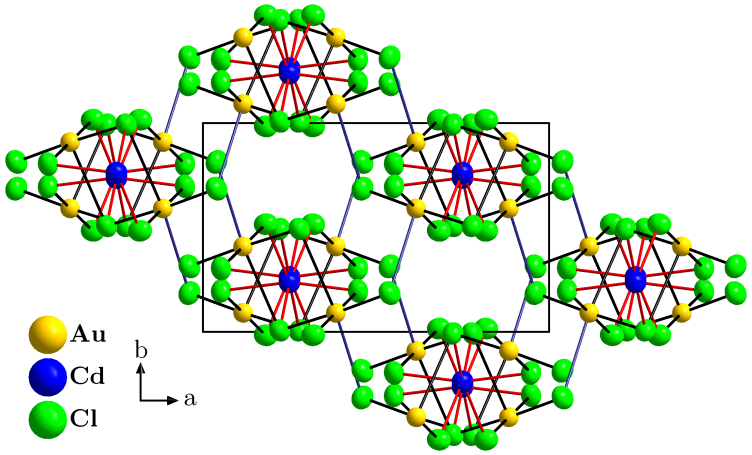

Figure 3.37: The extended unit cell of $Cd[AuCl_4]_2$ viewed along the crystallographic c axis. The blue bonds are the long Au··Cl(1) contacts, which link the chains. The displacement ellipsoids represent a probability of 90 %.

3.7.2 The Incommensurate Composite Structure of $Zn[AuCl_4]_2 \cdot (AuCl_3)_{1.115}$

Crystal structure

The compound $Zn[AuCl_4]_2 \cdot (AuCl_3)_{1.115}$ forms transparent, orange crystals and crystallizes in the (3+1)D superspace group $C2/c(\alpha 0\gamma)0s$. DSC measurements indicate that the compound is stable up to about 250 °C, which coincides with the decomposition temperature of $AuCl_3$. The recorded single crystal dataset of the compound cannot be indexed with three indices without choosing unreliable large direct lattice constants. Indexing as a modulated crystal structure using four indices ($hklm$) leads to a complete explanation of the diffraction pattern. Figure 3.38 shows the ($1kl$) layer of the diffraction pattern to illustrate the necessity for $hklm$ indexing. It displays the characteristic diffraction pattern of stronger main reflections and sharp, but weaker satellite reflections.

Additionally, this particular structure is best described as an incommensurately modulated composite crystal structure. This is advised, if the electron density of an atom, which is represented by a string in 2D projections of the modulated structure, does not run (in average) parallel to the fourth superspace axis (see Figure 3.39). By dividing a structure into multiple subsystems the complete structure description becomes easier to model and understand. Each subsystem has its own unit cell, but at least one, and in this case two lattice directions, are shared among all subsystems, to make sure that the cell contents never overlap. Usually, all subsystem unit cells are modulated crystal structures by themselves, because the subsystems influence each other. This means that main reflections of one subsystem are seen as satellite reflections by another subsystem and *vice versa* (see Figure 3.38). The first subsystem contains zinc(II) tetrachloroaurate(III) and possesses the same superspace symmetry as the whole crystal description. The second subsystem contains gold(III) chloride dimers (Au_2Cl_6) within the superspace group $C2/m(\alpha 0\gamma)0s$.

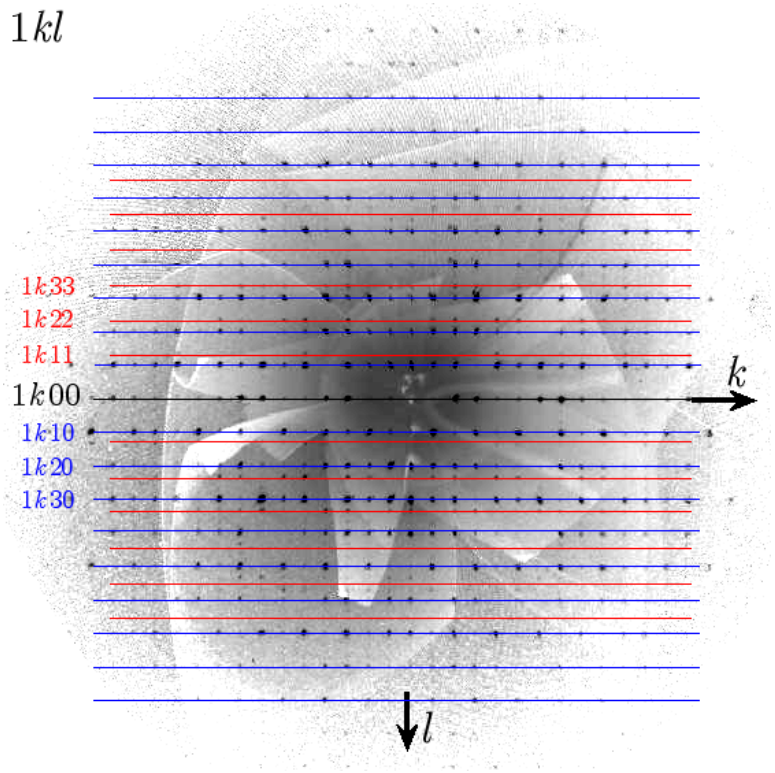

Figure 3.38: Reconstructed precession image of the diffraction pattern of $Zn[AuCl_4]_2 \cdot (AuCl_3)_{1.115}$. The Bragg indexing on the left corresponds to the first subsystem. The black coloured $1k0$ lattice direction is common to both subsystems. The blue coloured reflections are main reflections of the first subsystem ($m = 0$), while the red coloured reflections are satellite reflections of subsystem I but main reflections of the second subsystem.

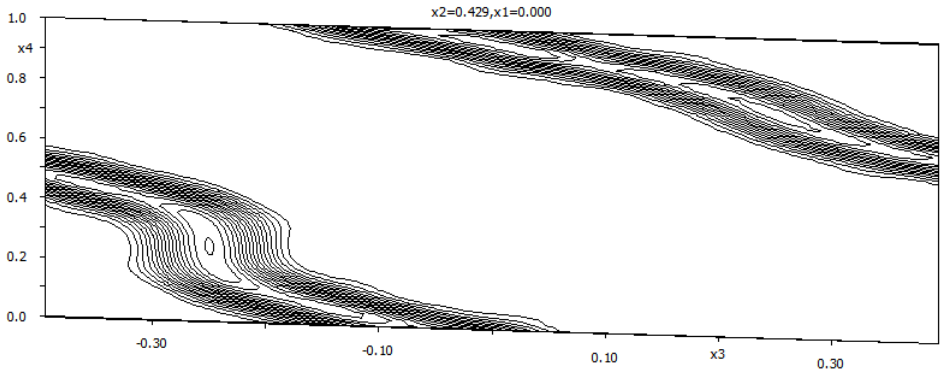

Figure 3.39: $x3$-$x4$-Section (in reference to subsystem I) of the four dimensional electron density in the crystal structure of $Zn[AuCl_4]_2 \cdot (AuCl_3)_{1.115}$ centred on atom Au(3). The string representing Au(3) runs almost perpendicular to the modulation axis $x4$, which encourages a composite crystal structure description.

Discussion of modulated compounds is usually based on t-plots. By definition a modulated crystal structure does not possess translation symmetry in three-dimensional space, which is the premise for "normal" 3D crystal structures. Usually, because of the translation symmetry, the full extent of the crystal structure can be described with only the small fragment of a single unit cell. Without translation symmetry discussion of crystal chemical features, i. e. interatomic distances, is bulky, because the modulation generates an infinite number of slightly

different unit cells, and therefore interatomic distances. Using t-plots, these infinite copies of the unit cell can be recovered into a periodic description by application of superspace.
The direct superspace can be constructed using four lattice vectors a_1 to a_4 and employing translation symmetry. The method of construction requires that a section perpendicular to the fourth superspace axis a_4 yields a three-dimensional subspace. The position t, where the section is cut, is defined for $0 \leq t < 1$, because for $t \geq 1$ the translation symmetry of the superspace generates equivalent sections. Additionally, cutting at $t = 0$ yields the three-dimensional section which matches the observed 3D structure (with modulation and therefore without translation symmetry in 3D space). Because of the translation symmetry in superspace, a section, taken at an arbitrary t, is found in every unit cell, and specifically in one unit cell, where this section corresponds to $t = 0$ (see Figure 3.40). Thus, every three-dimensional section taken at t corresponds to one of the infinite copies of the 3D unit cell. So examining a property as a function of t along a_4 recovers all information in one period owing to the periodicity in superspace.

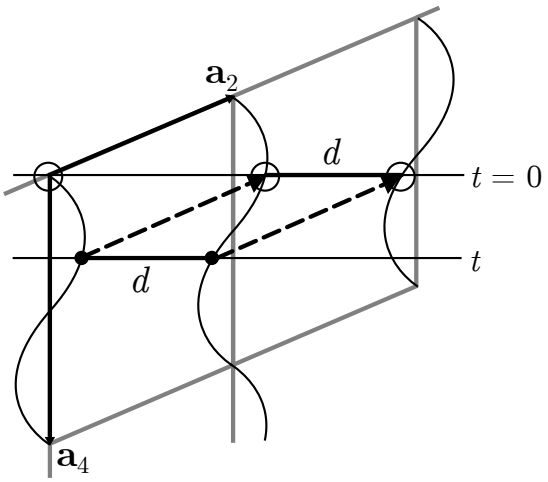

Figure 3.40: An interatomic distance in the first unit cell taken at section t is (by translation symmetry) equal to an interatomic distance at $t = 0$ in a different unit cell – not necessarily the neighbouring one. Figure taken from [91].

Consequently, crystal chemical properties, like interatomic distances, cannot be expressed by a single numerical value, but instead can be displayed as a t-plot. Most properties only show small changes over t and it is sufficient to give the range in which the t-plot meanders. However, sometimes displaying the full t-plot is necessary to emphasise a specific feature of the crystal structure. The Appendix A.1.16 holds additional t-plots not displayed here.

The asymmetric unit of the first subsystem contains one zinc atom and two halves of a tetrachloroaurate(III) anion. As common for Au^{III}, gold atoms are surrounded by four chlorine atoms in a square-planar arrangement. The Au–Cl bonding distances vary between 2.25 Å and 2.30 Å, with the shorter distances corresponding to the terminal bound chlorine atoms. The Cl–Au–Cl angles are close to the ideal angle of 90°, ranging from 88° to 92°.

Three bidentate tetrachloroaurate(III) anions coordinate the zinc atoms in a distorted octahedron (see blue octahedron Figure 3.41). One anion is terminally coordinated, while the other

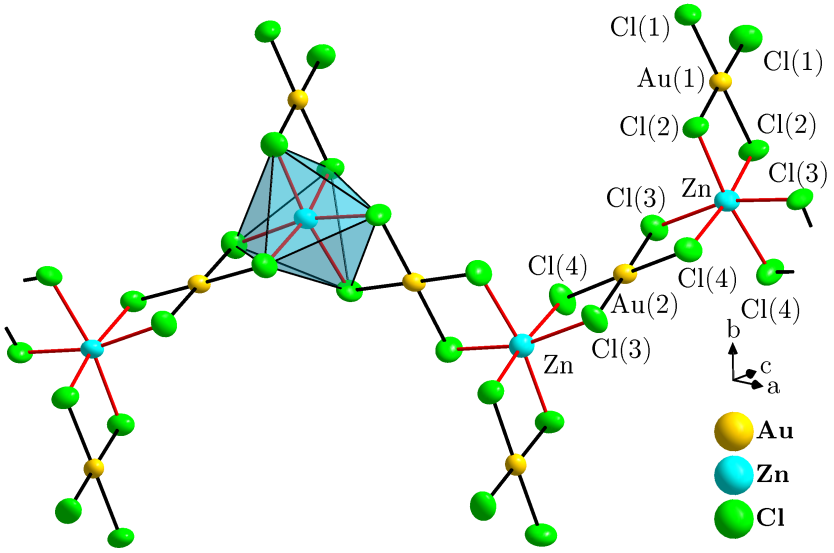

Figure 3.41: Zinc(II) tetrachloroaurate chain taken from the crystal structure of $Zn[AuCl_4]_2 \cdot (AuCl_3)_{1.115}$ at $t = 0$. The chain runs along the (101) direction and can be described by the Niggli formula $^1_\infty\left\{Zn\,[AuCl_4]_{1/1}\,[AuCl_4]_{2/2}\right\}$. Symmetry codes for equivalent atoms have been omitted. The displacement ellipsoids represent a probability of 90 %.

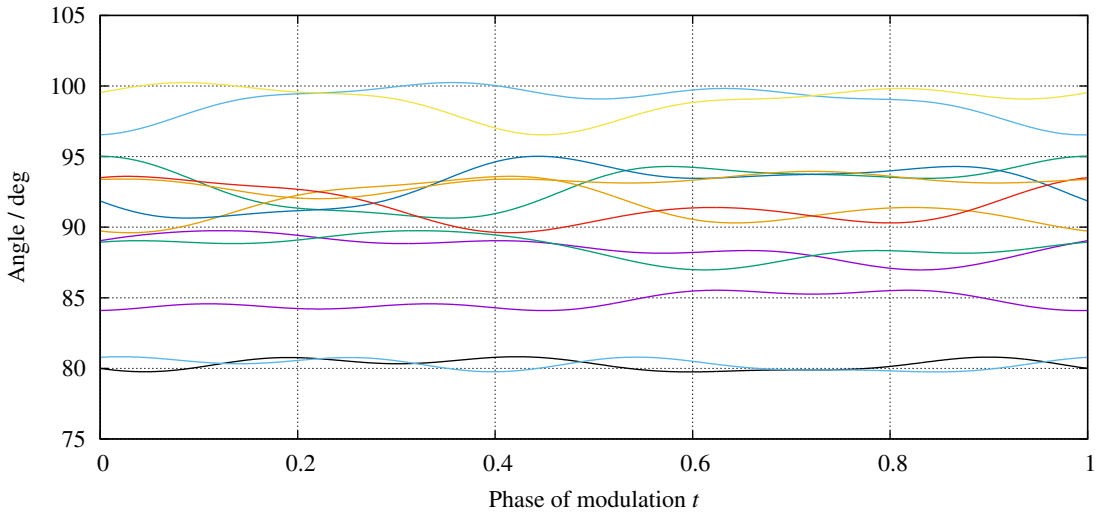

Figure 3.42: t-Plot of all Cl–Zn(1)–Cl angles in the first subsystem of the modulated crystal structure of $Zn[AuCl_4]_2 \cdot (AuCl_3)_{1.115}$. The assignment to the actual angles has been omitted to only focus on the distribution and the small change along t.

two bridge to different neighbouring zinc atoms, thus building up zig-zag chains running along the (101) direction (see Figure 3.41). These chains can be described by the Niggli formula $^1_\infty\left\{Zn\,[AuCl_4]_{1/1}\,[AuCl_4]_{2/2}\right\}$. The Zn–Cl distances cover slightly different ranges for the three symmetrically independent chlorine atoms. The terminal coordinated $[AuCl_4]^-$ anion exhibits the shortest Zn–Cl distances of roughly 2.40 Å, while the two independent Zn–Cl distances to a bridging anion are about 2.46 Å and 2.52 Å. In a perfect octahedral coordination, there are twelve right angles centred on the central atom. In this case, these are Cl–Zn–Cl angles, which are displayed in Figure 3.42. It shows that the change of a single angle versus t is rather small,

but the overall distribution of the twelve angles ranges from 80° to 100°, which clearly reflects the distorted character of the octahedron.

The zig-zag chains formed by the first subsystem build a honeycomb-like structure, leaving flat channels inside the crystal packing (see Figure 3.43). These channels run along the crystallographic c axis and are filled by the second subsystem. The common reciprocal lattice plane of both subsystems is therefore the $(hk0)$ plane.

The asymmetric unit of the second subsystem contains one gold atom and two chlorine atoms, which form Au_2Cl_6 molecules. These planar moieties are stacked along their longer edge inside the channels built up by the first subsystem. The molecules are tilted towards each other. This suggests that the dimers are slightly too small to fill the channels completely (see Figure 3.44). Another property, which allows to observe the arrangement of the gold(III) chloride dimers is the distance between the terminal chlorine atoms of adjacent dimers as shown in Figure 3.45. The much larger distance around $t = 0.8$ corresponds to sections where the tipping direction of the dimers switches. The structure of the second subsystem changes much more over t than the structure of the first subsystem. This seems plausible as these dimers are less tightly coordinated inside the crystal packing than the network structure of the first subsystem, allowing the gold(III) chloride more freedom to maximize the interaction between both subsystems.

The Au–Cl bond lengths differ slightly for the terminal and the bridging chlorine atom. As expected, the bond to the terminal atom is slightly shorter (2.25 Å) than the one to the bridging atom (2.35 Å). The Cl–Au–Cl angle between bridging chlorine atoms is slightly compressed (86°; red line), while, consequently, the other three angles are – with a small exception – wider than 90° (see Figure 3.46). Overall, the structural parameters of the dimers in this compound are very close to those of neat gold(III) chloride (see Table 3.15).

The similarity still holds up, when the examined coordination sphere of the gold atom is enlarged. In gold(III) chloride the dimers are arranged in a fashion which can be described as

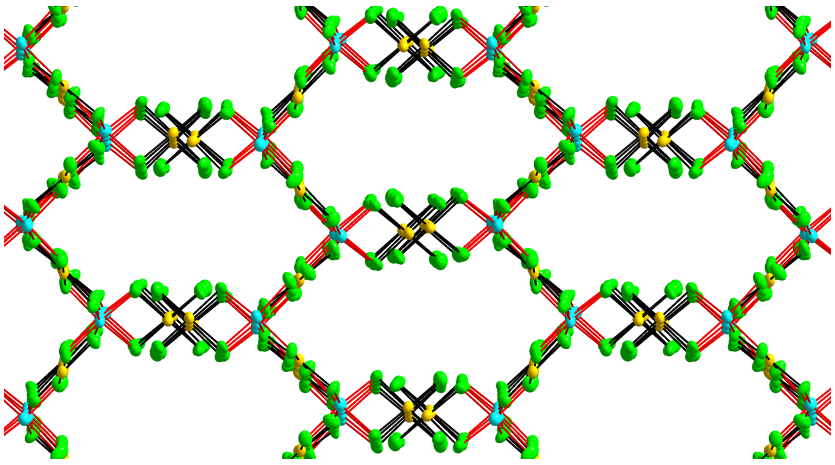

Figure 3.43: Network built up by subsystem I in the structure of $Zn[AuCl_4]_2 \cdot (AuCl_3)_{1.115}$. Structural detail taken at $t = 0$. The displacement ellipsoids represent a probability of 90 %.

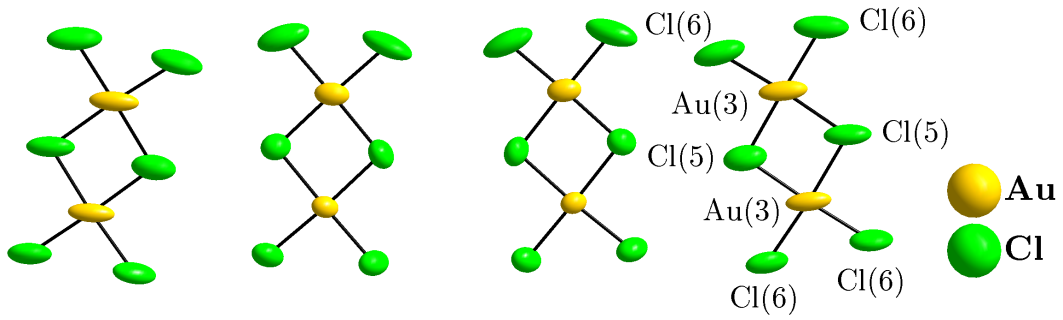

Figure 3.44: Au_2Cl_6 molecules taken from the crystal structure of $Zn[AuCl_4]_2 \cdot (AuCl_3)_{1.115}$ at $t = 0$. The channel built by subsystem I is slightly too large, the molecules are tipped in different directions. Symmetry codes for equivalent atoms have been omitted. The displacement ellipsoids represent a probability of 90 %.

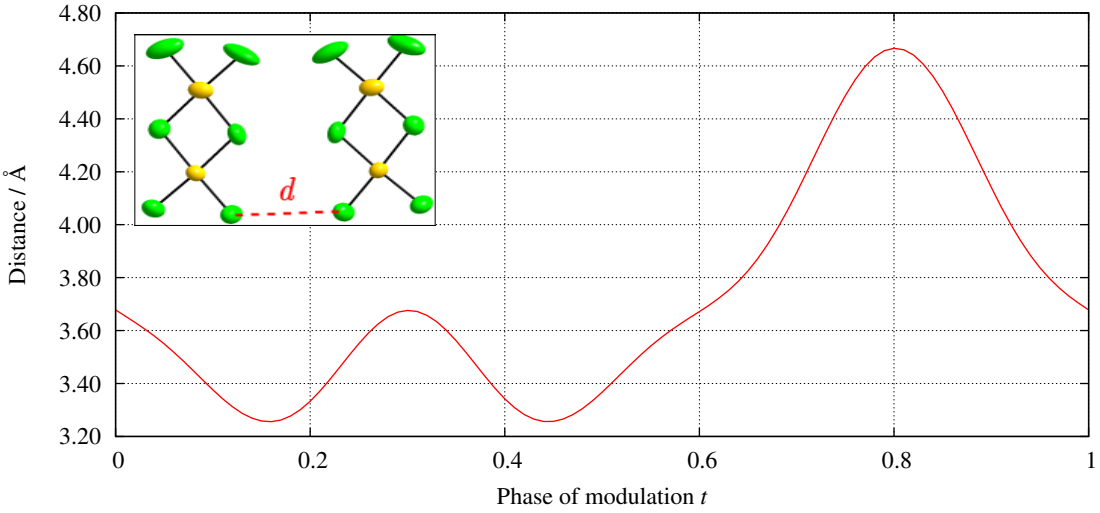

Figure 3.45: *t*-Plot of the distance between the terminal chlorine atom of adjacent Au_2Cl_6 dimers in the modulated crystal structure of $Zn[AuCl_4]_2 \cdot (AuCl_3)_{1.115}$. The longer distance around $t = 0.8$, corresponds to sections, where the tilting direction switches.

an elongated octahedral coordination, or rather as a 4+2 coordination of the gold atom. The two longer (3.46 Å) axial contacts are contacts to chlorine atoms of adjacent dimers. This coordination sphere is also found in this compound, but the chlorine atoms belong to the terminally coordinated anions from the first subsystem (see blue and orange contacts in Figure 3.48). These contacts cover a range from 3.20 Å to 3.60 Å (see Figure 3.47 *(top)*). There are at least two contacts below 3.60 Å. In the first half of the modulation ($t < 0.5$) the close contacts are between Au(3) and Cl(2) and for the second half they are between Au(3) and Cl(1). The gold coordination sphere around $t = 0.5$ even shows up to four contacts when the search radius is slightly enlarged to roughly 3.75 Å, which is obviously a small deviation from neat $AuCl_3$. In this context, the tilting of the dimers can also be interpreted as an effort to achieve the strongest 4+2 coordination.

The varying intersubsystem contacts are also reflected by the anisotropic displacement parameters (ADP) of the dimers as shown in Figure 3.47 (*bottom*; green line) for the maximal ADP of Au(3) exemplarily. When the distances to the chlorine atoms of subsystem I are longer

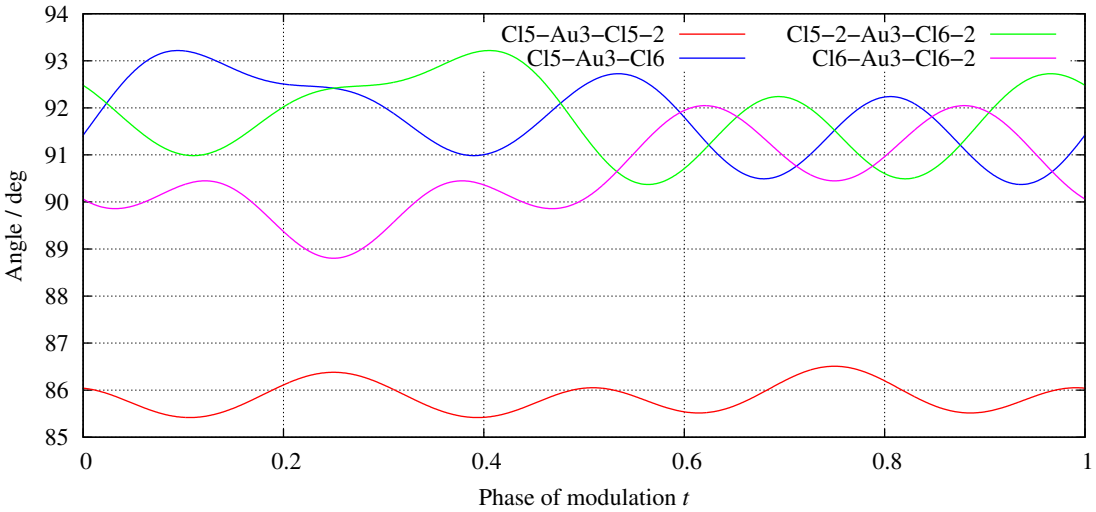

Figure 3.46: *t*-Plot of all Cl–Au(3)–Cl angles in the second subsystem of the modulated crystal structure of $Zn[AuCl_4]_2 \cdot (AuCl_3)_{1.115}$.

Table 3.15: Comparison of the structural features of the second subsystem of $Zn[AuCl_4]_2 \cdot (AuCl_3)_{1.115}$ to actual gold(III) chloride (see Appendix A.1.13). For gold(III) chloride all symmetrically independent values are listed, the value ranges for subsystem II are taken from *t*-plots.

	$AuCl_3$ individual values	Subsystem II range from *t*-plot
d(Au — Cl_{term})	2.245(2) Å; 2.251(2) Å	2.23 - 2.27 Å
d(Au — Cl_{bridge})	2.333(2) Å; 2.343(2) Å	2.32 - 2.38 Å
d(Au — Cl_{ax})	3.454(2) Å; 3.460(2) Å	3.25 - 3.60 Å
$\angle$(Cl_{bridge} — Au — Cl_{bridge})	85.71(6)°	85 - 87°
$\angle$(Cl_{bridge} — Au — Cl_{term})	91.58(6)°; 92.40(6)°	90 - 93°
$\angle$(Cl_{term} — Au — Cl_{term})	90.31(7)°	89 - 92°

(for $t = 0.0; 0.5$), the dimers are bound less tightly allowing them to slightly rattle inside the channel. The consequence is an enlarged displacement ellipsoid as can been seen in structure detail in Figure 3.44 as well as in the *t*-plot in Figure 3.47. Likewise, for short Au··Cl distances (for $t = 0.25; 0.75$), the interaction between the two subsystems is stronger and the dimers move less freely, which is reflected by smaller ellipsoids.

The extended 4+2 coordination is also achieved for the two gold atoms of the first subsystem (see pink contacts in Figure 3.48). The gold atom Au(2) in the bridging tetrachloroaurate ligand shows contacts between 3.30 Å and 3.60 Å to the terminal chlorine atoms Cl(6) from the second subsystem. The gold atom Au(1) in the terminal $[AuCl_4]^-$ ligands completes its coordination sphere without the second subsystem. It is coordinated by chlorine atoms Cl(1) and Cl(2) from terminal ligands below and above with Au··Cl distance between 3.40 Å and 3.60 Å.

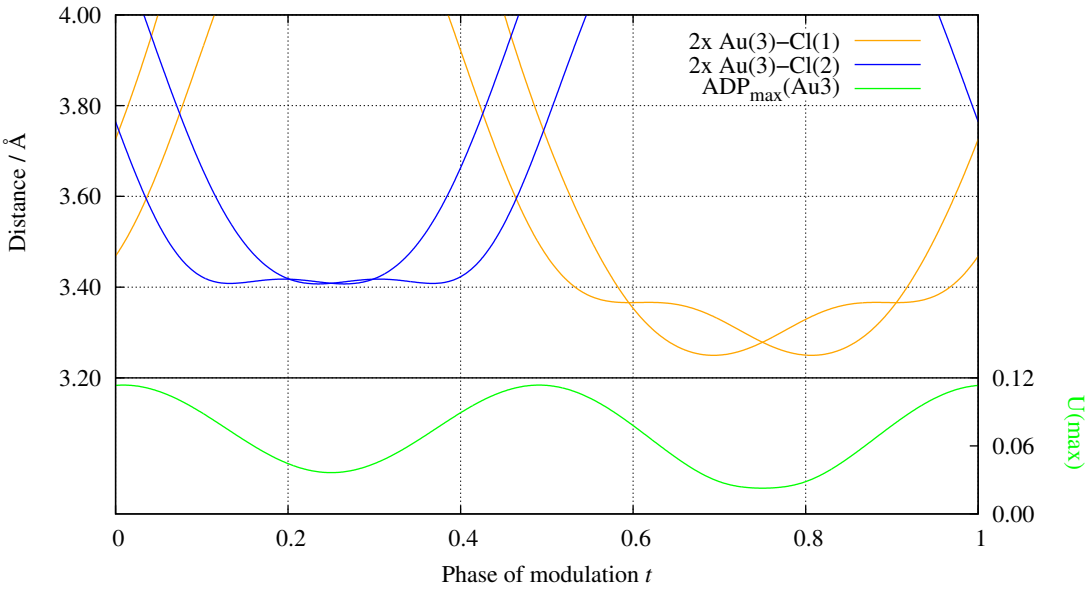

Figure 3.47: t-Plot of the intersubsystem Au(3)··Cl(1/2) contacts *(top)* and the maximal anisotropic displacement parameter (ADP) of Au(3) *(bottom)* in the modulated crystal structure of $Zn[AuCl_4]_2 \cdot (AuCl_3)_{1.115}$. There are always at least two Au··Cl contacts below 3.60 Å to complete the 4+2 coordination sphere. The ADP parameter for Au(3) behaves accordingly: for shorter contacts ($t = 0.25; 0.75$) the displacement ellipsoid is smaller, while it is longer for longer contacts ($t = 0.0; 0.5$). The blue and orange distances correspond to the same coloured contacts in Figure 3.48.

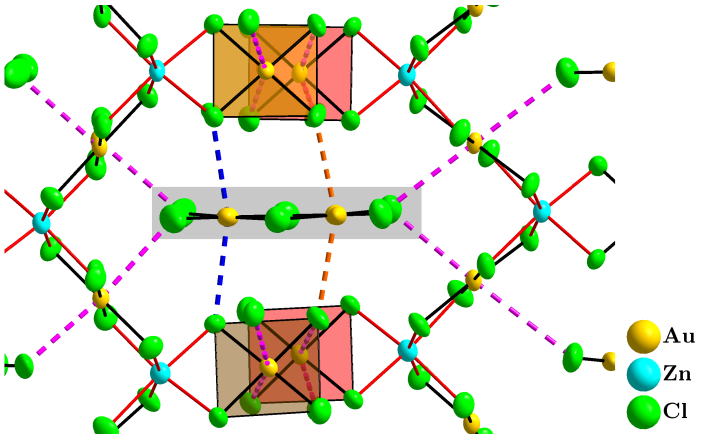

Figure 3.48: Extended gold coordination (depicted as dashed lines) in the crystal structure of $Zn[AuCl_4]_2 \cdot (AuCl_3)_{1.115}$ at $t = 0$. A dimer from the second subsystem is highlighted in grey, all other atoms belong to the first subsystem. All three independent gold atoms show the 4+2 coordination usually found for tetrachloroaurate(III) salts. The blue and orange coloured contacts are those depicted in the t-plot in Figure 3.47. The displacement ellipsoids represent a probability of 90 %.

An explanation why this intercalate compound, and consequently this composite crystal structure, is formed instead of a “simple” pseudo-binary salt, lies in the extended 4+2 coordination discussed above. The zinc(II) tetrachloroaurate(III) substructure is only able to complete the coordination sphere of one of the two independent gold atoms by itself. A different conformation or stacking of the formed chains might fail because of the strong geometric constraints an octahedral coordination around the rather small Zn^{2+} cation generates. So the reactant gold(III) chloride is intercalated to satisfy the 4+2 coordination for all gold atoms.

Why the obtained crystal structure is incommensurately modulated, is not as obvious, as there are plenty of intercalate compounds which crystallize in a 3D space group. Again, an explanation is provided by the 4+2 coordination. The translation period required for building the honeycomb-like network of subsystem I, only allows a more or less dense filling of the channels with Au_2Cl_6 dimers than the presented modulated structure. The denser filling is physically unreasonable and for the less dense filling not all gold atoms can complete their 4+2 coordination sphere, which is the reason for the intercalated guest molecules in the first place. Additionally, the mismatched translation periods are reflected by the irregular $AuCl_3$ stacking itself, which is a compromise between a most efficient space filling and the effort of the gold atoms to achieve a strong 4+2 coordination.

Raman Spectroscopy

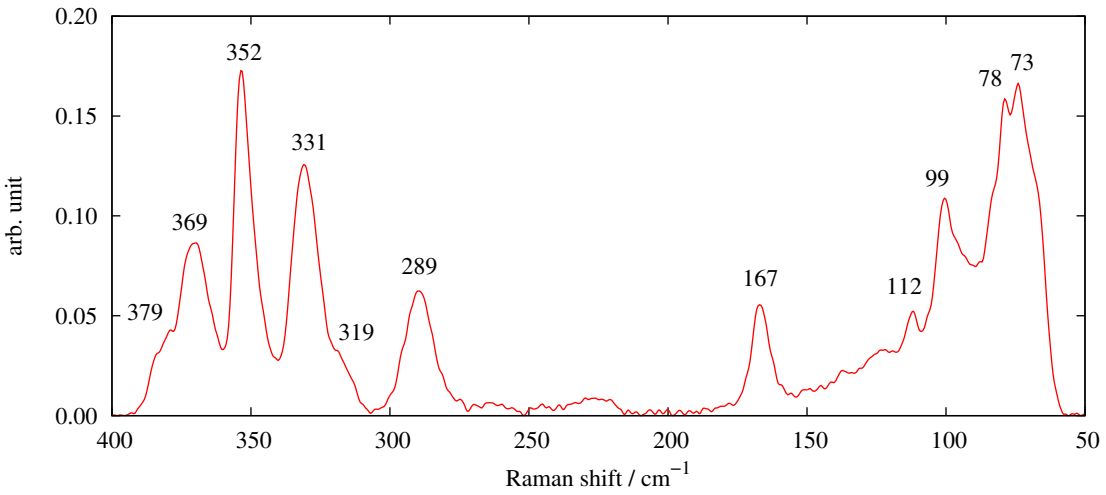

Figure 3.49: Raman spectrum of $Zn[AuCl_4]_2 \cdot (AuCl_3)_{1.115}$. Data was collected up to 1000 cm^{-1}, but no bands in the region above 400 cm^{-1} were observed. The bands at 73 and 78 cm^{-1} originate from the excitation laser itself. All other labelled bands are assigned according to the literature (see Table 3.16).

The vibrational raman spectrum of the compound was recorded. The compound contains two similar but slightly different square-planar gold coordination spheres as discussed above. The first subsystem contains square-planar $[AuCl_4]^-$ anions with an idealized D_{4h} point symmetry, while the second subsystem contains edge-connected Au_2Cl_6 dimers, which also contain square-planar coordinated gold atoms, but the whole dimer only possesses an idealized D_{2h} point symmetry. Individually both moieties have been reported in the literature [92, 93]. All bands in the recorded spectrum are assigned by comparison with the respective publication which supports the finding of undisturbed $AuCl_3$ molecules in the crystal structure. Table 3.16 holds the complete assignment together with the corresponding vibration. The bands are not broadened which is again in compliance with the small modulation-induced variation of the gold-chlorine distances.

Vibrations of the $ZnCl_6$ octahedra of the first subsystem must also exist, but their discussion is

Table 3.16: Band assignment for the Raman spectrum of $Zn[AuCl_4]_2 \cdot (AuCl_3)_{1.115}$. The point symmetry is idealized and does not correspond to the site symmetry of the crystal structure.

Observed / cm^{-1}	$AuCl_3$ (D_{2h}) [92] / cm^{-1}	$[AuCl_4]^-$ (D_{4h}) [93] / cm^{-1}	Vibration
379	378		A_g
369	365		B_{1g}
352		347	A_{1g}
331	328		A_g
319		324	B_{2g}
289	289		B_{1g}
167		171	B_{1g}
167	165		A_g
112	122		B_{1g}
99	104		B_{2g}/B_{3g}
99	97		A_g

complicated, because there is no reference data available in the literature. The raman spectra of compounds containing the tetrahedral $[ZnCl_4]^{2-}$ anion are known, but the transition from a tetrahedral to an octahedral coordination has probably a large impact on the vibrational spectrum. Still, the bands of $Cs_2[ZnCl_4]$ [94], for example, are reported with raman shifts of about 300 cm^{-1} and 120 cm^{-1}, the same region discussed here. This suggests that the broad signal between 150 cm^{-1} and 120 cm^{-1} belongs to the Zn–Cl vibrations. The bands around 300 cm^{-1} might be masked by the strong bonds belonging to the Au–Cl vibrations.

Chapter 4

Summary and Outlook

4.1 Compounds Containing the $(Au_6Te_{18}X_n)^{(6-n)+}$ Cation

Starting from the idea of modifying the unusual compound $AuTe_2Br$, a new compound family with seven different representatives was synthesized and characterized. The common building block for this compound family is the $(Au_6Te_{18}X_n)^{(6-n)+}$ cation (with n = 0, 1, 2 and X = Cl, Br), which was crystallized with a wide variety of anions: $[AlX_4]^-$, $[ZrCl_6]^{2-}$, $[Bi_4Cl_{16}]^{4-}$, $[MoOCl_4]^-$, $[Mo_2O_2Cl_8]^{2-}$, $[NbCl_6]^-$ and $[TaCl_6]^-$. All crystals were of black-metallic appearance and sensitive towards air, especially towards moisture. The cation can be described as a $3 \times 3 \times 3$ cube, where each of the 27 blocks represents a possible atom position. The central position of each face is occupied by a gold atom, the cube's centre and two corners are unoccupied, the remaining 18 positions are occupied by tellurium. For $(Au_6Te_{18}X)^{5+}$ and $(Au_6Te_{18}X_2)^{4+}$ the empty corner positions are occupied by halide atoms (see Figure 4.1).

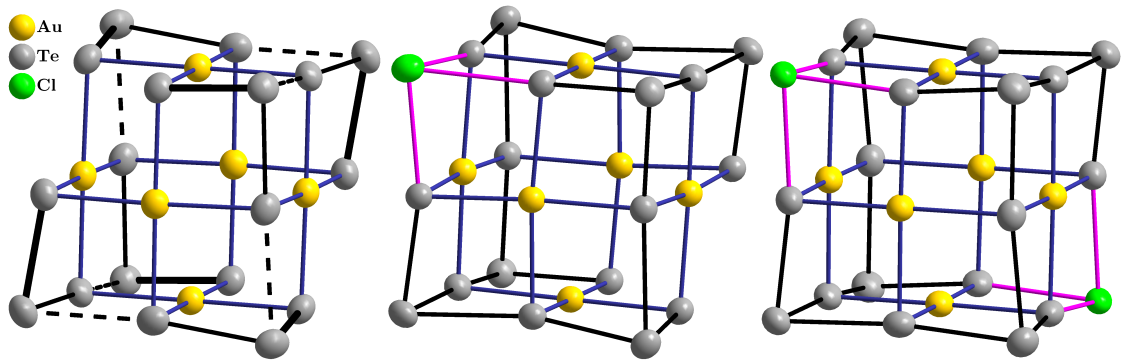

Figure 4.1: From left to right: The $(Au_6Te_{18})^{6+}$ cation, an idealized $(Au_6Te_{18}Cl)^{5+}$ cation and the $(Au_6Te_{18}Cl_2)^{4+}$ cation taken, from crystal structures of this work. Short bonds are emphasized by thick lines. The displacement ellipsoids represent a probability of 90 %.

The crystal structures of all compounds except the hexachloroniobate and -tantalate were determined successfully. At first glance, all crystal structures may be explained by a purely ionic model, consisting of $(Au_6Te_{18}X_n)^{(6-n)+}$ cations and the respective anions. Halide atoms

of the anions are located in axial positions above the square-planar coordinated gold atoms of the cations. Further examination, however, revealed that there are additional covalent interactions below the sum of the van-der-Waals radii present, for example between the cations themselves as indicated by Te-Te contacts between adjacent cations. The compounds containing a disordered cation were ambiguous towards the element assignment of atoms located on the corner positions, but this could be resolved through investigation of other properties later on.

Apart from the characterization by single crystal x-ray diffraction, the compounds were subjected to further experiments to examine their physical properties. Magnetic behaviour and electrical conductivity were investigated. In temperature dependent conductivity measurements all tested compounds showed typical semi-conducting behaviour. The actual conductivity varied among the tested compounds and was absolutely relatively low. This proved as problematic, because the offset voltage had to be chosen carefully to enable an electrical current through the samples without generating redox reactions in the sample itself. The large similarities among all presented compounds suggests that the untested compounds are semi-conductors, too. This assumption is substantiated by the fact that all compounds are of black-metallic appearance. Additionally, this observation is backed by the performed theoretical calculations. The three compounds investigated by DFT electronic structure calculations revealed fundamental band gaps ranging form 0.4 eV to 2.0 eV.

The cation itself, regardless of its halide contents, possesses a high diamagnetic moment of $\chi_{\mathrm{mol}} = -8.198 \cdot 10^{-4} \frac{\mathrm{cm}^3}{\mathrm{mol}}$, which was determined from a magnetic measurement of $(Au_6Te_{18}Cl)[AlCl_4]_5$ after subtraction of diamagnetic increments for the anionic parts. Because of this result the only other investigated compounds towards their magnetic properties were $(Au_6Te_{18}Cl)[MoOCl_4]_5$ and $(Au_6Te_{18}Cl_2)[Mo_2O_2Cl_8]_2$, since the respective anions were expected to exhibit paramagnetic behaviour originating from isolated Mo^{V} atoms with d^1 configuration. The measurement of the latter compound provided data in very good agreement with the Curie-Weiss law resulting in a magnetic moment of 1.67 μ_{B} for a single Mo^{V} atom. This value is only slightly lower than the spin-only value of 1.73 μ_{B} and in good agreement with similar compounds (1.64 μ_{B} [86]). The data obtained for $(Au_6Te_{18}Cl)[MoOCl_4]_5$ yielded a magnetic moment of 1.83 μ_{B}, but the agreement according the Curie-Weiss law was slightly worse, which was attributed to impurities.

In summary, this new, exciting compound family was successfully investigated but leaves room for further investigations. Starting from the unusual compound $AuTe_2Br$, which shows metallic conductivity despite its seemingly ionic composition, this whole family carries the same characteristics. All discussed compounds can be broken down to trivial ions, but from their properties (i. e. appearance, conductivity), it is clear that this is not a viable description. A distinct charge distribution has not been found, yet. Measurements further investigating the conductivity might help to better understand the bonding interactions. Enhanced in-depth theoretical calculations could provide new insights, too. However, the large and sometimes disordered unit cells are a serious handicap. The synthesis of new family members is not fully exhausted and maybe a better model system is found, for example a compound with a

smaller unit cell to reduce CPU time in calculations. In this context the reaction conditions might still be improvable to yield pure samples, which would open up further experimental analysis methods. From a crystallographic point of view there are also still some problems to tackle. Two compounds of the series, $(Au_6Te_{18}Cl_2)[NbCl_6]_4$ and $(Au_6Te_{18}Cl_2)[TaCl_6]_4$, have been synthesized, but their crystal structure could not be determined reliably. The crystals might have been multiply twinned and the data sets might contain unexpected crystallographic traps.

Expanding the series with compounds with lighter homologous of either tellurium or gold seems improbable due to the unique role the gold/tellurium element pair holds.

4.2 Salts of Tetrachloroaurate(III) with Group 12 Cations

In this work, the first two properly characterized salts of tetrachloroaurate(III) with divalent metal cations were presented: $Zn[AuCl_4]_2 \cdot (AuCl_3)_{1.115}$ and $Cd[AuCl_4]_2$. The relevant parameter for the successful synthesis was probably the usage of an unusual solvent: liquid chlorine. Both compounds could be characterized by single crystal x-ray diffraction.

The single crystal x-ray diffraction data set of the zinc compound was not trivial to solve and refine. The compound was best described as an incommensurately modulated composite crystal. The obtained structure solution places the polymeric chain formed by the zinc(II) tetrachloroaurate(III) substructure in one subsystem and Au_2Cl_6 dimers in the other subsystem. These dimers are, compared to neat gold(III) chloride, almost undisturbed. The first subsystem builds up channels, in which the gold(III) chloride dimers are stacked. The necessity for an incommensurately modulated crystal structure results from the incompatible translation periods of the stacked dimers and the polymeric chains.

Closer examination of the crystal structure revealed that the extended 4+2 coordination sphere, usually found for Au^{3+}, is only achieved for both subsystems through interactions with each other. Consequently, completion of this coordination is probably the driving force, for obtaining this intercalate compound instead of the “pure” tetrachloroaurate. The zinc cation is coordinated in form of a heavily distorted octahedron. The small radius of Zn^{2+} generates geometric constraints, which probably prevent a structure with a fulfilled 4+2 coordination sphere for all gold atoms without the guest molecule.

The compound was further examined by Raman spectroscopy. Vibrational spectra of square-planar $[AuCl_4]^-$ anions and neat $AuCl_3$ fragments have both been reported in literature. Since this compound contains gold in both coordination spheres, the $[AuCl_4]^-$ anion in subsystem I and the gold(III) chloride dimers in subsystem II, bands for both coordination spheres were expected and actually observed. It was possible to assign all observed bands by matching the literature data.

The crystal structure of the cadmium compound, on the other hand, was solved to be, more or less, as expected for a pseudo-binary compound. Octahedral coordinated cadmium atoms are

connected to a polymeric chain by the tetrachloroaurate anions. This arrangement, however, is able to complete the extended gold coordination sphere without problems. Additionally, a long known diffraction pattern, recorded by S. Wagner during his Ph.D. work in 1997, was found to already contain the reflections of badly crystallized $Cd[AuCl_4]_2$ (see Figure A.20). So the use of liquid chlorine is not essential for the reaction but seems to be very beneficial.

The literature holds almost no examples wherein liquid chlorine is used as a solvent or reactant. The discovery of $AsCl_5$ by Seppelt *et al.* [95–97] is one example and the use of liquid chlorine to chlorinate rubber [98] another. This promotes the question whether this element is underrated as a solvent or reactant. Obviously, the reactivity of elemental chlorine makes it unsuitable to explore redox sensitive compounds. But it might prove helpful to synthesize already known compounds easier, like it was done in this work to yield gold(III) chloride, without the need for a large experimental setup. Admittedly, after many years of focused research, the amount of undiscovered compounds with highly oxidized atoms is very low. The general interest currently seems more focused on lower and harder to reach oxidation states and mild reaction conditions, which reads like the opposite of liquid chlorine. On the other hand, there are still many blanks in the available databases, which seem easy to fill in, but turn out to be empty not for a lack of trying, but for a lack of success. This work fills one of these gaps with two new salts of tetrachloroaurate containing a divalent metal cation. For the future it might turn out to be gainful to look for “trivial” compounds, which could be synthesized in liquid chlorine.

Bibliography

[1] L. Grande, A. Augustyn, *Gems and Gemstones: Timeless Natural Beauty of the Mineral World*, University of Chicago Press, **2009**.

[2] A. Gopher, T. Tsuk, S. Shalev, R. Gophna, *Curr. Anthropol.* **1990**, *31*(4), 436–443, DOI 10.1086/203868.

[3] S. Wolfsried, Gold Tellurium Minerals, `http://www.mindat.org/photo-608982.html`, *personally submitted*, `http://www.mindat.org/photo-608996.html`, `http://www.mindat.org/photo-672366.html` and `http://www.mindat.org/photo-687137.html`, courtsey of S. Wolfsried, **2004**–**2015**.

[4] V. Goldschmidt, C. Palache, M. Peacock, *Uber Calaverit Neves Jahrbuch Fur Mineralogic*, Bd. 63, **1931**.

[5] K. Balzuweit, H. Meekes, P. Bennema, *J. Phys. D: Appl. Phys.* **1991**, *24*(2), 203, DOI 10.1088/0022-3727/24/2/017.

[6] G. Tunnel, C. J. Ksanda, *J. Wash. Acad. Sci.* **1935**, *25*, 32–33.

[7] W. J. Schutte, J. L. de Boer, *Acta Cryst. B* **1988**, *44*(5), 486–494, DOI 10.1107/S0108768188007001.

[8] L. Bindi, A. Arakcheeva, G. Chapuis, *Am. Mineral.* **2009**, *94*(5-6), 728–736, DOI 10.2138/am.2009.3159.

[9] A. F. Holleman, E. Wiberg, *Lehrbuch Der Anorganischen Chemie*, 101., verb. u. stark erw. Aufl., Gruyter, **1995**.

[10] R. Hoppe, R. Homann, *Z. anorg. allg. Chem.* **1970**, *379*(2), 193–198, DOI 10.1002/zaac.19703790210.

[11] A. J. Edwards, G. R. Jones, *J. Chem. Soc. A* **1969**, 1936–1938, DOI 10.1039/J19690001936.

[12] U. Engelmann, B. G. Müller, *Z. anorg. allg. Chem.* **1991**, *598*(1), 103–110, DOI 10.1002/zaac.19915980110.

[13] R. Schmidt, B. G. Müller, *Z. anorg. allg. Chem.* **2004**, *630*(13-14), 2393–2397, DOI 10.1002/zaac.200400123.

[14] O. Graudejus, A. P. Wilkinson, N. Bartlett, *Inorg. Chem.* **2000**, *39*(7), 1545–1548, DOI 10.1021/ic991178t.

[15] P. G. Jones, R. Hohbein, E. Schwarzmann, *Acta Cryst. C* **1988**, *44*(7), 1164–1166, DOI 10.1107/S0108270188002756.

[16] P. G. Jones, E. Bembenek, *J. Cryst. Spectrosc.* **1992**, *22*(4), 397–401, DOI 10.1007/BF01195399.

[17] J. Strähle, H. Bärnighausen, *Z. Kristallogr.* **1971**, *134*, 471–472, DOI 10.1524/zkri.1971.134.16.448.

[18] F. Kraus, *Z. Naturforsch. B* **2011**, *66*(8), 871–872.

[19] P. Werner, J. Strähle, *Z. Naturforsch. B* **1977**, *32*, 741–744.

[20] P. G. Jones, R. Schelbach, E. Schwarzmann, *Acta Cryst. C* **1987**, *43*(9), 1674–1675, DOI 10.1107/S0108270187090619.

[21] H. Omrani, R. Welter, R. Vangelisti, *Acta Cryst. C* **1999**, *55*(1), 13–14, DOI 10.1107/S010827019801110X.

[22] P. Gütlich, B. Lehnis, K. Römhild, J. Strähle, *Z. Naturforsch. B* **1982**, *37*, 550–556.

[23] E. Schulz Lang, U. Abram, J. Strähle, *Z. anorg. allg. Chem.* **1997**, *623*(11), 1791–1795, DOI 10.1002/zaac.19976231122.

[24] B. G. Müller, *Z. anorg. allg. Chem.* **1987**, *555*(12), 57–63, DOI 10.1002/zaac.19875551207.

[25] H. Bialowons, B. G. Müller, *Z. anorg. allg. Chem.* **1997**, *623*(1-6), 434–438, DOI 10.1002/zaac.19976230169.

[26] R. Fischer, B. G. Müller, *Z. anorg. allg. Chem.* **1997**, *623*(11), 1729–1733, DOI 10.1002/zaac.19976231110.

[27] R. Schmidt, B. G. Müller, *Z. anorg. allg. Chem.* **1999**, *625*(4), 605–608, DOI 10.1002/(SICI)1521-3749(199904)625:4<605::AID-ZAAC605>3.0.CO;2-6.

[28] H. Bialowons, B. G. Müller, *Z. anorg. allg. Chem.* **1997**, *623*(11), 1719–1722, DOI 10.1002/zaac.19976231108.

[29] P. G. Jones, R. Schelbach, E. Schwarzmann, C. Thöne, *Acta Cryst. C* **1988**, *44*(7), 1162–1164, DOI 10.1107/S0108270188002744.

[30] P. E. Plyusnin, I. A. Baidina, Y. V. Shubin, S. V. Korenev, *Russ. J. Inorg. Chem.* **2007**, *52*(3), 371–377, DOI 10.1134/S0036023607030138.

[31] O. Graudejus, B. G. Müller, *Z. anorg. allg. Chem.* **1996**, *622*(1), 187–190, DOI 10.1002/zaac.19966220127.

[32] S. Wagner, Dissertation, Universität Gießen, **1999**.

[33] J. Beck, S. Wagner, *Z. anorg. allg. Chem.* **1997**, *623*(11), 1810–1814, DOI 10.1002/zaac.19976231125.

[34] F. J. M. von Reichenstein, *Physikalische Arbeiten der einträchtigen Freunde in Wien* **1783**, *1*, 63–69.

[35] M. Klaproth, *Chemical Annals for the Friends of Science, Medicine, Economics, and Manufacturing* **1798**, *1*, 91–104.

[36] I. D. Brown, D. B. Crump, R. J. Gillespie, *Inorg. Chem.* **1971**, *10*(10), 2319–2323, DOI 10.1021/ic50104a046.

[37] T. W. Couch, D. A. Lokken, J. D. Corbett, *Inorg. Chem.* **1972**, *11*(2), 357–362, DOI 10.1021/ic50108a031.

[38] J. Beck, *Angew. Chem. Int. Ed. Engl.* **1994**, *33*(2), 163–172, DOI 10.1002/anie.199401631; J. Beck, *Angew. Chem.* **1994**, *106*(2), 172–182, DOI 10.1002/ange.19941060205.

[39] J. Beck, A. Fischer, A. Stankowski, *Z. anorg. allg. Chem.* **2002**, *628*(11), 2542–2548, DOI 10.1002/1521-3749(200211)628:11<2542::AID-ZAAC2542>3.0.CO;2-1.

[40] C. Hugot, *Ann. Chim. Phys.* **1900**, *21*.

[41] D. M. Smith, J. A. Ibers, *Coord. Chem. Rev.* **2000**, *200–202*, 187–205, DOI 10.1016/S0010-8545(00)00256-3.

[42] *ICSD Find It, Version 2015.2*, FIZ Karlsruhe, Eggenstein-Leopoldshafen, **2015**.

[43] F. Bachechi, *Nature* **1971**, *231*(20), 67–68, DOI 10.1038/10.1038/physci231067a0.

[44] W. Bronger, H. Kathage, *J. Alloy. Compd.* **1992**, *184*(1), 87–94, DOI 10.1016/0925-8388(92)90457-K.

[45] P. Messien, M. Baiwir, *Bull. Soc. Roy. Sci. Lieg.* **1966**, *35*, 234–243.

[46] G. Tunell, L. Pauling, *Acta Cryst.* **1952**, *5*(3), 375–381, DOI 10.1107/S0365110X52001106.

[47] T. K. Reynolds, M. A. McGuire, F. J. DiSalvo, *J. Solid State Chem.* **2004**, *177*(9), 2998–3006, DOI 10.1016/j.jssc.2004.04.029.

[48] P. Chai, J. D. Corbett, *Inorg. Chem.* **2011**, *50*(21), 10949–10955, DOI 10.1021/ic201492z.

[49] P. Chai, J. D. Corbett, *Inorg. Chem.* **2012**, *51*(6), 3548–3556, DOI 10.1021/ic202342v.

[50] A. Rabenau, H. Rau, G. Rosenstein, *J. Less-Common Met.* **1970**, *21*(4), 395–401, DOI 10.1016/0022-5088(70)90043-3.

[51] B. L. Zhou, E. Gmelin, R. Villar, *J. Phys. C: Solid State Phys.* **1981**, *14*(30), 4393, DOI 10.1088/0022-3719/14/30/007.

[52] *STOE Win XPOW v1.05*, STOE & Cie GmbH, Darmstadt, **1999**.

[53] M. Kienle, M. Jacob, *DIFFRACplus Measurement Part 2.5*, Bruker AXS, Karlsruhe, **2000**.

[54] *COLLECT*, Nonius BV, Delft, **1999**.

[55] Z. Otwinowski, W. Minor, J. Charles W. Carter, in *Macromolecular Crystallography Part A*, Bd. 276, Academic Press, **1997**, 307–326.

[56] L. Palatinus, G. Chapuis, *J. Appl. Crystallogr.* **2007**, *40*(4), 786–790, DOI 10.1107/S0021889807029238.

[57] G. M. Sheldrick, *Acta Cryst. A* **2007**, *64*, 112–122, DOI 10.1107/S0108767307043930.

[58] G. M. Sheldrick, *Acta Cryst. A* **2008**, *64*(1), 112–122, DOI 10.1107/S0108767307043930.

[59] R. H. Blessing, *Acta Cryst. A* **1995**, *51*(1), 33–38, DOI 10.1107/S0108767394005726.

[60] A. L. Spek, *J. Appl. Crystallogr.* **2003**, *36*(1), 7–13, DOI 10.1107/S0021889802022112.

[61] A. L. Spek, *Acta Cryst. D* **2009**, *65*, 148–155, DOI 10.1107/S090744490804362X.

[62] L. J. Farrugia, *J. Appl. Crystallogr.* **2012**, *45*(4), 849–854, DOI 10.1107/S0021889812029111.

[63] K. Brandenburg, *Diamond 3.2g*, Crystal Impact GbR, Bonn, **2011**.

[64] *APEX2, SAINT Und SADABS*, Bruker AXS Inc., Madison, Wisconsin, USA, **2004**.

[65] V. Petříček, M. Dušek, L. Palatinus, *Z. Kristallogr.* **2014**, *229*(5), 345–352, DOI 10.1515/zkri-2014-1737.

[66] H. Lueken, *Magnetochemie*, Teubner Studienbücher Chemie, Vieweg+Teubner Verlag, Wiesbaden, **1999**.

[67] R. Dovesi, R. Orlando, A. Erba, C. M. Zicovich-Wilson, B. Civalleri, S. Casassa, L. Maschio, M. Ferrabone, M. De La Pierre, P. D'Arco, Y. Noël, M. Causà, M. Rérat, B. Kirtman, *Int. J. Quantum Chem.* **2014**, *114*(19), 1287–1317, DOI 10.1002/qua.24658.

[68] T. Bredow, A. R. Gerson, *Phys. Rev. B* **2000**, *61*(8), 5194–5201, DOI 10.1103/PhysRevB.61.5194.

[69] J. P. Perdew, K. Burke, M. Ernzerhof, *Phys. Rev. Lett.* **1996**, *77*(18), 3865–3868, DOI 10.1103/PhysRevLett.77.3865.

[70] S. Grimme, J. Antony, S. Ehrlich, H. Krieg, *J. Chem. Phys.* **2010**, *132*(15), 154104, DOI 10.1063/1.3382344.

[71] S. Grimme, S. Ehrlich, L. Goerigk, *J. Comput. Chem.* **2011**, *32*(7), 1456–1465, DOI 10.1002/jcc.21759.

[72] J. G. Brandenburg, S. Grimme, in *Prediction and Calculation of Crystal Structures*, (Herausgegeben von S. Atahan-Evrenk, A. Aspuru-Guzik), Springer International Publishing, Nr. 345 in *Topics in Current Chemistry*, **2013**, 1–23, DOI 10.1007/128_2013_488.

[73] J. P. Perdew, Y. Wang, *Phys. Rev. B* **1992**, *45*(23), 13244–13249, DOI 10.1103/PhysRevB.45.13244.

[74] J. P. Perdew, J. A. Chevary, S. H. Vosko, K. A. Jackson, M. R. Pederson, D. J. Singh, C. Fiolhais, *Phys. Rev. B* **1992**, *46*(11), 6671–6687, DOI 10.1103/PhysRevB.46.6671.

[75] C. Pisani, R. Dovesi, C. Roetti, *Hartree-Fock Ab Initio Treatment of Crystalline Systems*, Bd. 48 von *Lecture Notes in Chemistry*, (Hrsg.: G. Berthier, M. J. S. Dewar, H. Fischer, K. Fukui, G. G. Hall, J. Hinze, H. H. Jaffé, J. Jortner, W. Kutzelnigg, K. Ruedenberg, J. Tomasi), Springer Berlin Heidelberg, Berlin, Heidelberg, **1988**.

[76] H. J. Monkhorst, J. D. Pack, *Phys. Rev. B* **1976**, *13*(12), 5188–5192, DOI 10.1103/PhysRevB.13.5188.

[77] T. Williams, C. Kelley and many others, *Gnuplot 5.0: An Interactive Plotting Program*, **2015**.

[78] G. Brauer, *Handbuch Der Präparativen Anorganischen Chemie*, 3., umgearb. Aufl., Ferdinand Enke Verlag, Stuttgart, **1975**.

[79] K.-P. Lörcher, J. Strähle, *Z. Naturforsch. B* **1975**, *30*, 662–664.

[80] R. Müller, Dissertation, Universität Bonn, **2012**.

[81] P. C. Crouch, G. W. A. Fowles, I. B. Tomkins, R. A. Walton, *J. Chem. Soc. A* **1969**, 2412–2415, DOI 10.1039/J19690002412.

[82] A. Bondi, *J. Phys. Chem.* **1964**, *68*(3), 441–451, DOI 10.1021/j100785a001.

[83] X. Zhang, J. L. Schindler, T. Hogan, J. Albritton-Thomas, C. R. Kannewurf, M. G. Kanatzidis, *Angew. Chem. Int. Ed. Engl.* **1995**, *34*(1), 68–71, DOI 10.1002/anie.199500681; X. Zhang, J. L. Schindler, T. Hogan, J. Albritton-Thomas, C. R. Kannewurf, M. G. Kanatzidis, *Angew. Chem.* **1995**, *107*(1), 117–120, DOI 10.1002/ange.19951070131;

[84] J. H. Shin, T. Hascall, G. Parkin, *Organometallics* **1999**, *18*(1), 6–9, DOI 10.1021/om9807396.

[85] B. Buss, B. Krebs, *Inorg. Chem.* **1971**, *10*(12), 2795–2800, DOI 10.1021/ic50106a035.

[86] J. Beck, M. Kellner, M. Kreuzinger, *Z. anorg. allg. Chem.* **2002**, *628*(12), 2656–2660, DOI 10.1002/1521-3749(200212)628:12<2656::AID-ZAAC2656>3.0.CO;2-2.

[87] G. R. Willey, H. Collins, M. G. B. Drew, *J. Chem. Soc., Dalton Trans.* **1991**, 961–965, DOI 10.1039/DT9910000961.

[88] K. A. Al-Farhan, A. I. Al-Wassil, *J. Chem. Crystallogr.* **1995**, *25*(12), 841–844, DOI 10.1007/BF01671080.

[89] I. A. Ahmed, R. Blachnik, H. Reuter, *Z. anorg. allg. Chem.* **2001**, *627*(9), 2057–2062, DOI 10.1002/1521-3749(200109)627:9<2057::AID-ZAAC2057>3.0.CO;2-7.

[90] P. Mahjoor, S. E. Latturner, *Cryst. Growth Des.* **2009**, *9*(3), 1385–1389, DOI 10.1021/cg800625w.

[91] S. van Smaalen, *Incommensurate Crystallography*, Oxford University Press, **2007**.

[92] G. N. P. L. Nalbandian, *Vib. Spectrosc.* **1992**, *4*(1), 25–34, DOI 10.1016/0924-2031(92)87010-D.

[93] K. Nakamoto, *Infrared and Raman Spectra of Inorganic and Coordination Compounds: Part A: Theory and Applications in Inorganic Chemistry*, 6. Aufl., John Wiley & Sons, Inc., Hoboken, New Jersey, **2009**.

[94] P. T. T. Wong, *J. Chem. Phys.* **1976**, *64*(5), 2186–2191, DOI 10.1063/1.432442.

[95] K. Seppelt, *Angew. Chem. Int. Ed. Engl.* **1976**, *15*(6), 377–378, DOI 10.1002/anie.197603771; K. Seppelt, *Angew. Chem.* **1976**, *88*(12), 410–411, DOI 10.1002/ange.19760881206.

[96] K. Seppelt, *Z. anorg. allg. Chem.* **1977**, *434*(1), 5–15, DOI 10.1002/zaac.19774340101.

[97] S. Haupt, K. Seppelt, *Z. anorg. allg. Chem.* **2002**, *628*(4), 729–734, DOI 10.1002/1521-3749(200205)628:4<729::AID-ZAAC729>3.0.CO;2-E.

[98] F. Cataldo, *J. Appl. Polym. Sci.* **1995**, *58*(11), 2063–2065, DOI 10.1002/app.1995.070581118.

[99] N. M. Harrison, Basisset 8-311G Al Atom from Scaled Si, `http://www.tcm.phy.cam.ac.uk/~mdt26/basis_sets/Al_basis.txt`, **1993**.

[100] D. Andrae, U. Häußermann, M. Dolg, H. Stoll, H. Preuß, *Theoret. Chim. Acta* **1990**, *77*(2), 123–141, DOI 10.1007/BF01114537.

[101] J. M. L. Martin, A. Sundermann, *J. Chem. Phys.* **2001**, *114*(8), 3408–3420, DOI 10.1063/1.1337864.

[102] M. F. Peintinger, D. V. Oliveira, T. Bredow, *J. Comput. Chem.* **2013**, *34*(6), 451–459, DOI 10.1002/jcc.23153.

[103] K. A. Peterson, D. Figgen, E. Goll, H. Stoll, M. Dolg, *J. Chem. Phys.* **2003**, *119*(21), 11113–11123, DOI 10.1063/1.1622924.

List of Figures

List of Tables

A.1 Single Crystal Datasheets

A.1.1 $(Au_6Te_{18})[AlCl_4]_6$

Table A.1: Crystal data and structure refinement for $(Au_6Te_{18})[AlCl_4]_6$.

Empirical formula	$Al_6\,Au_6\,Cl_{24}\,Te_{18}$
Formula weight / $g \cdot mol^{-1}$	4491.28
Temperature / K	123(2)
Crystal system; space group	Orthorhombic; *Pbca*
Lattice constants / $Å$	$a = 22.1041(2)$
	$b = 12.4304(1)$
	$c = 23.1555(3)$
Volume / $Å^3$	6362.3(1)
Z; F(000); calc. density / $g \cdot cm^{-3}$	4; 7584; 4.689
Wavelength	$Mo_{K\alpha}$ ($\lambda = 0.71073$ Å)
Crystal size / mm^3	$0.064 \times 0.059 \times 0.054$
Theta range for data collection / °	$3.030 \leq \theta \leq 27.472$
Limiting indices	$-28 \leq h \leq 28$; $-16 \leq k \leq 16$; $-29 \leq l \leq 30$
Reflections collected / unique	113679 / 7281
Completeness to $\theta = 25.242°$	99.9 %
R_{int}; R_σ	0.1002; 0.0353
Absorption coefficient / mm^{-1}	22.981; Semi-empirical from equivalents
Max. / min. transmission	0.2116 / 0.1281
Refinement method	Full-matrix least-squares on F^2
Data / restraints / parameters	7281 / 0 / 244
R indices (all data) R_1; wR_2	0.0386; 0.0493
R indices $[I > 4\sigma(I)]$ R_1; wR_2	0.0267; 0.0470; n = 6102 reflections
Goodness-of-fit for F^2	1.102
Largest diff. peak / $e^- \cdot Å^{-3}$	+1.225 (1.66 Å from Te1)
	-1.517 (0.76 Å from Au1)
Avg. diff. density / $e^- \cdot Å^{-3}$	0.270

Table A.2: Fractional coordinates and equivalent isotropic displacement parameter U_{eq} for the independent atoms in the structure of $(Au_6Te_{18})[AlCl_4]_6$.

Atom	Wyck.	Site	x / a	y / b	z / c	U_{eq} / $Å^2$
Au(1)	8*c*	1	0.01043(2)	0.42975(2)	0.39031(2)	0.01683(6)
Au(2)	8*c*	1	-0.12031(2)	0.51202(2)	0.48642(2)	0.01671(6)
Au(3)	8*c*	1	0.01526(2)	0.70156(2)	0.46445(2)	0.01705(6)
Te(1)	8*c*	1	-0.00409(2)	0.22648(3)	0.42740(2)	0.01874(9)
Te(2)	8*c*	1	-0.12431(2)	0.21855(3)	0.40035(2)	0.02045(10)
Te(3)	8*c*	1	-0.11009(2)	0.44357(3)	0.37689(2)	0.01846(9)
Te(4)	8*c*	1	0.13076(2)	0.42159(3)	0.40383(2)	0.01843(9)
Te(5)	8*c*	1	0.16177(2)	0.61588(3)	0.35881(2)	0.02110(10)
Te(6)	8*c*	1	-0.13592(2)	0.31057(3)	0.52400(2)	0.02013(10)
Te(7)	8*c*	1	-0.10459(2)	0.71447(3)	0.45087(2)	0.01797(9)
Te(8)	8*c*	1	-0.10363(2)	0.67812(3)	0.33502(2)	0.01941(9)
Te(9)	8*c*	1	0.02218(2)	0.63374(3)	0.35499(2)	0.01877(9)
Cl(1)	8*c*	1	-0.25946(7)	-0.04976(15)	-0.03549(9)	0.0347(4)
Cl(2)	8*c*	1	-0.30534(8)	-0.09060(14)	0.10544(8)	0.0346(4)
Cl(3)	8*c*	1	-0.40884(7)	0.00179(13)	-0.00020(8)	0.0271(4)
Cl(4)	8*c*	1	-0.29716(9)	0.17182(14)	0.05192(10)	0.0419(5)
Al(1)	8*c*	1	-0.31831(9)	0.00807(15)	0.03168(10)	0.0240(5)
Cl(5)	8*c*	1	-0.00382(7)	0.33452(13)	0.26148(7)	0.0249(4)
Cl(6)	8*c*	1	-0.07546(8)	0.57466(14)	0.21484(8)	0.0322(4)
Cl(7)	8*c*	1	-0.00232(8)	0.41667(13)	0.11610(8)	0.0317(4)
Cl(8)	8*c*	1	0.08216(8)	0.55214(15)	0.21936(9)	0.0367(4)
Al(2)	8*c*	1	0.00002(9)	0.46873(15)	0.20341(9)	0.0210(4)
Cl(9)	8*c*	1	-0.31853(8)	0.30574(15)	0.22269(8)	0.0324(4)
Cl(10)	8*c*	1	-0.25868(7)	0.30850(14)	0.36355(7)	0.0275(4)
Cl(11)	8*c*	1	-0.24642(8)	0.53690(14)	0.27738(10)	0.0380(5)
Cl(12)	8*c*	1	-0.16248(7)	0.30527(14)	0.24703(8)	0.0277(4)
Al(3)	8*c*	1	-0.24757(8)	0.36666(15)	0.27555(9)	0.0221(4)

Table A.3: Anisotropic displacement parameters U_{ij} / $Å^2$ for the independent atoms in the structure of $(Au_6Te_{18})[AlCl_4]_6$.

Atom	U_{11}	U_{22}	U_{33}	U_{23}	U_{13}	U_{12}
Au(1)	0.01901(12)	0.01613(12)	0.01534(14)	-0.00005(10)	0.00042(10)	0.00082(9)

continued on next page

Atom	U_{11}	U_{22}	U_{33}	U_{23}	U_{13}	U_{12}
Au(2)	0.01738(12)	0.01681(12)	0.01594(14)	0.00018(10)	0.00053(10)	0.00021(9)
Au(3)	0.01907(12)	0.01539(12)	0.01668(14)	0.00110(10)	0.00027(10)	-0.00007(9)
Te(1)	0.0221(2)	0.0153(2)	0.0189(2)	-0.00110(17)	-0.00102(18)	0.00090(16)
Te(2)	0.0235(2)	0.0175(2)	0.0203(2)	-0.00186(18)	-0.00273(18)	-0.00343(16)
Te(3)	0.0194(2)	0.0191(2)	0.0169(2)	-0.00207(17)	-0.00253(17)	0.00058(16)
Te(4)	0.0191(2)	0.0197(2)	0.0164(2)	-0.00020(17)	0.00249(17)	0.00265(16)
Te(5)	0.0189(2)	0.0258(2)	0.0186(2)	0.00358(18)	0.00310(17)	-0.00111(17)
Te(6)	0.0191(2)	0.0173(2)	0.0240(3)	0.00144(18)	0.00123(18)	-0.00206(16)
Te(7)	0.0198(2)	0.0167(2)	0.0174(2)	0.00055(17)	0.00057(17)	0.00247(16)
Te(8)	0.0206(2)	0.0205(2)	0.0172(2)	0.00307(17)	-0.00178(17)	0.00198(16)
Te(9)	0.0229(2)	0.0178(2)	0.0156(2)	0.00253(17)	0.00198(17)	0.00167(16)
Cl(1)	0.0216(8)	0.0457(11)	0.0367(12)	-0.0013(9)	0.0012(8)	-0.0032(7)
Cl(2)	0.0491(11)	0.0277(9)	0.0270(10)	0.0040(8)	-0.0081(8)	0.0021(8)
Cl(3)	0.0219(8)	0.0253(8)	0.0341(10)	-0.0030(8)	-0.0049(7)	0.0013(6)
Cl(4)	0.0456(11)	0.0191(8)	0.0610(15)	-0.0023(9)	-0.0288(10)	0.0003(8)
Al(1)	0.0240(10)	0.0186(10)	0.0294(13)	0.0022(9)	-0.0078(9)	-0.0003(8)
Cl(5)	0.0339(9)	0.0217(8)	0.0191(9)	0.0006(7)	0.0032(7)	0.0000(7)
Cl(6)	0.0360(10)	0.0295(9)	0.0311(11)	-0.0061(8)	0.0021(8)	0.0090(7)
Cl(7)	0.0534(11)	0.0231(8)	0.0186(10)	-0.0026(7)	0.0011(8)	0.0064(8)
Cl(8)	0.0371(10)	0.0403(11)	0.0325(11)	0.0019(9)	-0.0003(8)	-0.0146(8)
Al(2)	0.0278(10)	0.0177(10)	0.0176(11)	-0.0032(8)	0.0018(8)	-0.0005(8)
Cl(9)	0.0313(9)	0.0398(10)	0.0262(10)	0.0094(8)	-0.0101(8)	-0.0133(8)
Cl(10)	0.0250(8)	0.0375(10)	0.0200(9)	0.0019(7)	-0.0007(7)	-0.0054(7)
Cl(11)	0.0336(10)	0.0207(9)	0.0597(14)	0.0018(9)	-0.0081(9)	-0.0006(7)
Cl(12)	0.0268(9)	0.0315(9)	0.0248(10)	-0.0009(7)	0.0003(7)	0.0004(7)
Al(3)	0.0214(10)	0.0207(10)	0.0243(12)	0.0019(9)	-0.0032(9)	-0.0017(8)

Table A.4: Selected bond lengths for $(Au_6Te_{18})[AlCl_4]_6$. Symmetry transformations used to generate equivalent atoms: (i) $-x$, $-y+1$, $-z+1$.

Atoms 1, 2	Distance / *Å*	Atoms 1, 2	Distance / *Å*
Au(1) — Te(9)	2.6769(5)	Te(5) — Te(6)^{i}	2.9198(6)
Au(1) — Te(4)	2.6800(4)	Te(5) — Te(9)	3.0948(5)
Au(1) — Te(3)	2.6875(4)	Te(6) — Au(3)^{i}	2.6848(5)
Au(1) — Te(1)	2.6879(5)	Te(6) — Te(5)^{i}	2.9199(6)
Au(2) — Te(7)	2.6705(5)	Te(7) — Te(8)	2.7205(6)

continued on next page

Atoms 1, 2	Distance / Å	Atoms 1, 2	Distance / Å
Au(2) — Te(6)	2.6734(5)	Te(8) — Te(9)	2.8726(6)
Au(2) — Te(4)^{i}	2.6820(5)	Cl(1) — Al(1)	2.151(3)
Au(2) — Te(3)	2.6848(5)	Cl(2) — Al(1)	2.122(3)
Au(3) — Te(1)^{i}	2.6706(5)	Cl(3) — Al(1)	2.134(2)
Au(3) — Te(7)	2.6726(4)	Cl(4) — Al(1)	2.140(3)
Au(3) — Te(9)	2.6755(5)	Cl(5) — Al(2)	2.144(3)
Au(3) — Te(6)^{i}	2.6848(5)	Cl(6) — Al(2)	2.142(2)
Te(1) — Au(3)^{i}	2.6705(5)	Cl(7) — Al(2)	2.123(3)
Te(1) — Te(2)	2.7319(6)	Cl(8) — Al(2)	2.123(3)
Te(2) — Te(3)	2.8666(6)	Cl(9) — Al(3)	2.129(3)
Te(2) — Te(6)	3.0939(6)	Cl(10) — Al(3)	2.176(3)
Te(3) — Te(8)	3.0759(6)	Cl(11) — Al(3)	2.117(3)
Te(4) — Au(2)^{i}	2.6818(5)	Cl(12) — Al(3)	2.134(3)
Te(4) — Te(5)	2.7183(6)		

Table A.5: Selected bond angles for $(Au_6Te_{18})[AlCl_4]_6$. Symmetry transformations used to generate equivalent atoms: (i) $-x, -y+1, -z+1$.

Atoms 1, 2, 3	Angle / °	Atoms 1, 2, 3	Angle / °
Te(9) — Au(1) — Te(4)	88.581(14)	Au(2) — Te(6) — Au(3)^{i}	87.523(13)
Te(9) — Au(1) — Te(3)	90.019(14)	Au(2) — Te(6) — Te(5)^{i}	91.975(16)
Te(4) — Au(1) — Te(3)	178.503(15)	Au(3)^{i} — Te(6) — Te(5)^{i}	96.861(16)
Te(9) — Au(1) — Te(1)	178.427(16)	Au(2) — Te(6) — Te(2)	91.971(16)
Te(4) — Au(1) — Te(1)	92.615(14)	Au(3)^{i} — Te(6) — Te(2)	89.367(15)
Te(3) — Au(1) — Te(1)	88.775(14)	Te(5)^{i} — Te(6) — Te(2)	172.764(18)
Te(7) — Au(2) — Te(6)	178.961(17)	Au(2) — Te(7) — Au(3)	92.071(14)
Te(7) — Au(2) — Te(4)^{i}	90.765(14)	Au(2) — Te(7) — Te(8)	98.539(16)
Te(6) — Au(2) — Te(4)^{i}	88.206(15)	Au(3) — Te(7) — Te(8)	95.642(16)
Te(7) — Au(2) — Te(3)	89.799(15)	Te(7) — Te(8) — Te(9)	83.148(16)
Te(6) — Au(2) — Te(3)	91.229(15)	Te(7) — Te(8) — Te(3)	81.157(16)
Te(4)^{i} — Au(2) — Te(3)	179.435(16)	Te(9) — Te(8) — Te(3)	79.173(14)
Te(1)^{i} — Au(3) — Te(7)	89.922(14)	Au(3) — Te(9) — Au(1)	90.204(15)
Te(1)^{i} — Au(3) — Te(9)	177.619(16)	Au(3) — Te(9) — Te(8)	92.101(16)
Te(7) — Au(3) — Te(9)	87.944(14)	Au(1) — Te(9) — Te(8)	97.884(16)
Te(1)^{i} — Au(3) — Te(6)^{i}	90.987(15)	Au(3) — Te(9) — Te(5)	93.011(15)
Te(7) — Au(3) — Te(6)^{i}	178.933(17)	Au(1) — Te(9) — Te(5)	91.150(15)

continued on next page

Atoms 1, 2, 3	Angle / °	Atoms 1, 2, 3	Angle / °
Te(9) — Au(3) — Te(6)^{i}	91.137(15)	Te(8) — Te(9) — Te(5)	169.60(2)
Au(3)^{i} — Te(1) — Au(1)	89.762(14)	Cl(2) — Al(1) — Cl(3)	112.57(11)
Au(3)^{i} — Te(1) — Te(2)	97.885(17)	Cl(2) — Al(1) — Cl(4)	110.12(12)
Au(1) — Te(1) — Te(2)	94.407(16)	Cl(3) — Al(1) — Cl(4)	108.38(10)
Te(1) — Te(2) — Te(3)	84.351(16)	Cl(2) — Al(1) — Cl(1)	107.88(11)
Te(1) — Te(2) — Te(6)	81.673(16)	Cl(3) — Al(1) — Cl(1)	107.74(11)
Te(3) — Te(2) — Te(6)	79.849(15)	Cl(4) — Al(1) — Cl(1)	110.12(12)
Au(2) — Te(3) — Au(1)	89.684(14)	Cl(8) — Al(2) — Cl(7)	109.59(11)
Au(2) — Te(3) — Te(2)	96.949(17)	Cl(8) — Al(2) — Cl(6)	110.15(11)
Au(1) — Te(3) — Te(2)	91.400(15)	Cl(7) — Al(2) — Cl(6)	106.63(11)
Au(2) — Te(3) — Te(8)	90.071(15)	Cl(8) — Al(2) — Cl(5)	107.74(11)
Au(1) — Te(3) — Te(8)	92.923(14)	Cl(7) — Al(2) — Cl(5)	111.04(11)
Te(2) — Te(3) — Te(8)	171.78(2)	Cl(6) — Al(2) — Cl(5)	111.71(11)
Au(1) — Te(4) — Au(2)^{i}	90.783(14)	Cl(11) — Al(3) — Cl(9)	112.08(11)
Au(1) — Te(4) — Te(5)	99.898(16)	Cl(11) — Al(3) — Cl(12)	110.67(11)
Au(2)^{i} — Te(4) — Te(5)	96.410(17)	Cl(9) — Al(3) — Cl(12)	110.14(11)
Te(4) — Te(5) — Te(6)^{i}	82.675(16)	Cl(11) — Al(3) — Cl(10)	108.34(12)
Te(4) — Te(5) — Te(9)	79.818(15)	Cl(9) — Al(3) — Cl(10)	109.70(10)
Te(6)^{i} — Te(5) — Te(9)	78.990(15)	Cl(12) — Al(3) — Cl(10)	105.69(10)

A.1.2 $(Au_6Te_{18})[AlBr_4]_6$

Table A.6: Crystal data and structure refinement for $(Au_6Te_{18})[AlBr_4]_6$.

Empirical formula	$Al_6\,Au_6\,Br_{24}\,Te_{18}$
Formula weight / $g \cdot mol^{-1}$	5558.32
Temperature / K	123(2)
Crystal system; space group	Orthorhombic; *Pbca*
Lattice constants / $Å$	a = 22.8174(2)
	b = 12.9160(1)
	c = 23.4623(1)
Volume / $Å^3$	6914.56(9)
Z; F(000); calc. density / $g \cdot cm^{-3}$	4; 9312; 5.339
Wavelength	$Mo_{K\alpha}$ (λ = 0.71073 Å)
Crystal size / mm^3	0.1 × 0.08 × 0.06
Theta range for data collection / °	$2.948 \leq \theta \leq 27.493$
Limiting indices	$-29 \leq h \leq 29$; $-16 \leq k \leq 16$; $-30 \leq l \leq 30$
Reflections collected / unique	237515 / 7926
Completeness to θ = 25.242°	99.9 %
R_{int}; R_σ	0.0920; 0.0208
Absorption coefficient / mm^{-1}	34.088; Semi-empirical from equivalents
Max. / min. transmission	0.0752 / 0.0248
Refinement method	Full-matrix least-squares on F^2
Data / restraints / parameters	7926 / 0 / 244
R indices (all data) R_1; wR_2	0.0301; 0.0498
R indices $[I > 4\sigma(I)]$ R_1; wR_2	0.0239; 0.0483; n = 7046 reflections
Goodness-of-fit for F^2	1.187
Largest diff. peak / $e^- \cdot Å^{-3}$	+1.273 (0.91 Å from Au3)
	-1.618 (0.78 Å from Au1)
Avg. diff. density / $e^- \cdot Å^{-3}$	0.295

Table A.7: Fractional coordinates and equivalent isotropic displacement parameter U_{eq} for the independent atoms in the structure of $(Au_6Te_{18})[AlBr_4]_6$.

Atom	Wyck.	Site	x / a	y / b	z / c	U_{eq} / $Å^2$
Au(1)	8*c*	1	0.00486(2)	0.42599(2)	0.39136(2)	0.01915(6)
Au(2)	8*c*	1	-0.11733(2)	0.51274(2)	0.49031(2)	0.01853(6)
Au(3)	8*c*	1	0.01627(2)	0.69130(2)	0.46189(2)	0.01863(6)
Te(1)	8*c*	1	-0.01049(2)	0.23355(3)	0.43250(2)	0.02026(9)
Te(2)	8*c*	1	-0.12785(2)	0.22965(3)	0.40755(2)	0.02183(9)
Te(3)	8*c*	1	-0.11199(2)	0.44302(3)	0.38255(2)	0.01973(9)
Te(4)	8*c*	1	0.12198(2)	0.41688(3)	0.40260(2)	0.02031(9)
Te(5)	8*c*	1	0.15455(2)	0.60001(4)	0.35455(2)	0.02287(9)
Te(6)	8*c*	1	-0.13333(2)	0.32186(3)	0.53164(2)	0.02072(9)
Te(7)	8*c*	1	-0.10014(2)	0.70734(3)	0.45576(2)	0.01925(9)
Te(8)	8*c*	1	-0.10362(2)	0.67391(3)	0.34066(2)	0.02108(9)
Te(9)	8*c*	1	0.01632(2)	0.62071(3)	0.35467(2)	0.01990(9)
Br(1)	8*c*	1	-0.25158(3)	-0.05973(6)	-0.04236(3)	0.02768(15)
Br(2)	8*c*	1	-0.30450(4)	-0.09346(6)	0.10584(3)	0.03252(17)
Br(3)	8*c*	1	-0.40594(3)	0.00699(5)	-0.01305(3)	0.02673(15)
Br(4)	8*c*	1	-0.28937(3)	0.17559(5)	0.04816(3)	0.03228(17)
Al(1)	8*c*	1	-0.31349(9)	0.00707(16)	0.02665(9)	0.0235(4)
Br(5)	8*c*	1	0.00075(3)	0.32152(5)	0.26626(3)	0.02386(14)
Br(6)	8*c*	1	-0.08104(3)	0.56620(5)	0.22073(3)	0.02788(15)
Br(7)	8*c*	1	-0.01957(3)	0.40025(6)	0.11222(3)	0.02882(16)
Br(8)	8*c*	1	0.08381(3)	0.54488(6)	0.20760(3)	0.03265(17)
Al(2)	8*c*	1	-0.00268(9)	0.45794(15)	0.20305(9)	0.0208(4)
Br(9)	8*c*	1	-0.32195(3)	0.29815(6)	0.22127(3)	0.02868(16)
Br(10)	8*c*	1	-0.26166(3)	0.30569(6)	0.37062(3)	0.02573(15)
Br(11)	8*c*	1	-0.24553(3)	0.53868(5)	0.27685(3)	0.03051(16)
Br(12)	8*c*	1	-0.15961(3)	0.29486(5)	0.24825(3)	0.02546(14)
Al(3)	8*c*	1	-0.24807(9)	0.36290(16)	0.27648(9)	0.0218(4)

Table A.8: Anisotropic displacement parameters U_{ij} / $Å^2$ for the independent atoms in the structure of $(Au_6Te_{18})[AlBr_4]_6$.

Atom	U_{11}	U_{22}	U_{33}	U_{23}	U_{13}	U_{12}
Au(1)	0.02023(13)	0.01877(12)	0.01845(12)	-0.00001(10)	0.00001(9)	0.00027(10)

continued on next page

Atom	U_{11}	U_{22}	U_{33}	U_{23}	U_{13}	U_{12}
Au(2)	0.01915(12)	0.01872(12)	0.01771(12)	0.00036(9)	0.00053(9)	0.00003(9)
Au(3)	0.01887(12)	0.01825(12)	0.01875(12)	0.00068(9)	-0.00001(9)	-0.00005(9)
Te(1)	0.0222(2)	0.0181(2)	0.0204(2)	-0.00081(16)	-0.00080(17)	0.00039(17)
Te(2)	0.0236(2)	0.0190(2)	0.0228(2)	-0.00163(17)	-0.00272(17)	-0.00271(17)
Te(3)	0.0199(2)	0.0209(2)	0.0184(2)	-0.00117(16)	-0.00167(16)	0.00016(17)
Te(4)	0.0209(2)	0.0217(2)	0.0183(2)	-0.00033(17)	0.00152(16)	0.00258(17)
Te(5)	0.0202(2)	0.0282(2)	0.0202(2)	0.00330(18)	0.00250(17)	-0.00061(18)
Te(6)	0.0189(2)	0.0199(2)	0.0233(2)	0.00183(17)	0.00079(17)	-0.00126(17)
Te(7)	0.0193(2)	0.0185(2)	0.0200(2)	0.00023(16)	0.00046(16)	0.00135(16)
Te(8)	0.0210(2)	0.0227(2)	0.0195(2)	0.00306(17)	-0.00165(16)	0.00118(17)
Te(9)	0.0222(2)	0.0195(2)	0.0180(2)	0.00172(16)	0.00071(16)	0.00103(17)
Br(1)	0.0218(3)	0.0302(4)	0.0310(4)	-0.0037(3)	0.0012(3)	-0.0014(3)
Br(2)	0.0421(4)	0.0293(4)	0.0262(4)	0.0041(3)	-0.0037(3)	0.0030(3)
Br(3)	0.0220(3)	0.0256(3)	0.0327(4)	-0.0007(3)	-0.0043(3)	-0.0004(3)
Br(4)	0.0300(4)	0.0211(3)	0.0458(4)	-0.0044(3)	-0.0127(3)	0.0014(3)
Al(1)	0.0231(10)	0.0206(10)	0.0268(11)	-0.0001(8)	-0.0022(8)	0.0005(8)
Br(5)	0.0288(4)	0.0217(3)	0.0211(3)	0.0004(3)	0.0017(3)	0.0013(3)
Br(6)	0.0290(4)	0.0251(4)	0.0295(4)	-0.0062(3)	0.0004(3)	0.0057(3)
Br(7)	0.0392(4)	0.0256(4)	0.0217(3)	-0.0048(3)	-0.0020(3)	0.0047(3)
Br(8)	0.0288(4)	0.0346(4)	0.0346(4)	0.0030(3)	-0.0016(3)	-0.0106(3)
Al(2)	0.0225(10)	0.0187(10)	0.0211(10)	-0.0019(8)	0.0008(8)	-0.0003(8)
Br(9)	0.0284(4)	0.0322(4)	0.0254(3)	0.0068(3)	-0.0078(3)	-0.0083(3)
Br(10)	0.0247(3)	0.0306(4)	0.0219(3)	0.0028(3)	-0.0005(3)	-0.0028(3)
Br(11)	0.0292(4)	0.0195(3)	0.0428(4)	0.0025(3)	-0.0027(3)	-0.0006(3)
Br(12)	0.0242(3)	0.0258(3)	0.0263(3)	-0.0005(3)	0.0009(3)	0.0017(3)
Al(3)	0.0212(10)	0.0201(10)	0.0240(10)	0.0021(8)	-0.0017(8)	-0.0013(8)

Table A.9: Selected bond lengths for $(Au_6Te_{18})[AlBr_4]_6$. Symmetry transformations used to generate equivalent atoms: (i): $-x$, $-y+1$, $-z+1$.

Atoms 1, 2	Distance / *Å*	Atoms 1, 2	Distance / *Å*
Au(1)-Te(9)	2.6711(5)	Te(5)-Te(6)^{i}	2.8953(6)
Au(1)-Te(3)	2.6832(5)	Te(5)-Te(9)	3.1655(6)
Au(1)-Te(4)	2.6880(5)	Te(6)-Au(3)^{i}	2.6808(5)
Au(1)-Te(1)	2.6893(5)	Te(6)-Te(5)^{i}	2.8953(6)
Au(2)-Te(7)	2.6700(5)	Te(7)-Te(8)	2.7359(6)

continued on next page

Atoms 1, 2	Distance / *Å*	Atoms 1, 2	Distance / *Å*
Au(2)-Te(4)^{i}	2.6742(5)	Te(8)-Te(9)	2.8406(6)
Au(2)-Te(6)	2.6743(5)	Br(1)-Al(1)	2.315(2)
Au(2)-Te(3)	2.6867(5)	Br(2)-Al(1)	2.276(2)
Au(3)-Te(1)^{i}	2.6643(5)	Br(3)-Al(1)	2.306(2)
Au(3)-Te(7)	2.6681(5)	Br(4)-Al(1)	2.301(2)
Au(3)-Te(9)	2.6757(5)	Br(5)-Al(2)	2.304(2)
Au(3)-Te(6)^{i}	2.6808(5)	Br(6)-Al(2)	2.308(2)
Te(1)-Au(3)^{i}	2.6643(5)	Br(7)-Al(2)	2.290(2)
Te(1)-Te(2)	2.7416(6)	Br(8)-Al(2)	2.273(2)
Te(2)-Te(3)	2.8407(6)	Br(9)-Al(3)	2.285(2)
Te(2)-Te(6)	3.1482(6)	Br(10)-Al(3)	2.350(2)
Te(3)-Te(8)	3.1457(6)	Br(11)-Al(3)	2.271(2)
Te(4)-Au(2)^{i}	2.6741(5)	Br(12)-Al(3)	2.299(2)
Te(4)-Te(5)	2.7235(6)		

Table A.10: Selected bond angles for $(Au_6Te_{18})[AlBr_4]_6$. Symmetry transformations used to generate equivalent atoms: (i): $-x$, $-y+1$, $-z+1$.

Atoms 1, 2, 3	Angle / °	Atoms 1, 2, 3	Angle / °
Te(9)-Au(1)-Te(3)	89.727(15)	Au(2)-Te(6)-Au(3)^{i}	86.730(15)
Te(9)-Au(1)-Te(4)	88.599(15)	Au(2)-Te(6)-Te(5)^{i}	92.058(17)
Te(3)-Au(1)-Te(4)	177.503(17)	Au(3)^{i}-Te(6)-Te(5)^{i}	97.850(17)
Te(9)-Au(1)-Te(1)	177.023(17)	Au(2)-Te(6)-Te(2)	90.457(15)
Te(3)-Au(1)-Te(1)	88.508(15)	Au(3)^{i}-Te(6)-Te(2)	89.357(15)
Te(4)-Au(1)-Te(1)	93.086(15)	Te(5)^{i}-Te(6)-Te(2)	172.49(2)
Te(7)-Au(2)-Te(4)^{i}	88.343(15)	Au(3)-Te(7)-Au(2)	93.252(15)
Te(7)-Au(2)-Te(6)	176.391(17)	Au(3)-Te(7)-Te(8)	94.004(17)
Te(4)^{i}-Au(2)-Te(6)	88.124(15)	Au(2)-Te(7)-Te(8)	98.444(17)
Te(7)-Au(2)-Te(3)	91.326(15)	Te(7)-Te(8)-Te(9)	84.032(17)
Te(4)^{i}-Au(2)-Te(3)	179.569(18)	Te(7)-Te(8)-Te(3)	80.970(16)
Te(6)-Au(2)-Te(3)	92.204(15)	Te(9)-Te(8)-Te(3)	78.056(16)
Te(1)^{i}-Au(3)-Te(7)	88.432(15)	Au(1)-Te(9)-Au(3)	91.022(14)
Te(1)^{i}-Au(3)-Te(9)	176.830(17)	Au(1)-Te(9)-Te(8)	99.832(17)
Te(7)-Au(3)-Te(9)	88.635(15)	Au(3)-Te(9)-Te(8)	91.489(16)
Te(1)^{i}-Au(3)-Te(6)^{i}	91.131(15)	Au(1)-Te(9)-Te(5)	91.045(15)
Te(7)-Au(3)-Te(6)^{i}	179.170(17)	Au(3)-Te(9)-Te(5)	91.722(15)

continued on next page

Atoms 1, 2, 3	Angle / °	Atoms 1, 2, 3	Angle / °
Te(9)-Au(3)-Te(6)^{i}	91.786(15)	Te(8)-Te(9)-Te(5)	168.60(2)
Au(3)^{i}-Te(1)-Au(1)	90.205(15)	Br(2)-Al(1)-Br(4)	109.81(9)
Au(3)^{i}-Te(1)-Te(2)	99.034(17)	Br(2)-Al(1)-Br(3)	114.32(9)
Au(1)-Te(1)-Te(2)	93.874(17)	Br(4)-Al(1)-Br(3)	107.93(9)
Te(1)-Te(2)-Te(3)	84.365(17)	Br(2)-Al(1)-Br(1)	107.66(9)
Te(1)-Te(2)-Te(6)	80.463(16)	Br(4)-Al(1)-Br(1)	111.10(9)
Te(3)-Te(2)-Te(6)	80.155(15)	Br(3)-Al(1)-Br(1)	105.99(9)
Au(1)-Te(3)-Au(2)	90.000(14)	Br(8)-Al(2)-Br(7)	110.52(9)
Au(1)-Te(3)-Te(2)	91.787(17)	Br(8)-Al(2)-Br(5)	108.54(9)
Au(2)-Te(3)-Te(2)	97.184(16)	Br(7)-Al(2)-Br(5)	110.84(8)
Au(1)-Te(3)-Te(8)	92.375(16)	Br(8)-Al(2)-Br(6)	111.40(9)
Au(2)-Te(3)-Te(8)	88.797(15)	Br(7)-Al(2)-Br(6)	103.54(8)
Te(2)-Te(3)-Te(8)	172.71(2)	Br(5)-Al(2)-Br(6)	111.96(9)
Au(2)^{i}-Te(4)-Au(1)	92.164(15)	Br(11)-Al(3)-Br(9)	112.76(9)
Au(2)^{i}-Te(4)-Te(5)	95.996(17)	Br(11)-Al(3)-Br(12)	111.15(9)
Au(1)-Te(4)-Te(5)	101.108(17)	Br(9)-Al(3)-Br(12)	110.16(9)
Te(4)-Te(5)-Te(6)^{i}	82.841(17)	Br(11)-Al(3)-Br(10)	108.31(9)
Te(4)-Te(5)-Te(9)	78.528(16)	Br(9)-Al(3)-Br(10)	108.69(9)
Te(6)^{i}-Te(5)-Te(9)	78.643(15)	Br(12)-Al(3)-Br(10)	105.46(8)

A.1.3 $(Au_6Te_{18})[ZrCl_6]_3$

Table A.11: Crystal data and structure refinement for $(Au_6Te_{18})[ZrCl_6]_3$.

Empirical formula	$Au_6\,Cl_{18}\,Te_{18}\,Zr_3$
Formula weight / $g \cdot mol^{-1}$	4390.36
Temperature / K	123(2)
Crystal system; space group	Monoclinic; Cc
Lattice constants / $Å$	a = 16.9079(3)
	b = 18.4442(3); β = 90.6160(10)°
	c = 17.4618(3)
Volume / $Å^3$	5445.19(16)
Z; F(000); calc. density / $g \cdot cm^{-3}$	4; 7344; 5.355
Wavelength	$Mo_{K\alpha}$ (λ = 0.71073 Å)
Crystal size / mm^3	0.050 × 0.040 × 0.035
Theta range for data collection / °	$3.213 \leq \theta \leq 27.463$
Limiting indices	$-21 \leq h \leq 21$; $-23 \leq k \leq 23$; $-22 \leq l \leq 22$
Reflections collected / unique	71853 / 12424
Completeness to θ = 25.242°	99.8 %
R_{int}; R_σ	0.0642; 0.0451
Absorption coefficient / mm^{-1}	26.996; Semi-empirical from equivalents
Max. / min. transmission	0.0937 / 0.0572
Refinement method	Full-matrix least-squares on F^2
Data / restraints / parameters	12424 / 2 / 407
R indices (all data) R_1; wR_2	0.0407; 0.0569
R indices $[I > 4\sigma(I)]$ R_1; wR_2	0.0294; 0.0543; n = 10581 reflections
Goodness-of-fit for F^2	1.011
Flack x	-0.005(4) (4591 reflections; Parson's method)
Largest diff. peak / $e^- \cdot Å^{-3}$	+1.494 (1.04 Å from Au3)
	-1.320 (0.50 Å from Au4)
Avg. diff. density / $e^- \cdot Å^{-3}$	0.239

Table A.12: Fractional coordinates and equivalent isotropic displacement parameter U_{eq} for the independent atoms in the structure of $(Au_6Te_{18})[ZrCl_6]_3$.

Atom	Wyck.	Site	x / a	y / b	z / c	U_{eq} / $Å^2$
Au(1)	4*a*	1	0.13480(5)	0.18570(4)	0.08086(5)	0.01937(18)
Au(2)	4*a*	1	0.35290(5)	0.14567(4)	0.05372(5)	0.01983(18)
Au(3)	4*a*	1	0.27600(5)	0.33204(4)	0.12245(5)	0.01989(19)
Au(4)	4*a*	1	0.86510(5)	0.19253(4)	0.42024(5)	0.01934(18)
Au(5)	4*a*	1	0.64774(5)	0.15527(4)	0.44556(5)	0.01932(19)
Au(6)	4*a*	1	0.72285(5)	0.34056(4)	0.37741(5)	0.02001(19)
Te(1)	4*a*	1	0.16779(9)	0.26307(7)	0.20771(8)	0.0215(3)
Te(2)	4*a*	1	0.26197(9)	0.15983(7)	0.27350(9)	0.0243(3)
Te(3)	4*a*	1	0.23602(9)	0.08467(7)	0.13356(8)	0.0201(3)
Te(4)	4*a*	1	0.96840(9)	0.29012(7)	0.47467(8)	0.0210(3)
Te(5)	4*a*	1	0.52093(9)	0.28805(7)	0.09718(9)	0.0228(3)
Te(6)	4*a*	1	0.38336(9)	0.23495(7)	0.17180(8)	0.0215(3)
Te(7)	4*a*	1	0.17639(9)	0.43294(7)	0.06458(8)	0.0214(3)
Te(8)	4*a*	1	0.79321(9)	0.01474(7)	0.00261(9)	0.0230(3)
Te(9)	4*a*	1	0.39153(9)	0.39401(7)	0.04105(8)	0.0207(3)
Te(10)	4*a*	1	0.83550(9)	0.27525(7)	0.29611(8)	0.0221(3)
Te(11)	4*a*	1	0.74648(9)	0.16986(7)	0.22698(8)	0.0233(3)
Te(12)	4*a*	1	0.76387(9)	0.09290(7)	0.36632(8)	0.0201(3)
Te(13)	4*a*	1	0.03038(8)	0.28212(7)	0.02337(8)	0.0207(3)
Te(14)	4*a*	1	0.48015(9)	0.29684(7)	0.40036(8)	0.0218(3)
Te(15)	4*a*	1	0.61682(9)	0.24293(7)	0.32639(8)	0.0212(3)
Te(16)	4*a*	1	0.82010(9)	0.44266(7)	0.43553(8)	0.0216(3)
Te(17)	4*a*	1	0.70368(9)	0.47778(7)	0.00053(8)	0.0227(3)
Te(18)	4*a*	1	0.60731(9)	0.40048(7)	0.45950(8)	0.0204(3)
Zr(1)	4*a*	1	0.49741(15)	-0.00527(8)	0.23792(11)	0.0209(4)
Zr(2)	4*a*	1	-0.00383(17)	0.01471(7)	0.24923(16)	0.0184(3)
Zr(3)	4*a*	1	0.75063(17)	0.24651(12)	-0.00206(17)	0.0177(3)
Cl(1)	4*a*	1	0.4874(3)	0.0425(3)	0.1070(2)	0.0353(11)
Cl(2)	4*a*	1	0.5243(3)	-0.1269(3)	0.1799(3)	0.0419(12)
Cl(3)	4*a*	1	0.5106(3)	-0.0610(3)	0.3640(3)	0.0559(15)
Cl(4)	4*a*	1	0.4747(3)	0.1123(3)	0.2948(3)	0.0436(12)
Cl(5)	4*a*	1	0.3547(3)	-0.0285(3)	0.2371(3)	0.0340(11)
Cl(6)	4*a*	1	0.6408(3)	0.0188(3)	0.2363(3)	0.0354(11)

continued on next page

Atom	Wyck.	Site	x / a	y / b	z / c	U_{eq} / $Å^2$
Cl(7)	4*a*	1	-0.0040(5)	0.14493(19)	0.2502(5)	0.0347(9)
Cl(8)	4*a*	1	0.0334(4)	0.0107(3)	0.1128(3)	0.0292(13)
Cl(9)	4*a*	1	0.4972(5)	0.37653(18)	0.2461(4)	0.0289(8)
Cl(10)	4*a*	1	0.9604(4)	0.0083(3)	0.3853(3)	0.0298(13)
Cl(11)	4*a*	1	0.8574(3)	0.0013(3)	0.2126(3)	0.0290(13)
Cl(12)	4*a*	1	0.1363(4)	0.0013(3)	0.2861(3)	0.0291(13)
Cl(13)	4*a*	1	0.6633(3)	0.1506(3)	0.0433(3)	0.0235(12)
Cl(14)	4*a*	1	0.7250(3)	0.3181(3)	0.1155(3)	0.0244(12)
Cl(15)	4*a*	1	0.3406(3)	0.1552(3)	0.4561(3)	0.0222(12)
Cl(16)	4*a*	1	0.2759(3)	0.3231(3)	0.3808(3)	0.0258(12)
Cl(17)	4*a*	1	0.1378(3)	0.1934(3)	0.4328(3)	0.0254(12)
Cl(18)	4*a*	1	0.8636(3)	0.1863(3)	0.0618(3)	0.0220(11)

Table A.13: Anisotropic displacement parameters U_{ij} / $Å^2$ for the independent atoms in the structure of $(Au_6Te_{18})[ZrCl_6]_3$.

Atom	U_{11}	U_{22}	U_{33}	U_{23}	U_{13}	U_{12}
Au(1)	0.0192(5)	0.0192(4)	0.0197(5)	-0.0001(3)	0.0007(3)	-0.0005(3)
Au(2)	0.0197(5)	0.0200(4)	0.0198(5)	-0.0001(3)	0.0003(3)	-0.0003(3)
Au(3)	0.0204(5)	0.0203(4)	0.0190(5)	-0.0015(3)	0.0011(4)	-0.0008(3)
Au(4)	0.0203(5)	0.0193(4)	0.0185(5)	0.0003(3)	0.0006(3)	0.0011(3)
Au(5)	0.0184(5)	0.0181(4)	0.0214(5)	0.0000(3)	-0.0005(3)	0.0003(3)
Au(6)	0.0211(5)	0.0197(4)	0.0192(5)	0.0013(3)	0.0008(4)	0.0004(3)
Te(1)	0.0212(8)	0.0234(7)	0.0200(8)	-0.0026(5)	0.0027(6)	-0.0018(5)
Te(2)	0.0287(8)	0.0270(7)	0.0173(8)	0.0013(5)	0.0000(6)	-0.0026(6)
Te(3)	0.0209(8)	0.0196(6)	0.0198(8)	0.0020(5)	0.0009(6)	-0.0011(6)
Te(4)	0.0195(8)	0.0210(7)	0.0227(8)	0.0007(5)	0.0017(6)	0.0000(6)
Te(5)	0.0184(8)	0.0250(7)	0.0250(9)	-0.0003(6)	-0.0004(6)	-0.0009(6)
Te(6)	0.0212(8)	0.0224(7)	0.0210(8)	-0.0008(5)	-0.0016(6)	-0.0015(6)
Te(7)	0.0214(8)	0.0192(6)	0.0237(8)	-0.0021(5)	0.0027(6)	0.0010(5)
Te(8)	0.0266(9)	0.0169(6)	0.0255(8)	-0.0012(5)	-0.0002(6)	-0.0013(5)
Te(9)	0.0209(8)	0.0198(6)	0.0213(8)	-0.0021(6)	0.0001(6)	-0.0028(6)
Te(10)	0.0239(8)	0.0223(7)	0.0200(8)	0.0027(5)	0.0027(6)	0.0011(5)
Te(11)	0.0290(8)	0.0235(6)	0.0173(8)	-0.0005(5)	0.0003(6)	0.0040(6)
Te(12)	0.0225(9)	0.0181(6)	0.0198(8)	-0.0014(5)	0.0000(6)	0.0011(5)
Te(13)	0.0175(8)	0.0208(7)	0.0237(8)	-0.0012(5)	0.0011(6)	0.0001(6)

continued on next page

Atom	U_{11}	U_{22}	U_{33}	U_{23}	U_{13}	U_{12}
Te(14)	0.0186(8)	0.0226(7)	0.0242(8)	0.0016(5)	-0.0021(6)	0.0011(5)
Te(15)	0.0213(8)	0.0225(7)	0.0198(8)	0.0014(5)	-0.0015(6)	0.0013(5)
Te(16)	0.0222(8)	0.0215(7)	0.0211(8)	0.0022(5)	0.0013(6)	-0.0018(5)
Te(17)	0.0251(9)	0.0175(6)	0.0257(8)	0.0002(5)	0.0007(6)	-0.0007(5)
Te(18)	0.0216(8)	0.0182(6)	0.0213(8)	0.0011(5)	0.0006(6)	0.0020(6)
Zr(1)	0.0200(7)	0.0197(7)	0.0229(13)	0.0010(7)	0.0025(8)	0.0028(8)
Zr(2)	0.0193(7)	0.0174(7)	0.0185(6)	0.0009(10)	-0.0004(5)	0.0005(10)
Zr(3)	0.0175(6)	0.0169(7)	0.0188(6)	0.0017(5)	0.0001(5)	-0.0007(5)
Cl(1)	0.030(2)	0.045(3)	0.032(2)	0.015(2)	0.0059(19)	0.012(2)
Cl(2)	0.043(3)	0.029(3)	0.053(3)	-0.010(2)	-0.008(2)	0.007(2)
Cl(3)	0.048(3)	0.079(4)	0.041(3)	0.028(3)	0.007(2)	0.024(3)
Cl(4)	0.046(3)	0.035(3)	0.050(3)	-0.016(2)	-0.001(2)	0.009(2)
Cl(5)	0.024(2)	0.038(3)	0.041(3)	0.009(2)	0.0009(19)	-0.003(2)
Cl(6)	0.025(2)	0.046(3)	0.036(3)	-0.008(2)	-0.0004(19)	-0.002(2)
Cl(7)	0.036(2)	0.0208(19)	0.048(2)	-0.004(3)	-0.0059(17)	0.002(3)
Cl(8)	0.031(4)	0.035(3)	0.021(3)	0.003(2)	0.000(2)	-0.008(2)
Cl(9)	0.039(2)	0.0198(18)	0.028(2)	-0.001(3)	-0.0026(16)	0.001(3)
Cl(10)	0.033(4)	0.035(3)	0.021(3)	0.000(2)	0.003(2)	0.010(2)
Cl(11)	0.020(3)	0.038(3)	0.029(3)	-0.006(2)	0.002(2)	0.001(2)
Cl(12)	0.024(3)	0.032(3)	0.031(3)	0.004(2)	-0.004(2)	0.000(2)
Cl(13)	0.024(3)	0.018(2)	0.028(3)	0.003(2)	0.000(2)	-0.002(2)
Cl(14)	0.028(3)	0.025(3)	0.020(3)	0.001(2)	0.002(2)	0.001(2)
Cl(15)	0.018(3)	0.022(2)	0.027(3)	-0.003(2)	0.000(2)	0.0007(19)
Cl(16)	0.026(3)	0.026(3)	0.026(3)	0.005(2)	-0.002(2)	0.000(2)
Cl(17)	0.025(3)	0.024(2)	0.026(3)	-0.005(2)	-0.001(2)	0.000(2)
Cl(18)	0.016(3)	0.024(2)	0.026(3)	0.002(2)	-0.003(2)	0.001(2)

Table A.14: Selected bond lengths for $(Au_6Te_{18})[ZrCl_6]_3$. Symmetry transformations used to generate equivalent atoms: (i) $x-\frac{1}{2}$, $-y+\frac{1}{2}$, $z-\frac{1}{2}$; (ii) $x+\frac{1}{2}$, $-y+\frac{1}{2}$, $z+\frac{1}{2}$; (iii) $x-\frac{1}{2}$, $y-\frac{1}{2}$, z; (iv) $x-\frac{1}{2}$,$y+\frac{1}{2}$,z; (v) $x+\frac{1}{2}$, $y-\frac{1}{2}$, z; (vi) x, $-y$, $z-\frac{1}{2}$; (vii) x, $-y$, $z+\frac{1}{2}$; (viii) x,$-y+1$,$z+\frac{1}{2}$; (ix) x, $-y+1$, $z-\frac{1}{2}$; (x) $x+\frac{1}{2}$, $y+\frac{1}{2}$, z; (xi) $x-1$, y, z; (xii) $x+\frac{1}{2}$, $-y+\frac{1}{2}$, $z-\frac{1}{2}$; (xiii) $x+1$, y, z; (xiv) $x-\frac{1}{2}$, $-y+\frac{1}{2}$, $z+\frac{1}{2}$.

Atoms 1, 2	Distance / Å	Atoms 1, 2	Distance / Å
Au(1) — Te(18)^{i}	2.6856(16)	Te(10) — Te(11)	2.732(2)
Au(1) — Te(3)	2.6861(16)	Te(11) — Te(12)	2.830(2)
Au(1) — Te(1)	2.6884(16)	Te(11) — Te(15)	3.117(2)

continued on next page

Atoms 1, 2	Distance / Å	Atoms 1, 2	Distance / Å
Au(1) — Te(13)	2.6924(16)	Te(12) — Te(8)^{vii}	3.135(2)
Au(2) — Te(3)	2.6785(17)	Te(13) — Au(5)^{i}	2.6787(17)
Au(2) — Te(4)^{i}	2.6794(17)	Te(13) — Te(14)^{i}	2.723(2)
Au(2) — Te(16)^{i}	2.6827(16)	Te(14) — Te(13)^{ii}	2.723(2)
Au(2) — Te(6)	2.6843(16)	Te(14) — Te(15)	2.839(2)
Au(3) — Te(9)	2.6838(18)	Te(14) — Te(18)	3.049(2)
Au(3) — Te(6)	2.6852(16)	Te(16) — Au(2)^{ii}	2.6827(16)
Au(3) — Te(1)	2.6908(17)	Te(16) — Te(17)^{viii}	2.714(2)
Au(3) — Te(7)	2.6990(16)	Te(17) — Te(16)^{ix}	2.714(2)
Au(4) — Te(12)	2.6754(16)	Te(17) — Te(18)^{ix}	2.861(2)
Au(4) — Te(4)	2.6755(16)	Te(17) — Te(3)^{x}	3.091(2)
Au(4) — Te(9)^{ii}	2.6790(16)	Te(18) — Au(1)^{ii}	2.6857(16)
Au(4) — Te(10)	2.6933(16)	Te(18) — Te(17)^{viii}	2.861(2)
Au(5) — Te(12)	2.6742(17)	Zr(1) — Cl(4)	2.418(5)
Au(5) — Te(13)^{ii}	2.6786(17)	Zr(1) — Cl(3)	2.438(5)
Au(5) — Te(7)^{ii}	2.6795(16)	Zr(1) — Cl(5)	2.451(5)
Au(5) — Te(15)	2.6822(16)	Zr(1) — Cl(1)	2.453(5)
Au(6) — Te(18)	2.6743(18)	Zr(1) — Cl(6)	2.465(5)
Au(6) — Te(10)	2.6744(17)	Zr(1) — Cl(2)	2.504(5)
Au(6) — Te(15)	2.6863(17)	Zr(2) — Cl(7)	2.402(4)
Au(6) — Te(16)	2.6914(16)	Zr(2) — Cl(11)^{xi}	2.438(6)
Te(1) — Te(2)	2.728(2)	Zr(2) — Cl(10)^{xi}	2.462(6)
Te(2) — Te(3)	2.839(2)	Zr(2) — Cl(12)	2.462(7)
Te(2) — Te(6)	3.060(2)	Zr(2) — Cl(8)	2.472(6)
Te(3) — Te(17)^{iii}	3.091(2)	Zr(2) — Cl(9)^{iii}	2.549(4)
Te(4) — Au(2)^{ii}	2.6793(17)	Zr(3) — Cl(13)	2.442(6)
Te(4) — Te(5)^{ii}	2.721(2)	Zr(3) — Cl(16)^{xii}	2.456(6)
Te(5) — Te(4)^{i}	2.721(2)	Zr(3) — Cl(18)	2.465(6)
Te(5) — Te(6)	2.852(2)	Zr(3) — Cl(17)^{xii}	2.472(6)
Te(5) — Te(9)	3.086(2)	Zr(3) — Cl(15)^{xii}	2.482(6)
Te(7) — Au(5)^{i}	2.6795(16)	Zr(3) — Cl(14)	2.483(6)
Te(7) — Te(8)^{iv}	2.719(2)	Cl(9) — Zr(2)^{x}	2.549(4)
Te(8) — Te(7)^{v}	2.719(2)	Cl(10) — Zr(2)^{xiii}	2.462(6)
Te(8) — Te(9)^{v}	2.855(2)	Cl(11) — Zr(2)^{xiii}	2.438(6)
Te(8) — Te(12)^{vi}	3.135(2)	Cl(15) — Zr(3)^{xiv}	2.482(6)

continued on next page

Atoms 1, 2	Distance / Å	Atoms 1, 2	Distance / Å
Te(9) — Au(4)^{i}	2.6790(16)	Cl(16) — Zr(3)^{xiv}	2.456(6)
Te(9) — Te(8)^{iv}	2.855(2)	Cl(17) — Zr(3)^{xiv}	2.472(6)

Table A.15: Selected bond angles for $(Au_6Te_{18})[ZrCl_6]_3$. Symmetry transformations used to generate equivalent atoms: (i) $x-\frac{1}{2}$, $-y+\frac{1}{2}$, $z-\frac{1}{2}$; (ii) $x+\frac{1}{2}$, $-y+\frac{1}{2}$, $z+\frac{1}{2}$; (iii) $x-\frac{1}{2}$, $y-\frac{1}{2}$, z; (iv) $x-\frac{1}{2}$,$y+\frac{1}{2}$,z; (v) $x+\frac{1}{2}$, $y-\frac{1}{2}$, z; (vi) x, $-y$, $z-\frac{1}{2}$; (vii) x, $-y$, $z+\frac{1}{2}$; (viii) x,$-y+1$,$z+\frac{1}{2}$; (ix) x, $-y+1$, $z-\frac{1}{2}$; (x) $x+\frac{1}{2}$, $y+\frac{1}{2}$, z; (xi) $x-1$, y, z; (xii) $x+\frac{1}{2}$, $-y+\frac{1}{2}$, $z-\frac{1}{2}$; (xiii) $x+1$, y, z; (xiv) $x-\frac{1}{2}$, $-y+\frac{1}{2}$, $z+\frac{1}{2}$.

Atoms 1, 2, 3	Angle / °	Atoms 1, 2, 3	Angle / °
Te(18)^{i} — Au(1) — Te(3)	87.93(5)	Te(12) — Te(11) — Te(15)	78.77(6)
Te(18)^{i} — Au(1) — Te(1)	175.52(6)	Au(5) — Te(12) — Au(4)	89.60(5)
Te(3) — Au(1) — Te(1)	87.72(5)	Au(5) — Te(12) — Te(11)	99.15(6)
Te(18)^{i} — Au(1) — Te(13)	89.40(5)	Au(4) — Te(12) — Te(11)	91.04(5)
Te(3) — Au(1) — Te(13)	177.22(5)	Au(5) — Te(12) — Te(8)^{vii}	89.47(5)
Te(1) — Au(1) — Te(13)	94.94(5)	Au(4) — Te(12) — Te(8)^{vii}	94.15(5)
Te(3) — Au(2) — Te(4)^{i}	178.61(5)	Te(11) — Te(12) — Te(8)^{vii}	169.97(7)
Te(3) — Au(2) — Te(16)^{i}	89.87(5)	Au(5)^{i} — Te(13) — Au(1)	89.29(5)
Te(4)^{i} — Au(2) — Te(16)^{i}	91.02(5)	Au(5)^{i} — Te(13) — Te(14)^{i}	93.26(6)
Te(3) — Au(2) — Te(6)	89.68(5)	Au(1) — Te(13) — Te(14)^{i}	97.96(5)
Te(4)^{i} — Au(2) — Te(6)	89.41(5)	Te(13)^{ii} — Te(14) — Te(15)	85.59(6)
Te(16)^{i} — Au(2) — Te(6)	179.08(6)	Te(13)^{ii} — Te(14) — Te(18)	81.68(5)
Te(9) — Au(3) — Te(6)	87.74(5)	Te(15) — Te(14) — Te(18)	78.42(5)
Te(9) — Au(3) — Te(1)	175.94(6)	Au(5) — Te(15) — Au(6)	91.32(5)
Te(6) — Au(3) — Te(1)	88.20(5)	Au(5) — Te(15) — Te(14)	90.63(6)
Te(9) — Au(3) — Te(7)	87.87(5)	Au(6) — Te(15) — Te(14)	99.08(6)
Te(6) — Au(3) — Te(7)	175.51(6)	Au(5) — Te(15) — Te(11)	92.24(5)
Te(1) — Au(3) — Te(7)	96.19(5)	Au(6) — Te(15) — Te(11)	90.21(6)
Te(12) — Au(4) — Te(4)	178.88(6)	Te(14) — Te(15) — Te(11)	170.21(7)
Te(12) — Au(4) — Te(9)^{ii}	88.20(5)	Au(2)^{ii} — Te(16) — Au(6)	89.17(5)
Te(4) — Au(4) — Te(9)^{ii}	91.05(5)	Au(2)^{ii} — Te(16) — Te(17)^{viii}	98.71(6)
Te(12) — Au(4) — Te(10)	89.61(5)	Au(6) — Te(16) — Te(17)^{viii}	95.34(6)
Te(4) — Au(4) — Te(10)	91.13(5)	Te(16)^{ix} — Te(17) — Te(18)^{ix}	83.38(6)
Te(9)^{ii} — Au(4) — Te(10)	177.77(6)	Te(16)^{ix} — Te(17) — Te(3)^{x}	81.15(5)
Te(12) — Au(5) — Te(13)^{ii}	179.31(6)	Te(18)^{ix} — Te(17) — Te(3)^{x}	77.48(5)
Te(12) — Au(5) — Te(7)^{ii}	90.72(5)	Au(6) — Te(18) — Au(1)^{ii}	93.28(5)
Te(13)^{ii} — Au(5) — Te(7)^{ii}	89.83(5)	Au(6) — Te(18) — Te(17)^{viii}	92.36(6)

continued on next page

Atoms 1, 2, 3	Angle / °	Atoms 1, 2, 3	Angle / °
Te(12) — Au(5) — Te(15)	89.77(5)	Au(1)^{ii} — Te(18) — Te(17)^{viii}	100.00(6)
Te(13)^{ii} — Au(5) — Te(15)	89.68(5)	Au(6) — Te(18) — Te(14)	94.35(5)
Te(7)^{ii} — Au(5) — Te(15)	179.15(6)	Au(1)^{ii} — Te(18) — Te(14)	90.67(5)
Te(18) — Au(6) — Te(10)	177.61(6)	Te(17)^{viii} — Te(18) — Te(14)	167.05(6)
Te(18) — Au(6) — Te(15)	88.05(5)	Cl(4) — Zr(1) — Cl(3)	91.1(2)
Te(10) — Au(6) — Te(15)	89.92(5)	Cl(4) — Zr(1) — Cl(5)	89.92(19)
Te(18) — Au(6) — Te(16)	87.46(5)	Cl(3) — Zr(1) — Cl(5)	90.70(19)
Te(10) — Au(6) — Te(16)	94.56(5)	Cl(4) — Zr(1) — Cl(1)	92.94(18)
Te(15) — Au(6) — Te(16)	175.51(6)	Cl(3) — Zr(1) — Cl(1)	175.9(2)
Au(1) — Te(1) — Au(3)	86.07(5)	Cl(5) — Zr(1) — Cl(1)	89.94(17)
Au(1) — Te(1) — Te(2)	95.25(6)	Cl(4) — Zr(1) — Cl(6)	90.22(18)
Au(3) — Te(1) — Te(2)	99.54(6)	Cl(3) — Zr(1) — Cl(6)	90.3(2)
Te(1) — Te(2) — Te(3)	83.93(6)	Cl(5) — Zr(1) — Cl(6)	178.94(18)
Te(1) — Te(2) — Te(6)	80.31(5)	Cl(1) — Zr(1) — Cl(6)	89.01(17)
Te(3) — Te(2) — Te(6)	79.63(6)	Cl(4) — Zr(1) — Cl(2)	178.7(2)
Au(2) — Te(3) — Au(1)	90.07(5)	Cl(3) — Zr(1) — Cl(2)	88.4(2)
Au(2) — Te(3) — Te(2)	97.75(6)	Cl(5) — Zr(1) — Cl(2)	91.36(18)
Au(1) — Te(3) — Te(2)	92.76(5)	Cl(1) — Zr(1) — Cl(2)	87.45(17)
Au(2) — Te(3) — Te(17)^{iii}	90.13(5)	Cl(6) — Zr(1) — Cl(2)	88.50(18)
Au(1) — Te(3) — Te(17)^{iii}	94.48(5)	Cl(7) — Zr(2) — Cl(11)^{xi}	95.8(3)
Te(2) — Te(3) — Te(17)^{iii}	169.29(6)	Cl(7) — Zr(2) — Cl(10)^{xi}	92.4(3)
Au(4) — Te(4) — Au(2)^{ii}	90.21(5)	Cl(11)^{xi} — Zr(2) — Cl(10)^{xi}	90.2(2)
Au(4) — Te(4) — Te(5)^{ii}	97.42(5)	Cl(7) — Zr(2) — Cl(12)	95.7(3)
Au(2)^{ii} — Te(4) — Te(5)^{ii}	93.60(6)	Cl(11)^{xi} — Zr(2) — Cl(12)	168.44(13)
Te(4)^{i} — Te(5) — Te(6)	85.20(6)	Cl(10)^{xi} — Zr(2) — Cl(12)	89.3(2)
Te(4)^{i} — Te(5) — Te(9)	82.04(5)	Cl(7) — Zr(2) — Cl(8)	92.1(3)
Te(6) — Te(5) — Te(9)	77.50(5)	Cl(11)^{xi} — Zr(2) — Cl(8)	89.9(2)
Au(2) — Te(6) — Au(3)	92.24(5)	Cl(10)^{xi} — Zr(2) — Cl(8)	175.50(14)
Au(2) — Te(6) — Te(5)	90.60(6)	Cl(12) — Zr(2) — Cl(8)	89.7(2)
Au(3) — Te(6) — Te(5)	100.15(6)	Cl(7) — Zr(2) — Cl(9)^{iii}	179.1(3)
Au(2) — Te(6) — Te(2)	92.50(5)	Cl(11)^{xi} — Zr(2) — Cl(9)^{iii}	84.3(2)
Au(3) — Te(6) — Te(2)	91.88(6)	Cl(10)^{xi} — Zr(2) — Cl(9)^{iii}	88.6(2)
Te(5) — Te(6) — Te(2)	167.45(7)	Cl(12) — Zr(2) — Cl(9)^{iii}	84.2(2)
Au(5)^{i} — Te(7) — Au(3)	88.77(5)	Cl(8) — Zr(2) — Cl(9)^{iii}	87.0(2)
Au(5)^{i} — Te(7) — Te(8)^{iv}	98.87(6)	Cl(13) — Zr(3) — Cl(16)^{xii}	90.2(2)

continued on next page

Atoms 1, 2, 3	Angle / °	Atoms 1, 2, 3	Angle / °
Au(3) — Te(7) — Te(8)^{iv}	94.51(6)	Cl(13) — Zr(3) — Cl(18)	89.76(19)
Te(7)^{v} — Te(8) — Te(9)^{v}	84.11(6)	Cl(16)^{xii} — Zr(3) — Cl(18)	90.0(2)
Te(7)^{v} — Te(8) — Te(12)^{vi}	80.85(5)	Cl(13) — Zr(3) — Cl(17)^{xii}	90.4(2)
Te(9)^{v} — Te(8) — Te(12)^{vi}	76.79(5)	Cl(16)^{xii} — Zr(3) — Cl(17)^{xii}	89.5(2)
Au(4)^{i} — Te(9) — Au(3)	92.70(5)	Cl(18) — Zr(3) — Cl(17)^{xii}	179.5(3)
Au(4)^{i} — Te(9) — Te(8)^{iv}	100.82(6)	Cl(13) — Zr(3) — Cl(15)^{xii}	178.2(3)
Au(3) — Te(9) — Te(8)^{iv}	91.80(6)	Cl(16)^{xii} — Zr(3) — Cl(15)^{xii}	91.4(2)
Au(4)^{i} — Te(9) — Te(5)	89.11(5)	Cl(18) — Zr(3) — Cl(15)^{xii}	89.3(2)
Au(3) — Te(9) — Te(5)	94.57(5)	Cl(17)^{xii} — Zr(3) — Cl(15)^{xii}	90.55(19)
Te(8)^{iv} — Te(9) — Te(5)	167.94(6)	Cl(13) — Zr(3) — Cl(14)	90.3(2)
Au(6) — Te(10) — Au(4)	87.43(5)	Cl(16)^{xii} — Zr(3) — Cl(14)	179.4(2)
Au(6) — Te(10) — Te(11)	99.38(6)	Cl(18) — Zr(3) — Cl(14)	90.4(2)
Au(4) — Te(10) — Te(11)	92.82(6)	Cl(17)^{xii} — Zr(3) — Cl(14)	90.1(2)
Te(10) — Te(11) — Te(12)	85.72(6)	Cl(15)^{xii} — Zr(3) — Cl(14)	88.16(19)
Te(10) — Te(11) — Te(15)	80.43(6)		

A.1.4 $(Au_6Te_{18}Cl)[AlCl_4]_5$

Table A.16: Crystal data and structure refinement for $(Au_6Te_{18}Cl)[AlCl_4]_5$.

Empirical formula	$Al_5\,Au_6\,Cl_{21}\,Te_{18}$
Formula weight / $g \cdot mol^{-1}$	4357.95
Temperature / K	123(2)
Crystal system; space group	Monoclinic; $P2_1/c$
Lattice constants / $Å$	a = 15.3118(2)
	b = 18.8757(3); β = 96.725(1)°
	c = 20.8541(2)
Volume / $Å^3$	5985.8(1)
Z; F(000); calc. density / $g \cdot cm^{-3}$	4; 7328; 4.836
Wavelength	$Mo_{K\alpha}$ (λ = 0.71073 Å)
Crystal size / mm^3	0.063 × 0.058 × 0.052
Theta range for data collection / °	$2.920 \leq \theta \leq 27.490$
Limiting indices	$-19 \leq h \leq 19$; $-24 \leq k \leq 24$; $-26 \leq l \leq 27$
Reflections collected / unique	108944 / 13712
Completeness to θ = 25.242°	99.8 %
R_{int}; R_σ	0.0904; 0.0492
Absorption coefficient / mm^{-1}	24.275; Semi-empirical from equivalents
Max. / min. transmission	0.1898 / 0.1332
Refinement method	Full-matrix least-squares on F^2
Data / restraints / parameters	13712 / 4 / 496
R indices (all data) R_1; wR_2	0.0683; 0.0939
R indices $[I > 4\sigma(I)]$ R_1; wR_2	0.0413; 0.0850; n = 10258 reflections
Goodness-of-fit for F^2	1.071
Largest diff. peak / $e^- \cdot Å^{-3}$	+2.104 (0.97 Å from Al5)
	-2.221 (0.62 Å from Cl24)
Avg. diff. density / $e^- \cdot Å^{-3}$	0.333

Table A.17: Fractional coordinates and equivalent isotropic displacement parameter U_{eq} for the independent atoms in the structure of $(Au_6Te_{18}Cl)[AlCl_4]_5$.

Atom	Wyck.	Site	*SOF*	*x / a*	*y / b*	*z / c*	U_{eq} / Å^2
Au(1)	4*e*	1		0.05221(3)	0.06740(2)	0.11068(2)	0.02187(10)
Au(2)	4*e*	1		0.14607(3)	0.03693(2)	-0.05023(2)	0.02356(10)
Au(3)	4*e*	1		-0.08044(3)	0.11933(2)	-0.04667(2)	0.02402(10)
Te(1)	4*e*	1		0.19942(5)	0.10357(4)	0.06118(3)	0.02533(17)
Te(2)	4*e*	1		-0.03094(5)	0.18594(4)	0.06517(4)	0.02712(17)
Te(3)	4*e*	1		0.13397(5)	-0.05052(4)	0.15713(4)	0.02769(17)
Te(4)	4*e*	1		-0.09258(5)	0.02810(4)	0.16232(3)	0.02723(17)
Te(5)	4*e*	1		-0.06656(5)	-0.15590(4)	0.09682(4)	0.02708(17)
Te(6)	4*e*	1		-0.22662(5)	0.08191(4)	0.00300(4)	0.03016(18)
Te(7)	4*e*	1		-0.18451(6)	0.16337(5)	0.12047(4)	0.0389(2)
Te(8)	4*e*	1		-0.01085(6)	-0.10231(4)	0.21834(4)	0.03175(19)
Te(9)	4*e*	1	0.702(1)	0.30568(8)	-0.00441(7)	0.11193(6)	0.0432(3)
Te(10)	4*e*	1	0.298(1)	0.1299(2)	0.23549(17)	0.02055(14)	0.0575(8)
Cl(21)	4*e*	1	0.251(1)	0.30568(8)	-0.00441(7)	0.11193(6)	0.0432(3)
Cl(22)	4*e*	1	0.249(1)	0.1299(2)	0.23549(17)	0.02055(14)	0.0575(8)
Au(4)	4*e*	1		0.66874(3)	0.51988(3)	0.05057(2)	0.02820(11)
Au(5)	4*e*	1		0.50232(3)	0.37336(3)	0.05717(2)	0.02881(11)
Au(6)	4*e*	1		0.55998(3)	0.44205(3)	-0.10434(2)	0.03085(11)
Te(11)	4*e*	1		0.66945(5)	0.39378(4)	0.10967(4)	0.03120(18)
Te(12)	4*e*	1		0.72767(6)	0.46501(5)	-0.05559(4)	0.0355(2)
Te(13)	4*e*	1		0.66430(6)	0.64783(4)	-0.00475(4)	0.03261(19)
Te(14)	4*e*	1		0.60843(6)	0.57889(5)	0.15359(4)	0.0375(2)
Te(15)	4*e*	1		0.44165(6)	0.68618(5)	0.04795(4)	0.0349(2)
Te(16)	4*e*	1		0.55945(6)	0.56934(5)	-0.16155(4)	0.0363(2)
Te(17)	4*e*	1		0.74315(6)	0.59336(6)	-0.11880(4)	0.0442(2)
Te(18)	4*e*	1		0.60734(6)	0.72205(5)	0.10791(4)	0.0406(2)
Te(19)	4*e*	1	0.645(1)	0.62382(9)	0.44040(8)	0.22536(6)	0.0451(3)
Te(20)	4*e*	1	0.355(1)	0.7406(2)	0.32644(18)	0.00979(16)	0.0751(9)
Cl(23)	4*e*	1	0.254(1)	0.62382(9)	0.44040(8)	0.22536(6)	0.0451(3)
Cl(24)	4*e*	1	0.246(1)	0.7406(2)	0.32644(18)	0.00979(16)	0.0751(9)
Al(1)	4*e*	1		0.4879(3)	0.1938(2)	0.1684(2)	0.0345(9)
Cl(1)	4*e*	1		0.4872(2)	0.08917(17)	0.20686(16)	0.0365(7)
Cl(2A)	4*e*	1	0.53(4)	0.6073(12)	0.2240(12)	0.1418(12)	0.057(5)

continued on next page

Atom	Wyck.	Site	*SOF*	*x / a*	*y / b*	*z / c*	U_{eq} / Å^2
Cl(3A)	4*e*	1	0.53(4)	0.4964(17)	0.2642(7)	0.2493(6)	0.079(5)
Cl(4A)	4*e*	1	0.53(4)	0.3728(10)	0.2178(10)	0.1093(13)	0.067(6)
Cl(2B)	4*e*	1	0.47(4)	0.5999(19)	0.2146(14)	0.1154(14)	0.072(7)
Cl(3B)	4*e*	1	0.47(4)	0.439(2)	0.2700(7)	0.2299(14)	0.093(10)
Cl(4B)	4*e*	1	0.47(4)	0.3983(12)	0.1943(10)	0.0780(11)	0.057(5)
Al(2)	4*e*	1		-0.0470(3)	0.4863(2)	0.11204(18)	0.0328(9)
Cl(5)	4*e*	1		-0.0941(2)	0.54536(19)	0.02810(15)	0.0403(8)
Cl(6)	4*e*	1		-0.1424(2)	0.4978(2)	0.18002(15)	0.0415(8)
Cl(7)	4*e*	1		0.0761(2)	0.5250(2)	0.15699(15)	0.0412(8)
Cl(8)	4*e*	1		-0.0367(4)	0.3761(2)	0.0954(2)	0.0712(14)
Al(3)	4*e*	1		0.7766(2)	0.2380(2)	0.32462(19)	0.0313(8)
Cl(9)	4*e*	1		0.8103(2)	0.29463(18)	0.24183(16)	0.0424(8)
Cl(10)	4*e*	1		0.6911(2)	0.30611(18)	0.37102(17)	0.0419(8)
Cl(11)	4*e*	1		0.8917(2)	0.21883(18)	0.39029(17)	0.0430(8)
Cl(12)	4*e*	1		0.7117(3)	0.14098(18)	0.29726(18)	0.0469(9)
Al(4)	4*e*	1		0.8398(2)	0.7070(2)	0.22994(17)	0.0292(8)
Cl(13)	4*e*	1		0.7916(3)	0.8119(2)	0.2389(2)	0.0606(11)
Cl(14)	4*e*	1		0.9748(2)	0.7021(2)	0.26684(16)	0.0480(9)
Cl(15)	4*e*	1		0.7624(2)	0.6346(2)	0.27817(15)	0.0422(8)
Cl(16)	4*e*	1		0.8266(2)	0.68139(18)	0.12962(14)	0.0384(8)
Al(5)	4*e*	1		0.6120(3)	0.9560(2)	0.1202(2)	0.0395(10)
Cl(17)	4*e*	1		0.5837(3)	1.0437(2)	0.0583(2)	0.0629(11)
Cl(18)	4*e*	1		0.4996(2)	0.90238(19)	0.14587(19)	0.0471(9)
Cl(19)	4*e*	1		0.6822(3)	0.8798(2)	0.0692(2)	0.0620(12)
Cl(20)	4*e*	1		0.6981(2)	0.9872(2)	0.20375(19)	0.0513(9)

Table A.18: Anisotropic displacement parameters U_{ij} / Å^2 for the independent atoms in the structure of $(Au_6Te_{18}Cl)[AlCl_4]_5$.

Atom	U_{11}	U_{22}	U_{33}	U_{23}	U_{13}	U_{12}
Au(1)	0.0249(2)	0.0210(2)	0.0193(2)	-0.00076(16)	0.00140(17)	-0.00293(18)
Au(2)	0.0242(2)	0.0258(2)	0.0205(2)	-0.00183(17)	0.00170(17)	-0.00387(18)
Au(3)	0.0275(2)	0.0214(2)	0.0225(2)	-0.00046(17)	0.00001(17)	-0.00023(18)
Te(1)	0.0262(4)	0.0276(4)	0.0219(4)	-0.0022(3)	0.0014(3)	-0.0082(3)
Te(2)	0.0353(4)	0.0207(4)	0.0245(4)	-0.0034(3)	0.0003(3)	0.0013(3)
Te(3)	0.0353(4)	0.0248(4)	0.0216(4)	0.0008(3)	-0.0027(3)	0.0017(3)

continued on next page

Atom	U_{11}	U_{22}	U_{33}	U_{23}	U_{13}	U_{12}
Te(4)	0.0285(4)	0.0323(4)	0.0213(4)	-0.0048(3)	0.0043(3)	-0.0074(3)
Te(5)	0.0329(4)	0.0235(4)	0.0245(4)	0.0032(3)	0.0018(3)	-0.0062(3)
Te(6)	0.0259(4)	0.0321(4)	0.0329(4)	0.0008(3)	0.0049(3)	0.0041(3)
Te(7)	0.0367(5)	0.0406(5)	0.0391(5)	-0.0110(4)	0.0034(4)	0.0061(4)
Te(8)	0.0420(5)	0.0304(4)	0.0216(4)	0.0038(3)	-0.0013(3)	-0.0094(4)
Te(9)	0.0421(7)	0.0441(7)	0.0422(7)	-0.0112(5)	0.0001(5)	-0.0042(6)
Te(10)	0.071(2)	0.0547(18)	0.0466(16)	-0.0010(13)	0.0037(14)	-0.0223(16)
Cl(21)	0.0421(7)	0.0441(7)	0.0422(7)	-0.0112(5)	0.0001(5)	-0.0042(6)
Cl(22)	0.071(2)	0.0547(18)	0.0466(16)	-0.0010(13)	0.0037(14)	-0.0223(16)
Au(4)	0.0273(2)	0.0306(3)	0.0256(2)	0.00093(18)	-0.00109(18)	-0.0014(2)
Au(5)	0.0296(3)	0.0294(3)	0.0266(2)	0.00291(19)	-0.00028(19)	-0.0008(2)
Au(6)	0.0302(3)	0.0370(3)	0.0248(2)	-0.0027(2)	0.00099(19)	0.0001(2)
Te(11)	0.0305(4)	0.0311(4)	0.0301(4)	0.0026(3)	-0.0045(3)	0.0034(4)
Te(12)	0.0273(4)	0.0473(5)	0.0320(4)	-0.0022(4)	0.0046(3)	0.0003(4)
Te(13)	0.0322(5)	0.0281(4)	0.0357(4)	0.0025(3)	-0.0035(3)	-0.0048(4)
Te(14)	0.0335(5)	0.0511(6)	0.0264(4)	-0.0090(4)	-0.0028(3)	-0.0045(4)
Te(15)	0.0353(5)	0.0319(5)	0.0370(5)	-0.0045(4)	0.0023(4)	0.0020(4)
Te(16)	0.0397(5)	0.0440(5)	0.0257(4)	0.0016(4)	0.0056(4)	-0.0061(4)
Te(17)	0.0353(5)	0.0579(6)	0.0410(5)	0.0148(4)	0.0109(4)	0.0007(4)
Te(18)	0.0442(5)	0.0309(5)	0.0452(5)	-0.0037(4)	-0.0016(4)	-0.0036(4)
Te(19)	0.0422(8)	0.0497(8)	0.0412(7)	-0.0019(6)	-0.0037(6)	0.0006(6)
Te(20)	0.068(2)	0.071(2)	0.085(2)	0.0161(16)	0.0055(16)	0.0087(16)
Cl(23)	0.0422(8)	0.0497(8)	0.0412(7)	-0.0019(6)	-0.0037(6)	0.0006(6)
Cl(24)	0.068(2)	0.071(2)	0.085(2)	0.0161(16)	0.0055(16)	0.0087(16)
Al(1)	0.030(2)	0.025(2)	0.048(2)	0.0024(17)	0.0013(17)	-0.0021(16)
Cl(1)	0.0329(17)	0.0306(17)	0.0459(18)	0.0073(14)	0.0037(14)	-0.0014(13)
Cl(2A)	0.030(5)	0.051(8)	0.092(13)	0.029(8)	0.020(7)	-0.007(4)
Cl(3A)	0.102(12)	0.046(6)	0.082(7)	-0.017(5)	-0.016(7)	0.002(7)
Cl(4A)	0.046(6)	0.061(8)	0.084(11)	0.034(8)	-0.030(7)	-0.025(5)
Cl(2B)	0.077(12)	0.050(8)	0.098(16)	0.029(10)	0.049(11)	0.022(7)
Cl(3B)	0.15(2)	0.038(6)	0.108(15)	-0.016(7)	0.083(16)	-0.004(9)
Cl(4B)	0.052(7)	0.050(7)	0.059(9)	0.031(6)	-0.029(6)	-0.022(6)
Al(2)	0.040(2)	0.030(2)	0.0277(19)	0.0026(15)	0.0023(16)	-0.0029(17)
Cl(5)	0.0429(19)	0.049(2)	0.0278(16)	0.0060(14)	0.0008(13)	0.0016(16)
Cl(6)	0.0391(19)	0.051(2)	0.0357(17)	0.0124(15)	0.0091(14)	-0.0001(16)

continued on next page

Atom	U_{11}	U_{22}	U_{33}	U_{23}	U_{13}	U_{12}
Cl(7)	0.0332(18)	0.056(2)	0.0337(17)	0.0072(15)	0.0018(13)	-0.0028(16)
Cl(8)	0.124(4)	0.031(2)	0.063(3)	-0.0033(18)	0.028(3)	-0.005(2)
Al(3)	0.028(2)	0.026(2)	0.039(2)	-0.0050(16)	-0.0047(16)	-0.0012(16)
Cl(9)	0.047(2)	0.0355(18)	0.0435(19)	-0.0001(14)	-0.0002(15)	-0.0034(15)
Cl(10)	0.0387(19)	0.0345(18)	0.053(2)	-0.0032(15)	0.0072(15)	0.0024(15)
Cl(11)	0.0381(19)	0.0347(18)	0.052(2)	-0.0054(15)	-0.0111(15)	0.0018(15)
Cl(12)	0.051(2)	0.0294(18)	0.056(2)	-0.0020(15)	-0.0141(17)	-0.0116(16)
Al(4)	0.030(2)	0.031(2)	0.0253(18)	0.0024(15)	-0.0009(15)	-0.0034(16)
Cl(13)	0.085(3)	0.043(2)	0.055(2)	-0.0012(18)	0.015(2)	0.017(2)
Cl(14)	0.0324(18)	0.073(3)	0.0361(18)	0.0129(17)	-0.0080(14)	-0.0093(17)
Cl(15)	0.0395(19)	0.058(2)	0.0272(15)	0.0087(15)	-0.0016(13)	-0.0166(17)
Cl(16)	0.050(2)	0.0418(19)	0.0221(14)	0.0035(13)	-0.0010(13)	-0.0130(16)
Al(5)	0.037(2)	0.037(2)	0.047(2)	-0.0004(18)	0.0147(19)	-0.0091(19)
Cl(17)	0.059(3)	0.068(3)	0.063(3)	0.023(2)	0.016(2)	0.004(2)
Cl(18)	0.0368(19)	0.040(2)	0.068(2)	0.0012(17)	0.0219(17)	-0.0068(16)
Cl(19)	0.065(3)	0.044(2)	0.086(3)	-0.011(2)	0.048(2)	-0.0128(19)
Cl(20)	0.040(2)	0.052(2)	0.061(2)	-0.0082(18)	0.0028(17)	0.0035(17)

Table A.19: Selected bond lengths for $(Au_6Te_{18}Cl)[AlCl_4]_5$. Symmetry transformations used to generate equivalent atoms: (i) $-x$, $-y$, $-z$; (ii) $-x+1$, $-y+1$, $-z$.

Atoms 1, 2	Distance / *Å*	Atoms 1, 2	Distance / *Å*
Au(1) — Te(1)	2.6752(9)	Te(11) — Te(19)	2.7346(16)
Au(1) — Te(3)	2.6787(9)	Te(11) — Te(20)	2.769(4)
Au(1) — Te(4)	2.6803(9)	Te(12) — Te(17)	2.7815(13)
Au(1) — Te(2)	2.6916(9)	Te(12) — Te(20)	2.945(3)
Au(2) — Te(5)^{i}	2.6818(9)	Te(13) — Au(5)^{ii}	2.6852(9)
Au(2) — Te(4)^{i}	2.6820(8)	Te(13) — Te(18)	2.9535(13)
Au(2) — Te(1)	2.6839(8)	Te(13) — Te(17)	2.9738(13)
Au(2) — Te(6)^{i}	2.6904(9)	Te(14) — Au(6)^{ii}	2.6908(10)
Au(3) — Te(6)	2.6692(9)	Te(14) — Te(18)	2.8647(13)
Au(3) — Te(2)	2.6798(8)	Te(14) — Te(19)	3.0077(17)
Au(3) — Te(5)^{i}	2.6811(9)	Te(15) — Au(5)^{ii}	2.6916(10)
Au(3) — Te(3)^{i}	2.6874(9)	Te(15) — Au(6)^{ii}	2.6923(10)
Te(1) — Te(9)	2.7419(15)	Te(15) — Te(18)	2.7778(13)
Te(1) — Te(10)	2.800(3)	Te(15) — Te(20)^{ii}	2.916(3)

continued on next page

Atoms 1, 2	Distance / Å	Atoms 1, 2	Distance / Å
Te(2) — Te(7)	2.7706(12)	Te(16) — Au(5)^{ii}	2.6991(10)
Te(2) — Te(10)	2.889(3)	Te(16) — Te(17)	2.8852(13)
Te(3) — Au(3)^{i}	2.6873(9)	Te(16) — Te(19)^{ii}	2.9672(16)
Te(3) — Te(8)	2.8575(12)	Te(19) — Te(16)^{ii}	2.9672(16)
Te(3) — Te(9)	3.0231(15)	Te(20) — Te(15)^{ii}	2.916(3)
Te(4) — Au(2)^{i}	2.6819(8)	Al(1) — Cl(2A)	2.053(18)
Te(4) — Te(8)	2.9407(12)	Al(1) — Cl(4A)	2.078(11)
Te(4) — Te(7)	2.9957(12)	Al(1) — Cl(3B)	2.119(12)
Te(5) — Au(3)^{i}	2.6810(9)	Al(1) — Cl(1)	2.133(5)
Te(5) — Au(2)^{i}	2.6818(9)	Al(1) — Cl(3A)	2.138(13)
Te(5) — Te(8)	2.7688(11)	Al(1) — Cl(2B)	2.18(2)
Te(5) — Te(10)^{i}	2.938(3)	Al(1) — Cl(4B)	2.197(13)
Te(6) — Au(2)^{i}	2.6904(9)	Al(2) — Cl(8)	2.119(6)
Te(6) — Te(7)	2.9003(12)	Al(2) — Cl(5)	2.129(5)
Te(6) — Te(9)^{i}	2.9445(14)	Al(2) — Cl(7)	2.132(5)
Te(9) — Te(6)^{i}	2.9445(14)	Al(2) — Cl(6)	2.163(5)
Te(10) — Te(5)^{i}	2.938(3)	Al(3) — Cl(12)	2.130(5)
Au(4) — Te(13)	2.6741(9)	Al(3) — Cl(11)	2.132(5)
Au(4) — Te(14)	2.6783(10)	Al(3) — Cl(9)	2.144(5)
Au(4) — Te(11)	2.6798(9)	Al(3) — Cl(10)	2.145(5)
Au(4) — Te(12)	2.6937(10)	Al(4) — Cl(14)	2.122(5)
Au(5) — Te(13)^{ii}	2.6853(9)	Al(4) — Cl(13)	2.128(5)
Au(5) — Te(11)	2.6907(9)	Al(4) — Cl(16)	2.134(5)
Au(5) — Te(15)^{ii}	2.6917(10)	Al(4) — Cl(15)	2.136(5)
Au(5) — Te(16)^{ii}	2.6990(10)	Al(5) — Cl(17)	2.113(6)
Au(6) — Te(16)	2.6823(10)	Al(5) — Cl(18)	2.118(5)
Au(6) — Te(12)	2.6838(10)	Al(5) — Cl(20)	2.142(6)
Au(6) — Te(14)^{ii}	2.6909(10)	Al(5) — Cl(19)	2.151(6)
Au(6) — Te(15)^{ii}	2.6923(10)		

Table A.20: Selected bond angles for $(Au_6Te_{18}Cl)[AlCl_4]_5$. Symmetry transformations used to generate equivalent atoms: (i) $-x$, $-y$, $-z$; (ii) $-x+1$, $-y+1$, $-z$.

Atoms 1, 2, 3	Angle / °	Atoms 1, 2, 3	Angle / °
Te(1) — Au(1) — Te(3)	88.42(3)	Au(4) — Te(11) — Au(5)	89.29(3)
Te(1) — Au(1) — Te(4)	178.28(3)	Au(4) — Te(11) — Te(19)	97.59(4)

continued on next page

Atoms 1, 2, 3	Angle / °	Atoms 1, 2, 3	Angle / °
Te(3) — Au(1) — Te(4)	89.90(3)	Au(5) — Te(11) — Te(19)	94.36(4)
Te(1) — Au(1) — Te(2)	92.12(3)	Au(4) — Te(11) — Te(20)	92.44(7)
Te(3) — Au(1) — Te(2)	179.36(3)	Au(5) — Te(11) — Te(20)	93.85(7)
Te(4) — Au(1) — Te(2)	89.56(3)	Te(19) — Te(11) — Te(20)	167.10(8)
Te(5)^{i} — Au(2) — Te(4)^{i}	89.32(3)	Au(6) — Te(12) — Au(4)	88.61(3)
Te(5)^{i} — Au(2) — Te(1)	90.03(3)	Au(6) — Te(12) — Te(17)	95.28(4)
Te(4)^{i} — Au(2) — Te(1)	179.29(3)	Au(4) — Te(12) — Te(17)	96.31(4)
Te(5)^{i} — Au(2) — Te(6)^{i}	179.62(3)	Au(6) — Te(12) — Te(20)	92.36(7)
Te(4)^{i} — Au(2) — Te(6)^{i}	91.01(3)	Au(4) — Te(12) — Te(20)	88.38(7)
Te(1) — Au(2) — Te(6)^{i}	89.65(3)	Te(17) — Te(12) — Te(20)	171.12(8)
Te(6) — Au(3) — Te(2)	87.19(3)	Au(4) — Te(13) — Au(5)^{ii}	90.92(3)
Te(6) — Au(3) — Te(5)^{i}	179.57(3)	Au(4) — Te(13) — Te(18)	94.60(3)
Te(2) — Au(3) — Te(5)^{i}	93.09(3)	Au(5)^{ii} — Te(13) — Te(18)	92.26(3)
Te(6) — Au(3) — Te(3)^{i}	91.10(3)	Au(4) — Te(13) — Te(17)	92.33(3)
Te(2) — Au(3) — Te(3)^{i}	178.25(3)	Au(5)^{ii} — Te(13) — Te(17)	94.49(3)
Te(5)^{i} — Au(3) — Te(3)^{i}	88.62(3)	Te(18) — Te(13) — Te(17)	170.25(4)
Au(1) — Te(1) — Au(2)	91.70(3)	Au(4) — Te(14) — Au(6)^{ii}	92.16(3)
Au(1) — Te(1) — Te(9)	98.63(4)	Au(4) — Te(14) — Te(18)	96.59(4)
Au(2) — Te(1) — Te(9)	95.30(4)	Au(6)^{ii} — Te(14) — Te(18)	92.50(3)
Au(1) — Te(1) — Te(10)	92.07(7)	Au(4) — Te(14) — Te(19)	91.34(4)
Au(2) — Te(1) — Te(10)	95.08(6)	Au(6)^{ii} — Te(14) — Te(19)	94.47(4)
Te(9) — Te(1) — Te(10)	164.84(7)	Te(18) — Te(14) — Te(19)	169.23(4)
Au(3) — Te(2) — Au(1)	89.47(3)	Au(5)^{ii} — Te(15) — Au(6)^{ii}	90.03(3)
Au(3) — Te(2) — Te(7)	97.06(3)	Au(5)^{ii} — Te(15) — Te(18)	96.14(4)
Au(1) — Te(2) — Te(7)	96.60(3)	Au(6)^{ii} — Te(15) — Te(18)	94.43(3)
Au(3) — Te(2) — Te(10)	92.09(6)	Au(5)^{ii} — Te(15) — Te(20)^{ii}	90.59(7)
Au(1) — Te(2) — Te(10)	89.82(7)	Au(6)^{ii} — Te(15) — Te(20)^{ii}	92.84(7)
Te(7) — Te(2) — Te(10)	168.86(7)	Te(18) — Te(15) — Te(20)^{ii}	170.08(8)
Au(1) — Te(3) — Au(3)^{i}	90.51(3)	Au(6) — Te(16) — Au(5)^{ii}	89.04(3)
Au(1) — Te(3) — Te(8)	95.25(3)	Au(6) — Te(16) — Te(17)	92.94(4)
Au(3)^{i} — Te(3) — Te(8)	92.45(3)	Au(5)^{ii} — Te(16) — Te(17)	96.25(3)
Au(1) — Te(3) — Te(9)	91.99(4)	Au(6) — Te(16) — Te(19)^{ii}	95.58(4)
Au(3)^{i} — Te(3) — Te(9)	93.50(3)	Au(5)^{ii} — Te(16) — Te(19)^{ii}	89.10(4)
Te(8) — Te(3) — Te(9)	170.58(4)	Te(17) — Te(16) — Te(19)^{ii}	170.02(5)
Au(1) — Te(4) — Au(2)^{i}	87.65(3)	Te(12) — Te(17) — Te(16)	82.85(4)

continued on next page

Atoms 1, 2, 3	Angle / °	Atoms 1, 2, 3	Angle / °
Au(1) — Te(4) — Te(8)	93.31(3)	Te(12) — Te(17) — Te(13)	81.78(3)
Au(2)^{i} — Te(4) — Te(8)	92.03(3)	Te(16) — Te(17) — Te(13)	80.16(3)
Au(1) — Te(4) — Te(7)	91.70(3)	Te(15) — Te(18) — Te(14)	83.64(4)
Au(2)^{i} — Te(4) — Te(7)	92.93(3)	Te(15) — Te(18) — Te(13)	82.27(3)
Te(8) — Te(4) — Te(7)	173.09(4)	Te(14) — Te(18) — Te(13)	80.00(3)
Au(3)^{i} — Te(5) — Au(2)^{i}	90.53(3)	Te(11) — Te(19) — Te(16)^{ii}	84.85(4)
Au(3)^{i} — Te(5) — Te(8)	94.60(3)	Te(11) — Te(19) — Te(14)	81.60(4)
Au(2)^{i} — Te(5) — Te(8)	95.96(3)	Te(16)^{ii} — Te(19) — Te(14)	79.39(4)
Au(3)^{i} — Te(5) — Te(10)^{i}	90.98(7)	Te(11) — Te(20) — Te(15)^{ii}	84.65(9)
Au(2)^{i} — Te(5) — Te(10)^{i}	92.00(7)	Te(11) — Te(20) — Te(12)	85.97(9)
Te(8) — Te(5) — Te(10)^{i}	170.23(7)	Te(15)^{ii} — Te(20) — Te(12)	82.67(8)
Au(3) — Te(6) — Au(2)^{i}	89.62(3)	Cl(2A) — Al(1) — Cl(4A)	120.0(10)
Au(3) — Te(6) — Te(7)	94.24(3)	Cl(2A) — Al(1) — Cl(1)	113.7(7)
Au(2)^{i} — Te(6) — Te(7)	94.92(3)	Cl(4A) — Al(1) — Cl(1)	112.6(4)
Au(3) — Te(6) — Te(9)^{i}	95.69(4)	Cl(3B) — Al(1) — Cl(1)	112.5(5)
Au(2)^{i} — Te(6) — Te(9)^{i}	90.63(4)	Cl(2A) — Al(1) — Cl(3A)	93.8(12)
Te(7) — Te(6) — Te(9)^{i}	168.65(4)	Cl(4A) — Al(1) — Cl(3A)	107.6(6)
Te(2) — Te(7) — Te(6)	81.11(3)	Cl(1) — Al(1) — Cl(3A)	106.3(4)
Te(2) — Te(7) — Te(4)	81.93(3)	Cl(3B) — Al(1) — Cl(2B)	122.5(11)
Te(6) — Te(7) — Te(4)	81.06(3)	Cl(1) — Al(1) — Cl(2B)	113.3(7)
Te(5) — Te(8) — Te(3)	83.58(3)	Cl(3B) — Al(1) — Cl(4B)	106.7(7)
Te(5) — Te(8) — Te(4)	82.59(3)	Cl(1) — Al(1) — Cl(4B)	107.2(4)
Te(3) — Te(8) — Te(4)	81.52(3)	Cl(2B) — Al(1) — Cl(4B)	90.8(14)
Te(1) — Te(9) — Te(6)^{i}	83.47(4)	Cl(8) — Al(2) — Cl(5)	113.8(2)
Te(1) — Te(9) — Te(3)	80.55(4)	Cl(8) — Al(2) — Cl(7)	109.3(3)
Te(6)^{i} — Te(9) — Te(3)	79.69(4)	Cl(5) — Al(2) — Cl(7)	112.3(2)
Te(1) — Te(10) — Te(2)	85.57(8)	Cl(8) — Al(2) — Cl(6)	105.9(2)
Te(1) — Te(10) — Te(5)^{i}	82.77(9)	Cl(5) — Al(2) — Cl(6)	107.2(2)
Te(2) — Te(10) — Te(5)^{i}	83.80(8)	Cl(7) — Al(2) — Cl(6)	107.9(2)
Te(13) — Au(4) — Te(14)	88.67(3)	Cl(12) — Al(3) — Cl(11)	110.5(2)
Te(13) — Au(4) — Te(11)	177.69(3)	Cl(12) — Al(3) — Cl(9)	111.2(2)
Te(14) — Au(4) — Te(11)	89.07(3)	Cl(11) — Al(3) — Cl(9)	110.1(2)
Te(13) — Au(4) — Te(12)	89.24(3)	Cl(12) — Al(3) — Cl(10)	110.2(2)
Te(14) — Au(4) — Te(12)	177.84(3)	Cl(11) — Al(3) — Cl(10)	108.3(2)
Te(11) — Au(4) — Te(12)	93.02(3)	Cl(9) — Al(3) — Cl(10)	106.4(2)

continued on next page

Atoms 1, 2, 3	Angle / °	Atoms 1, 2, 3	Angle / °
Te(13)^{ii} — Au(5) — Te(11)	179.66(3)	Cl(14) — Al(4) — Cl(13)	110.0(2)
Te(13)^{ii} — Au(5) — Te(15)^{ii}	89.11(3)	Cl(14) — Al(4) — Cl(16)	108.8(2)
Te(11) — Au(5) — Te(15)^{ii}	90.72(3)	Cl(13) — Al(4) — Cl(16)	107.7(2)
Te(13)^{ii} — Au(5) — Te(16)^{ii}	88.97(3)	Cl(14) — Al(4) — Cl(15)	111.9(2)
Te(11) — Au(5) — Te(16)^{ii}	91.19(3)	Cl(13) — Al(4) — Cl(15)	109.6(2)
Te(15)^{ii} — Au(5) — Te(16)^{ii}	177.94(3)	Cl(16) — Al(4) — Cl(15)	108.8(2)
Te(16) — Au(6) — Te(12)	88.67(3)	Cl(17) — Al(5) — Cl(18)	114.5(3)
Te(16) — Au(6) — Te(14)^{ii}	90.52(3)	Cl(17) — Al(5) — Cl(20)	110.1(3)
Te(12) — Au(6) — Te(14)^{ii}	179.15(4)	Cl(18) — Al(5) — Cl(20)	111.5(2)
Te(16) — Au(6) — Te(15)^{ii}	179.19(4)	Cl(17) — Al(5) — Cl(19)	107.5(3)
Te(12) — Au(6) — Te(15)^{ii}	92.12(3)	Cl(18) — Al(5) — Cl(19)	105.9(2)
Te(14)^{ii} — Au(6) — Te(15)^{ii}	88.69(3)	Cl(20) — Al(5) — Cl(19)	106.9(3)

A.1.5 $(Au_6Te_{18}Cl)[GaCl_4]_5$

Table A.21: Crystal data and structure refinement for $(Au_6Te_{18}Cl)[GaCl_4]_5$.

Empirical formula	$Au_6\,Cl_{21}\,Ga_5\,Te_{18}$
Formula weight / $g \cdot mol^{-1}$	4571.65
Temperature / K	123(2)
Crystal system; space group	Monoclinic; $P2_1/c$
Lattice constants / $Å$	a = 15.3182(2)
	b = 18.8797(2); β = 96.804(1)°
	c = 20.8264(3)
Volume / $Å^3$	5980.6(1)
Z; F(000); calc. density / $g \cdot cm^{-3}$	4; 7688; 5.077
Wavelength	$Mo_{K\alpha}$ (λ = 0.71073 Å)
Crystal size / mm^3	0.074 × 0.072 × 0.070
Theta range for data collection / °	$2.922 \leq \theta \leq 27.486$
Limiting indices	$-19 \leq h \leq 19$; $-23 \leq k \leq 24$; $-27 \leq l \leq 27$
Reflections collected / unique	108007 / 13704
Completeness to θ = 25.242°	99.8 %
R_{int}; R_σ	0.0725; 0.0421
Absorption coefficient / mm^{-1}	26.426; Semi-empirical from equivalents
Max. / min. transmission	0.1217 / 0.0693
Refinement method	Full-matrix least-squares on F^2
Data / restraints / parameters	13704 / 4 / 496
R indices (all data) R_1; wR_2	0.0600; 0.0763
R indices $[I > 4\sigma(I)]$ R_1; wR_2	0.0362; 0.0691; n = 10450 reflections
Goodness-of-fit for F^2	1.066
Largest diff. peak / $e^- \cdot Å^{-3}$	+1.330 (1.34 Å from Au3)
	-2.151 (0.78 Å from Au4)
Avg. diff. density / $e^- \cdot Å^{-3}$	0.304

Table A.22: Fractional coordinates and equivalent isotropic displacement parameter U_{eq} for the independent atoms in the structure of $(Au_6Te_{18}Cl)[GaCl_4]_5$.

Atom	Wyck.	Site	*SOF*	*x / a*	*y / b*	*z / c*	U_{eq} / Å^2
Au(1)	4*e*	1		0.05203(2)	0.06731(2)	0.11095(2)	0.02048(8)
Au(2)	4*e*	1		0.14611(3)	0.03702(2)	-0.05025(2)	0.02229(9)
Au(3)	4*e*	1		-0.08023(3)	0.11931(2)	-0.04693(2)	0.02282(9)
Te(1)	4*e*	1		0.19901(4)	0.10360(4)	0.06140(3)	0.02408(15)
Te(2)	4*e*	1		-0.03101(5)	0.18578(4)	0.06519(3)	0.02574(15)
Te(3)	4*e*	1		0.13365(5)	-0.05071(4)	0.15757(3)	0.02624(15)
Te(4)	4*e*	1		-0.09279(4)	0.02801(4)	0.16248(3)	0.02579(15)
Te(5)	4*e*	1		-0.06671(5)	-0.15587(4)	0.09701(3)	0.02608(15)
Te(6)	4*e*	1		-0.22638(5)	0.08181(4)	0.00278(4)	0.02913(16)
Te(7)	4*e*	1		-0.18478(5)	0.16339(4)	0.12022(4)	0.03722(18)
Te(8)	4*e*	1		-0.01099(5)	-0.10216(4)	0.21872(3)	0.03026(16)
Te(9)	4*e*	1	0.695(1)	0.30537(7)	-0.00419(6)	0.11241(5)	0.0428(3)
Te(10)	4*e*	1	0.305(1)	0.1298(2)	0.23515(15)	0.02075(13)	0.0607(8)
Cl(21)	4*e*	1	0.249(1)	0.30537(7)	-0.00419(6)	0.11241(5)	0.0428(3)
Cl(22)	4*e*	1	0.251(1)	0.1298(2)	0.23515(15)	0.02075(13)	0.0607(8)
Au(4)	4*e*	1		0.66895(3)	0.52000(2)	0.05014(2)	0.02643(9)
Au(5)	4*e*	1		0.50315(3)	0.37310(2)	0.05702(2)	0.02734(10)
Au(6)	4*e*	1		0.55948(3)	0.44260(2)	-0.10479(2)	0.02931(10)
Te(11)	4*e*	1		0.67036(5)	0.39386(4)	0.10914(3)	0.02958(16)
Te(12)	4*e*	1		0.72717(5)	0.46563(4)	-0.05645(4)	0.03347(17)
Te(13)	4*e*	1		0.66357(5)	0.64808(4)	-0.00499(4)	0.03089(16)
Te(14)	4*e*	1		0.60896(5)	0.57875(5)	0.15354(4)	0.03599(18)
Te(15)	4*e*	1		0.44156(5)	0.68589(4)	0.04875(4)	0.03337(17)
Te(16)	4*e*	1		0.55811(5)	0.57009(4)	-0.16188(4)	0.03451(18)
Te(17)	4*e*	1		0.74183(5)	0.59382(5)	-0.11973(4)	0.0424(2)
Te(18)	4*e*	1		0.60783(5)	0.72199(4)	0.10801(4)	0.03834(19)
Te(19)	4*e*	1	0.641(1)	0.62551(8)	0.44001(7)	0.22534(6)	0.0431(3)
Te(20)	4*e*	1	0.359(1)	0.7404(2)	0.32669(16)	0.00876(15)	0.0760(8)
Cl(23)	4*e*	1	0.258(1)	0.62551(8)	0.44001(7)	0.22534(6)	0.0431(3)
Cl(24)	4*e*	1	0.242(1)	0.7404(2)	0.32669(16)	0.00876(15)	0.0760(8)
Ga(1)	4*e*	1		0.48860(8)	0.19322(6)	0.16908(6)	0.0319(3)
Cl(1)	4*e*	1		0.48821(18)	0.08659(15)	0.20736(14)	0.0353(6)
Cl(2A)	4*e*	1	0.54(3)	0.6129(10)	0.2256(11)	0.1411(11)	0.071(5)

continued on next page

Atom	Wy.	Site	*SOF*	*x / a*	*y / b*	*z / c*	U_{eq} / Å^2
Cl(3A)	4*e*	1	0.54(3)	0.4981(13)	0.2652(5)	0.2517(5)	0.069(4)
Cl(4A)	4*e*	1	0.54(3)	0.3701(9)	0.2186(8)	0.1089(9)	0.060(5)
Cl(2B)	4*e*	1	0.46(3)	0.5962(13)	0.2151(10)	0.1140(11)	0.055(4)
Cl(3B)	4*e*	1	0.46(3)	0.439(2)	0.2707(6)	0.2317(13)	0.099(10)
Cl(4B)	4*e*	1	0.46(3)	0.3986(10)	0.1942(8)	0.0777(10)	0.056(5)
Ga(2)	4*e*	1		-0.04635(8)	0.48622(6)	0.11123(6)	0.0292(3)
Cl(5)	4*e*	1		-0.09409(19)	0.54635(16)	0.02550(13)	0.0375(7)
Cl(6)	4*e*	1		-0.14354(19)	0.49812(17)	0.18079(14)	0.0395(7)
Cl(7)	4*e*	1		0.07880(18)	0.52532(17)	0.15792(14)	0.0396(7)
Cl(8)	4*e*	1		-0.0361(3)	0.37347(18)	0.09548(19)	0.0678(12)
Ga(3)	4*e*	1		0.77780(8)	0.23717(6)	0.32455(6)	0.0302(3)
Cl(9)	4*e*	1		0.8118(2)	0.29590(16)	0.24035(14)	0.0383(7)
Cl(10)	4*e*	1		0.69102(19)	0.30679(16)	0.37191(16)	0.0407(7)
Cl(11)	4*e*	1		0.8947(2)	0.21780(16)	0.39147(16)	0.0422(7)
Cl(12)	4*e*	1		0.7113(2)	0.13924(16)	0.29568(16)	0.0467(8)
Ga(4)	4*e*	1		0.84004(8)	0.70682(6)	0.22905(5)	0.0270(3)
Cl(13)	4*e*	1		0.7900(3)	0.81364(18)	0.23757(18)	0.0588(10)
Cl(14)	4*e*	1		0.97718(19)	0.70225(19)	0.26680(15)	0.0464(8)
Cl(15)	4*e*	1		0.76057(19)	0.63388(17)	0.27856(14)	0.0412(7)
Cl(16)	4*e*	1		0.8273(2)	0.68017(15)	0.12706(13)	0.0358(6)
Ga(5)	4*e*	1		0.61078(8)	0.95664(7)	0.11930(7)	0.0364(3)
Cl(17)	4*e*	1		0.5822(2)	1.0466(2)	0.05641(19)	0.0607(10)
Cl(18)	4*e*	1		0.49647(19)	0.90173(17)	0.14486(17)	0.0439(7)
Cl(19)	4*e*	1		0.6815(3)	0.87866(19)	0.0666(2)	0.0638(11)
Cl(20)	4*e*	1		0.6991(2)	0.98693(19)	0.20455(17)	0.0495(8)

Table A.23: Anisotropic displacement parameters U_{ij} / Å^2 for the independent atoms in the structure of$(Au_6Te_{18}Cl)[GaCl_4]_5$.

Atom	U_{11}	U_{22}	U_{33}	U_{23}	U_{13}	U_{12}
Au(1)	0.02357(19)	0.02014(19)	0.01771(19)	-0.00053(15)	0.00230(15)	-0.00256(16)
Au(2)	0.02330(19)	0.0249(2)	0.01875(19)	-0.00159(16)	0.00284(15)	-0.00362(16)
Au(3)	0.0270(2)	0.0206(2)	0.0205(2)	-0.00041(16)	0.00105(15)	0.00061(16)
Te(1)	0.0249(3)	0.0273(4)	0.0199(3)	-0.0021(3)	0.0025(3)	-0.0079(3)
Te(2)	0.0345(4)	0.0196(3)	0.0227(3)	-0.0028(3)	0.0018(3)	0.0020(3)
Te(3)	0.0348(4)	0.0240(4)	0.0189(3)	0.0007(3)	-0.0011(3)	0.0026(3)

continued on next page

Atom	U_{11}	U_{22}	U_{33}	U_{23}	U_{13}	U_{12}
Te(4)	0.0274(3)	0.0312(4)	0.0194(3)	-0.0047(3)	0.0057(3)	-0.0067(3)
Te(5)	0.0330(4)	0.0226(3)	0.0226(3)	0.0031(3)	0.0029(3)	-0.0057(3)
Te(6)	0.0249(4)	0.0316(4)	0.0315(4)	0.0004(3)	0.0060(3)	0.0045(3)
Te(7)	0.0359(4)	0.0394(4)	0.0364(4)	-0.0102(3)	0.0042(3)	0.0064(4)
Te(8)	0.0421(4)	0.0288(4)	0.0190(3)	0.0042(3)	0.0001(3)	-0.0090(3)
Te(9)	0.0405(6)	0.0459(7)	0.0411(6)	-0.0121(5)	0.0010(5)	-0.0037(5)
Te(10)	0.0777(19)	0.0595(17)	0.0444(15)	-0.0027(12)	0.0059(13)	-0.0238(15)
Cl(21)	0.0405(6)	0.0459(7)	0.0411(6)	-0.0121(5)	0.0010(5)	-0.0037(5)
Cl(22)	0.0777(19)	0.0595(17)	0.0444(15)	-0.0027(12)	0.0059(13)	-0.0238(15)
Au(4)	0.0253(2)	0.0296(2)	0.0238(2)	0.00088(17)	0.00009(16)	-0.00116(17)
Au(5)	0.0277(2)	0.0289(2)	0.0248(2)	0.00238(17)	0.00028(17)	-0.00060(18)
Au(6)	0.0279(2)	0.0369(2)	0.0229(2)	-0.00300(18)	0.00187(17)	-0.00017(19)
Te(11)	0.0290(4)	0.0301(4)	0.0280(4)	0.0028(3)	-0.0033(3)	0.0034(3)
Te(12)	0.0258(4)	0.0461(5)	0.0290(4)	-0.0028(3)	0.0053(3)	0.0006(3)
Te(13)	0.0312(4)	0.0273(4)	0.0327(4)	0.0027(3)	-0.0026(3)	-0.0047(3)
Te(14)	0.0318(4)	0.0503(5)	0.0248(4)	-0.0090(3)	-0.0014(3)	-0.0043(4)
Te(15)	0.0334(4)	0.0320(4)	0.0344(4)	-0.0051(3)	0.0026(3)	0.0018(3)
Te(16)	0.0375(4)	0.0430(5)	0.0237(4)	0.0013(3)	0.0066(3)	-0.0059(4)
Te(17)	0.0335(4)	0.0585(5)	0.0369(4)	0.0147(4)	0.0108(3)	0.0009(4)
Te(18)	0.0428(5)	0.0294(4)	0.0413(5)	-0.0037(3)	-0.0012(4)	-0.0032(3)
Te(19)	0.0408(6)	0.0482(7)	0.0386(7)	-0.0013(5)	-0.0024(5)	0.0004(5)
Te(20)	0.0677(17)	0.0740(19)	0.086(2)	0.0120(15)	0.0073(15)	0.0112(14)
Cl(23)	0.0408(6)	0.0482(7)	0.0386(7)	-0.0013(5)	-0.0024(5)	0.0004(5)
Cl(24)	0.0677(17)	0.0740(19)	0.086(2)	0.0120(15)	0.0073(15)	0.0112(14)
Ga(1)	0.0302(6)	0.0239(6)	0.0412(7)	-0.0002(5)	0.0022(5)	-0.0047(5)
Cl(1)	0.0351(15)	0.0300(15)	0.0413(16)	0.0090(12)	0.0064(12)	-0.0002(12)
Cl(2A)	0.029(4)	0.066(8)	0.115(13)	0.051(9)	-0.007(6)	-0.015(4)
Cl(3A)	0.106(10)	0.044(4)	0.055(5)	-0.019(3)	-0.002(5)	-0.002(5)
Cl(4A)	0.042(5)	0.051(6)	0.078(8)	0.032(6)	-0.025(5)	-0.021(4)
Cl(2B)	0.038(9)	0.039(6)	0.094(12)	0.026(7)	0.026(7)	0.002(6)
Cl(3B)	0.17(2)	0.035(5)	0.111(15)	-0.011(7)	0.098(16)	-0.011(8)
Cl(4B)	0.041(6)	0.048(6)	0.072(9)	0.027(6)	-0.024(6)	-0.013(5)
Ga(2)	0.0353(7)	0.0276(6)	0.0251(6)	0.0025(5)	0.0050(5)	-0.0007(5)
Cl(5)	0.0401(16)	0.0457(17)	0.0264(14)	0.0091(13)	0.0029(12)	0.0013(13)
Cl(6)	0.0362(15)	0.0513(18)	0.0322(15)	0.0109(14)	0.0094(12)	0.0010(14)

continued on next page

Atom	U_{11}	U_{22}	U_{33}	U_{23}	U_{13}	U_{12}
Cl(7)	0.0318(14)	0.0546(19)	0.0319(15)	0.0072(14)	0.0020(12)	-0.0037(14)
Cl(8)	0.121(4)	0.0284(17)	0.057(2)	-0.0009(16)	0.026(2)	0.000(2)
Ga(3)	0.0300(6)	0.0233(6)	0.0355(7)	-0.0036(5)	-0.0027(5)	-0.0017(5)
Cl(9)	0.0409(16)	0.0350(16)	0.0389(17)	-0.0005(13)	0.0039(13)	-0.0016(13)
Cl(10)	0.0369(16)	0.0332(16)	0.0524(19)	-0.0023(14)	0.0074(14)	0.0054(13)
Cl(11)	0.0368(16)	0.0364(16)	0.0500(19)	-0.0053(14)	-0.0092(14)	0.0008(13)
Cl(12)	0.0568(19)	0.0280(15)	0.0506(19)	-0.0014(14)	-0.0127(15)	-0.0138(14)
Ga(4)	0.0299(6)	0.0291(6)	0.0212(6)	0.0036(5)	0.0000(5)	-0.0035(5)
Cl(13)	0.086(3)	0.0413(19)	0.050(2)	-0.0009(16)	0.0144(19)	0.0227(18)
Cl(14)	0.0308(15)	0.069(2)	0.0367(17)	0.0141(15)	-0.0053(12)	-0.0076(15)
Cl(15)	0.0393(16)	0.057(2)	0.0266(14)	0.0108(13)	-0.0003(12)	-0.0169(15)
Cl(16)	0.0478(17)	0.0383(16)	0.0207(13)	0.0035(11)	0.0013(12)	-0.0126(13)
Ga(5)	0.0333(7)	0.0353(7)	0.0433(8)	-0.0013(6)	0.0155(6)	-0.0068(6)
Cl(17)	0.057(2)	0.066(2)	0.062(2)	0.0255(19)	0.0186(18)	0.0007(19)
Cl(18)	0.0348(16)	0.0404(17)	0.060(2)	0.0016(15)	0.0203(14)	-0.0089(13)
Cl(19)	0.075(2)	0.044(2)	0.083(3)	-0.0124(18)	0.056(2)	-0.0171(18)
Cl(20)	0.0360(16)	0.053(2)	0.059(2)	-0.0055(16)	0.0016(15)	0.0017(15)

Table A.24: Selected bond lengths for $(Au_6Te_{18}Cl)[GaCl_4]_5$. Symmetry transformations used to generate equivalent atoms: (i) $-x$, $-y$, $-z$; (ii) $-x+1$, $-y+1$, $-z$.

Atoms 1, 2	Distance / *Å*	Atoms 1, 2	Distance / *Å*
Au(1) — Te(1)	2.6746(8)	Te(11) — Te(19)	2.7352(14)
Au(1) — Te(3)	2.6801(8)	Te(11) — Te(20)	2.768(3)
Au(1) — Te(4)	2.6810(8)	Te(12) — Te(17)	2.7775(12)
Au(1) — Te(2)	2.6911(8)	Te(12) — Te(20)	2.950(3)
Au(2) — Te(5)^{i}	2.6798(8)	Te(13) — Au(5)^{ii}	2.6834(8)
Au(2) — Te(4)^{i}	2.6804(8)	Te(13) — Te(18)	2.9480(11)
Au(2) — Te(1)	2.6827(8)	Te(13) — Te(17)	2.9793(12)
Au(2) — Te(6)^{i}	2.6897(8)	Te(14) — Au(6)^{ii}	2.6888(8)
Au(3) — Te(6)	2.6710(8)	Te(14) — Te(18)	2.8651(12)
Au(3) — Te(2)	2.6793(8)	Te(14) — Te(19)	3.0119(15)
Au(3) — Te(5)^{i}	2.6809(8)	Te(15) — Au(6)^{ii}	2.6928(9)
Au(3) — Te(3)^{i}	2.6848(8)	Te(15) — Au(5)^{ii}	2.6930(9)
Te(1) — Te(9)	2.7412(14)	Te(15) — Te(18)	2.7803(11)
Te(1) — Te(10)	2.792(3)	Te(15) — Te(20)^{ii}	2.910(3)

continued on next page

Atoms 1, 2	Distance / *Å*	Atoms 1, 2	Distance / *Å*
Te(2) — Te(7)	2.7715(11)	Te(16) — Au(5)^{ii}	2.6991(9)
Te(2) — Te(10)	2.887(3)	Te(16) — Te(17)	2.8820(11)
Te(3) — Au(3)^{i}	2.6849(8)	Te(16) — Te(19)^{ii}	2.9689(14)
Te(3) — Te(8)	2.8535(10)	Te(19) — Te(16)^{ii}	2.9689(14)
Te(3) — Te(9)	3.0268(13)	Te(20) — Te(15)^{ii}	2.910(3)
Te(4) — Au(2)^{i}	2.6804(8)	Ga(1) — Cl(4A)	2.135(8)
Te(4) — Te(8)	2.9383(10)	Ga(1) — Cl(2A)	2.145(17)
Te(4) — Te(7)	2.9999(11)	Ga(1) — Cl(2B)	2.157(18)
Te(5) — Au(2)^{i}	2.6799(8)	Ga(1) — Cl(3B)	2.160(11)
Te(5) — Au(3)^{i}	2.6809(8)	Ga(1) — Cl(1)	2.165(3)
Te(5) — Te(8)	2.7695(10)	Ga(1) — Cl(3A)	2.184(9)
Te(5) — Te(10)^{i}	2.937(3)	Ga(1) — Cl(4B)	2.214(12)
Te(6) — Au(2)^{i}	2.6897(8)	Ga(2) — Cl(8)	2.162(4)
Te(6) — Te(7)	2.8968(11)	Ga(2) — Cl(5)	2.168(3)
Te(6) — Te(9)^{i}	2.9460(13)	Ga(2) — Cl(7)	2.173(3)
Te(9) — Te(6)^{i}	2.9459(13)	Ga(2) — Cl(6)	2.208(3)
Te(10) — Te(5)^{i}	2.937(3)	Ga(3) — Cl(12)	2.162(3)
Au(4) — Te(13)	2.6740(8)	Ga(3) — Cl(11)	2.166(3)
Au(4) — Te(11)	2.6787(8)	Ga(3) — Cl(10)	2.186(3)
Au(4) — Te(14)	2.6798(9)	Ga(3) — Cl(9)	2.189(3)
Au(4) — Te(12)	2.6917(9)	Ga(4) — Cl(14)	2.156(3)
Au(5) — Te(13)^{ii}	2.6835(8)	Ga(4) — Cl(16)	2.169(3)
Au(5) — Te(11)	2.6895(8)	Ga(4) — Cl(13)	2.172(3)
Au(5) — Te(15)^{ii}	2.6930(9)	Ga(4) — Cl(15)	2.177(3)
Au(5) — Te(16)^{ii}	2.6992(9)	Ga(5) — Cl(18)	2.155(3)
Au(6) — Te(12)	2.6811(8)	Ga(5) — Cl(17)	2.158(4)
Au(6) — Te(16)	2.6837(9)	Ga(5) — Cl(20)	2.177(4)
Au(6) — Te(14)^{ii}	2.6888(8)	Ga(5) — Cl(19)	2.197(4)
Au(6) — Te(15)^{ii}	2.6928(9)		

Table A.25: Selected bond angles for $(Au_6Te_{18}Cl)[GaCl_4]_5$. Symmetry transformations used to generate equivalent atoms: (i) $-x$, $-y$, $-z$; (ii) $-x+1$, $-y+1$, $-z$.

Atoms 1, 2, 3	Angle / °	Atoms 1, 2, 3	Angle / °
Te(1) — Au(1) — Te(3)	88.56(2)	Au(4) — Te(11) — Au(5)	89.37(2)
Te(1) — Au(1) — Te(4)	178.39(3)	Au(4) — Te(11) — Te(19)	97.67(4)

continued on next page

Atoms 1, 2, 3	Angle / °	Atoms 1, 2, 3	Angle / °
Te(3) — Au(1) — Te(4)	89.85(2)	Au(5) — Te(11) — Te(19)	94.39(3)
Te(1) — Au(1) — Te(2)	91.98(2)	Au(4) — Te(11) — Te(20)	92.50(6)
Te(3) — Au(1) — Te(2)	179.38(3)	Au(5) — Te(11) — Te(20)	93.67(7)
Te(4) — Au(1) — Te(2)	89.60(2)	Te(19) — Te(11) — Te(20)	167.08(7)
Te(5)^{i} — Au(2) — Te(4)^{i}	89.33(2)	Au(6) — Te(12) — Au(4)	88.58(2)
Te(5)^{i} — Au(2) — Te(1)	90.00(2)	Au(6) — Te(12) — Te(17)	95.21(3)
Te(4)^{i} — Au(2) — Te(1)	179.32(3)	Au(4) — Te(12) — Te(17)	96.46(3)
Te(5)^{i} — Au(2) — Te(6)^{i}	179.66(3)	Au(6) — Te(12) — Te(20)	92.24(6)
Te(4)^{i} — Au(2) — Te(6)^{i}	90.99(3)	Au(4) — Te(12) — Te(20)	88.32(7)
Te(1) — Au(2) — Te(6)^{i}	89.67(2)	Te(17) — Te(12) — Te(20)	171.23(6)
Te(6) — Au(3) — Te(2)	87.06(2)	Au(4) — Te(13) — Au(5)^{ii}	91.03(2)
Te(6) — Au(3) — Te(5)^{i}	179.55(3)	Au(4) — Te(13) — Te(18)	94.72(3)
Te(2) — Au(3) — Te(5)^{i}	93.20(2)	Au(5)^{ii} — Te(13) — Te(18)	92.36(3)
Te(6) — Au(3) — Te(3)^{i}	91.18(3)	Au(4) — Te(13) — Te(17)	92.21(3)
Te(2) — Au(3) — Te(3)^{i}	178.20(3)	Au(5)^{ii} — Te(13) — Te(17)	94.53(3)
Te(5)^{i} — Au(3) — Te(3)^{i}	88.56(2)	Te(18) — Te(13) — Te(17)	170.14(4)
Au(1) — Te(1) — Au(2)	91.88(2)	Au(4) — Te(14) — Au(6)^{ii}	92.27(3)
Au(1) — Te(1) — Te(9)	98.58(3)	Au(4) — Te(14) — Te(18)	96.54(3)
Au(2) — Te(1) — Te(9)	95.32(3)	Au(6)^{ii} — Te(14) — Te(18)	92.79(3)
Au(1) — Te(1) — Te(10)	92.19(6)	Au(4) — Te(14) — Te(19)	91.28(4)
Au(2) — Te(1) — Te(10)	95.12(6)	Au(6)^{ii} — Te(14) — Te(19)	94.46(3)
Te(9) — Te(1) — Te(10)	164.73(7)	Te(18) — Te(14) — Te(19)	169.12(4)
Au(3) — Te(2) — Au(1)	89.53(2)	Au(6)^{ii} — Te(15) — Au(5)^{ii}	90.03(3)
Au(3) — Te(2) — Te(7)	97.11(3)	Au(6)^{ii} — Te(15) — Te(18)	94.62(3)
Au(1) — Te(2) — Te(7)	96.66(3)	Au(5)^{ii} — Te(15) — Te(18)	95.98(3)
Au(3) — Te(2) — Te(10)	91.99(6)	Au(6)^{ii} — Te(15) — Te(20)^{ii}	92.88(6)
Au(1) — Te(2) — Te(10)	89.79(6)	Au(5)^{ii} — Te(15) — Te(20)^{ii}	90.47(7)
Te(7) — Te(2) — Te(10)	168.87(6)	Te(18) — Te(15) — Te(20)^{ii}	170.09(7)
Au(1) — Te(3) — Au(3)^{i}	90.49(2)	Au(6) — Te(16) — Au(5)^{ii}	89.04(3)
Au(1) — Te(3) — Te(8)	95.23(3)	Au(6) — Te(16) — Te(17)	92.77(3)
Au(3)^{i} — Te(3) — Te(8)	92.58(3)	Au(5)^{ii} — Te(16) — Te(17)	96.45(3)
Au(1) — Te(3) — Te(9)	91.80(3)	Au(6) — Te(16) — Te(19)^{ii}	95.56(3)
Au(3)^{i} — Te(3) — Te(9)	93.50(3)	Au(5)^{ii} — Te(16) — Te(19)^{ii}	89.07(3)
Te(8) — Te(3) — Te(9)	170.66(4)	Te(17) — Te(16) — Te(19)^{ii}	170.08(4)
Au(2)^{i} — Te(4) — Au(1)	87.64(2)	Te(12) — Te(17) — Te(16)	83.00(3)

continued on next page

Atoms 1, 2, 3	Angle / °	Atoms 1, 2, 3	Angle / °
Au(2)^{i} — Te(4) — Te(8)	92.07(3)	Te(12) — Te(17) — Te(13)	81.73(3)
Au(1) — Te(4) — Te(8)	93.27(3)	Te(16) — Te(17) — Te(13)	80.01(3)
Au(2)^{i} — Te(4) — Te(7)	92.89(3)	Te(15) — Te(18) — Te(14)	83.39(3)
Au(1) — Te(4) — Te(7)	91.66(3)	Te(15) — Te(18) — Te(13)	82.32(3)
Te(8) — Te(4) — Te(7)	173.15(3)	Te(14) — Te(18) — Te(13)	80.01(3)
Au(2)^{i} — Te(5) — Au(3)^{i}	90.51(2)	Te(11) — Te(19) — Te(16)^{ii}	84.82(4)
Au(2)^{i} — Te(5) — Te(8)	95.93(3)	Te(11) — Te(19) — Te(14)	81.54(4)
Au(3)^{i} — Te(5) — Te(8)	94.58(3)	Te(16)^{ii} — Te(19) — Te(14)	79.35(4)
Au(2)^{i} — Te(5) — Te(10)^{i}	91.89(6)	Te(11) — Te(20) — Te(15)^{ii}	84.86(8)
Au(3)^{i} — Te(5) — Te(10)^{i}	90.86(6)	Te(11) — Te(20) — Te(12)	85.91(8)
Te(8) — Te(5) — Te(10)^{i}	170.42(6)	Te(15)^{ii} — Te(20) — Te(12)	82.70(7)
Au(3) — Te(6) — Au(2)^{i}	89.77(2)	Cl(4A) — Ga(1) — Cl(2A)	119.8(8)
Au(3) — Te(6) — Te(7)	94.34(3)	Cl(2B) — Ga(1) — Cl(3B)	122.6(8)
Au(2)^{i} — Te(6) — Te(7)	95.04(3)	Cl(4A) — Ga(1) — Cl(1)	112.7(2)
Au(3) — Te(6) — Te(9)^{i}	95.65(3)	Cl(2A) — Ga(1) — Cl(1)	114.0(5)
Au(2)^{i} — Te(6) — Te(9)^{i}	90.59(3)	Cl(2B) — Ga(1) — Cl(1)	114.2(5)
Te(7) — Te(6) — Te(9)^{i}	168.55(4)	Cl(3B) — Ga(1) — Cl(1)	113.0(4)
Te(2) — Te(7) — Te(6)	81.06(3)	Cl(4A) — Ga(1) — Cl(3A)	107.2(4)
Te(2) — Te(7) — Te(4)	81.87(3)	Cl(2A) — Ga(1) — Cl(3A)	93.3(10)
Te(6) — Te(7) — Te(4)	80.99(3)	Cl(1) — Ga(1) — Cl(3A)	106.9(3)
Te(5) — Te(8) — Te(3)	83.54(3)	Cl(2B) — Ga(1) — Cl(4B)	88.7(11)
Te(5) — Te(8) — Te(4)	82.57(3)	Cl(3B) — Ga(1) — Cl(4B)	106.5(7)
Te(3) — Te(8) — Te(4)	81.62(3)	Cl(1) — Ga(1) — Cl(4B)	107.2(3)
Te(1) — Te(9) — Te(6)^{i}	83.44(4)	Cl(8) — Ga(2) — Cl(5)	114.46(15)
Te(1) — Te(9) — Te(3)	80.64(3)	Cl(8) — Ga(2) — Cl(7)	109.04(17)
Te(6)^{i} — Te(9) — Te(3)	79.66(3)	Cl(5) — Ga(2) — Cl(7)	112.60(12)
Te(1) — Te(10) — Te(2)	85.60(8)	Cl(8) — Ga(2) — Cl(6)	105.44(15)
Te(1) — Te(10) — Te(5)^{i}	82.84(8)	Cl(5) — Ga(2) — Cl(6)	107.40(12)
Te(2) — Te(10) — Te(5)^{i}	83.92(7)	Cl(7) — Ga(2) — Cl(6)	107.42(12)
Te(13) — Au(4) — Te(11)	177.59(3)	Cl(12) — Ga(3) — Cl(11)	111.17(13)
Te(13) — Au(4) — Te(14)	88.55(3)	Cl(12) — Ga(3) — Cl(10)	110.37(14)
Te(11) — Au(4) — Te(14)	89.10(3)	Cl(11) — Ga(3) — Cl(10)	108.17(13)
Te(13) — Au(4) — Te(12)	89.26(3)	Cl(12) — Ga(3) — Cl(9)	111.07(13)
Te(11) — Au(4) — Te(12)	93.09(3)	Cl(11) — Ga(3) — Cl(9)	110.09(13)
Te(14) — Au(4) — Te(12)	177.72(3)	Cl(10) — Ga(3) — Cl(9)	105.79(13)

continued on next page

Atoms 1, 2, 3	Angle / °	Atoms 1, 2, 3	Angle / °
Te(13)^{ii} — Au(5) — Te(11)	179.81(3)	Cl(14) — Ga(4) — Cl(16)	108.57(13)
Te(13)^{ii} — Au(5) — Te(15)^{ii}	89.11(3)	Cl(14) — Ga(4) — Cl(13)	110.20(16)
Te(11) — Au(5) — Te(15)^{ii}	90.78(3)	Cl(16) — Ga(4) — Cl(13)	107.69(13)
Te(13)^{ii} — Au(5) — Te(16)^{ii}	88.88(3)	Cl(14) — Ga(4) — Cl(15)	112.17(13)
Te(11) — Au(5) — Te(16)^{ii}	91.22(3)	Cl(16) — Ga(4) — Cl(15)	109.07(12)
Te(15)^{ii} — Au(5) — Te(16)^{ii}	177.87(3)	Cl(13) — Ga(4) — Cl(15)	109.03(15)
Te(12) — Au(6) — Te(16)	88.72(3)	Cl(18) — Ga(5) — Cl(17)	114.57(15)
Te(12) — Au(6) — Te(14)^{ii}	179.28(3)	Cl(18) — Ga(5) — Cl(20)	111.69(14)
Te(16) — Au(6) — Te(14)^{ii}	90.60(3)	Cl(17) — Ga(5) — Cl(20)	110.50(16)
Te(12) — Au(6) — Te(15)^{ii}	92.18(3)	Cl(18) — Ga(5) — Cl(19)	105.32(13)
Te(16) — Au(6) — Te(15)^{ii}	179.07(3)	Cl(17) — Ga(5) — Cl(19)	107.53(16)
Te(14)^{ii} — Au(6) — Te(15)^{ii}	88.51(3)	Cl(20) — Ga(5) — Cl(19)	106.71(16)

A.1.6 $(Au_6Te_{18}Br)[AlCl_4]_5$

Table A.26: Crystal data and structure refinement for $(Au_6Te_{18}Br)[AlCl_4]_5$.

Empirical formula	$Al_5\,Au_6\,Br\,Cl_{20}\,Te_{18}$
Formula weight / $g \cdot mol^{-1}$	4402.41
Temperature / K	123(2)
Crystal system; space group	Monoclinic; $P2_1/c$
Lattice constants / $Å$	$a = 15.3779(2)$
	$b = 19.0170(3)$; $\beta = 96.508(1)°$
	$c = 21.0065(3)$
Volume / $Å^3$	6103.6(2)
Z; F(000); calc. density / $g \cdot cm^{-3}$	4; 7400; 4.791
Wavelength	$Mo_{K\alpha}$ ($\lambda = 0.71073$ Å)
Crystal size / mm^3	0.130 × 0.064 × 0.014
Theta range for data collection / °	$2.936 \leq \theta \leq 27.492$
Limiting indices	$-19 \leq h \leq 19$; $-24 \leq k \leq 23$; $-27 \leq l \leq 27$
Reflections collected / unique	115032 / 13973
Completeness to $\theta = 25.242°$	99.8 %
R_{int}; R_σ	0.1112; 0.0671
Absorption coefficient / mm^{-1}	24.417; Semi-empirical from equivalents
Max. / min. transmission	0.2025 / 0.0895
Refinement method	Full-matrix least-squares on F^2
Data / restraints / parameters	13973 / 4 / 496
R indices (all data) R_1; wR_2	0.0813; 0.1164
R indices $[I > 4\sigma(I)]$ R_1; wR_2	0.0430; 0.1040; n = 9364 reflections
Goodness-of-fit for F^2	1.039
Largest diff. peak / $e^- \cdot Å^{-3}$	+2.879 (0.58 Å from Cl7)
	-2.021 (0.81 Å from Au5)
Avg. diff. density / $e^- \cdot Å^{-3}$	0.369

Table A.27: Fractional coordinates and equivalent isotropic displacement parameter U_{eq} for the independent atoms in the structure of $(Au_6Te_{18}Br)[AlCl_4]_5$.

Atom	Wyck.	Site	*SOF*	*x / a*	*y / b*	*z / c*	U_{eq} / Å^2
Au(1)	4*e*	1		0.05139(4)	0.06592(3)	0.11068(2)	0.02307(12)
Au(2)	4*e*	1		0.14496(4)	0.03942(3)	-0.05013(2)	0.02400(13)
Au(3)	4*e*	1		-0.08177(4)	0.11858(3)	-0.04479(2)	0.02446(13)
Te(1)	4*e*	1		0.19741(6)	0.10450(5)	0.06139(4)	0.0256(2)
Te(2)	4*e*	1		-0.03431(7)	0.18322(5)	0.06740(4)	0.0274(2)
Te(3)	4*e*	1		0.13478(7)	-0.05111(5)	0.15501(4)	0.0278(2)
Te(4)	4*e*	1		-0.09213(6)	0.02383(5)	0.16207(4)	0.0279(2)
Te(5)	4*e*	1		-0.06397(6)	-0.15713(5)	0.09526(4)	0.0266(2)
Te(6)	4*e*	1		-0.22665(6)	0.07882(5)	0.00488(5)	0.0299(2)
Te(7)	4*e*	1		-0.18596(7)	0.15721(5)	0.12402(5)	0.0346(2)
Te(8)	4*e*	1		-0.00771(7)	-0.10541(5)	0.21646(4)	0.0303(2)
Te(9)	4*e*	1	0.632(1)	0.30570(7)	-0.00203(6)	0.10896(5)	0.0222(3)
Te(10)	4*e*	1	0.368(1)	0.12790(11)	0.24375(8)	0.02300(7)	0.0213(4)
Br(1)	4*e*	1	0.204(1)	0.30570(7)	-0.00203(6)	0.10896(5)	0.0222(3)
Br(2)	4*e*	1	0.296(1)	0.12790(11)	0.24375(8)	0.02300(7)	0.0213(4)
Au(4)	4*e*	1		0.66774(4)	0.51994(3)	0.05083(3)	0.02834(14)
Au(5)	4*e*	1		0.50231(4)	0.37395(3)	0.05665(3)	0.02839(14)
Au(6)	4*e*	1		0.56054(4)	0.44215(3)	-0.10382(3)	0.03003(14)
Te(11)	4*e*	1		0.66837(7)	0.39446(5)	0.10937(5)	0.0315(2)
Te(12)	4*e*	1		0.72704(7)	0.46620(5)	-0.05501(5)	0.0346(2)
Te(13)	4*e*	1		0.66312(7)	0.64711(5)	-0.00395(5)	0.0325(2)
Te(14)	4*e*	1		0.60672(7)	0.57929(6)	0.15302(5)	0.0360(2)
Te(15)	4*e*	1		0.44102(7)	0.68530(5)	0.04778(5)	0.0336(2)
Te(16)	4*e*	1		0.56095(7)	0.56903(5)	-0.16011(5)	0.0349(2)
Te(17)	4*e*	1		0.74299(7)	0.59402(6)	-0.11771(5)	0.0403(3)
Te(18)	4*e*	1		0.60636(7)	0.72113(5)	0.10779(5)	0.0365(2)
Te(19)	4*e*	1	0.589(1)	0.62186(9)	0.44260(7)	0.22493(6)	0.0268(3)
Te(20)	4*e*	1	0.411(1)	0.74682(11)	0.32361(8)	0.01035(8)	0.0323(4)
Br(3)	4*e*	1	0.217(1)	0.62186(9)	0.44260(7)	0.22493(6)	0.0268(3)
Br(4)	4*e*	1	0.283(1)	0.74682(11)	0.32361(8)	0.01035(8)	0.0323(4)
Al(1)	4*e*	1		0.4865(3)	0.1944(2)	0.1669(2)	0.0341(11)
Cl(1)	4*e*	1		0.4870(2)	0.09026(18)	0.20629(18)	0.0329(8)
Cl(2A)	4*e*	1	0.45(7)	0.610(2)	0.219(2)	0.137(2)	0.058(7)

continued on next page

Atom	Wyck.	Site	*SOF*	*x / a*	*y / b*	*z / c*	U_{eq} / Å^2
Cl(3A)	4*e*	1	0.45(7)	0.491(3)	0.2674(9)	0.2474(7)	0.044(6)
Cl(4A)	4*e*	1	0.45(7)	0.3709(16)	0.2183(17)	0.106(2)	0.051(8)
Cl(2B)	4*e*	1	0.55(7)	0.596(2)	0.2198(18)	0.118(2)	0.075(10)
Cl(3B)	4*e*	1	0.55(7)	0.445(3)	0.2708(7)	0.2328(17)	0.064(9)
Cl(4B)	4*e*	1	0.55(7)	0.3948(19)	0.1972(13)	0.0807(15)	0.055(7)
Al(2)	4*e*	1		-0.0449(3)	0.4859(2)	0.1148(2)	0.0321(10)
Cl(5)	4*e*	1		-0.0944(3)	0.5438(2)	0.02923(17)	0.0351(8)
Cl(6)	4*e*	1		-0.1432(2)	0.49544(19)	0.18201(16)	0.0313(8)
Cl(7)	4*e*	1		0.0787(2)	0.52884(17)	0.16019(14)	0.0202(7)
Cl(8)	4*e*	1		-0.0277(3)	0.37451(19)	0.09920(19)	0.0458(11)
Al(3)	4*e*	1		0.7748(3)	0.2396(2)	0.3237(2)	0.0325(10)
Cl(9)	4*e*	1		0.8072(2)	0.29569(17)	0.23916(16)	0.0299(8)
Cl(10)	4*e*	1		0.6905(3)	0.30768(19)	0.37154(18)	0.0369(9)
Cl(11)	4*e*	1		0.8938(2)	0.21827(16)	0.38882(16)	0.0249(7)
Cl(12)	4*e*	1		0.7067(2)	0.14198(17)	0.29678(16)	0.0308(8)
Al(4)	4*e*	1		0.8397(3)	0.7059(2)	0.2302(2)	0.0305(10)
Cl(13)	4*e*	1		0.7918(3)	0.81286(18)	0.23870(18)	0.0397(10)
Cl(14)	4*e*	1		0.9751(2)	0.6996(2)	0.26647(18)	0.0399(9)
Cl(15)	4*e*	1		0.7603(3)	0.6354(2)	0.27830(17)	0.0420(10)
Cl(16)	4*e*	1		0.8255(3)	0.6802(2)	0.13060(17)	0.0402(10)
Al(5)	4*e*	1		0.6120(3)	0.9552(3)	0.1202(2)	0.0411(12)
Cl(17)	4*e*	1		0.5813(3)	1.0435(2)	0.0577(2)	0.0487(11)
Cl(18)	4*e*	1		0.4996(3)	0.9010(2)	0.1438(2)	0.0438(10)
Cl(19)	4*e*	1		0.6835(3)	0.8798(2)	0.0696(2)	0.0563(13)
Cl(20)	4*e*	1		0.6979(2)	0.98740(18)	0.20549(17)	0.0291(8)

Table A.28: Anisotropic displacement parameters U_{ij} / Å^2 for the independent atoms in the structure of $(Au_6Te_{18}Br)[AlCl_4]_5$.

Atom	U_{11}	U_{22}	U_{33}	U_{23}	U_{13}	U_{12}
Au(1)	0.0269(3)	0.0212(3)	0.0211(3)	-0.0004(2)	0.0023(2)	-0.0021(2)
Au(2)	0.0265(3)	0.0237(3)	0.0216(3)	-0.0005(2)	0.0023(2)	-0.0025(2)
Au(3)	0.0281(3)	0.0212(3)	0.0239(3)	0.0003(2)	0.0019(2)	-0.0007(2)
Te(1)	0.0283(5)	0.0258(5)	0.0223(4)	-0.0018(4)	0.0012(4)	-0.0064(4)
Te(2)	0.0355(6)	0.0209(5)	0.0254(5)	-0.0026(4)	0.0020(4)	-0.0002(4)
Te(3)	0.0356(6)	0.0248(5)	0.0222(5)	0.0004(4)	-0.0007(4)	0.0010(4)

continued on next page

Atom	U_{11}	U_{22}	U_{33}	U_{23}	U_{13}	U_{12}
Te(4)	0.0308(5)	0.0314(5)	0.0221(4)	-0.0034(4)	0.0055(4)	-0.0063(4)
Te(5)	0.0318(5)	0.0228(5)	0.0250(5)	0.0036(4)	0.0029(4)	-0.0035(4)
Te(6)	0.0280(5)	0.0283(5)	0.0341(5)	0.0038(4)	0.0063(4)	0.0030(4)
Te(7)	0.0354(6)	0.0329(5)	0.0355(5)	-0.0076(4)	0.0035(4)	0.0033(4)
Te(8)	0.0383(6)	0.0295(5)	0.0222(5)	0.0048(4)	-0.0001(4)	-0.0064(4)
Te(9)	0.0211(6)	0.0239(6)	0.0205(6)	-0.0043(5)	-0.0026(4)	-0.0023(5)
Te(10)	0.0300(9)	0.0158(7)	0.0178(7)	-0.0021(6)	0.0021(6)	-0.0098(6)
Br(1)	0.0211(6)	0.0239(6)	0.0205(6)	-0.0043(5)	-0.0026(4)	-0.0023(5)
Br(2)	0.0300(9)	0.0158(7)	0.0178(7)	-0.0021(6)	0.0021(6)	-0.0098(6)
Au(4)	0.0305(3)	0.0276(3)	0.0264(3)	0.0000(2)	0.0006(2)	-0.0024(2)
Au(5)	0.0327(3)	0.0259(3)	0.0263(3)	0.0010(2)	0.0023(2)	-0.0016(2)
Au(6)	0.0336(3)	0.0312(3)	0.0251(3)	-0.0024(2)	0.0028(2)	-0.0016(3)
Te(11)	0.0339(6)	0.0278(5)	0.0313(5)	0.0018(4)	-0.0025(4)	0.0021(4)
Te(12)	0.0311(6)	0.0402(6)	0.0330(5)	-0.0033(5)	0.0061(4)	-0.0017(5)
Te(13)	0.0341(6)	0.0263(5)	0.0361(5)	0.0018(4)	-0.0002(4)	-0.0063(4)
Te(14)	0.0372(6)	0.0430(6)	0.0269(5)	-0.0070(5)	-0.0006(4)	-0.0054(5)
Te(15)	0.0397(6)	0.0274(5)	0.0340(5)	-0.0040(4)	0.0048(4)	0.0008(4)
Te(16)	0.0435(6)	0.0357(6)	0.0266(5)	0.0004(4)	0.0090(4)	-0.0045(5)
Te(17)	0.0369(6)	0.0479(6)	0.0376(6)	0.0081(5)	0.0112(5)	-0.0032(5)
Te(18)	0.0442(7)	0.0259(5)	0.0383(6)	-0.0045(4)	0.0003(5)	-0.0061(5)
Te(19)	0.0329(8)	0.0277(7)	0.0187(6)	0.0005(5)	-0.0024(5)	0.0008(5)
Te(20)	0.0278(9)	0.0301(9)	0.0389(9)	0.0066(7)	0.0035(7)	0.0070(7)
Br(3)	0.0329(8)	0.0277(7)	0.0187(6)	0.0005(5)	-0.0024(5)	0.0008(5)
Br(4)	0.0278(9)	0.0301(9)	0.0389(9)	0.0066(7)	0.0035(7)	0.0070(7)
Al(1)	0.030(3)	0.028(2)	0.044(3)	0.003(2)	0.002(2)	-0.005(2)
Cl(1)	0.032(2)	0.0264(18)	0.040(2)	0.0050(16)	0.0054(16)	-0.0034(15)
Cl(2A)	0.032(10)	0.036(9)	0.104(17)	0.047(9)	0.000(9)	-0.005(8)
Cl(3A)	0.074(15)	0.018(5)	0.037(6)	-0.010(4)	-0.002(8)	-0.002(7)
Cl(4A)	0.032(8)	0.043(10)	0.074(14)	0.030(10)	-0.014(8)	-0.015(7)
Cl(2B)	0.041(12)	0.053(9)	0.14(3)	0.056(13)	0.040(15)	0.023(8)
Cl(3B)	0.11(2)	0.029(5)	0.062(12)	-0.002(6)	0.055(14)	0.002(8)
Cl(4B)	0.044(10)	0.046(8)	0.068(11)	0.026(8)	-0.029(8)	-0.019(7)
Al(2)	0.037(3)	0.032(2)	0.027(2)	0.0037(19)	0.003(2)	0.000(2)
Cl(5)	0.036(2)	0.044(2)	0.0252(18)	0.0038(16)	0.0010(15)	0.0016(17)
Cl(6)	0.030(2)	0.039(2)	0.0258(17)	0.0087(16)	0.0092(15)	0.0009(16)

continued on next page

Atom	U_{11}	U_{22}	U_{33}	U_{23}	U_{13}	U_{12}
Cl(7)	0.0171(16)	0.0280(17)	0.0149(14)	0.0053(13)	0.0000(12)	-0.0027(13)
Cl(8)	0.080(3)	0.0195(18)	0.040(2)	-0.0016(17)	0.016(2)	-0.0007(19)
Al(3)	0.036(3)	0.024(2)	0.037(2)	-0.002(2)	-0.002(2)	-0.0017(19)
Cl(9)	0.034(2)	0.0231(17)	0.0313(18)	0.0003(15)	-0.0011(15)	-0.0027(15)
Cl(10)	0.039(2)	0.0279(19)	0.044(2)	-0.0029(17)	0.0042(18)	0.0027(16)
Cl(11)	0.0204(17)	0.0206(16)	0.0318(17)	-0.0072(14)	-0.0046(14)	-0.0028(13)
Cl(12)	0.039(2)	0.0175(16)	0.0334(19)	0.0005(14)	-0.0077(16)	-0.0105(15)
Al(4)	0.038(3)	0.029(2)	0.024(2)	0.0041(19)	0.0009(19)	-0.002(2)
Cl(13)	0.061(3)	0.0221(18)	0.037(2)	-0.0010(16)	0.0114(19)	0.0150(17)
Cl(14)	0.027(2)	0.059(3)	0.0315(19)	0.0131(18)	-0.0059(16)	-0.0047(18)
Cl(15)	0.044(2)	0.054(2)	0.0269(18)	0.0101(18)	-0.0006(17)	-0.013(2)
Cl(16)	0.055(3)	0.041(2)	0.0242(18)	0.0031(17)	0.0043(17)	-0.0114(19)
Al(5)	0.039(3)	0.040(3)	0.048(3)	0.003(2)	0.017(2)	-0.007(2)
Cl(17)	0.048(3)	0.050(3)	0.050(2)	0.015(2)	0.018(2)	0.001(2)
Cl(18)	0.036(2)	0.040(2)	0.059(3)	0.005(2)	0.022(2)	-0.0017(18)
Cl(19)	0.062(3)	0.041(2)	0.073(3)	-0.006(2)	0.042(3)	-0.012(2)
Cl(20)	0.0238(19)	0.0287(18)	0.0355(19)	-0.0015(15)	0.0055(15)	0.0026(14)

Table A.29: Selected bond lengths for $(Au_6Te_{18}Br)[AlCl_4]_5$. Symmetry transformations used to generate equivalent atoms: (i) $-x$, $-y$, $-z$; (ii) $-x+1$, $-y+1$, $-z$.

Atoms 1, 2	Distance / Å	Atoms 1, 2	Distance / Å
Au(1) — Te(1)	2.6795(11)	Te(11) — Te(19)	2.7634(15)
Au(1) — Te(3)	2.6823(11)	Te(11) — Te(20)	2.8575(19)
Au(1) — Te(4)	2.6865(11)	Te(12) — Te(17)	2.7887(15)
Au(1) — Te(2)	2.6958(11)	Te(12) — Te(20)	3.0392(19)
Au(2) — Te(5)^{i}	2.6821(11)	Te(13) — Au(5)^{ii}	2.6868(12)
Au(2) — Te(4)^{i}	2.6837(10)	Te(13) — Te(18)	2.9527(14)
Au(2) — Te(1)	2.6911(10)	Te(13) — Te(17)	2.9838(15)
Au(2) — Te(6)^{i}	2.6958(11)	Te(14) — Au(6)^{ii}	2.6921(12)
Au(3) — Te(6)	2.6740(11)	Te(14) — Te(18)	2.8596(15)
Au(3) — Te(2)	2.6848(10)	Te(14) — Te(19)	3.0023(16)
Au(3) — Te(5)^{i}	2.6876(11)	Te(15) — Au(6)^{ii}	2.6959(11)
Au(3) — Te(3)^{i}	2.6913(10)	Te(15) — Au(5)^{ii}	2.6973(11)
Te(1) — Te(9)	2.7383(15)	Te(15) — Te(18)	2.7913(15)
Te(1) — Te(10)	2.9344(18)	Te(15) — Te(20)^{ii}	3.011(2)

continued on next page

Atoms 1, 2	Distance / Å	Atoms 1, 2	Distance / Å
Te(2) — Te(7)	2.7797(14)	Te(16) — Au(5)^{ii}	2.7063(11)
Te(2) — Te(10)	2.9908(18)	Te(16) — Te(17)	2.8792(16)
Te(3) — Au(3)^{i}	2.6913(10)	Te(16) — Br(3)^{ii}	2.9898(17)
Te(3) — Te(8)	2.8592(14)	Te(16) — Te(19)^{ii}	2.9898(17)
Te(3) — Te(9)	3.0482(15)	Te(19) — Te(16)^{ii}	2.9897(17)
Te(4) — Au(2)^{i}	2.6839(10)	Te(20) — Te(15)^{ii}	3.011(2)
Te(4) — Te(8)	2.9487(14)	Al(1) — Cl(4A)	2.114(16)
Te(4) — Te(7)	2.9821(14)	Al(1) — Cl(2A)	2.12(4)
Te(5) — Au(2)^{i}	2.6821(11)	Al(1) — Cl(2B)	2.13(3)
Te(5) — Au(3)^{i}	2.6875(11)	Al(1) — Cl(1)	2.147(6)
Te(5) — Te(8)	2.7746(13)	Al(1) — Cl(3B)	2.155(14)
Te(5) — Te(10)^{i}	3.0492(17)	Al(1) — Cl(4B)	2.166(15)
Te(6) — Au(2)^{i}	2.6957(11)	Al(1) — Cl(3A)	2.184(17)
Te(6) — Te(7)	2.9194(14)	Al(2) — Cl(8)	2.165(6)
Te(6) — Br(1)^{i}	2.9444(14)	Al(2) — Cl(5)	2.171(6)
Te(6) — Te(9)^{i}	2.9444(14)	Al(2) — Cl(7)	2.185(6)
Te(9) — Te(6)^{i}	2.9444(14)	Al(2) — Cl(6)	2.189(6)
Te(10) — Te(5)^{i}	3.0492(17)	Al(3) — Cl(10)	2.159(6)
Au(4) — Te(13)	2.6757(11)	Al(3) — Cl(12)	2.173(5)
Au(4) — Te(11)	2.6841(11)	Al(3) — Cl(9)	2.178(6)
Au(4) — Te(14)	2.6869(11)	Al(3) — Cl(11)	2.195(6)
Au(4) — Te(12)	2.6979(11)	Al(4) — Cl(16)	2.134(5)
Au(5) — Te(13)^{ii}	2.6869(12)	Al(4) — Cl(14)	2.137(6)
Au(5) — Te(11)	2.6943(12)	Al(4) — Cl(15)	2.142(6)
Au(5) — Te(15)^{ii}	2.6971(11)	Al(4) — Cl(13)	2.179(6)
Au(5) — Te(16)^{ii}	2.7064(11)	Al(5) — Cl(18)	2.119(6)
Au(6) — Te(12)	2.6872(12)	Al(5) — Cl(17)	2.151(7)
Au(6) — Te(16)	2.6872(11)	Al(5) — Cl(19)	2.158(7)
Au(6) — Te(14)^{ii}	2.6921(12)	Al(5) — Cl(20)	2.190(6)
Au(6) — Te(15)^{ii}	2.6960(11)		

Table A.30: Selected bond angles for $(Au_6Te_{18}Br)[AlCl_4]_5$. Symmetry transformations used to generate equivalent atoms: (i) $-x$, $-y$, $-z$; (ii) $-x+1$, $-y+1$, $-z$.

Atoms 1, 2, 3	Angle / °	Atoms 1, 2, 3	Angle / °
Te(1) — Au(1) — Te(3)	88.44(3)	Au(4) — Te(11) — Au(5)	89.22(3)

continued on next page

Atoms 1, 2, 3	Angle / °	Atoms 1, 2, 3	Angle / °
Te(1) — Au(1) — Te(4)	178.15(4)	Au(4) — Te(11) — Te(19)	96.90(4)
Te(3) — Au(1) — Te(4)	89.74(3)	Au(5) — Te(11) — Te(19)	94.67(4)
Te(1) — Au(1) — Te(2)	92.42(3)	Au(4) — Te(11) — Te(20)	93.76(4)
Te(3) — Au(1) — Te(2)	179.11(4)	Au(5) — Te(11) — Te(20)	95.24(5)
Te(4) — Au(1) — Te(2)	89.40(3)	Te(19) — Te(11) — Te(20)	165.53(6)
Te(5)^{i} — Au(2) — Te(4)^{i}	88.97(3)	Au(6) — Te(12) — Au(4)	89.00(3)
Te(5)^{i} — Au(2) — Te(1)	90.30(3)	Au(6) — Te(12) — Te(17)	95.69(4)
Te(4)^{i} — Au(2) — Te(1)	179.25(4)	Au(4) — Te(12) — Te(17)	96.61(4)
Te(5)^{i} — Au(2) — Te(6)^{i}	179.89(4)	Au(6) — Te(12) — Te(20)	93.60(5)
Te(4)^{i} — Au(2) — Te(6)^{i}	91.02(3)	Au(4) — Te(12) — Te(20)	89.52(4)
Te(1) — Au(2) — Te(6)^{i}	89.71(3)	Te(17) — Te(12) — Te(20)	168.95(6)
Te(6) — Au(3) — Te(2)	86.71(3)	Au(4) — Te(13) — Au(5)^{ii}	91.16(3)
Te(6) — Au(3) — Te(5)^{i}	179.38(4)	Au(4) — Te(13) — Te(18)	94.86(4)
Te(2) — Au(3) — Te(5)^{i}	93.75(3)	Au(5)^{ii} — Te(13) — Te(18)	92.71(4)
Te(6) — Au(3) — Te(3)^{i}	90.94(3)	Au(4) — Te(13) — Te(17)	92.60(4)
Te(2) — Au(3) — Te(3)^{i}	177.61(4)	Au(5)^{ii} — Te(13) — Te(17)	94.36(4)
Te(5)^{i} — Au(3) — Te(3)^{i}	88.59(3)	Te(18) — Te(13) — Te(17)	169.61(5)
Au(1) — Te(1) — Au(2)	91.65(3)	Au(4) — Te(14) — Au(6)^{ii}	91.98(3)
Au(1) — Te(1) — Te(9)	99.09(4)	Au(4) — Te(14) — Te(18)	96.81(4)
Au(2) — Te(1) — Te(9)	95.01(4)	Au(6)^{ii} — Te(14) — Te(18)	92.84(4)
Au(1) — Te(1) — Te(10)	93.33(4)	Au(4) — Te(14) — Te(19)	91.38(4)
Au(2) — Te(1) — Te(10)	96.42(4)	Au(6)^{ii} — Te(14) — Te(19)	94.49(4)
Te(9) — Te(1) — Te(10)	162.84(5)	Te(18) — Te(14) — Te(19)	168.81(5)
Au(3) — Te(2) — Au(1)	89.49(3)	Au(6)^{ii} — Te(15) — Au(5)^{ii}	89.96(3)
Au(3) — Te(2) — Te(7)	97.84(4)	Au(6)^{ii} — Te(15) — Te(18)	94.30(4)
Au(1) — Te(2) — Te(7)	96.33(4)	Au(5)^{ii} — Te(15) — Te(18)	96.18(4)
Au(3) — Te(2) — Te(10)	93.20(4)	Au(6)^{ii} — Te(15) — Te(20)^{ii}	94.07(5)
Au(1) — Te(2) — Te(10)	91.75(4)	Au(5)^{ii} — Te(15) — Te(20)^{ii}	91.73(4)
Te(7) — Te(2) — Te(10)	166.35(5)	Te(18) — Te(15) — Te(20)^{ii}	168.48(5)
Au(1) — Te(3) — Au(3)^{i}	90.61(3)	Au(6) — Te(16) — Au(5)^{ii}	89.28(3)
Au(1) — Te(3) — Te(8)	95.49(4)	Au(6) — Te(16) — Te(17)	93.60(4)
Au(3)^{i} — Te(3) — Te(8)	92.48(4)	Au(5)^{ii} — Te(16) — Te(17)	96.36(4)
Au(1) — Te(3) — Te(9)	91.79(4)	Au(6) — Te(16) — Br(3)^{ii}	94.88(4)
Au(3)^{i} — Te(3) — Te(9)	93.50(4)	Au(5)^{ii} — Te(16) — Br(3)^{ii}	89.45(4)
Te(8) — Te(3) — Te(9)	170.53(4)	Te(17) — Te(16) — Br(3)^{ii}	169.78(5)

continued on next page

Atoms 1, 2, 3	Angle / °	Atoms 1, 2, 3	Angle / °
Au(2)^{i} — Te(4) — Au(1)	87.84(3)	Au(6) — Te(16) — Te(19)^{ii}	94.88(4)
Au(2)^{i} — Te(4) — Te(8)	92.42(3)	Au(5)^{ii} — Te(16) — Te(19)^{ii}	89.45(4)
Au(1) — Te(4) — Te(8)	93.35(4)	Te(17) — Te(16) — Te(19)^{ii}	169.78(5)
Au(2)^{i} — Te(4) — Te(7)	93.28(4)	Br(3)^{ii} — Te(16) — Te(19)^{ii}	0.0
Au(1) — Te(4) — Te(7)	91.92(4)	Te(12) — Te(17) — Te(16)	82.40(4)
Te(8) — Te(4) — Te(7)	172.38(4)	Te(12) — Te(17) — Te(13)	81.40(4)
Au(2)^{i} — Te(5) — Au(3)^{i}	90.43(3)	Te(16) — Te(17) — Te(13)	80.19(4)
Au(2)^{i} — Te(5) — Te(8)	96.46(4)	Te(15) — Te(18) — Te(14)	83.52(4)
Au(3)^{i} — Te(5) — Te(8)	94.47(4)	Te(15) — Te(18) — Te(13)	82.00(4)
Au(2)^{i} — Te(5) — Te(10)^{i}	93.95(4)	Te(14) — Te(18) — Te(13)	79.91(4)
Au(3)^{i} — Te(5) — Te(10)^{i}	91.85(4)	Te(11) — Te(19) — Te(16)^{ii}	84.21(4)
Te(8) — Te(5) — Te(10)^{i}	167.77(5)	Te(11) — Te(19) — Te(14)	81.83(4)
Au(3) — Te(6) — Au(2)^{i}	89.88(3)	Te(16)^{ii} — Te(19) — Te(14)	79.61(4)
Au(3) — Te(6) — Te(7)	94.76(4)	Te(11) — Te(20) — Te(15)^{ii}	81.78(5)
Au(2)^{i} — Te(6) — Te(7)	94.45(4)	Te(11) — Te(20) — Te(12)	83.07(5)
Au(3) — Te(6) — Br(1)^{i}	96.25(4)	Te(15)^{ii} — Te(20) — Te(12)	79.90(5)
Au(2)^{i} — Te(6) — Br(1)^{i}	90.33(4)	Cl(4A) — Al(1) — Cl(2A)	119.4(16)
Te(7) — Te(6) — Br(1)^{i}	168.00(5)	Cl(4A) — Al(1) — Cl(1)	113.3(6)
Au(3) — Te(6) — Te(9)^{i}	96.25(4)	Cl(2A) — Al(1) — Cl(1)	111.0(10)
Au(2)^{i} — Te(6) — Te(9)^{i}	90.33(4)	Cl(2B) — Al(1) — Cl(1)	115.4(9)
Te(7) — Te(6) — Te(9)^{i}	168.00(5)	Cl(2B) — Al(1) — Cl(3B)	118.0(17)
Br(1)^{i} — Te(6) — Te(9)^{i}	0.0	Cl(1) — Al(1) — Cl(3B)	111.2(6)
Te(2) — Te(7) — Te(6)	80.37(4)	Cl(2B) — Al(1) — Cl(4B)	94(2)
Te(2) — Te(7) — Te(4)	82.08(4)	Cl(1) — Al(1) — Cl(4B)	108.6(5)
Te(6) — Te(7) — Te(4)	81.12(4)	Cl(3B) — Al(1) — Cl(4B)	107.9(6)
Te(5) — Te(8) — Te(3)	83.63(4)	Cl(4A) — Al(1) — Cl(3A)	106.2(8)
Te(5) — Te(8) — Te(4)	82.08(4)	Cl(2A) — Al(1) — Cl(3A)	98.0(17)
Te(3) — Te(8) — Te(4)	81.39(3)	Cl(1) — Al(1) — Cl(3A)	106.8(5)
Te(1) — Te(9) — Te(6)^{i}	83.83(4)	Cl(8) — Al(2) — Cl(5)	114.1(2)
Te(1) — Te(9) — Te(3)	80.32(4)	Cl(8) — Al(2) — Cl(7)	108.5(3)
Te(6)^{i} — Te(9) — Te(3)	79.30(4)	Cl(5) — Al(2) — Cl(7)	112.2(2)
Te(1) — Te(10) — Te(2)	81.81(4)	Cl(8) — Al(2) — Cl(6)	106.5(2)
Te(1) — Te(10) — Te(5)^{i}	79.06(4)	Cl(5) — Al(2) — Cl(6)	106.8(2)
Te(2) — Te(10) — Te(5)^{i}	80.96(4)	Cl(7) — Al(2) — Cl(6)	108.5(2)
Te(13) — Au(4) — Te(11)	177.65(4)	Cl(10) — Al(3) — Cl(12)	109.7(3)

continued on next page

Atoms 1, 2, 3	Angle / °	Atoms 1, 2, 3	Angle / °
Te(13) — Au(4) — Te(14)	88.24(4)	Cl(10) — Al(3) — Cl(9)	106.9(2)
Te(11) — Au(4) — Te(14)	89.48(3)	Cl(12) — Al(3) — Cl(9)	110.8(2)
Te(13) — Au(4) — Te(12)	89.02(4)	Cl(10) — Al(3) — Cl(11)	108.8(2)
Te(11) — Au(4) — Te(12)	93.25(4)	Cl(12) — Al(3) — Cl(11)	110.3(2)
Te(14) — Au(4) — Te(12)	177.20(4)	Cl(9) — Al(3) — Cl(11)	110.3(2)
Te(13)^{ii} — Au(5) — Te(11)	179.74(4)	Cl(16) — Al(4) — Cl(14)	108.9(3)
Te(13)^{ii} — Au(5) — Te(15)^{ii}	88.90(4)	Cl(16) — Al(4) — Cl(15)	108.6(2)
Te(11) — Au(5) — Te(15)^{ii}	90.93(4)	Cl(14) — Al(4) — Cl(15)	112.4(2)
Te(13)^{ii} — Au(5) — Te(16)^{ii}	88.90(4)	Cl(16) — Al(4) — Cl(13)	107.2(2)
Te(11) — Au(5) — Te(16)^{ii}	91.27(4)	Cl(14) — Al(4) — Cl(13)	110.3(3)
Te(15)^{ii} — Au(5) — Te(16)^{ii}	177.68(4)	Cl(15) — Al(4) — Cl(13)	109.2(3)
Te(12) — Au(6) — Te(16)	88.02(4)	Cl(18) — Al(5) — Cl(17)	113.2(3)
Te(12) — Au(6) — Te(14)^{ii}	178.91(4)	Cl(18) — Al(5) — Cl(19)	105.5(3)
Te(16) — Au(6) — Te(14)^{ii}	90.97(4)	Cl(17) — Al(5) — Cl(19)	107.9(3)
Te(12) — Au(6) — Te(15)^{ii}	92.39(4)	Cl(18) — Al(5) — Cl(20)	112.1(3)
Te(16) — Au(6) — Te(15)^{ii}	179.59(4)	Cl(17) — Al(5) — Cl(20)	110.6(3)
Te(14)^{ii} — Au(6) — Te(15)^{ii}	88.63(4)	Cl(19) — Al(5) — Cl(20)	107.2(3)

A.1.7 $(Au_6Te_{18}Br)[AlBr_4]_5$ Enantiomer 1

Table A.31: Crystal data and structure refinement for $(Au_6Te_{18}Br)[AlBr_4]_5$.

Empirical formula	$Al_5\,Au_6\,Br_{21}\,Te_{18}$
Formula weight / $g \cdot mol^{-1}$	5291.61
Temperature / K	123(2)
Crystal system; space group	Trigonal; $P31c$
Lattice constants / $Å$	$a = 12.8029(2)$
	$c = 23.0476(3)$
Volume / $Å^3$	3271.7(1)
Z; F(000); calc. density / $g \cdot cm^{-3}$	2; 4420; 5.371
Wavelength	$Mo_{K\alpha}$ ($\lambda = 0.71073$ Å)
Crystal size / mm^3	0.090 × 0.060 × 0.040
Theta range for data collection / °	$3.182 \leq \theta \leq 27.446$
Limiting indices	$-16 \leq h \leq 16$; $-16 \leq k \leq 16$; $-29 \leq l \leq 29$
Reflections collected / unique	56165 / 4993
Completeness to $\theta = 25.242°$	99.8 %
R_{int}; R_σ	0.0866; 0.0320
Absorption coefficient / mm^{-1}	34.173; Semi-empirical from equivalents
Max. / min. transmission	0.1200 / 0.0555
Refinement method	Full-matrix least-squares on F^2
Data / restraints / parameters	4993 / 3 / 158
R indices (all data) R_1; wR_2	0.0439; 0.0876
R indices $[I > 4\sigma(I)]$ R_1; wR_2	0.0346; 0.0829; n = 4354 reflections
Goodness-of-fit for F^2	1.051
Flack x	0.013(7) (1932 reflections; Parson's method)
Largest diff. peak / $e^- \cdot Å^{-3}$	+1.202 (0.47 Å from Br2)
	-2.291 (2.49 Å from Au2)
Avg. diff. density / $e^- \cdot Å^{-3}$	0.374

Table A.32: Fractional coordinates and equivalent isotropic displacement parameter U_{eq} for the independent atoms in the structure of $(Au_6Te_{18}Br)[AlBr_4]_5$.

Atom	Wyck.	Site	*SOF*	*x / a*	*y / b*	*z / c*	U_{eq} / $Å^2$
Au(1)	6*c*	1		0.32952(7)	0.49699(7)	0.31834(3)	0.01997(18)
Au(2)	6*c*	1		0.50044(7)	0.66277(6)	0.18044(2)	0.01989(19)
Te(1)	6*c*	1		0.49777(14)	0.49345(14)	0.25031(8)	0.0240(2)
Te(2)	6*c*	1		0.32889(12)	0.49235(13)	0.11226(6)	0.0251(3)
Te(3)	6*c*	1		0.16131(13)	0.49841(13)	0.38743(6)	0.0249(3)
Te(4)	6*c*	1		0.15863(15)	0.32892(9)	0.24961(8)	0.0247(2)
Te(5)	2*b*	3..		0.3333	0.6667	0.03367(11)	0.0255(5)
Te(6)	2*b*	3..		0.3333	0.6667	0.46849(10)	0.0279(6)
Te(7)	6*c*	1..	0.6666(13)	0.32648(16)	0.29150(16)	0.18346(8)	0.0254(4)
Te(8)	6*c*	1	0.6667(13)	0.70119(17)	0.66006(17)	0.31867(8)	0.0263(4)
Br(1)	6*c*	1	0.1563(13)	0.32648(16)	0.29150(16)	0.18346(8)	0.0254(4)
Br(2)	6*c*	1	0.1771(13)	0.70119(17)	0.66006(17)	0.31867(8)	0.0263(4)
Al(1)	2*b*	3..		0.0000	0.0000	0.3483(4)	0.0238(18)
Br(3)	2*b*	3..		0.0000	0.0000	0.24776(18)	0.0239(5)
Br(4)	6*c*	1		0.1651(2)	0.1738(2)	0.37904(11)	0.0382(6)
Al(3)	2*b*	3..		0.6667	0.3333	0.3595(4)	0.0217(19)
Br(5)	2*b*	3..		0.6667	0.3333	0.25904(14)	0.0245(7)
Br(6)	6*c*	1		0.65570(19)	0.15861(18)	0.39216(10)	0.0269(5)
Al(2)	6*c*	1		0.3361(5)	0.0822(5)	0.0596(2)	0.0255(12)
Br(7)	6*c*	1		0.5051(2)	0.1481(2)	0.11679(12)	0.0404(6)
Br(8)	6*c*	1		0.1663(2)	-0.0110(2)	0.11469(12)	0.0393(6)
Br(9)	6*c*	1		0.3558(2)	0.24890(19)	0.01205(9)	0.0338(4)
Br(10)	6*c*	1		0.3314(3)	-0.0588(2)	-0.00373(10)	0.0522(7)

Table A.33: Anisotropic displacement parameters U_{ij} / $Å^2$ for the independent atoms in the structure of $(Au_6Te_{18}Br)[AlBr_4]_5$.

Atom	U_{11}	U_{22}	U_{33}	U_{23}	U_{13}	U_{12}
Au(1)	0.0211(4)	0.0198(4)	0.0200(4)	0.0021(3)	0.0008(3)	0.0109(3)
Au(2)	0.0194(4)	0.0211(4)	0.0194(4)	0.0006(3)	0.0016(3)	0.0103(3)
Te(1)	0.0278(7)	0.0264(7)	0.0246(5)	0.0016(5)	0.0018(5)	0.0186(4)
Te(2)	0.0257(8)	0.0256(7)	0.0228(7)	-0.0059(5)	0.0009(5)	0.0120(6)
Te(3)	0.0271(7)	0.0271(7)	0.0214(7)	0.0052(5)	0.0064(6)	0.0142(7)

continued on next page

Atom	U_{11}	U_{22}	U_{33}	U_{23}	U_{13}	U_{12}
Te(4)	0.0265(7)	0.0171(4)	0.0270(5)	0.0006(6)	-0.0009(5)	0.0084(6)
Te(5)	0.0297(8)	0.0297(8)	0.0171(10)	0.000	0.000	0.0149(4)
Te(6)	0.0333(9)	0.0333(9)	0.0171(10)	0.000	0.000	0.0167(5)
Te(7)	0.0315(10)	0.0191(9)	0.0280(9)	-0.0027(7)	0.0039(7)	0.0144(8)
Te(8)	0.0210(9)	0.0316(10)	0.0307(9)	0.0024(7)	-0.0033(7)	0.0164(7)
Br(1)	0.0315(10)	0.0191(9)	0.0280(9)	-0.0027(7)	0.0039(7)	0.0144(8)
Br(2)	0.0210(9)	0.0316(10)	0.0307(9)	0.0024(7)	-0.0033(7)	0.0164(7)
Al(1)	0.024(3)	0.024(3)	0.023(4)	0.000	0.000	0.0120(14)
Br(3)	0.0248(7)	0.0248(7)	0.0219(12)	0.000	0.000	0.0124(4)
Br(4)	0.0344(13)	0.0321(13)	0.0410(12)	-0.0094(10)	-0.0122(10)	0.0114(11)
Al(3)	0.022(3)	0.022(3)	0.021(5)	0.000	0.000	0.0110(14)
Br(5)	0.0258(8)	0.0258(8)	0.0220(19)	0.000	0.000	0.0129(4)
Br(6)	0.0285(11)	0.0242(10)	0.0294(10)	0.0018(8)	-0.0003(8)	0.0142(9)
Al(2)	0.029(3)	0.027(3)	0.023(3)	0.002(2)	0.003(2)	0.015(2)
Br(7)	0.0338(13)	0.0362(13)	0.0491(14)	0.0116(10)	-0.0079(10)	0.0159(11)
Br(8)	0.0345(13)	0.0400(14)	0.0445(14)	0.0092(11)	0.0122(10)	0.0193(11)
Br(9)	0.0473(12)	0.0302(10)	0.0276(9)	0.0035(8)	-0.0038(9)	0.0221(9)
Br(10)	0.098(2)	0.0336(12)	0.0300(10)	0.0029(9)	0.0189(13)	0.0367(14)

Table A.34: Selected bond lengths for $(Au_6Te_{18}Br)[AlBr_4]_5$. Symmetry transformations used to generate equivalent atoms: (i) $-y+1$, $x-y+1$, z; (ii) $-x+y$, $-x+1$, z; (iii) $-y$, $x-y$, z (iv) $-x+y$, $-x$, z; (v) $-y+1$, $x-y$, z; (vi) $-x+y+1$, $-x+1$, z.

Atoms 1, 2	Distance / *Å*	Atoms 1, 2	Distance / *Å*
Au(1) — Te(1)	2.6859(16)	Te(4) — Te(8)^{ii}	2.872(3)
Au(1) — Te(3)	2.6880(15)	Te(5) — Te(2)^{i}	2.855(2)
Au(1) — Te(4)	2.6886(17)	Te(5) — Te(2)^{ii}	2.855(2)
Au(1) — Te(3)^{i}	2.6887(16)	Te(6) — Te(3)^{ii}	2.872(2)
Au(2) — Te(4)^{i}	2.6856(17)	Te(6) — Te(3)^{i}	2.872(2)
Au(2) — Te(1)	2.6869(16)	Te(8) — Te(4)^{i}	2.872(3)
Au(2) — Te(2)^{i}	2.6882(15)	Te(8) — Te(3)^{i}	3.025(3)
Au(2) — Te(2)	2.6967(16)	Al(1) — Br(4)^{iii}	2.291(4)
Te(1) — Te(7)	2.864(3)	Al(1) — Br(4)^{iv}	2.291(4)
Te(1) — Te(8)	2.873(3)	Al(1) — Br(4)	2.291(4)
Te(2) — Au(2)^{ii}	2.6880(15)	Al(1) — Br(3)	2.310(11)
Te(2) — Te(5)	2.855(2)	Al(3) — Br(6)	2.295(4)

continued on next page

Atoms 1, 2	Distance / *Å*	Atoms 1, 2	Distance / *Å*
Te(2) — Te(7)	3.037(2)	Al(3) — Br(6)^{v}	2.295(4)
Te(3) — Au(1)^{ii}	2.6888(16)	Al(3) — Br(6)^{vi}	2.295(4)
Te(3) — Te(6)	2.872(2)	Al(3) — Br(5)	2.319(10)
Te(3) — Te(8)^{ii}	3.025(3)	Al(2) — Br(8)	2.282(6)
Te(4) — Au(2)^{ii}	2.6856(17)	Al(2) — Br(9)	2.296(6)
Te(4) — Te(7)	2.864(3)	Al(2) — Br(7)	2.297(6)
Te(4) — Br(2)^{ii}	2.872(3)	Al(2) — Br(10)	2.307(6)

Table A.35: Selected bond angles for $(Au_6Te_{18}Br)[AlBr_4]_5$. Symmetry transformations used to generate equivalent atoms: (i) $-y+1$, $x-y+1$, z; (ii) $-x+y$, $-x+1$, z; (iii) $-y$, $x-y$, z (iv) $-x+y$, $-x$, z; (v) $-y+1$, $x-y$, z; (vi) $-x+y+1$, $-x+1$, z.

Atoms 1, 2, 3	Angle / °	Atoms 1, 2, 3	Angle / °
Te(1) — Au(1) — Te(3)	179.28(6)	Te(7) — Te(4) — Br(2)^{ii}	164.96(6)
Te(1) — Au(1) — Te(4)	88.94(6)	Au(2)^{ii} — Te(4) — Te(8)^{ii}	95.20(7)
Te(3) — Au(1) — Te(4)	91.18(6)	Au(1) — Te(4) — Te(8)^{ii}	95.43(7)
Te(1) — Au(1) — Te(3)^{i}	90.66(6)	Te(7) — Te(4) — Te(8)^{ii}	164.96(6)
Te(3) — Au(1) — Te(3)^{i}	89.21(7)	Br(2)^{ii} — Te(4) — Te(8)^{ii}	0.00(8)
Te(4) — Au(1) — Te(3)^{i}	179.24(6)	Te(2)^{i} — Te(5) — Te(2)^{ii}	83.91(8)
Te(4)^{i} — Au(2) — Te(1)	87.87(6)	Te(2)^{i} — Te(5) — Te(2)	83.91(8)
Te(4)^{i} — Au(2) — Te(2)^{i}	90.63(6)	Te(2)^{ii} — Te(5) — Te(2)	83.91(8)
Te(1) — Au(2) — Te(2)^{i}	178.50(6)	Te(3) — Te(6) — Te(3)^{ii}	82.19(8)
Te(4)^{i} — Au(2) — Te(2)	179.06(6)	Te(3) — Te(6) — Te(3)^{i}	82.19(8)
Te(1) — Au(2) — Te(2)	91.19(6)	Te(3)^{ii} — Te(6) — Te(3)^{i}	82.19(8)
Te(2)^{i} — Au(2) — Te(2)	90.30(7)	Te(4) — Te(7) — Te(1)	82.19(6)
Au(1) — Te(1) — Au(2)	91.31(4)	Te(4) — Te(7) — Te(2)	80.65(6)
Au(1) — Te(1) — Te(7)	93.97(6)	Te(1) — Te(7) — Te(2)	81.29(6)
Au(2) — Te(1) — Te(7)	95.74(7)	Te(4)^{i} — Te(8) — Te(1)	80.93(6)
Au(1) — Te(1) — Te(8)	96.00(7)	Te(4)^{i} — Te(8) — Te(3)^{i}	81.24(6)
Au(2) — Te(1) — Te(8)	95.15(6)	Te(1) — Te(8) — Te(3)^{i}	80.75(6)
Te(7) — Te(1) — Te(8)	165.05(6)	Br(4)^{iii} — Al(1) — Br(4)^{iv}	110.5(2)
Au(2)^{ii} — Te(2) — Au(2)	88.27(5)	Br(4)^{iii} — Al(1) — Br(4)	110.5(2)
Au(2)^{ii} — Te(2) — Te(5)	92.95(6)	Br(4)^{iv} — Al(1) — Br(4)	110.5(2)
Au(2) — Te(2) — Te(5)	92.77(6)	Br(4)^{iii} — Al(1) — Br(3)	108.4(2)
Au(2)^{ii} — Te(2) — Te(7)	92.31(6)	Br(4)^{iv} — Al(1) — Br(3)	108.4(2)
Au(2) — Te(2) — Te(7)	91.63(6)	Br(4) — Al(1) — Br(3)	108.4(2)

continued on next page

Atoms 1, 2, 3	Angle / °	Atoms 1, 2, 3	Angle / °
Te(5) — Te(2) — Te(7)	173.24(8)	Br(6) — Al(3) — Br(6)^{v}	109.9(2)
Au(1) — Te(3) — Au(1)^{ii}	87.68(6)	Br(6) — Al(3) — Br(6)^{vi}	109.9(2)
Au(1) — Te(3) — Te(6)	94.26(6)	Br(6)^{v} — Al(3) — Br(6)^{vi}	109.9(2)
Au(1)^{ii} — Te(3) — Te(6)	94.24(6)	Br(6) — Al(3) — Br(5)	109.0(2)
Au(1) — Te(3) — Te(8)^{ii}	91.98(6)	Br(6)^{v} — Al(3) — Br(5)	109.0(2)
Au(1)^{ii} — Te(3) — Te(8)^{ii}	92.46(6)	Br(6)^{vi} — Al(3) — Br(5)	109.0(2)
Te(6) — Te(3) — Te(8)^{ii}	171.02(8)	Br(8) — Al(2) — Br(9)	112.5(3)
Au(2)^{ii} — Te(4) — Au(1)	91.31(4)	Br(8) — Al(2) — Br(7)	110.4(2)
Au(2)^{ii} — Te(4) — Te(7)	96.33(7)	Br(9) — Al(2) — Br(7)	107.0(2)
Au(1) — Te(4) — Te(7)	93.93(7)	Br(8) — Al(2) — Br(10)	107.3(3)
Au(2)^{ii} — Te(4) — Br(2)^{ii}	95.20(7)	Br(9) — Al(2) — Br(10)	111.9(2)
Au(1) — Te(4) — Br(2)^{ii}	95.43(7)	Br(7) — Al(2) — Br(10)	107.7(3)

A.1.8 $(Au_6Te_{18}Br)[AlBr_4]_5$ Enantiomer 2

Table A.36: Crystal data and structure refinement for $(Au_6Te_{18}Br)[AlBr_4]_5$.

Empirical formula	$Al_5\,Au_6\,Br_{21}\,Te_{18}$
Formula weight / $g \cdot mol^{-1}$	5291.61
Temperature / K	123(2)
Crystal system; space group	Trigonal; $P31c$
Lattice constants / $Å$	a = 12.8097(2)
	c = 23.0638(4)
Volume / $Å^3$	3277.5(1)
Z; F(000); calc. density / $g \cdot cm^{-3}$	2; 4420; 5.362
Wavelength	$Mo_{K\alpha}$ (λ = 0.71073 Å)
Crystal size / mm^3	0.075 × 0.060 × 0.040
Theta range for data collection / °	$3.181 \leq \theta \leq 27.430$
Limiting indices	$-16 \leq h \leq 16$; $-16 \leq k \leq 16$; $-29 \leq l \leq 29$
Reflections collected / unique	48291 / 4992
Completeness to θ = 25.242°	99.8 %
R_{int}; R_σ	0.0810; 0.0340
Absorption coefficient / mm^{-1}	34.113; Semi-empirical from equivalents
Max. / min. transmission	0.1326 / 0.0503
Refinement method	Full-matrix least-squares on F^2
Data / restraints / parameters	4992 / 3 / 158
R indices (all data) R_1; wR_2	0.0461; 0.0844
R indices $[I > 4\sigma(I)]$ R_1; wR_2	0.0344; 0.0792; n = 4243 reflections
Goodness-of-fit for F^2	1.077
Flack x	0.018(6) (1858 reflections; Parson's method)
Largest diff. peak / $e^- \cdot Å^{-3}$	+1.055 (1.51 Å from Br1)
	-1.985 (2.44 Å from Au1)
Avg. diff. density / $e^- \cdot Å^{-3}$	0.276

Table A.37: Fractional coordinates and equivalent isotropic displacement parameter U_{eq} for the independent atoms in the structure of $(Au_6Te_{18}Br)[AlBr_4]_5$.

Atom	Wyck.	Site	*SOF*	*x* / *a*	*y* / *b*	*z* / *c*	U_{eq} / Å^2
Au(1)	6*c*	1		-0.32954(7)	-0.49694(8)	-0.31835(3)	0.02093(19)
Au(2)	6*c*	1		-0.50035(7)	-0.66277(7)	-0.18047(3)	0.02096(19)
Te(1)	6*c*	1		-0.49798(14)	-0.49365(14)	-0.25027(8)	0.0249(2)
Te(2)	6*c*	1		-0.32881(12)	-0.49238(13)	-0.11225(6)	0.0258(3)
Te(3)	6*c*	1		-0.16130(13)	-0.49843(13)	-0.38744(6)	0.0258(3)
Te(4)	6*c*	1		-0.15864(15)	-0.32901(9)	-0.24955(9)	0.0255(2)
Te(5)	2*b*	3..		-0.3333	-0.6667	-0.03356(11)	0.0261(5)
Te(6)	2*b*	3..		-0.3333	-0.6667	-0.46852(11)	0.0297(6)
Te(7)	6*c*	1	0.6656(13)	-0.32652(16)	-0.29181(17)	-0.18346(8)	0.0265(5)
Te(8)	6*c*	1	0.6677(13)	-0.70114(17)	-0.65999(17)	-0.31860(8)	0.0268(4)
Br(1)	6*c*	1	0.1595(13)	-0.32652(16)	-0.29181(17)	-0.18346(8)	0.0265(5)
Br(2)	6*c*	1	0.1738(13)	-0.70114(17)	-0.65999(17)	-0.31860(8)	0.0268(4)
Al(1)	2*b*	3..		0.0000	0.0000	-0.3477(4)	0.0229(18)
Br(3)	2*b*	3..		0.0000	0.0000	-0.2476(2)	0.0247(5)
Br(4)	6*c*	1		-0.1651(2)	-0.1740(2)	-0.37911(11)	0.0394(6)
Al(3)	2*b*	3..		-0.6667	-0.3333	-0.3595(4)	0.024(2)
Br(5)	2*b*	3..		-0.6667	-0.3333	-0.25896(15)	0.0257(7)
Br(6)	6*c*	1		-0.6558(2)	-0.15877(19)	-0.39195(10)	0.0277(5)
Al(2)	6*c*	1		-0.3370(5)	-0.0828(5)	-0.0597(2)	0.0263(12)
Br(7)	6*c*	1		-0.5052(2)	-0.1481(2)	-0.11677(13)	0.0421(7)
Br(8)	6*c*	1		-0.1665(2)	0.0105(2)	-0.11484(12)	0.0406(6)
Br(9)	6*c*	1		-0.3558(2)	-0.24879(19)	-0.01205(9)	0.0348(5)
Br(10)	6*c*	1		-0.3314(3)	0.0590(2)	0.00382(10)	0.0536(7)

Table A.38: Anisotropic displacement parameters U_{ij} / Å^2 for the independent atoms in the structure of $(Au_6Te_{18}Br)[AlBr_4]_5$.

Atom	U_{11}	U_{22}	U_{33}	U_{23}	U_{13}	U_{12}
Au(1)	0.0220(4)	0.0205(4)	0.0211(4)	0.0020(3)	0.0009(3)	0.0112(3)
Au(2)	0.0201(4)	0.0224(5)	0.0210(4)	0.0004(3)	0.0014(3)	0.0111(3)
Te(1)	0.0283(7)	0.0267(7)	0.0260(5)	0.0016(5)	0.0021(5)	0.0186(4)
Te(2)	0.0265(8)	0.0271(7)	0.0230(8)	-0.0052(6)	0.0013(5)	0.0128(6)
Te(3)	0.0277(8)	0.0275(8)	0.0224(8)	0.0053(6)	0.0065(6)	0.0140(7)

continued on next page

Atom	U_{11}	U_{22}	U_{33}	U_{23}	U_{13}	U_{12}
Te(4)	0.0281(7)	0.0179(5)	0.0275(5)	0.0000(7)	-0.0011(5)	0.0094(6)
Te(5)	0.0301(9)	0.0301(9)	0.0179(11)	0.000	0.000	0.0151(4)
Te(6)	0.0354(10)	0.0354(10)	0.0183(12)	0.000	0.000	0.0177(5)
Te(7)	0.0320(10)	0.0209(10)	0.0289(10)	-0.0026(7)	0.0040(7)	0.0150(8)
Te(8)	0.0214(9)	0.0322(10)	0.0313(10)	0.0021(7)	-0.0031(7)	0.0168(8)
Br(1)	0.0320(10)	0.0209(10)	0.0289(10)	-0.0026(7)	0.0040(7)	0.0150(8)
Br(2)	0.0214(9)	0.0322(10)	0.0313(10)	0.0021(7)	-0.0031(7)	0.0168(8)
Al(1)	0.022(3)	0.022(3)	0.025(4)	0.000	0.000	0.0110(14)
Br(3)	0.0253(8)	0.0253(8)	0.0234(12)	0.000	0.000	0.0127(4)
Br(4)	0.0360(13)	0.0337(13)	0.0420(14)	-0.0085(10)	-0.0130(11)	0.0125(11)
Al(3)	0.025(3)	0.025(3)	0.023(5)	0.000	0.000	0.0125(15)
Br(5)	0.0266(8)	0.0266(8)	0.024(2)	0.000	0.000	0.0133(4)
Br(6)	0.0294(11)	0.0247(11)	0.0307(11)	0.0027(9)	-0.0005(9)	0.0147(9)
Al(2)	0.031(3)	0.027(3)	0.022(3)	0.002(2)	0.004(2)	0.015(3)
Br(7)	0.0350(13)	0.0375(14)	0.0516(16)	0.0116(11)	-0.0063(11)	0.0166(11)
Br(8)	0.0355(13)	0.0412(15)	0.0461(15)	0.0092(11)	0.0121(11)	0.0201(12)
Br(9)	0.0481(13)	0.0310(10)	0.0292(10)	0.0035(8)	-0.0038(9)	0.0228(10)
Br(10)	0.100(2)	0.0344(12)	0.0309(11)	0.0036(10)	0.0196(13)	0.0368(14)

Table A.39: Selected bond lengths for $(Au_6Te_{18}Br)[AlBr_4]_5$. Symmetry transformations used to generate equivalent atoms: (i) $-y+1$, $x-y+1$, z; (ii) $-x+y$, $-x+1$, z; (iii) $-y$, $x-y$, z (iv) $-x+y$, $-x$, z; (v) $-y+1$, $x-y$, z; (vi) $-x+y+1$, $-x+1$, z.

Atoms 1, 2	Distance / Å	Atoms 1, 2	Distance / Å
Au(1) — Te(1)	2.6829(15)	Te(4) — Te(8)^{ii}	2.870(2)
Au(1) — Te(3)	2.6858(15)	Te(5) — Te(2)^{i}	2.853(2)
Au(1) — Te(4)	2.6866(16)	Te(5) — Te(2)^{ii}	2.853(2)
Au(1) — Te(3)^{i}	2.6874(15)	Te(6) — Te(3)^{ii}	2.870(2)
Au(2) — Te(4)^{i}	2.6858(16)	Te(6) — Te(3)^{i}	2.870(2)
Au(2) — Te(1)	2.6870(15)	Te(8) — Te(4)^{i}	2.870(2)
Au(2) — Te(2)^{i}	2.6873(15)	Te(8) — Te(3)^{i}	3.023(2)
Au(2) — Te(2)	2.6947(15)	Al(1) — Br(4)^{iii}	2.284(4)
Te(1) — Te(7)	2.863(2)	Al(1) — Br(4)^{iv}	2.284(4)
Te(1) — Te(8)	2.874(2)	Al(1) — Br(4)	2.284(4)
Te(2) — Au(2)^{ii}	2.6872(15)	Al(1) — Br(3)	2.317(11)
Te(2) — Te(5)	2.853(2)	Al(3) — Br(6)	2.297(4)

continued on next page

Atoms 1, 2	Distance / *Å*	Atoms 1, 2	Distance / *Å*
Te(2) — Te(7)	3.037(2)	Al(3) — Br(6)^{v}	2.297(4)
Te(3) — Au(1)^{ii}	2.6874(15)	Al(3) — Br(6)^{vi}	2.297(4)
Te(3) — Te(6)	2.870(2)	Al(3) — Br(5)	2.314(9)
Te(3) — Te(8)^{ii}	3.023(2)	Al(2) — Br(8)	2.273(6)
Te(4) — Au(2)^{ii}	2.6859(16)	Al(2) — Br(9)	2.298(6)
Te(4) — Te(7)	2.864(3)	Al(2) — Br(10)	2.299(6)
Te(4) — Br(2)^{ii}	2.870(2)	Al(2) — Br(7)	2.303(6)

Table A.40: Selected bond angles for $(Au_6Te_{18}Br)[AlBr_4]_5$. Symmetry transformations used to generate equivalent atoms: (i) $-y+1$, $x-y+1$, z; (ii) $-x+y$, $-x+1$, z; (iii) $-y$, $x-y$, z (iv) $-x+y$, $-x$, z; (v) $-y+1$, $x-y$, z; (vi) $-x+y+1$, $-x+1$, z.

Atoms 1, 2, 3	Angle / °	Atoms 1, 2, 3	Angle / °
Te(1) — Au(1) — Te(3)	179.22(5)	Te(7) — Te(4) — Br(2)^{ii}	164.93(6)
Te(1) — Au(1) — Te(4)	88.92(6)	Au(2)^{ii} — Te(4) — Te(8)^{ii}	95.20(6)
Te(3) — Au(1) — Te(4)	91.16(6)	Au(1) — Te(4) — Te(8)^{ii}	95.44(7)
Te(1) — Au(1) — Te(3)^{i}	90.68(5)	Te(7) — Te(4) — Te(8)^{ii}	164.93(6)
Te(3) — Au(1) — Te(3)^{i}	89.22(7)	Br(2)^{ii} — Te(4) — Te(8)^{ii}	0.00(5)
Te(4) — Au(1) — Te(3)^{i}	179.18(6)	Te(2) — Te(5) — Te(2)^{i}	83.99(7)
Te(4)^{i} — Au(2) — Te(1)	87.90(6)	Te(2) — Te(5) — Te(2)^{ii}	83.99(7)
Te(4)^{i} — Au(2) — Te(2)^{i}	90.61(6)	Te(2)^{i} — Te(5) — Te(2)^{ii}	83.98(7)
Te(1) — Au(2) — Te(2)^{i}	178.52(6)	Te(3)^{ii} — Te(6) — Te(3)^{i}	82.21(7)
Te(4)^{i} — Au(2) — Te(2)	179.03(6)	Te(3)^{ii} — Te(6) — Te(3)	82.21(7)
Te(1) — Au(2) — Te(2)	91.13(5)	Te(3)^{i} — Te(6) — Te(3)	82.21(7)
Te(2)^{i} — Au(2) — Te(2)	90.35(7)	Te(1) — Te(7) — Te(4)	82.09(6)
Au(1) — Te(1) — Au(2)	91.32(4)	Te(1) — Te(7) — Te(2)	81.21(6)
Au(1) — Te(1) — Te(7)	94.06(6)	Te(4) — Te(7) — Te(2)	80.61(6)
Au(2) — Te(1) — Te(7)	95.80(6)	Te(4)^{i} — Te(8) — Te(1)	80.96(6)
Au(1) — Te(1) — Te(8)	95.99(7)	Te(4)^{i} — Te(8) — Te(3)^{i}	81.22(6)
Au(2) — Te(1) — Te(8)	95.07(6)	Te(1) — Te(8) — Te(3)^{i}	80.71(6)
Te(7) — Te(1) — Te(8)	165.00(6)	Br(4)^{iii} — Al(1) — Br(4)^{iv}	110.8(2)
Au(2)^{ii} — Te(2) — Au(2)	88.32(5)	Br(4)^{iii} — Al(1) — Br(4)	110.8(2)
Au(2)^{ii} — Te(2) — Te(5)	92.87(6)	Br(4)^{iv} — Al(1) — Br(4)	110.8(2)
Au(2) — Te(2) — Te(5)	92.72(6)	Br(4)^{iii} — Al(1) — Br(3)	108.1(2)
Au(2)^{ii} — Te(2) — Te(7)	92.34(6)	Br(4)^{iv} — Al(1) — Br(3)	108.1(2)
Au(2) — Te(2) — Te(7)	91.70(6)	Br(4) — Al(1) — Br(3)	108.1(2)

continued on next page

Atoms 1, 2, 3	Angle / °	Atoms 1, 2, 3	Angle / °
Te(5) — Te(2) — Te(7)	173.26(7)	Br(6) — Al(3) — Br(6)^{v}	109.8(2)
Au(1) — Te(3) — Au(1)^{ii}	87.66(5)	Br(6) — Al(3) — Br(6)^{vi}	109.8(2)
Au(1) — Te(3) — Te(6)	94.25(6)	Br(6)^{v} — Al(3) — Br(6)^{vi}	109.8(2)
Au(1)^{ii} — Te(3) — Te(6)	94.21(6)	Br(6) — Al(3) — Br(5)	109.2(2)
Au(1) — Te(3) — Te(8)^{ii}	92.00(5)	Br(6)^{v} — Al(3) — Br(5)	109.2(2)
Au(1)^{ii} — Te(3) — Te(8)^{ii}	92.50(6)	Br(6)^{vi} — Al(3) — Br(5)	109.2(2)
Te(6) — Te(3) — Te(8)^{ii}	171.00(7)	Br(8) — Al(2) — Br(9)	112.7(2)
Au(2)^{ii} — Te(4) — Au(1)	91.28(4)	Br(8) — Al(2) — Br(10)	107.4(3)
Au(2)^{ii} — Te(4) — Te(7)	96.34(7)	Br(9) — Al(2) — Br(10)	112.0(2)
Au(1) — Te(4) — Te(7)	93.96(6)	Br(8) — Al(2) — Br(7)	110.5(2)
Au(2)^{ii} — Te(4) — Br(2)^{ii}	95.20(6)	Br(9) — Al(2) — Br(7)	106.6(2)
Au(1) — Te(4) — Br(2)^{ii}	95.44(7)	Br(10) — Al(2) — Br(7)	107.6(2)

A.1.9 $(Au_6Te_{18}Cl)[MoOCl_4]_5$

Table A.41: Crystal data and structure refinement for $(Au_6Te_{18}Cl)[MoOCl_4]_5$.

Empirical formula	$Au_6\,Cl_{21}\,Mo_5\,O_5\,Te_{18}$
Formula weight / $g \cdot mol^{-1}$	4782.75
Temperature / K	123(2)
Crystal system; space group	Triclinic; $P\bar{1}$
Lattice constants / $Å$	$a = 10.3239(1)$; $\alpha = 96.019(1)°$
	$b = 13.1127(2)$; $\beta = 93.894(1)°$
	$c = 22.7623(4)$; $\gamma = 103.178(1)°$
Volume / $Å^3$	2970.30(8)
Z; F(000); calc. density / $g \cdot cm^{-3}$	2; 4034; 5.348
Wavelength	$Mo_{K\alpha}$ ($\lambda = 0.71073$ Å)
Crystal size / mm^3	0.094 × 0.078 × 0.068
Theta range for data collection / °	$2.976 \leq \theta \leq 27.514$
Limiting indices	$-13 \leq h \leq 13$; $-17 \leq k \leq 17$; $-29 \leq l \leq 29$
Reflections collected / unique	79755 / 13631
Completeness to $\theta = 25.242°$	99.8 %
R_{int}; R_σ	0.0822; 0.0462
Absorption coefficient / mm^{-1}	25.404; Semi-empirical from equivalents
Max. / min. transmission	0.1269 / 0.0583
Refinement method	Full-matrix least-squares on F^2
Data / restraints / parameters	13631 / 0 / 500
R indices (all data) R_1; wR_2	0.0580; 0.0859
R indices $[I > 4\sigma(I)]$ R_1; wR_2	0.0365; 0.0792; n = 10073 reflections
Goodness-of-fit for F^2	1.044
Largest diff. peak / $e^- \cdot Å^{-3}$	+4.168 (1.32 Å from Cl12)
	-2.686 (0.68 Å from Mo3)
Avg. diff. density / $e^- \cdot Å^{-3}$	0.378

Table A.42: Fractional coordinates and equivalent isotropic displacement parameter U_{eq} for the independent atoms in the structure of $(Au_6Te_{18}Cl)[MoOCl_4]_5$.

Atom	Wyck.	Site	x / a	y / b	z / c	U_{eq} / $Å^2$
Au(1)	2*i*	1	-0.11844(4)	0.11694(3)	-0.42583(2)	0.01567(9)
Au(2)	2*i*	1	0.19250(4)	0.17511(3)	-0.50974(2)	0.01519(9)
Au(3)	2*i*	1	0.15969(4)	-0.04638(3)	-0.41263(2)	0.01530(9)
Te(1)	2*i*	1	-0.26478(6)	0.17373(5)	-0.51429(3)	0.01583(14)
Te(2)	2*i*	1	-0.08526(7)	0.36156(5)	-0.52068(3)	0.01861(15)
Te(3)	2*i*	1	0.07376(7)	0.28962(5)	-0.43434(3)	0.01676(14)
Te(4)	2*i*	1	-0.29801(6)	-0.06124(5)	-0.40983(3)	0.01615(14)
Te(5)	2*i*	1	-0.17293(7)	-0.11884(5)	-0.31303(3)	0.01847(15)
Te(6)	2*i*	1	-0.03902(6)	-0.21444(5)	-0.39978(3)	0.01607(14)
Te(7)	2*i*	1	0.34528(6)	0.13329(5)	-0.41941(3)	0.01557(14)
Te(8)	2*i*	1	0.25927(7)	0.25269(5)	-0.33096(3)	0.01782(15)
Te(9)	2*i*	1	0.04325(7)	0.07120(5)	-0.34004(3)	0.01612(14)
Au(4)	2*i*	1	0.38726(4)	0.62314(3)	0.07264(2)	0.01595(9)
Au(5)	2*i*	1	0.34764(4)	0.54864(3)	-0.08916(2)	0.01574(9)
Au(6)	2*i*	1	0.69493(4)	0.67139(3)	-0.01187(2)	0.01538(9)
Te(10)	2*i*	1	0.79603(6)	0.55147(5)	-0.09052(3)	0.01617(14)
Te(11)	2*i*	1	0.66817(7)	0.58461(5)	-0.19358(3)	0.01907(15)
Te(12)	2*i*	1	0.54100(7)	0.57515(5)	0.16032(3)	0.01669(14)
Te(13)	2*i*	1	0.24257(6)	0.67738(5)	-0.01738(3)	0.01686(14)
Te(14)	2*i*	1	0.42470(7)	0.85724(5)	-0.03466(3)	0.01833(15)
Te(15)	2*i*	1	0.54696(6)	0.71446(5)	-0.10328(3)	0.01650(14)
Te(16)	2*i*	1	0.84175(6)	0.62713(5)	0.08027(3)	0.01621(14)
Te(17)	2*i*	1	0.76962(7)	0.76833(5)	0.16135(3)	0.01781(15)
Te(18)	2*i*	1	0.58669(7)	0.79253(5)	0.06407(3)	0.01728(15)
Mo(1)	2*i*	1	0.74793(10)	0.19712(8)	-0.24429(4)	0.0234(2)
Cl(1)	2*i*	1	0.6962(3)	0.2135(2)	-0.34383(12)	0.0312(7)
Cl(2)	2*i*	1	0.5329(3)	0.2182(2)	-0.22987(13)	0.0278(6)
Cl(3)	2*i*	1	0.8096(3)	0.2738(2)	-0.14584(13)	0.0308(6)
Cl(4)	2*i*	1	0.9711(3)	0.2697(2)	-0.26063(13)	0.0286(6)
O(1)	2*i*	1	0.7385(8)	0.0702(6)	-0.2432(4)	0.0326(19)
Mo(2)	2*i*	1	0.54138(9)	0.55638(7)	-0.40879(4)	0.0209(2)
Cl(5)	2*i*	1	0.3070(3)	0.5125(2)	-0.41440(12)	0.0229(6)
Cl(6)	2*i*	1	0.5452(3)	0.4290(2)	-0.34437(13)	0.0302(6)

continued on next page

Atom	Wyck.	Site	x / a	y / b	z / c	U_{eq} / Å^2
Cl(7)	2i	1	0.7602(3)	0.5457(2)	-0.42799(13)	0.0269(6)
Cl(8)	2i	1	0.5216(3)	0.6317(2)	-0.50071(12)	0.0249(6)
O(2)	2i	1	0.5754(8)	0.6663(6)	-0.3634(4)	0.035(2)
Mo(3)	2i	1	-0.04775(10)	-0.00574(8)	-0.09196(5)	0.0284(2)
Cl(9)	2i	1	0.1756(3)	-0.0228(2)	-0.08930(14)	0.0325(7)
Cl(10)	2i	1	-0.1120(3)	-0.1789(3)	-0.13890(17)	0.0460(9)
Cl(11)	2i	1	-0.2700(3)	-0.0205(3)	-0.06751(16)	0.0415(8)
Cl(12)	2i	1	0.0260(3)	0.1303(2)	-0.01008(14)	0.0349(7)
O(3)	2i	1	-0.0479(7)	0.0621(6)	-0.1485(4)	0.033(2)
Mo(4)	2i	1	0.36890(9)	-0.10530(7)	-0.23240(4)	0.0217(2)
Cl(13)	2i	1	0.5399(3)	-0.1958(2)	-0.23913(13)	0.0267(6)
Cl(14)	2i	1	0.4354(3)	-0.0321(2)	-0.31825(12)	0.0265(6)
Cl(15)	2i	1	0.1658(3)	-0.0519(2)	-0.24566(13)	0.0284(6)
Cl(16)	2i	1	0.2495(3)	-0.2414(2)	-0.17959(11)	0.0225(6)
O(4)	2i	1	0.4413(7)	-0.0135(6)	-0.1750(3)	0.0272(18)
Mo(5)	2i	1	0.11763(9)	0.59099(7)	-0.27116(4)	0.0222(2)
Cl(17)	2i	1	0.3202(3)	0.5391(2)	-0.25460(12)	0.0285(6)
Cl(18)	2i	1	0.0468(3)	0.5206(2)	-0.18511(12)	0.0281(6)
Cl(19)	2i	1	-0.0552(3)	0.6811(2)	-0.26705(13)	0.0279(6)
Cl(20)	2i	1	0.2357(2)	0.7267(2)	-0.32466(11)	0.0220(5)
O(5)	2i	1	0.0471(8)	0.4980(6)	-0.3265(3)	0.0292(18)
Cl(21)	1f	$\bar{1}$	-0.5000	0.0000	-0.5000	0.0207(8)
Cl(22)	1c	$\bar{1}$	0.0000	0.5000	0.0000	0.0192(7)

Table A.43: Anisotropic displacement parameters U_{ij} / Å^2 for the independent atoms in the structure of $(Au_6Te_{18}Cl)[MoOCl_4]_5$.

Atom	U_{11}	U_{22}	U_{33}	U_{23}	U_{13}	U_{12}
Au(1)	0.0157(2)	0.0160(2)	0.0154(2)	0.00229(16)	0.00124(16)	0.00374(16)
Au(2)	0.0148(2)	0.0156(2)	0.0154(2)	0.00300(15)	0.00106(16)	0.00357(15)
Au(3)	0.0154(2)	0.01523(19)	0.0154(2)	0.00253(15)	0.00138(16)	0.00366(15)
Te(1)	0.0150(3)	0.0162(3)	0.0168(4)	0.0032(3)	0.0019(3)	0.0040(3)
Te(2)	0.0186(3)	0.0145(3)	0.0233(4)	0.0043(3)	0.0008(3)	0.0044(3)
Te(3)	0.0166(3)	0.0151(3)	0.0179(4)	0.0010(3)	0.0011(3)	0.0031(3)
Te(4)	0.0146(3)	0.0178(3)	0.0165(4)	0.0032(3)	0.0020(3)	0.0043(3)
Te(5)	0.0185(3)	0.0221(4)	0.0160(4)	0.0051(3)	0.0034(3)	0.0056(3)

continued on next page

Atom	U_{11}	U_{22}	U_{33}	U_{23}	U_{13}	U_{12}
Te(6)	0.0161(3)	0.0160(3)	0.0166(4)	0.0040(3)	0.0013(3)	0.0040(3)
Te(7)	0.0140(3)	0.0169(3)	0.0155(3)	0.0019(3)	0.0007(3)	0.0033(3)
Te(8)	0.0172(3)	0.0188(3)	0.0159(4)	-0.0005(3)	-0.0005(3)	0.0029(3)
Te(9)	0.0170(3)	0.0171(3)	0.0145(3)	0.0019(3)	0.0015(3)	0.0045(3)
Au(4)	0.0156(2)	0.0162(2)	0.0159(2)	0.00187(15)	0.00121(16)	0.00363(16)
Au(5)	0.0160(2)	0.0163(2)	0.0148(2)	0.00248(15)	0.00076(16)	0.00361(16)
Au(6)	0.0153(2)	0.0160(2)	0.0149(2)	0.00272(15)	0.00102(16)	0.00362(16)
Te(10)	0.0148(3)	0.0186(3)	0.0154(3)	0.0030(3)	0.0018(3)	0.0039(3)
Te(11)	0.0185(4)	0.0229(4)	0.0155(4)	0.0059(3)	0.0024(3)	0.0024(3)
Te(12)	0.0161(3)	0.0182(3)	0.0155(4)	0.0016(3)	0.0011(3)	0.0040(3)
Te(13)	0.0153(3)	0.0178(3)	0.0176(4)	0.0028(3)	0.0013(3)	0.0041(3)
Te(14)	0.0189(3)	0.0156(3)	0.0211(4)	0.0035(3)	0.0003(3)	0.0053(3)
Te(15)	0.0164(3)	0.0172(3)	0.0163(4)	0.0053(3)	0.0007(3)	0.0037(3)
Te(16)	0.0146(3)	0.0186(3)	0.0153(3)	0.0023(3)	0.0007(3)	0.0039(3)
Te(17)	0.0180(3)	0.0181(3)	0.0157(4)	0.0002(3)	-0.0001(3)	0.0023(3)
Te(18)	0.0168(3)	0.0157(3)	0.0186(4)	0.0007(3)	0.0008(3)	0.0032(3)
Mo(1)	0.0210(5)	0.0263(5)	0.0231(5)	-0.0024(4)	0.0012(4)	0.0089(4)
Cl(1)	0.0321(16)	0.0455(18)	0.0208(15)	0.0002(12)	0.0040(12)	0.0206(14)
Cl(2)	0.0199(14)	0.0326(15)	0.0309(16)	-0.0052(12)	0.0025(12)	0.0106(12)
Cl(3)	0.0259(15)	0.0426(17)	0.0224(15)	-0.0071(12)	0.0022(12)	0.0102(13)
Cl(4)	0.0219(14)	0.0301(15)	0.0321(16)	-0.0046(12)	0.0062(12)	0.0054(12)
O(1)	0.031(5)	0.031(5)	0.037(5)	0.000(4)	-0.004(4)	0.014(4)
Mo(2)	0.0190(5)	0.0190(5)	0.0236(5)	0.0022(4)	0.0046(4)	0.0019(4)
Cl(5)	0.0192(13)	0.0264(14)	0.0239(14)	0.0039(11)	0.0057(11)	0.0057(11)
Cl(6)	0.0269(15)	0.0364(16)	0.0299(16)	0.0132(13)	0.0039(12)	0.0081(12)
Cl(7)	0.0178(13)	0.0289(15)	0.0324(16)	0.0047(12)	0.0045(12)	0.0014(11)
Cl(8)	0.0265(14)	0.0192(13)	0.0297(16)	0.0062(11)	0.0084(12)	0.0036(11)
O(2)	0.029(5)	0.035(5)	0.035(5)	-0.009(4)	0.008(4)	0.002(4)
Mo(3)	0.0264(5)	0.0278(5)	0.0257(6)	0.0068(4)	-0.0003(4)	-0.0051(4)
Cl(9)	0.0290(16)	0.0332(16)	0.0366(18)	0.0068(13)	0.0055(13)	0.0082(13)
Cl(10)	0.0390(19)	0.0306(17)	0.059(2)	-0.0051(15)	0.0053(17)	-0.0062(14)
Cl(11)	0.0286(16)	0.0423(18)	0.048(2)	-0.0018(15)	0.0129(15)	-0.0021(14)
Cl(12)	0.0362(17)	0.0267(15)	0.0399(18)	0.0026(13)	0.0052(14)	0.0036(13)
O(3)	0.016(4)	0.046(5)	0.036(5)	0.021(4)	-0.003(4)	0.000(4)
Mo(4)	0.0194(5)	0.0250(5)	0.0217(5)	0.0052(4)	0.0007(4)	0.0065(4)

continued on next page

Atom	U_{11}	U_{22}	U_{33}	U_{23}	U_{13}	U_{12}
Cl(13)	0.0221(14)	0.0349(16)	0.0277(15)	0.0124(12)	0.0049(12)	0.0117(12)
Cl(14)	0.0269(15)	0.0292(15)	0.0236(15)	0.0105(12)	0.0026(12)	0.0038(12)
Cl(15)	0.0263(15)	0.0348(16)	0.0304(16)	0.0125(12)	0.0045(12)	0.0155(12)
Cl(16)	0.0241(14)	0.0290(14)	0.0172(13)	0.0073(11)	0.0031(11)	0.0095(11)
O(4)	0.026(4)	0.029(4)	0.026(4)	0.003(3)	0.001(3)	0.005(3)
Mo(5)	0.0220(5)	0.0242(5)	0.0219(5)	0.0074(4)	0.0010(4)	0.0066(4)
Cl(17)	0.0322(16)	0.0372(16)	0.0222(15)	0.0090(12)	0.0021(12)	0.0187(13)
Cl(18)	0.0339(16)	0.0298(15)	0.0237(15)	0.0100(12)	0.0072(12)	0.0099(12)
Cl(19)	0.0201(14)	0.0354(16)	0.0335(16)	0.0179(13)	0.0051(12)	0.0106(12)
Cl(20)	0.0197(13)	0.0304(14)	0.0166(13)	0.0070(11)	-0.0004(10)	0.0060(11)
O(5)	0.036(5)	0.026(4)	0.026(5)	0.009(3)	0.008(4)	0.004(4)
Cl(21)	0.0167(18)	0.0216(18)	0.024(2)	0.0063(15)	0.0020(15)	0.0031(14)
Cl(22)	0.0195(18)	0.0198(18)	0.0177(19)	0.0039(14)	0.0011(15)	0.0027(14)

Table A.44: Selected bond lengths for $(Au_6Te_{18}Cl)[MoOCl_4]_5$. Symmetry transformations used to generate equivalent atoms: (i) $-x$, $-y$, $-z-1$; (ii) $-x+1$, $-y+1$, $-z$.

Atoms 1, 2	Distance / *Å*	Atoms 1, 2	Distance / *Å*
Au(1) — Te(3)	2.6828(8)	Te(10) — Te(11)	2.7366(9)
Au(1) — Te(9)	2.6867(8)	Te(11) — Te(12)^{ii}	2.8490(9)
Au(1) — Te(1)	2.7030(8)	Te(11) — Te(15)	3.0459(10)
Au(1) — Te(4)	2.7062(7)	Te(12) — Au(5)^{ii}	2.6708(8)
Au(2) — Te(6)^{i}	2.6778(8)	Te(12) — Te(11)^{ii}	2.8491(9)
Au(2) — Te(4)^{i}	2.6845(8)	Te(12) — Te(17)	3.0402(9)
Au(2) — Te(7)	2.6846(8)	Te(13) — Te(14)	2.7433(9)
Au(2) — Te(3)	2.6996(8)	Te(14) — Te(15)	2.8757(9)
Au(3) — Te(9)	2.6708(8)	Te(14) — Te(18)	3.0173(9)
Au(3) — Te(1)^{i}	2.6875(8)	Te(16) — Au(5)^{ii}	2.6968(7)
Au(3) — Te(7)	2.7025(7)	Te(16) — Te(17)	2.7363(9)
Au(3) — Te(6)	2.7029(7)	Te(17) — Te(18)	2.9021(10)
Te(1) — Au(3)^{i}	2.6874(8)	Mo(1) — O(1)	1.648(8)
Te(1) — Te(2)	2.7482(9)	Mo(1) — Cl(1)	2.336(3)
Te(2) — Te(3)	2.8468(9)	Mo(1) — Cl(2)	2.339(3)
Te(2) — Te(6)^{i}	3.0590(9)	Mo(1) — Cl(3)	2.341(3)
Te(3) — Te(8)	3.0804(9)	Mo(1) — Cl(4)	2.354(3)
Te(4) — Au(2)^{i}	2.6845(8)	Mo(2) — O(2)	1.636(8)

continued on next page

Atoms 1, 2	Distance / *Å*	Atoms 1, 2	Distance / *Å*
Te(4) — Te(5)	2.7386(9)	Mo(2) — Cl(6)	2.341(3)
Te(5) — Te(6)	2.8326(9)	Mo(2) — Cl(5)	2.348(3)
Te(5) — Te(9)	3.0888(9)	Mo(2) — Cl(7)	2.363(3)
Te(6) — Au(2)^{i}	2.6778(8)	Mo(2) — Cl(8)	2.422(3)
Te(6) — Te(2)^{i}	3.0591(9)	Mo(3) — O(3)	1.639(8)
Te(7) — Te(8)	2.7402(9)	Mo(3) — Cl(10)	2.333(3)
Te(8) — Te(9)	2.8451(9)	Mo(3) — Cl(9)	2.364(3)
Au(4) — Te(12)	2.6809(8)	Mo(3) — Cl(11)	2.367(3)
Au(4) — Te(18)	2.6964(8)	Mo(3) — Cl(12)	2.393(3)
Au(4) — Te(13)	2.7037(8)	Mo(4) — O(4)	1.686(8)
Au(4) — Te(10)^{ii}	2.7044(7)	Mo(4) — Cl(14)	2.343(3)
Au(5) — Te(12)^{ii}	2.6708(8)	Mo(4) — Cl(13)	2.345(3)
Au(5) — Te(13)	2.6820(8)	Mo(4) — Cl(15)	2.368(3)
Au(5) — Te(15)	2.6948(7)	Mo(4) — Cl(16)	2.408(3)
Au(5) — Te(16)^{ii}	2.6968(7)	Mo(5) — O(5)	1.660(8)
Au(6) — Te(10)	2.6795(8)	Mo(5) — Cl(18)	2.343(3)
Au(6) — Te(15)	2.6814(8)	Mo(5) — Cl(19)	2.356(3)
Au(6) — Te(18)	2.6936(8)	Mo(5) — Cl(17)	2.361(3)
Au(6) — Te(16)	2.6940(8)	Mo(5) — Cl(20)	2.409(3)
Te(10) — Au(4)^{ii}	2.7044(7)		

Table A.45: Selected bond angles for $(Au_6Te_{18}Cl)[MoOCl_4]_5$. Symmetry transformations used to generate equivalent atoms: (i) $-x$, $-y$, $-z-1$; (ii) $-x+1$, $-y+1$, $-z$.

Atoms 1, 2, 3	Angle / °	Atoms 1, 2, 3	Angle / °
Te(3) — Au(1) — Te(9)	87.87(2)	Au(5)^{ii} — Te(12) — Te(11)^{ii}	98.18(3)
Te(3) — Au(1) — Te(1)	87.90(2)	Au(4) — Te(12) — Te(11)^{ii}	94.13(3)
Te(9) — Au(1) — Te(1)	175.63(3)	Au(5)^{ii} — Te(12) — Te(17)	93.77(2)
Te(3) — Au(1) — Te(4)	175.03(3)	Au(4) — Te(12) — Te(17)	95.42(2)
Te(9) — Au(1) — Te(4)	87.17(2)	Te(11)^{ii} — Te(12) — Te(17)	163.99(3)
Te(1) — Au(1) — Te(4)	97.07(2)	Au(5) — Te(13) — Au(4)	86.21(2)
Te(6)^{i} — Au(2) — Te(4)^{i}	87.30(2)	Au(5) — Te(13) — Te(14)	94.57(3)
Te(6)^{i} — Au(2) — Te(7)	179.34(3)	Au(4) — Te(13) — Te(14)	97.21(3)
Te(4)^{i} — Au(2) — Te(7)	92.34(2)	Te(13) — Te(14) — Te(15)	84.46(3)
Te(6)^{i} — Au(2) — Te(3)	89.11(2)	Te(13) — Te(14) — Te(18)	82.30(3)
Te(4)^{i} — Au(2) — Te(3)	176.30(3)	Te(15) — Te(14) — Te(18)	80.49(2)

continued on next page

Atoms 1, 2, 3	Angle / °	Atoms 1, 2, 3	Angle / °
Te(7) — Au(2) — Te(3)	91.25(2)	Au(6) — Te(15) — Au(5)	90.03(2)
Te(9) — Au(3) — Te(1)^{i}	176.78(3)	Au(6) — Te(15) — Te(14)	96.33(3)
Te(9) — Au(3) — Te(7)	86.54(2)	Au(5) — Te(15) — Te(14)	91.33(2)
Te(1)^{i} — Au(3) — Te(7)	96.64(2)	Au(6) — Te(15) — Te(11)	92.55(2)
Te(9) — Au(3) — Te(6)	87.95(2)	Au(5) — Te(15) — Te(11)	93.06(2)
Te(1)^{i} — Au(3) — Te(6)	88.86(2)	Te(14) — Te(15) — Te(11)	170.09(3)
Te(7) — Au(3) — Te(6)	174.46(3)	Au(6) — Te(16) — Au(5)^{ii}	90.89(2)
Au(3)^{i} — Te(1) — Au(1)	85.76(2)	Au(6) — Te(16) — Te(17)	94.28(3)
Au(3)^{i} — Te(1) — Te(2)	98.87(3)	Au(5)^{ii} — Te(16) — Te(17)	100.48(3)
Au(1) — Te(1) — Te(2)	94.87(3)	Te(16) — Te(17) — Te(18)	84.60(3)
Te(1) — Te(2) — Te(3)	83.81(3)	Te(16) — Te(17) — Te(12)	78.77(2)
Te(1) — Te(2) — Te(6)^{i}	80.85(2)	Te(18) — Te(17) — Te(12)	77.96(2)
Te(3) — Te(2) — Te(6)^{i}	79.32(2)	Au(6) — Te(18) — Au(4)	89.34(2)
Au(1) — Te(3) — Au(2)	90.28(2)	Au(6) — Te(18) — Te(17)	90.61(2)
Au(1) — Te(3) — Te(2)	93.07(3)	Au(4) — Te(18) — Te(17)	98.36(3)
Au(2) — Te(3) — Te(2)	97.84(3)	Au(6) — Te(18) — Te(14)	92.82(3)
Au(1) — Te(3) — Te(8)	94.29(2)	Au(4) — Te(18) — Te(14)	91.13(2)
Au(2) — Te(3) — Te(8)	89.05(2)	Te(17) — Te(18) — Te(14)	169.94(3)
Te(2) — Te(3) — Te(8)	169.89(3)	O(1) — Mo(1) — Cl(1)	104.6(3)
Au(2)^{i} — Te(4) — Au(1)	90.81(2)	O(1) — Mo(1) — Cl(2)	105.2(3)
Au(2)^{i} — Te(4) — Te(5)	95.27(3)	Cl(1) — Mo(1) — Cl(2)	86.09(10)
Au(1) — Te(4) — Te(5)	100.54(3)	O(1) — Mo(1) — Cl(3)	105.3(3)
Te(4) — Te(5) — Te(6)	83.25(3)	Cl(1) — Mo(1) — Cl(3)	150.16(12)
Te(4) — Te(5) — Te(9)	79.04(2)	Cl(2) — Mo(1) — Cl(3)	86.93(10)
Te(6) — Te(5) — Te(9)	77.99(2)	O(1) — Mo(1) — Cl(4)	104.9(3)
Au(2)^{i} — Te(6) — Au(3)	91.66(2)	Cl(1) — Mo(1) — Cl(4)	85.87(11)
Au(2)^{i} — Te(6) — Te(5)	93.26(3)	Cl(2) — Mo(1) — Cl(4)	149.92(11)
Au(3) — Te(6) — Te(5)	99.50(3)	Cl(3) — Mo(1) — Cl(4)	85.79(10)
Au(2)^{i} — Te(6) — Te(2)^{i}	93.36(2)	O(2) — Mo(2) — Cl(6)	102.6(3)
Au(3) — Te(6) — Te(2)^{i}	91.35(2)	O(2) — Mo(2) — Cl(5)	100.7(3)
Te(5) — Te(6) — Te(2)^{i}	167.11(3)	Cl(6) — Mo(2) — Cl(5)	89.28(10)
Au(2) — Te(7) — Au(3)	89.71(2)	O(2) — Mo(2) — Cl(7)	99.8(3)
Au(2) — Te(7) — Te(8)	96.98(3)	Cl(6) — Mo(2) — Cl(7)	87.24(10)
Au(3) — Te(7) — Te(8)	95.63(3)	Cl(5) — Mo(2) — Cl(7)	159.43(11)
Te(7) — Te(8) — Te(9)	82.49(3)	O(2) — Mo(2) — Cl(8)	97.9(3)

continued on next page

Atoms 1, 2, 3	Angle / °	Atoms 1, 2, 3	Angle / °
Te(7) — Te(8) — Te(3)	82.56(3)	Cl(6) — Mo(2) — Cl(8)	159.42(11)
Te(9) — Te(8) — Te(3)	77.80(2)	Cl(5) — Mo(2) — Cl(8)	87.45(10)
Au(3) — Te(9) — Au(1)	95.56(2)	Cl(7) — Mo(2) — Cl(8)	88.73(10)
Au(3) — Te(9) — Te(8)	93.92(3)	O(3) — Mo(3) — Cl(10)	101.7(3)
Au(1) — Te(9) — Te(8)	99.83(3)	O(3) — Mo(3) — Cl(9)	98.7(3)
Au(3) — Te(9) — Te(5)	94.11(2)	Cl(10) — Mo(3) — Cl(9)	87.58(12)
Au(1) — Te(9) — Te(5)	92.68(2)	O(3) — Mo(3) — Cl(11)	100.3(3)
Te(8) — Te(9) — Te(5)	164.40(3)	Cl(10) — Mo(3) — Cl(11)	88.76(12)
Te(12) — Au(4) — Te(18)	88.12(2)	Cl(9) — Mo(3) — Cl(11)	160.99(12)
Te(12) — Au(4) — Te(13)	177.32(3)	O(3) — Mo(3) — Cl(12)	102.2(3)
Te(18) — Au(4) — Te(13)	89.34(2)	Cl(10) — Mo(3) — Cl(12)	155.98(13)
Te(12) — Au(4) — Te(10)^{ii}	85.84(2)	Cl(9) — Mo(3) — Cl(12)	86.89(11)
Te(18) — Au(4) — Te(10)^{ii}	173.96(3)	Cl(11) — Mo(3) — Cl(12)	88.91(12)
Te(13) — Au(4) — Te(10)^{ii}	96.70(2)	O(4) — Mo(4) — Cl(14)	105.9(3)
Te(12)^{ii} — Au(5) — Te(13)	178.31(3)	O(4) — Mo(4) — Cl(13)	98.1(3)
Te(12)^{ii} — Au(5) — Te(15)	89.09(2)	Cl(14) — Mo(4) — Cl(13)	88.05(10)
Te(13) — Au(5) — Te(15)	89.27(2)	O(4) — Mo(4) — Cl(15)	97.5(3)
Te(12)^{ii} — Au(5) — Te(16)^{ii}	86.35(2)	Cl(14) — Mo(4) — Cl(15)	89.16(10)
Te(13) — Au(5) — Te(16)^{ii}	95.28(2)	Cl(13) — Mo(4) — Cl(15)	164.34(12)
Te(15) — Au(5) — Te(16)^{ii}	175.43(3)	O(4) — Mo(4) — Cl(16)	100.2(3)
Te(10) — Au(6) — Te(15)	87.72(2)	Cl(14) — Mo(4) — Cl(16)	153.92(11)
Te(10) — Au(6) — Te(18)	177.93(3)	Cl(13) — Mo(4) — Cl(16)	88.92(9)
Te(15) — Au(6) — Te(18)	90.24(2)	Cl(15) — Mo(4) — Cl(16)	86.83(9)
Te(10) — Au(6) — Te(16)	92.43(2)	O(5) — Mo(5) — Cl(18)	105.0(3)
Te(15) — Au(6) — Te(16)	179.52(3)	O(5) — Mo(5) — Cl(19)	97.9(3)
Te(18) — Au(6) — Te(16)	89.61(2)	Cl(18) — Mo(5) — Cl(19)	87.64(10)
Au(6) — Te(10) — Au(4)^{ii}	91.12(2)	O(5) — Mo(5) — Cl(17)	98.0(3)
Au(6) — Te(10) — Te(11)	99.92(3)	Cl(18) — Mo(5) — Cl(17)	89.18(10)
Au(4)^{ii} — Te(10) — Te(11)	96.21(3)	Cl(19) — Mo(5) — Cl(17)	164.06(12)
Te(10) — Te(11) — Te(12)^{ii}	82.05(3)	O(5) — Mo(5) — Cl(20)	101.0(3)
Te(10) — Te(11) — Te(15)	79.74(3)	Cl(18) — Mo(5) — Cl(20)	154.00(11)
Te(12)^{ii} — Te(11) — Te(15)	79.28(2)	Cl(19) — Mo(5) — Cl(20)	88.09(9)
Au(5)^{ii} — Te(12) — Au(4)	94.94(2)	Cl(17) — Mo(5) — Cl(20)	87.95(9)

A.1.10 $(Au_6Te_{18}Cl_2)[Mo_2O_2Cl_8]_2$

Table A.46: Crystal data and structure refinement for $(Au_6Te_{18}Cl_2)[Mo_2O_2Cl_8]_2$.

Empirical formula	$Au_6\,Cl_{18}\,Mo_4\,O_4\,Te_{18}$
Formula weight / $g \cdot mol^{-1}$	4564.46
Temperature / K	123(2)
Crystal system; space group	Monoclinic; $P2_1/n$
Lattice constants / $Å$	a = 11.7360(2)
	b = 17.6378(5); β = 105.670(1)°
	c = 13.4546(3)
Volume / $Å^3$	2681.6(1)
Z; F(000); calc. density / $g \cdot cm^{-3}$	2; 3832; 5.653
Wavelength	$Mo_{K\alpha}$ (λ = 0.71073 Å)
Crystal size / mm^3	0.103 × 0.067 × 0.022
Theta range for data collection / °	$2.930 \leq \theta \leq 27.501$
Limiting indices	$-15 \leq h \leq 15$; $-22 \leq k \leq 22$; $-17 \leq l \leq 17$
Reflections collected / unique	73228 / 6152
Completeness to θ = 25.242°	99.9 %
R_{int}; R_σ	0.1036; 0.0398
Absorption coefficient / mm^{-1}	27.761; Semi-empirical from equivalents
Max. / min. transmission	0.1644 / 0.0584
Refinement method	Full-matrix least-squares on F^2
Data / restraints / parameters	6152 / 0 / 226
R indices (all data) R_1; wR_2	0.0458; 0.0754
R indices $[I > 4\sigma(I)]$ R_1; wR_2	0.0323; 0.0713; n = 5043 reflections
Goodness-of-fit for F^2	1.068
Largest diff. peak / $e^- \cdot Å^{-3}$	+2.974 (0.91 Å from Au1)
	-1.783 (0.83 Å from Au1)
Avg. diff. density / $e^- \cdot Å^{-3}$	0.351

Table A.47: Fractional coordinates and equivalent isotropic displacement parameter U_{eq} for the independent atoms in the structure of $(Au_6Te_{18}Cl_2)[Mo_2O_2Cl_8]_2$.

Atom	Wyck.	Site	x / a	y / b	z / c	U_{eq} / $Å^2$
Au(1)	4*e*	1	0.86951(3)	0.49932(2)	0.13857(2)	0.01752(9)
Au(2)	4*e*	1	1.19714(3)	0.47696(2)	0.15372(3)	0.01779(9)
Au(3)	4*e*	1	0.97179(3)	0.34935(2)	-0.02163(2)	0.01738(9)
Te(1)	4*e*	1	0.84360(5)	0.34892(4)	0.11651(4)	0.01849(14)
Te(2)	4*e*	1	1.03412(5)	0.31088(4)	0.28215(4)	0.01954(14)
Te(3)	4*e*	1	1.06818(5)	0.47602(4)	0.29197(4)	0.01948(14)
Te(4)	4*e*	1	0.67270(5)	0.52659(4)	-0.01637(4)	0.01892(14)
Te(5)	4*e*	1	0.67258(5)	0.68153(4)	0.01397(5)	0.02220(14)
Te(6)	4*e*	1	1.16944(5)	0.32575(4)	0.13161(4)	0.02055(14)
Te(7)	4*e*	1	1.22209(5)	0.62804(4)	0.17816(4)	0.01907(14)
Te(8)	4*e*	1	1.11600(5)	0.63822(4)	0.33794(4)	0.02203(14)
Te(9)	4*e*	1	0.90070(5)	0.64978(4)	0.16043(4)	0.01980(14)
Cl(1)	4*e*	1	0.62136(18)	0.36590(13)	-0.04508(15)	0.0173(4)
Mo(1)	4*e*	1	0.88372(7)	0.88798(5)	0.13450(6)	0.01750(17)
Mo(2)	4*e*	1	0.81220(7)	1.11494(5)	0.12283(6)	0.01839(18)
O(1)	4*e*	1	0.8995(6)	0.8176(4)	0.0574(5)	0.0252(15)
O(2)	4*e*	1	0.7944(6)	1.1838(4)	0.2016(5)	0.0260(15)
Cl(2)	4*e*	1	1.07914(19)	0.92940(15)	0.19036(17)	0.0250(5)
Cl(3)	4*e*	1	0.9124(2)	0.82537(15)	0.29369(17)	0.0248(5)
Cl(4)	4*e*	1	0.67660(19)	0.87629(15)	0.11054(17)	0.0242(5)
Cl(5)	4*e*	1	0.84428(19)	0.98927(14)	0.01064(16)	0.0201(5)
Cl(6)	4*e*	1	0.84945(19)	1.01630(14)	0.25325(16)	0.0221(5)
Cl(7)	4*e*	1	0.7882(2)	1.18009(14)	-0.03407(17)	0.0239(5)
Cl(8)	4*e*	1	1.01717(19)	1.12918(15)	0.14636(17)	0.0237(5)
Cl(9)	4*e*	1	0.61212(19)	1.07640(15)	0.06420(18)	0.0263(5)

Table A.48: Anisotropic displacement parameters U_{ij} / $Å^2$ for the independent atoms in the structure of $(Au_6Te_{18}Cl_2)[Mo_2O_2Cl_8]_2$.

Atom	U_{11}	U_{22}	U_{33}	U_{23}	U_{13}	U_{12}
Au(1)	0.01619(17)	0.0211(2)	0.01494(16)	0.00010(14)	0.00369(12)	-0.00055(15)
Au(2)	0.01568(17)	0.0216(2)	0.01515(16)	0.00067(14)	0.00258(13)	-0.00030(14)
Au(3)	0.01557(17)	0.0202(2)	0.01584(17)	-0.00003(14)	0.00344(13)	-0.00057(14)

continued on next page

Atom	U_{11}	U_{22}	U_{33}	U_{23}	U_{13}	U_{12}
Te(1)	0.0177(3)	0.0205(4)	0.0172(3)	0.0010(2)	0.0046(2)	-0.0017(2)
Te(2)	0.0195(3)	0.0222(4)	0.0164(3)	0.0032(2)	0.0040(2)	0.0005(3)
Te(3)	0.0174(3)	0.0260(4)	0.0143(3)	0.0010(2)	0.0028(2)	-0.0011(3)
Te(4)	0.0152(3)	0.0239(4)	0.0172(3)	0.0009(2)	0.0037(2)	0.0002(2)
Te(5)	0.0184(3)	0.0246(4)	0.0237(3)	0.0012(3)	0.0059(2)	0.0027(3)
Te(6)	0.0178(3)	0.0217(4)	0.0201(3)	0.0020(2)	0.0016(2)	0.0015(3)
Te(7)	0.0167(3)	0.0225(4)	0.0163(3)	-0.0005(2)	0.0015(2)	-0.0021(2)
Te(8)	0.0228(3)	0.0250(4)	0.0170(3)	-0.0029(2)	0.0033(2)	-0.0015(3)
Te(9)	0.0207(3)	0.0201(4)	0.0200(3)	-0.0015(2)	0.0078(2)	-0.0003(3)
Cl(1)	0.0150(10)	0.0210(12)	0.0149(9)	0.0018(8)	0.0026(8)	-0.0024(9)
Mo(1)	0.0165(4)	0.0203(5)	0.0156(4)	-0.0003(3)	0.0041(3)	-0.0007(3)
Mo(2)	0.0174(4)	0.0211(5)	0.0169(4)	-0.0004(3)	0.0049(3)	-0.0003(3)
O(1)	0.025(3)	0.026(4)	0.026(4)	-0.003(3)	0.009(3)	-0.002(3)
O(2)	0.029(4)	0.022(4)	0.029(4)	-0.005(3)	0.009(3)	0.002(3)
Cl(2)	0.0171(11)	0.0337(15)	0.0221(11)	-0.0019(10)	0.0014(8)	-0.0019(10)
Cl(3)	0.0279(12)	0.0284(14)	0.0187(10)	0.0022(9)	0.0072(9)	0.0025(11)
Cl(4)	0.0187(11)	0.0325(15)	0.0221(11)	0.0017(10)	0.0065(9)	-0.0046(10)
Cl(5)	0.0196(10)	0.0246(13)	0.0157(10)	0.0008(9)	0.0041(8)	0.0006(9)
Cl(6)	0.0231(11)	0.0272(14)	0.0167(10)	-0.0005(9)	0.0067(8)	-0.0008(10)
Cl(7)	0.0255(12)	0.0242(14)	0.0210(11)	0.0035(9)	0.0047(9)	0.0006(10)
Cl(8)	0.0177(11)	0.0301(14)	0.0226(11)	-0.0006(10)	0.0041(9)	-0.0023(10)
Cl(9)	0.0167(11)	0.0343(15)	0.0288(12)	-0.0001(11)	0.0075(9)	0.0001(10)

Table A.49: Selected bond lengths for $(Au_6Te_{18}Cl_2)[Mo_2O_2Cl_8]_2$. Symmetry transformations used to generate equivalent atoms: (i) $-x+2$, $-y+1$, $-z$.

Atoms 1, 2	Distance / *Å*	Atoms 1, 2	Distance / *Å*
Au(1) —Te(1)	2.6775(7)	Te(5) —Te(9)	2.9179(8)
Au(1) —Te(9)	2.6841(7)	Te(5) —Te(6)^{i}	3.0418(8)
Au(1) —Te(3)	2.6954(6)	Te(6) —Te(5)^{i}	3.0419(8)
Au(1) —Te(4)	2.7039(6)	Te(7) —Au(3)^{i}	2.6801(6)
Au(2) —Te(7)	2.6912(8)	Te(7) —Te(8)	2.7659(8)
Au(2) —Te(6)	2.6934(8)	Te(8) —Te(9)	2.9783(8)
Au(2) —Te(3)	2.6966(7)	Te(9) —Au(3)^{i}	2.6902(7)
Au(2) —Te(4)^{i}	2.6975(7)	Mo(1) —O(1)	1.660(7)
Au(3) —Te(7)^{i}	2.6801(6)	Mo(1) —Cl(2)	2.330(2)

continued on next page

Atoms 1, 2	Distance / *Å*	Atoms 1, 2	Distance / *Å*
Au(3) —Te(6)	2.6873(6)	Mo(1) —Cl(3)	2.352(2)
Au(3) —Te(1)	2.6885(7)	Mo(1) —Cl(4)	2.373(2)
Au(3) —Te(9)^{i}	2.6903(7)	Mo(1) —Cl(5)	2.401(2)
Te(1) —Te(2)	2.7792(8)	Mo(2) —O(2)	1.661(7)
Te(2) —Te(6)	2.9035(8)	Mo(2) —Cl(7)	2.353(2)
Te(2) —Te(3)	2.9382(9)	Mo(2) —Cl(8)	2.353(2)
Te(3) —Te(8)	2.9487(9)	Mo(2) —Cl(9)	2.366(2)
Te(4) —Au(2)^{i}	2.6975(7)	Mo(2) —Cl(6)	2.426(2)
Te(4) —Te(5)	2.7633(9)	Mo(2) —Cl(5)	2.764(2)

Table A.50: Selected bond angles for $(Au_6Te_{18}Cl_2)[Mo_2O_2Cl_8]_2$. Symmetry transformations used to generate equivalent atoms: (i) $-x+2$, $-y+1$, $-z$.

Atoms 1, 2, 3	Angle / °	Atoms 1, 2, 3	Angle / °
Te(1) —Au(1) —Te(9)	178.67(2)	Au(2) —Te(6) —Te(5)^{i}	92.09(2)
Te(1) —Au(1) —Te(3)	89.01(2)	Te(2) —Te(6) —Te(5)^{i}	171.39(3)
Te(9) —Au(1) —Te(3)	90.15(2)	Au(3)^{i} —Te(7) —Au(2)	90.58(2)
Te(1) —Au(1) —Te(4)	92.46(2)	Au(3)^{i} —Te(7) —Te(8)	97.83(2)
Te(9) —Au(1) —Te(4)	88.36(2)	Au(2) —Te(7) —Te(8)	95.87(2)
Te(3) —Au(1) —Te(4)	178.36(2)	Te(7) —Te(8) —Te(3)	82.77(2)
Te(7) —Au(2) —Te(6)	178.92(2)	Te(7) —Te(8) —Te(9)	81.01(2)
Te(7) —Au(2) —Te(3)	89.12(2)	Te(3) —Te(8) —Te(9)	79.98(2)
Te(6) —Au(2) —Te(3)	89.81(2)	Au(1) —Te(9) —Au(3)^{i}	90.83(2)
Te(7) —Au(2) —Te(4)^{i}	92.50(2)	Au(1) —Te(9) —Te(5)	92.45(2)
Te(6) —Au(2) —Te(4)^{i}	88.58(2)	Au(3)^{i} —Te(9) —Te(5)	96.37(2)
Te(3) —Au(2) —Te(4)^{i}	178.29(3)	Au(1) —Te(9) —Te(8)	94.66(2)
Te(7)^{i} —Au(3) —Te(6)	178.46(2)	Au(3)^{i} —Te(9) —Te(8)	92.67(2)
Te(7)^{i} —Au(3) —Te(1)	91.65(2)	Te(5) —Te(9) —Te(8)	168.41(3)
Te(6) —Au(3) —Te(1)	89.85(2)	O(1) —Mo(1) —Cl(2)	99.8(2)
Te(7)^{i} —Au(3) —Te(9)^{i}	88.11(2)	O(1) —Mo(1) —Cl(3)	101.9(2)
Te(6) —Au(3) —Te(9)^{i}	90.39(2)	Cl(2) —Mo(1) —Cl(3)	88.11(9)
Te(1) —Au(3) —Te(9)^{i}	179.73(3)	O(1) —Mo(1) —Cl(4)	97.6(2)
Au(1) —Te(1) —Au(3)	90.33(2)	Cl(2) —Mo(1) —Cl(4)	162.57(9)
Au(1) —Te(1) —Te(2)	96.18(2)	Cl(3) —Mo(1) —Cl(4)	88.42(8)
Au(3) —Te(1) —Te(2)	94.35(2)	O(1) —Mo(1) —Cl(5)	98.9(2)
Te(1) —Te(2) —Te(6)	83.80(2)	Cl(2) —Mo(1) —Cl(5)	88.80(9)

continued on next page

Atoms 1, 2, 3	Angle / °	Atoms 1, 2, 3	Angle / °
Te(1) —Te(2) —Te(3)	82.35(2)	Cl(3) —Mo(1) —Cl(5)	159.19(9)
Te(6) —Te(2) —Te(3)	81.28(2)	Cl(4) —Mo(1) —Cl(5)	88.40(8)
Au(1) —Te(3) —Au(2)	90.085(19)	O(2) —Mo(2) —Cl(7)	102.1(2)
Au(1) —Te(3) —Te(2)	92.16(2)	O(2) —Mo(2) —Cl(8)	97.8(2)
Au(2) —Te(3) —Te(2)	94.01(2)	Cl(7) —Mo(2) —Cl(8)	86.50(8)
Au(1) —Te(3) —Te(8)	95.10(2)	O(2) —Mo(2) —Cl(9)	98.0(2)
Au(2) —Te(3) —Te(8)	91.62(2)	Cl(7) —Mo(2) —Cl(9)	88.49(9)
Te(2) —Te(3) —Te(8)	170.80(3)	Cl(8) —Mo(2) —Cl(9)	164.13(9)
$Au(2)^{i}$ —Te(4) —Au(1)	90.013(19)	O(2) —Mo(2) —Cl(6)	95.3(2)
$Au(2)^{i}$ —Te(4) —Te(5)	98.46(2)	Cl(7) —Mo(2) —Cl(6)	162.56(9)
Au(1) —Te(4) —Te(5)	95.53(2)	Cl(8) —Mo(2) —Cl(6)	90.08(8)
Te(4) —Te(5) —Te(9)	82.70(2)	Cl(9) —Mo(2) —Cl(6)	90.22(9)
Te(4) —Te(5) —$Te(6)^{i}$	80.70(2)	O(2) —Mo(2) —Cl(5)	173.4(2)
Te(9) —Te(5) —$Te(6)^{i}$	79.58(2)	Cl(7) —Mo(2) —Cl(5)	84.41(8)
Au(3) —Te(6) —Au(2)	89.13(2)	Cl(8) —Mo(2) —Cl(5)	82.76(8)
Au(3) —Te(6) —Te(2)	91.59(2)	Cl(9) —Mo(2) —Cl(5)	81.77(8)
Au(2) —Te(6) —Te(2)	94.87(2)	Cl(6) —Mo(2) —Cl(5)	78.19(7)
Au(3) —Te(6) —$Te(5)^{i}$	93.58(2)	Mo(1) —Cl(5) —Mo(2)	104.29(8)

A.1.11 $(Au_6Te_{18}Cl_2)[Bi_4Cl_{16}]$

Table A.51: Crystal data and structure refinement for $(Au_6Te_{18}Cl_2)[Bi_4Cl_{16}]$.

Empirical formula	$Au_6\,Bi_4\,Cl_{18}\,Te_{18}$
Formula weight / $g \cdot mol^{-1}$	4952.62
Temperature / K	123(2)
Crystal system; space group	Monoclinic; $P21/c$
Lattice constants / $\AA$	$a = 19.2955(7)$
	$b = 18.9948(7)$; $\beta = 99.419(2)^\circ$
	$c = 15.5236(4)$
Volume / $\AA^3$	5612.9(3)
Z; F(000); calc. density / $g \cdot cm^{-3}$	4; 8192; 5.861
Wavelength	$Mo_{K\alpha}$ ($\lambda = 0.71073$ Å)
Crystal size / mm^3	0.074 × 0.050 × 0.024
Theta range for data collection / °	$2.904 \leq \theta \leq 27.398$
Limiting indices	$-24 \leq h \leq 24$; $-24 \leq k \leq 24$; $-20 \leq l \leq 19$
Reflections collected / unique	73266 / 12355
Completeness to $\theta = 25.242^\circ$	98.3 %
R_{int}; R_σ	0.1054; 0.0722
Absorption coefficient / mm^{-1}	38.147; Semi-empirical from equivalents
Max. / min. transmission	0.1329 / 0.0647
Refinement method	Full-matrix least-squares on F^2
Data / restraints / parameters	12355 / 2 / 421
R indices (all data) R_1; wR_2	0.0883; 0.1052
R indices $[I > 4\sigma(I)]$ R_1; wR_2	0.0465; 0.0936; n = 8186 reflections
Goodness-of-fit for F^2	1.037
Largest diff. peak / $e^- \cdot \AA^{-3}$	+3.016 (2.39 Å from Cl2)
	-2.079 (0.78 Å from Bi1)
Avg. diff. density / $e^- \cdot \AA^{-3}$	0.366

Table A.52: Fractional coordinates and equivalent isotropic displacement parameter U_{eq} for the independent atoms in the structure of $(Au_6Te_{18}Cl_2)[Bi_4Cl_{16}]$.

Atom	Wyck.	Site	*SOF*	*x / a*	*y / b*	*z / c*	U_{eq} / Å^2
Au(1)	4*e*	1	1	0.13947(3)	-0.48027(4)	0.53267(4)	0.03703(17)
Au(2)	4*e*	1	1	0.00611(3)	-0.51996(4)	0.32677(4)	0.03518(16)
Au(3)	4*e*	1	1	-0.01868(3)	-0.36120(4)	0.47083(4)	0.03667(17)
Te(1)	4*e*	1	1	-0.13297(6)	-0.54057(8)	0.29645(8)	0.0447(3)
Te(2)	4*e*	1	1	0.15837(6)	-0.61931(7)	0.56020(8)	0.0425(3)
Te(3)	4*e*	1	1	0.12087(6)	-0.34159(7)	0.50167(8)	0.0408(3)
Te(4)	4*e*	1	1	0.14554(6)	-0.50124(7)	0.36232(7)	0.0409(3)
Te(5)	4*e*	1	1	-0.01201(6)	-0.38032(7)	0.30002(7)	0.0412(3)
Te(6)	4*e*	1	1	0.02748(6)	-0.65819(7)	0.35912(7)	0.0412(3)
Te(7)	4*e*	1	1	0.17802(7)	-0.64997(8)	0.38488(8)	0.0510(3)
Te(8)	4*e*	1	0.781(2)	0.13605(9)	-0.35075(9)	0.31964(11)	0.0544(4)
Te(9)	4*e*	1	0.662(2)	-0.12627(9)	-0.6909(1)	0.31735(11)	0.0480(4)
Te(10)	4*e*	1	0.557(2)	-0.16227(9)	-0.3923(1)	0.24923(12)	0.0452(5)
Cl(17)	4*e*	1	0.220(2)	0.13605(9)	-0.35075(9)	0.31964(11)	0.0544(4)
Cl(18)	4*e*	1	0.338(2)	-0.12627(9)	-0.6909(1)	0.31735(11)	0.0480(4)
Cl(19)	4*e*	1	0.442(2)	-0.16227(9)	-0.3923(1)	0.24923(12)	0.0452(5)
Au(4)	4*e*	1	1	0.47197(3)	-0.13558(4)	0.52815(4)	0.03404(16)
Au(5)	4*e*	1	1	0.63348(3)	-0.03376(4)	0.48622(4)	0.03305(16)
Au(6)	4*e*	1	1	0.53959(3)	0.02011(4)	0.67361(4)	0.03361(16)
Te(11)	4*e*	1	1	0.60418(6)	-0.17007(6)	0.51115(7)	0.0358(3)
Te(12)	4*e*	1	1	0.50868(6)	-0.11514(6)	0.70118(7)	0.0374(3)
Te(13)	4*e*	1	1	0.43370(6)	-0.15601(6)	0.35573(7)	0.0376(3)
Te(14)	4*e*	1	1	0.33906(6)	-0.10207(7)	0.54432(7)	0.0371(3)
Te(15)	4*e*	1	1	0.32737(6)	0.01267(7)	0.34135(7)	0.0390(3)
Te(16)	4*e*	1	1	0.40610(6)	0.05358(7)	0.68607(7)	0.0370(3)
Te(17)	4*e*	1	1	0.37060(6)	-0.09582(7)	0.73119(8)	0.0453(3)
Te(18)	4*e*	1	0.749(2)	0.28587(7)	-0.12849(8)	0.35707(9)	0.0409(4)
Te(19)	4*e*	1	0.955(2)	0.57562(7)	-0.20214(7)	0.33046(8)	0.0426(3)
Te(20)	4*e*	1	0.296(2)	0.65650(14)	-0.1611(1)	0.69504(16)	0.0475(7)
Cl(20)	4*e*	1	0.251(2)	0.28587(7)	-0.12849(8)	0.35707(9)	0.0409(4)
Cl(21)	4*e*	1	0.045(2)	0.57562(7)	-0.20214(7)	0.33046(8)	0.0426(3)
Cl(22)	4*e*	1	0.704(2)	0.65650(14)	-0.1611(1)	0.69504(16)	0.0475(7)
Bi(1)	4*e*	1	1	0.62840(4)	-0.63403(4)	0.46266(4)	0.04011(18)

continued on next page

Atom	Wyck.	Site	*SOF*	*x / a*	*y / b*	*z / c*	U_{eq} / Å^2
Bi(2)	4*e*	1	1	0.41431(3)	-0.58125(4)	0.48895(4)	0.03464(16)
Cl(1)	4*e*	1	1	0.7069(3)	-0.5818(4)	0.3652(3)	0.0717(18)
Cl(2)	4*e*	1	1	0.7125(3)	-0.7171(4)	0.5488(5)	0.093(2)
Cl(3)	4*e*	1	1	0.5716(4)	-0.7236(3)	0.3528(3)	0.0770(19)
Cl(4)	4*e*	1	1	0.5214(2)	-0.5289(2)	0.3845(3)	0.0386(10)
Cl(5)	4*e*	1	1	0.5185(2)	-0.6686(3)	0.5677(3)	0.0459(11)
Cl(6)	4*e*	1	1	0.3201(2)	-0.4835(3)	0.4170(3)	0.0455(11)
Cl(7)	4*e*	1	1	0.3658(3)	-0.6666(3)	0.3711(3)	0.0504(12)
Cl(8)	4*e*	1	1	0.3360(2)	-0.6259(3)	0.5914(3)	0.0525(13)
Bi(3)	4*e*	1	1	0.14146(4)	0.12284(4)	0.56910(5)	0.04419(19)
Bi(4)	4*e*	1	1	0.07947(3)	-0.08821(4)	0.50658(4)	0.03949(17)
Cl(9)	4*e*	1	1	0.1096(3)	0.2170(3)	0.6705(4)	0.0621(14)
Cl(10)	4*e*	1	1	0.2280(3)	0.2002(3)	0.5081(5)	0.0797(19)
Cl(11)	4*e*	1	1	0.2322(3)	0.0681(3)	0.6858(3)	0.0607(14)
Cl(12)	4*e*	1	1	0.0367(2)	0.0256(3)	0.6255(3)	0.0445(11)
Cl(13)	4*e*	1	1	0.1693(2)	0.0052(3)	0.4526(3)	0.0504(12)
Cl(14)	4*e*	1	1	-0.0190(2)	-0.1715(3)	0.5639(3)	0.0505(12)
Cl(15)	4*e*	1	1	0.1780(3)	-0.1413(3)	0.6142(4)	0.0689(17)
Cl(16)	4*e*	1	1	0.0970(3)	-0.1745(3)	0.3899(4)	0.0624(14)

Table A.53: Anisotropic displacement parameters U_{ij} / Å^2 for the independent atoms in the structure of $(Au_6Te_{18}Cl_2)[Bi_4Cl_{16}]$.

Atom	U_{11}	U_{22}	U_{33}	U_{23}	U_{13}	U_{12}
Au(1)	0.0278(3)	0.0517(5)	0.0313(4)	-0.0008(3)	0.0040(3)	-0.0015(3)
Au(2)	0.0297(3)	0.0468(5)	0.0288(4)	-0.0009(3)	0.0040(3)	-0.0013(3)
Au(3)	0.0334(4)	0.0463(5)	0.0303(4)	0.0012(3)	0.0052(3)	0.0010(3)
Te(1)	0.0296(6)	0.0724(10)	0.0313(6)	-0.0057(6)	0.0024(5)	-0.0050(6)
Te(2)	0.0306(6)	0.0534(8)	0.0423(7)	0.0003(6)	0.0027(5)	0.0056(5)
Te(3)	0.0349(6)	0.0505(8)	0.0369(7)	0.0005(5)	0.0056(5)	-0.0074(5)
Te(4)	0.0287(6)	0.0613(9)	0.0331(6)	-0.0029(5)	0.0064(5)	-0.0004(5)
Te(5)	0.0460(7)	0.0473(8)	0.0299(6)	0.0029(5)	0.0051(5)	-0.0007(6)
Te(6)	0.0452(7)	0.0460(8)	0.0333(6)	-0.0021(5)	0.0089(5)	-0.0011(6)
Te(7)	0.0403(7)	0.0696(10)	0.0451(8)	0.0040(6)	0.0131(6)	0.0140(6)
Te(8)	0.0569(10)	0.0595(11)	0.0501(10)	0.0011(8)	0.0186(8)	-0.0054(8)
Te(9)	0.0487(10)	0.0572(12)	0.0384(9)	-0.0014(8)	0.0086(7)	-0.0024(8)

continued on next page

Atom	U_{11}	U_{22}	U_{33}	U_{23}	U_{13}	U_{12}
Te(10)	0.0354(10)	0.0618(13)	0.0363(10)	-0.0029(9)	0.0001(7)	-0.0018(9)
Cl(17)	0.0569(10)	0.0595(11)	0.0501(10)	0.0011(8)	0.0186(8)	-0.0054(8)
Cl(18)	0.0487(10)	0.0572(12)	0.0384(9)	-0.0014(8)	0.0086(7)	-0.0024(8)
Cl(19)	0.0354(10)	0.0618(13)	0.0363(10)	-0.0029(9)	0.0001(7)	-0.0018(9)
Au(4)	0.0311(3)	0.0443(4)	0.0265(3)	-0.0023(3)	0.0038(3)	0.0006(3)
Au(5)	0.0297(3)	0.0429(4)	0.0260(3)	-0.0013(3)	0.0031(3)	0.0018(3)
Au(6)	0.0305(3)	0.0446(4)	0.0249(3)	-0.0021(3)	0.0023(3)	0.0011(3)
Te(11)	0.0347(6)	0.0415(7)	0.0309(6)	-0.0010(5)	0.0044(5)	0.0039(5)
Te(12)	0.0401(6)	0.0457(8)	0.0258(6)	0.0003(5)	0.0038(5)	-0.0004(5)
Te(13)	0.0424(7)	0.0420(7)	0.0266(6)	-0.0032(5)	0.0006(5)	0.0009(5)
Te(14)	0.0301(6)	0.0472(8)	0.0342(6)	0.0000(5)	0.0055(5)	-0.0019(5)
Te(15)	0.0301(6)	0.0584(8)	0.0270(6)	-0.0055(5)	0.0002(4)	0.0003(5)
Te(16)	0.0322(6)	0.0540(8)	0.0249(6)	-0.0034(5)	0.0044(4)	0.0022(5)
Te(17)	0.0449(7)	0.0556(9)	0.0373(7)	0.0010(6)	0.0121(5)	0.0027(6)
Te(18)	0.0332(8)	0.0552(10)	0.0326(8)	0.0004(7)	0.0004(6)	0.0009(7)
Te(19)	0.0478(7)	0.0470(8)	0.0337(7)	-0.0047(6)	0.0090(5)	-0.0004(6)
Te(20)	0.0492(15)	0.0591(19)	0.0342(14)	-0.0022(12)	0.0064(11)	-0.0013(13)
Cl(20)	0.0332(8)	0.0552(10)	0.0326(8)	0.0004(7)	0.0004(6)	0.0009(7)
Cl(21)	0.0478(7)	0.0470(8)	0.0337(7)	-0.0047(6)	0.0090(5)	-0.0004(6)
Cl(22)	0.0492(15)	0.0591(19)	0.0342(14)	-0.0022(12)	0.0064(11)	-0.0013(13)
Bi(1)	0.0370(4)	0.0482(5)	0.0336(4)	0.0040(3)	0.0012(3)	-0.0086(3)
Bi(2)	0.0322(3)	0.0423(4)	0.0294(3)	0.0009(3)	0.0049(3)	-0.0049(3)
Cl(1)	0.041(3)	0.138(6)	0.037(3)	0.003(3)	0.011(2)	-0.014(3)
Cl(2)	0.061(4)	0.083(5)	0.126(6)	0.036(4)	-0.013(4)	0.001(3)
Cl(3)	0.128(5)	0.060(4)	0.038(3)	0.002(3)	-0.001(3)	-0.028(4)
Cl(4)	0.034(2)	0.049(3)	0.032(2)	0.0050(19)	0.0049(17)	-0.0033(19)
Cl(5)	0.040(3)	0.058(3)	0.040(3)	0.004(2)	0.0067(19)	-0.005(2)
Cl(6)	0.038(2)	0.058(3)	0.039(3)	0.002(2)	0.0006(19)	-0.009(2)
Cl(7)	0.063(3)	0.048(3)	0.037(3)	-0.003(2)	-0.002(2)	-0.007(2)
Cl(8)	0.036(3)	0.080(4)	0.041(3)	0.016(2)	0.006(2)	-0.007(2)
Bi(3)	0.0386(4)	0.0513(5)	0.0453(4)	0.0035(3)	0.0147(3)	0.0057(3)
Bi(4)	0.0391(4)	0.0466(5)	0.0355(4)	0.0046(3)	0.0143(3)	0.0063(3)
Cl(9)	0.068(3)	0.057(4)	0.064(3)	-0.006(3)	0.020(3)	0.014(3)
Cl(10)	0.057(3)	0.066(4)	0.127(6)	0.012(4)	0.047(4)	-0.002(3)
Cl(11)	0.044(3)	0.086(4)	0.053(3)	0.002(3)	0.010(2)	0.011(3)

continued on next page

Atom	U_{11}	U_{22}	U_{33}	U_{23}	U_{13}	U_{12}
Cl(12)	0.045(3)	0.055(3)	0.036(2)	0.003(2)	0.0131(19)	0.007(2)
Cl(13)	0.051(3)	0.058(3)	0.047(3)	0.008(2)	0.023(2)	0.011(2)
Cl(14)	0.050(3)	0.062(3)	0.041(3)	0.008(2)	0.012(2)	0.002(2)
Cl(15)	0.052(3)	0.085(4)	0.069(4)	0.036(3)	0.009(3)	0.000(3)
Cl(16)	0.075(4)	0.058(4)	0.061(3)	0.000(3)	0.032(3)	0.007(3)

Table A.54: Selected bond lengths for $(Au_6Te_{18}Cl_2)[Bi_4Cl_{16}]$. Symmetry transformations used to generate equivalent atoms: (i) $-x, -y-1, -z+1$; (ii) $-x+1, -y, -z+1$; (iii) $-x+1, -y-1, -z+1$; (iv) $-x, -y, -z+1$.

Atoms 1, 2	Distance / Å	Atoms 1, 2	Distance / Å
Au(1) — Te(2)	2.6908(15)	Te(12) — Te(20)	2.999(3)
Au(1) — Te(3)	2.6911(15)	Te(13) — Au(6)^{ii}	2.6859(14)
Au(1) — Te(4)	2.6958(13)	Te(13) — Te(18)	2.9033(18)
Au(1) — Te(1)^{i}	2.7052(13)	Te(13) — Te(19)	2.9618(17)
Au(2) — Te(1)	2.6765(13)	Te(14) — Au(5)^{ii}	2.6915(14)
Au(2) — Te(4)	2.6802(13)	Te(14) — Te(17)	2.8674(16)
Au(2) — Te(6)	2.6923(15)	Te(14) — Te(18)	2.9628(18)
Au(2) — Te(5)	2.6986(15)	Te(15) — Au(6)^{ii}	2.6881(13)
Au(3) — Te(3)	2.6826(13)	Te(15) — Au(5)^{ii}	2.6897(12)
Au(3) — Te(2)^{i}	2.6849(13)	Te(15) — Te(18)	2.820(2)
Au(3) — Te(6)^{i}	2.6981(13)	Te(15) — Te(20)^{ii}	2.902(3)
Au(3) — Te(5)	2.7002(13)	Te(16) — Au(5)^{ii}	2.6851(12)
Te(1) — Au(1)^{i}	2.7052(13)	Te(16) — Te(19)^{ii}	2.8606(19)
Te(1) — Te(9)	2.874(2)	Te(16) — Te(17)	3.0281(19)
Te(1) — Te(10)	2.941(2)	Te(19) — Te(16)^{ii}	2.8605(19)
Te(2) — Au(3)^{i}	2.6850(13)	Te(20) — Te(15)^{ii}	2.902(3)
Te(2) — Te(7)	2.8684(18)	Bi(1) — Cl(2)	2.491(6)
Te(2) — Te(10)^{i}	2.955(2)	Bi(1) — Cl(1)	2.513(5)
Te(3) — Te(9)^{i}	2.861(2)	Bi(1) — Cl(3)	2.528(5)
Te(3) — Te(8)	2.893(2)	Bi(1) — Cl(5)	2.954(4)
Te(4) — Te(7)	2.902(2)	Bi(1) — Cl(6)^{iii}	2.976(5)
Te(4) — Te(8)	2.933(2)	Bi(1) — Cl(4)	2.984(4)
Te(5) — Te(8)	2.878(2)	Bi(2) — Cl(7)	2.508(5)
Te(5) — Te(10)	2.887(2)	Bi(2) — Cl(8)	2.514(4)
Te(6) — Au(3)^{i}	2.6981(13)	Bi(2) — Cl(6)	2.708(5)

continued on next page

Atoms 1, 2	Distance / Å	Atoms 1, 2	Distance / Å
Te(6) — Te(7)	2.8708(17)	Bi(2) — Cl(5)	2.736(5)
Te(6) — Te(9)	2.996(2)	Bi(2) — Cl(4)^{iii}	2.996(4)
Te(9) — Te(3)^{i}	2.861(2)	Bi(2) — Cl(4)	2.997(4)
Te(10) — Te(2)^{i}	2.955(2)	Cl(4) — Bi(2)^{iii}	2.996(4)
Au(4) — Te(13)	2.6857(12)	Cl(6) — Bi(1)^{iii}	2.976(5)
Au(4) — Te(11)	2.6884(13)	Bi(3) — Cl(10)	2.523(5)
Au(4) — Te(12)	2.6915(12)	Bi(3) — Cl(9)	2.524(5)
Au(4) — Te(14)	2.6935(13)	Bi(3) — Cl(11)	2.528(5)
Au(5) — Te(16)^{ii}	2.6852(12)	Bi(3) — Cl(12)	2.974(5)
Au(5) — Te(15)^{ii}	2.6897(12)	Bi(3) — Cl(13)	2.979(5)
Au(5) — Te(11)	2.6915(14)	Bi(3) — Cl(14)^{iv}	3.017(5)
Au(5) — Te(14)^{ii}	2.6915(14)	Bi(4) — Cl(16)	2.506(5)
Au(6) — Te(13)^{ii}	2.6858(14)	Bi(4) — Cl(15)	2.527(5)
Au(6) — Te(12)	2.6874(14)	Bi(4) — Cl(13)	2.708(5)
Au(6) — Te(15)^{ii}	2.6882(13)	Bi(4) — Cl(14)	2.730(5)
Au(6) — Te(16)	2.6906(12)	Bi(4) — Cl(12)^{iv}	3.023(5)
Te(11) — Te(19)	2.8349(16)	Bi(4) — Cl(12)	3.043(5)
Te(11) — Te(20)	2.873(3)	Cl(12) — Bi(4)^{iv}	3.023(5)
Te(12) — Te(17)	2.8030(16)	Cl(14) — Bi(3)^{iv}	3.017(5)

Table A.55: Selected bond angles for $(Au_6Te_{18}Cl_2)[Bi_4Cl_{16}]$. Symmetry transformations used to generate equivalent atoms: (i) $-x, -y-1, -z+1$; (ii) $-x+1, -y, -z+1$; (iii) $-x+1, -y-1, -z+1$; (iv) $-x, -y, -z+1$.

Atoms 1, 2, 3	Angle / °	Atoms 1, 2, 3	Angle / °
Te(2) — Au(1) — Te(3)	178.82(5)	Te(18) — Te(13) — Te(19)	170.05(6)
Te(2) — Au(1) — Te(4)	89.10(4)	Au(5)^{ii} — Te(14) — Au(4)	89.55(4)
Te(3) — Au(1) — Te(4)	89.73(4)	Au(5)^{ii} — Te(14) — Te(17)	97.08(5)
Te(2) — Au(1) — Te(1)^{i}	90.84(5)	Au(4) — Te(14) — Te(17)	93.23(4)
Te(3) — Au(1) — Te(1)^{i}	90.34(4)	Au(5)^{ii} — Te(14) — Te(18)	92.07(5)
Te(4) — Au(1) — Te(1)^{i}	179.82(5)	Au(4) — Te(14) — Te(18)	92.91(5)
Te(1) — Au(2) — Te(4)	178.12(5)	Te(17) — Te(14) — Te(18)	169.01(6)
Te(1) — Au(2) — Te(6)	90.50(5)	Au(6)^{ii} — Te(15) — Au(5)^{ii}	90.22(4)
Te(4) — Au(2) — Te(6)	88.46(4)	Au(6)^{ii} — Te(15) — Te(18)	94.36(5)
Te(1) — Au(2) — Te(5)	90.91(4)	Au(5)^{ii} — Te(15) — Te(18)	95.34(5)
Te(4) — Au(2) — Te(5)	90.10(4)	Au(6)^{ii} — Te(15) — Te(20)^{ii}	94.23(6)

continued on next page

Atoms 1, 2, 3	Angle / °	Atoms 1, 2, 3	Angle / °
Te(6) — Au(2) — Te(5)	177.84(4)	Au(5)^{ii} — Te(15) — Te(20)^{ii}	91.57(6)
Te(3) — Au(3) — Te(2)^{i}	179.92(6)	Te(18) — Te(15) — Te(20)^{ii}	168.95(7)
Te(3) — Au(3) — Te(6)^{i}	91.63(4)	Au(5)^{ii} — Te(16) — Au(6)	90.85(4)
Te(2)^{i} — Au(3) — Te(6)^{i}	88.41(4)	Au(5)^{ii} — Te(16) — Te(19)^{ii}	93.90(5)
Te(3) — Au(3) — Te(5)	89.21(4)	Au(6) — Te(16) — Te(19)^{ii}	95.35(5)
Te(2)^{i} — Au(3) — Te(5)	90.75(4)	Au(5)^{ii} — Te(16) — Te(17)	93.48(5)
Te(6)^{i} — Au(3) — Te(5)	179.13(5)	Au(6) — Te(16) — Te(17)	92.90(5)
Au(2) — Te(1) — Au(1)^{i}	90.70(4)	Te(19)^{ii} — Te(16) — Te(17)	168.83(5)
Au(2) — Te(1) — Te(9)	95.75(5)	Te(12) — Te(17) — Te(14)	82.91(4)
Au(1)^{i} — Te(1) — Te(9)	92.47(5)	Te(12) — Te(17) — Te(16)	80.05(5)
Au(2) — Te(1) — Te(10)	92.87(5)	Te(14) — Te(17) — Te(16)	79.83(4)
Au(1)^{i} — Te(1) — Te(10)	93.81(6)	Te(15) — Te(18) — Te(13)	82.95(5)
Te(9) — Te(1) — Te(10)	169.27(6)	Te(15) — Te(18) — Te(14)	82.31(5)
Au(3)^{i} — Te(2) — Au(1)	90.05(4)	Te(13) — Te(18) — Te(14)	81.63(5)
Au(3)^{i} — Te(2) — Te(7)	94.96(5)	Te(11) — Te(19) — Te(16)^{ii}	82.53(5)
Au(1) — Te(2) — Te(7)	94.82(5)	Te(11) — Te(19) — Te(13)	80.77(4)
Au(3)^{i} — Te(2) — Te(10)^{i}	92.88(5)	Te(16)^{ii} — Te(19) — Te(13)	81.39(5)
Au(1) — Te(2) — Te(10)^{i}	93.80(6)	Te(11) — Te(20) — Te(15)^{ii}	84.01(8)
Te(7) — Te(2) — Te(10)^{i}	168.33(6)	Te(11) — Te(20) — Te(12)	82.38(7)
Au(3) — Te(3) — Au(1)	89.81(4)	Te(15)^{ii} — Te(20) — Te(12)	81.73(8)
Au(3) — Te(3) — Te(9)^{i}	94.55(5)	Cl(2) — Bi(1) — Cl(1)	99.7(2)
Au(1) — Te(3) — Te(9)^{i}	93.05(5)	Cl(2) — Bi(1) — Cl(3)	96.2(2)
Au(3) — Te(3) — Te(8)	94.38(5)	Cl(1) — Bi(1) — Cl(3)	95.5(2)
Au(1) — Te(3) — Te(8)	94.82(5)	Cl(2) — Bi(1) — Cl(5)	91.5(2)
Te(9)^{i} — Te(3) — Te(8)	168.11(7)	Cl(1) — Bi(1) — Cl(5)	168.00(18)
Au(2) — Te(4) — Au(1)	91.04(4)	Cl(3) — Bi(1) — Cl(5)	87.23(18)
Au(2) — Te(4) — Te(7)	94.89(5)	Cl(2) — Bi(1) — Cl(6)^{iii}	91.0(2)
Au(1) — Te(4) — Te(7)	93.94(5)	Cl(1) — Bi(1) — Cl(6)^{iii}	84.83(17)
Au(2) — Te(4) — Te(8)	93.40(5)	Cl(3) — Bi(1) — Cl(6)^{iii}	172.59(18)
Au(1) — Te(4) — Te(8)	93.81(5)	Cl(5) — Bi(1) — Cl(6)^{iii}	90.94(13)
Te(7) — Te(4) — Te(8)	168.54(6)	Cl(2) — Bi(1) — Cl(4)	171.6(2)
Au(2) — Te(5) — Au(3)	90.40(4)	Cl(1) — Bi(1) — Cl(4)	86.32(16)
Au(2) — Te(5) — Te(8)	94.26(5)	Cl(3) — Bi(1) — Cl(4)	88.92(18)
Au(3) — Te(5) — Te(8)	94.35(5)	Cl(5) — Bi(1) — Cl(4)	82.05(12)
Au(2) — Te(5) — Te(10)	93.64(6)	Cl(6)^{iii} — Bi(1) — Cl(4)	83.72(12)

continued on next page

Atoms 1, 2, 3	Angle / °	Atoms 1, 2, 3	Angle / °
Au(3) — Te(5) — Te(10)	94.11(5)	Cl(7) — Bi(2) — Cl(8)	92.98(17)
Te(8) — Te(5) — Te(10)	168.38(7)	Cl(7) — Bi(2) — Cl(6)	89.85(15)
Au(2) — Te(6) — Au(3)^{i}	90.98(4)	Cl(8) — Bi(2) — Cl(6)	93.43(15)
Au(2) — Te(6) — Te(7)	95.37(5)	Cl(7) — Bi(2) — Cl(5)	95.32(15)
Au(3)^{i} — Te(6) — Te(7)	94.62(5)	Cl(8) — Bi(2) — Cl(5)	89.22(15)
Au(2) — Te(6) — Te(9)	92.63(5)	Cl(6) — Bi(2) — Cl(5)	174.06(14)
Au(3)^{i} — Te(6) — Te(9)	91.22(5)	Cl(7) — Bi(2) — Cl(4)^{iii}	174.04(14)
Te(7) — Te(6) — Te(9)	170.01(7)	Cl(8) — Bi(2) — Cl(4)^{iii}	92.77(15)
Te(2) — Te(7) — Te(6)	81.68(5)	Cl(6) — Bi(2) — Cl(4)^{iii}	88.25(13)
Te(2) — Te(7) — Te(4)	81.81(5)	Cl(5) — Bi(2) — Cl(4)^{iii}	86.31(13)
Te(6) — Te(7) — Te(4)	80.94(5)	Cl(7) — Bi(2) — Cl(4)	91.61(14)
Te(5) — Te(8) — Te(3)	81.82(5)	Cl(8) — Bi(2) — Cl(4)	173.32(13)
Te(5) — Te(8) — Te(4)	81.83(5)	Cl(6) — Bi(2) — Cl(4)	91.43(13)
Te(3) — Te(8) — Te(4)	81.41(5)	Cl(5) — Bi(2) — Cl(4)	85.52(13)
Te(3)^{i} — Te(9) — Te(1)	83.71(6)	Cl(4)^{iii} — Bi(2) — Cl(4)	82.79(12)
Te(3)^{i} — Te(9) — Te(6)	82.37(5)	Bi(1) — Cl(4) — Bi(2)^{iii}	90.94(11)
Te(1) — Te(9) — Te(6)	80.98(6)	Bi(1) — Cl(4) — Bi(2)	92.89(12)
Te(5) — Te(10) — Te(1)	82.18(6)	Bi(2)^{iii} — Cl(4) — Bi(2)	97.21(12)
Te(5) — Te(10) — Te(2)^{i}	82.00(5)	Bi(2) — Cl(5) — Bi(1)	99.19(14)
Te(1) — Te(10) — Te(2)^{i}	81.36(6)	Bi(2) — Cl(6) — Bi(1)^{iii}	97.06(13)
Te(13) — Au(4) — Te(11)	88.71(4)	Cl(10) — Bi(3) — Cl(9)	93.8(2)
Te(13) — Au(4) — Te(12)	179.31(4)	Cl(10) — Bi(3) — Cl(11)	94.9(2)
Te(11) — Au(4) — Te(12)	91.95(4)	Cl(9) — Bi(3) — Cl(11)	93.18(18)
Te(13) — Au(4) — Te(14)	90.94(4)	Cl(10) — Bi(3) — Cl(12)	174.90(19)
Te(11) — Au(4) — Te(14)	179.47(5)	Cl(9) — Bi(3) — Cl(12)	90.55(16)
Te(12) — Au(4) — Te(14)	88.40(4)	Cl(11) — Bi(3) — Cl(12)	87.58(15)
Te(16)^{ii} — Au(5) — Te(15)^{ii}	179.46(5)	Cl(10) — Bi(3) — Cl(13)	90.71(18)
Te(16)^{ii} — Au(5) — Te(11)	88.63(4)	Cl(9) — Bi(3) — Cl(13)	175.42(16)
Te(15)^{ii} — Au(5) — Te(11)	91.81(4)	Cl(11) — Bi(3) — Cl(13)	87.35(16)
Te(16)^{ii} — Au(5) — Te(14)^{ii}	89.49(4)	Cl(12) — Bi(3) — Cl(13)	84.93(13)
Te(15)^{ii} — Au(5) — Te(14)^{ii}	90.07(4)	Cl(10) — Bi(3) — Cl(14)^{iv}	93.30(18)
Te(11) — Au(5) — Te(14)^{ii}	178.11(4)	Cl(9) — Bi(3) — Cl(14)^{iv}	88.05(16)
Te(13)^{ii} — Au(6) — Te(12)	178.25(4)	Cl(11) — Bi(3) — Cl(14)^{iv}	171.63(16)
Te(13)^{ii} — Au(6) — Te(15)^{ii}	89.74(4)	Cl(12) — Bi(3) — Cl(14)^{iv}	84.12(13)
Te(12) — Au(6) — Te(15)^{ii}	91.85(4)	Cl(13) — Bi(3) — Cl(14)^{iv}	90.78(14)

continued on next page

Atoms 1, 2, 3	Angle / °	Atoms 1, 2, 3	Angle / °
Te(13)^{ii} — Au(6) — Te(16)	89.86(4)	Cl(16) — Bi(4) — Cl(15)	92.3(2)
Te(12) — Au(6) — Te(16)	88.54(4)	Cl(16) — Bi(4) — Cl(13)	92.05(17)
Te(15)^{ii} — Au(6) — Te(16)	179.14(4)	Cl(15) — Bi(4) — Cl(13)	90.88(16)
Au(4) — Te(11) — Au(5)	90.27(4)	Cl(16) — Bi(4) — Cl(14)	92.28(17)
Au(4) — Te(11) — Te(19)	96.64(4)	Cl(15) — Bi(4) — Cl(14)	92.40(16)
Au(5) — Te(11) — Te(19)	94.35(5)	Cl(13) — Bi(4) — Cl(14)	174.46(15)
Au(4) — Te(11) — Te(20)	94.17(6)	Cl(16) — Bi(4) — Cl(12)^{iv}	86.55(16)
Au(5) — Te(11) — Te(20)	92.18(7)	Cl(15) — Bi(4) — Cl(12)^{iv}	178.71(17)
Te(19) — Te(11) — Te(20)	167.33(8)	Cl(13) — Bi(4) — Cl(12)^{iv}	88.47(14)
Au(6) — Te(12) — Au(4)	90.46(4)	Cl(14) — Bi(4) — Cl(12)^{iv}	88.33(13)
Au(6) — Te(12) — Te(17)	98.22(5)	Cl(16) — Bi(4) — Cl(12)	170.05(16)
Au(4) — Te(12) — Te(17)	94.74(4)	Cl(15) — Bi(4) — Cl(12)	97.58(18)
Au(6) — Te(12) — Te(20)	92.08(7)	Cl(13) — Bi(4) — Cl(12)	88.48(14)
Au(4) — Te(12) — Te(20)	91.30(6)	Cl(14) — Bi(4) — Cl(12)	86.66(14)
Te(17) — Te(12) — Te(20)	168.00(7)	Cl(12)^{iv} — Bi(4) — Cl(12)	83.53(13)
Au(4) — Te(13) — Au(6)^{ii}	90.06(4)	Bi(3) — Cl(12) — Bi(4)^{iv}	91.14(13)
Au(4) — Te(13) — Te(18)	94.42(5)	Bi(3) — Cl(12) — Bi(4)	89.87(12)
Au(6)^{ii} — Te(13) — Te(18)	92.53(5)	Bi(4)^{iv} — Cl(12) — Bi(4)	96.47(13)
Au(4) — Te(13) — Te(19)	93.75(4)	Bi(4) — Cl(13) — Bi(3)	96.62(13)
Au(6)^{ii} — Te(13) — Te(19)	93.14(5)	Bi(4) — Cl(14) — Bi(3)^{iv}	96.23(14)

A.1.12 $(Au_6Te_{18}Cl_2)[MCl_6]$

Table A.56: Unit cell parameters for $(Au_6Te_{18}Cl_2)[NbCl_6]_4$.

Empirical formula	$(Au_6Te_{18}Cl_2)[NbCl_6]_4$
Formula weight / $g \cdot mol^{-1}$	4771.995
Temperature / K	123(2)
Crystal system; space group	Triclinc; $P\overline{1}$
Lattice constants / $\AA$	$a = 14.4637(4)$; $\alpha = 86.643(2)^\circ$
	$b = 15.0536(4)$; $\beta = 88.142(2)^\circ$
	$c = 15.5090(4)$; $\gamma = 66.176(2)^\circ$
Volume / $\AA^3$	3083.6(3)

Table A.57: Unit cell parameters for $(Au_6Te_{18}Cl_2)[TaCl_6]_4$.

Empirical formula	$(Au_6Te_{18}Cl_2)[TaCl_6]_4$
Formula weight / $g \cdot mol^{-1}$	5124.161
Temperature / K	123(2)
Crystal system; space group	Triclinc; $P\overline{1}$
Lattice constants / $\AA$	$a = 14.7629(5)$; $\alpha = 86.345(2)^\circ$
	$b = 15.1084(6)$; $\beta = 88.197(3)^\circ$
	$c = 15.4564(6)$; $\gamma = 65.808(2)^\circ$
Volume / $\AA^3$	3138.2(3)

A.1.13 $AuCl_3$

Table A.58: Crystal data and structure refinement for $AuCl_3$.

Empirical formula	$Au_2\,Cl_6$
Formula weight / $g \cdot mol^{-1}$	606.63
Temperature / K	123(2)
Crystal system; space group	Monoclinic; $P2_1/c$
Lattice constants / $Å$	$a = 6.5316(5)$
	$b = 10.9011(7)$; $\beta = 113.477(4)^\circ$
	$c = 6.4072(5)$
Volume / $Å^3$	418.44(5)
Z; F(000); calc. density / $g \cdot cm^{-3}$	2; 520; 4.815
Wavelength	$Mo_{K\alpha}$ ($\lambda = 0.71073$ Å)
Crystal size / mm^3	0.067 × 0.04 × 0.024
Theta range for data collection / °	$3.401 \leq \theta \leq 27.467$
Limiting indices	$-8 \leq h \leq 8$; $-14 \leq k \leq 14$; $-8 \leq l \leq 8$
Reflections collected / unique	6653 / 958
Completeness to $\theta = 25.242^\circ$	99.9 %
R_{int}; R_σ	0.0680; 0.0305
Absorption coefficient / mm^{-1}	36.836; Semi-empirical from equivalents
Max. / min. transmission	0.087 / 0.024
Refinement method	Full-matrix least-squares on F^2
Data / restraints / parameters	958 / 0 / 37
R indices (all data) R_1; wR_2	0.0315; 0.0626
R indices $[I > 4\sigma(I)]$ R_1; wR_2	0.0256; 0.0602; n = 845 reflections
Goodness-of-fit for F^2	1.045
Largest diff. peak / $e^- \cdot Å^{-3}$	+2.382 0.96 Å from Au)
	-1.647 (0.74 Å from Au)
Avg. diff. density / $e^- \cdot Å^{-3}$	0.290

Table A.59: Fractional coordinates and equivalent isotropic displacement parameter U_{eq} for the independent atoms in the structure of $AuCl_3$.

Atom	Wyck.	Site	x / a	y / b	z / c	U_{eq} / $Å^2$
Au	4*e*	1	0.45901(4)	-0.08691(2)	0.76370(4)	0.02445(12)
Cl(1)	4*e*	1	0.2396(3)	-0.00530(15)	0.9415(3)	0.0297(4)
Cl(2)	4*e*	1	0.6847(3)	-0.16084(14)	0.6042(3)	0.0312(4)
Cl(3)	4*e*	1	0.1619(3)	-0.16994(15)	0.4829(3)	0.0328(4)

Table A.60: Anisotropic displacement parameters U_{ij} / $Å^2$ for the independent atoms in the structure of $AuCl_3$.

Atom	U_{11}	U_{22}	U_{33}	U_{23}	U_{13}	U_{12}
Au	0.02721(18)	0.02189(17)	0.02362(18)	-0.00040(9)	0.00947(13)	0.00100(9)
Cl(1)	0.0269(8)	0.0326(8)	0.0303(9)	-0.0056(7)	0.0119(7)	-0.0003(7)
Cl(2)	0.0371(9)	0.0288(8)	0.0322(10)	-0.0016(6)	0.0185(8)	0.0046(7)
Cl(3)	0.0334(8)	0.0335(9)	0.0271(10)	-0.0047(7)	0.0073(7)	-0.0024(7)

Table A.61: Selected bond lengths and angles for $AuCl_3$. Symmetry transformations used to generate equivalent atoms: (i) $-x+1$, $-y$, $-z+2$.

Atoms 1, 2	Distance / $Å$	Atoms 1, 2, 3	Angle / °
Au(1) — Cl(3)	2.2452(17)	Cl(3) — Au(1) — Cl(2)	90.31(7)
Au(1) — Cl(2)	2.2511(17)	Cl(3) — Au(1) — Cl(1)	92.40(6)
Au(1) — Cl(1)	2.3334(17)	Cl(2) — Au(1) — Cl(1)	177.27(6)
Au(1) — Cl(1)^{i}	2.3434(16)	Cl(3) — Au(1) — Cl(1)^{i}	177.88(6)
Cl(1) — Au(1)^{i}	2.3433(16)	Cl(2) — Au(1) — Cl(1)^{i}	91.58(6)
		Cl(1) — Au(1) — Cl(1)^{i}	85.71(6)
		Au(1) — Cl(1) — Au(1)^{i}	94.29(6)

A.1.14 $AuTe_2Br$

Table A.62: Crystal data and structure refinement for $AuTe_2Br$.

Empirical formula	Au Te_2 Br
Formula weight / $g \cdot mol^{-1}$	532.08
Temperature / K	123(2)
Crystal system; space group	Orthorhombic; $Cmcm$
Lattice constants / $Å$	$a = 4.0292(3)$
	$b = 12.3167(9)$
	$c = 8.9184(4)$
Volume / $Å^3$	442.59(5)
Z; F(000); calc. density / $g \cdot cm^{-3}$	4; 872; 7.985
Wavelength	$Mo_{K\alpha}$ ($\lambda = 0.71073$ Å)
Crystal size / mm^3	0.030 × 0.008 × 0.006
Theta range for data collection / °	$3.308 \leq \theta \leq 27.493$
Limiting indices	$-5 \leq h \leq 5$; $-16 \leq k \leq 16$; $-11 \leq l \leq 10$
Reflections collected / unique	3432 / 312
Completeness to $\theta = 25.242$ °	100.0%
R_{int}; R_σ	0.0509; 0.0253
Absorption coefficient / mm^{-1}	54.968; Analytical
Max. / min. transmission	0.730 / 0.287
Refinement method	Full-matrix least-squares on F^2
Data / restraints / parameters	312 / 0 / 16
R indices (all data) R_1; wR_2	0.0241; 0.0424
R indices $[I > 2\sigma(I)]$ R_1; wR_2	0.0198; 0.0401; n = 289 reflections
Goodness-of-fit for F^2	1.147
Largest diff. peak / $e^- \cdot Å^{-3}$	+1.737 (1.39 Å from Te)
	-1.862 (0.86 Å from Au)
Avg. diff. density / $e^- \cdot Å^{-3}$	0.413

Table A.63: Fractional coordinates and equivalent isotropic displacement parameter U_{eq} for the independent atoms in the structure of $AuTe_2Br$.

Atom	Wyck.	Site	x / a	y / b	z / c	U_{eq} / $Å^2$
Au	4*c*	4	0.0000	-0.08157(4)	0.2500	0.00847(19)
Te	8*f*	2	0.5000	-0.10615(5)	0.05438(6)	0.00835(19)
Br	4*c*	4	0.0000	0.16522(10)	0.2500	0.0117(3)

Table A.64: Anisotropic displacement parameters U_{ij} / $Å^2$ for the independent atoms in the structure of $AuTe_2Br$.

Atom	U_{11}	U_{22}	U_{33}	U_{23}	U_{13}	U_{12}
Au	0.0061(3)	0.0117(3)	0.0076(3)	0.000	0.000	0.000
Te	0.0062(3)	0.0115(3)	0.0074(3)	0.00000(19)	0.000	0.000
Br	0.0120(6)	0.0107(6)	0.0123(7)	0.000	0.000	0.000

Table A.65: Selected bond lengths and angles for $AuTe_2Br$. Symmetry transformations used to generate equivalent atoms: (i) $x-1$, y, z; (ii) x, y, $-z+\frac{1}{2}$; (iii) $x-1$, y, $-z+\frac{1}{2}$; (iv) $x+1$, y, z; (v) $-x+1$, $-y$, $-z$.

Atoms 1, 2	Distance / $Å$	Atoms 1, 2, 3	Angle / °
Au — Te	2.6822(4)	Te — Au — Te^{i}	97.373(18)
Au — Te^{i}	2.6822(4)	Te — Au — Te^{ii}	81.153(19)
Au — Te^{ii}	2.6822(4)	Te^{i} — Au — Te^{ii}	167.04(3)
Au — Te^{iii}	2.6822(4)	Te — Au — Te^{iii}	167.04(3)
Au — Br	3.0397(13)	Te^{i} — Au — Te^{iii}	81.153(19)
Te — Au^{iv}	2.6822(4)	Te^{ii} — Au — Te^{iii}	97.373(18)
Te — Te^{v}	2.7889(12)	Te — Au — Br	96.479(16)
		Te^{i} — Au — Br	96.480(16)
		Te^{ii} — Au — Br	96.480(16)
		Te^{iii} — Au — Br	96.480(16)
		Au^{iv} — Te — Au	97.374(18)
		Au^{iv} — Te — Te^{v}	96.92(2)
		Au — Te — Te^{v}	96.92(2)

A.1.15 $TeBr_4$

Table A.66: Crystal data and structure refinement for $TeBr_4$.

Empirical formula	$TeBr_4$
Formula weight / $g \cdot mol^{-1}$	447.24
Temperature / K	123(2)
Crystal system; space group	Tetragonal; $I4_1/amd$
Lattice constants / $Å$	a = 15.6369(4)
	b = 15.6369(4)
	c = 11.0114(5)
Volume / $Å^3$	2692.4(2)
Z; F(000); calc. density / $g \cdot cm^{-3}$	16; 3072; 4.413
Wavelength	$Mo_{K\alpha}$ (λ = 0.71073 Å)
Crystal size / mm^3	0.070 × 0.050 × 0.031
Theta range for data collection / °	$3.451 \leq \theta \leq 27.484$
Limiting indices	$-20 \leq h \leq 20$; $-20 \leq k \leq 20$; $-14 \leq l \leq 14$
Reflections collected / unique	21251 / 830
Completeness to θ = 25.242°	99.7 %
R_{int}; R_σ	0.0894; 0.0239
Absorption coefficient / mm^{-1}	28.025; Semi-empirical from equivalents
Max. / min. transmission	0.0632 / 0.0279
Refinement method	Full-matrix least-squares on F^2
Data / restraints / parameters	830 / 0 / 28
R indices (all data) R_1; wR_2	0.0465; 0.0530
R indices [$I > 4\sigma(I)$] R_1; wR_2	0.0274; 0.0496; n = 634 reflections
Goodness-of-fit for F^2	1.039
Largest diff. peak / $e^- \cdot Å^{-3}$	+0.845 (1.93 Å from Br3)
	-1.103 (0.27 Å from Br3)
Avg. diff. density / $e^- \cdot Å^{-3}$	0.235

Table A.67: Fractional coordinates and equivalent isotropic displacement parameter U_{eq} for the independent atoms in the structure of $TeBr_4$.

Atom	Wyck.	Site	x / a	y / b	z / c	U_{eq} / $Å^2$
Te	16h	.m.	0.14047(3)	0.2500	0.02174(4)	0.02382(15)
Br(1)	16h	.m.	0.12398(4)	0.2500	0.24767(6)	0.0287(2)
Br(2)	32i	1	0.24762(3)	0.36964(3)	0.01627(5)	0.03022(16)
Br(3)	16h	.m.	0.0000	0.11807(4)	0.00614(6)	0.02506(18)

Table A.68: Anisotropic displacement parameters U_{ij} / $Å^2$ for the independent atoms in the structure of $TeBr_4$.

Atom	U_{11}	U_{22}	U_{33}	U_{23}	U_{13}	U_{12}
Te	0.0242(3)	0.0243(3)	0.0230(3)	0.000	-0.0009(2)	0.000
Br(1)	0.0296(4)	0.0340(4)	0.0227(4)	0.000	-0.0010(3)	0.000
Br(2)	0.0273(3)	0.0291(3)	0.0342(3)	-0.0003(2)	-0.0006(2)	-0.0048(2)
Br(3)	0.0260(4)	0.0234(4)	0.0257(4)	0.0009(3)	0.000	0.000

Table A.69: Selected bond lengths and angles for $TeBr_4$. Symmetry transformations used to generate equivalent atoms: (i) x, $-y+\frac{1}{2}$, z.

Atoms 1, 2	Distance / $Å$	Atoms 1, 2, 3	Angle / °
Te — Br(1)	2.5011(8)	Br(1) — Te — Br(2)^{i}	95.31(2)
Te — Br(2)^{i}	2.5120(6)	Br(1) — Te — Br(2)	95.31(2)
Te — Br(2)	2.5121(6)	Br(2)^{i} — Te — Br(2)	96.27(3)

A.1.16 $Zn[AuCl_4]_2 \cdot (AuCl_3)_{1.114}$

Table A.70: Crystal data and structure refinement for $Zn[AuCl_4]_2 \cdot (AuCl_3)_{1.114}$.

Empirical formula	$Zn[AuCl_4]_2 \cdot (AuCl_3)_{1.114}$
Formula weight / $g \cdot mol^{-1}$	1081.1
Temperature / K	123(2)
Crystal system; space group	Monoclinic; $C2/c\,(\alpha 0 \gamma)\,0s$
Lattice constants / $Å$	$a = 9.248(3)$
	$b = 23.799(7)$; $\beta = 93.41(1)^\circ$
	$c = 7.593(2)$
	$q = (0.6600(4); 0; 0.1143(4))$
Volume / $Å^3$	1668.3(9)
Z; F(000); calc. density / $g \cdot cm^{-3}$	4; 1875; 4.3035
Wavelength	$Mo_{K\alpha}$ ($\lambda = 0.71073$ Å)
Crystal size / mm^3	0.086 × 0.070 × 0.046
Theta range for data collection / °	$0.92 \leq \theta \leq 47.43$
Limiting indices	$-17 \leq h \leq 17$; $-37 \leq k \leq 37$
	$-12 \leq l \leq 12$; $-4 \leq m \leq 4$
Reflections collected / unique / $I > 3\sigma(I)$	117367 / 29752 / 11923
Completeness to $\theta = 26.62^\circ$	98 %
R_{int}; R_σ	0.1341; 0.0894
Absorption coefficient / mm^{-1}	30.502; SADABS
Max. / min. transmission	0.4357 / 0.2649
Refinement method	Full-matrix least-squares on F
Data / restraints / parameters	29752 / 0 / 433
R indices (all data) R_1; wR	0.1721; 0.0631
R indices $[I > 3\sigma(I)]$ R_1; wR	0.0555; 0.0576
R_1 main / 1st / 2nd	3.46 % / 5.66 % / 7.98 %
R_1 3rd / 4th	14.09 % / 21.19 %
Goodness-of-fit for F	1.57
Largest diff. peak / $e^- \cdot Å^{-3}$	14.44 / -16.48

Table A.71: Composite crystal data of $Zn[AuCl_4]_2 \cdot (AuCl_3)_{1.114}$.

	Subsystem I	Subsystem II
Composite matrix	$W^1 = \begin{pmatrix} 1 & 0 & 0 & 0 \\ 0 & 1 & 0 & 0 \\ 0 & 0 & 1 & 0 \\ 0 & 0 & 0 & 1 \end{pmatrix}$	$W^2 = \begin{pmatrix} 1 & 0 & 0 & 0 \\ 0 & 1 & 0 & 0 \\ 0 & 0 & 1 & 1 \\ 0 & 0 & 1 & 0 \end{pmatrix}$
Space group	$C2/c(\alpha 0 \gamma)0s$	$C2/m(\alpha 0 \gamma)0s$
Lattice constants / $\AA$	$a = 9.2485$	$a = 10.5213$
	$b = 23.7995$	$b = 23.7995$
	$c = 7.5926$	$c = 6.8136$
	$\beta = 93.405°$	$\beta = 118.661°$
	$q = (0.6600; 0; 0.1143)$	$q = (-0.5923; 0; 0.8974)$
Volume / $\AA^3$	$V = 1668.3$	$V = 1497.1$
Contents	$Zn[AuCl_4]_2$; $Z = 4$	$\frac{1}{2}$ Au_2Cl_6; $Z = 4$

Table A.72: Fractional coordinates and equivalent isotropic displacement parameter U_{eq} for the independent atoms in the structure of $Zn[AuCl_4]_2 \cdot (AuCl_3)_{1.114}$.

Atom	Mult.	x / a	y / b	z / c	U_{eq} / $\AA^2$	Subsystem
Au1	2	0	0.977408(9)	0.25	0.01535(6)	1
Au2	2	0.25	0.75	0.5	0.01367(5)	1
Zn1	2	0	0.83346(3)	0.25	0.01739(19)	1
Cl1	1	0.15752(11)	1.04475(5)	0.17400(17)	0.0258(3)	1
Cl2	1	-0.16011(10)	0.90804(4)	0.32537(15)	0.0200(3)	1
Cl3	1	0.08850(11)	0.81889(4)	0.55794(13)	0.0196(3)	1
Cl4	1	0.19171(11)	0.76095(4)	0.20611(13)	0.0202(3)	1
Au3	2	0	0.429166(10)	0	0.03348(12)	2
Cl5	2	-0.00495(18)	0.5	0.2270(4)	0.0389(9)	2
Cl6	1	-0.00625(13)	0.36390(5)	0.2257(3)	0.0457(8)	2

Table A.73: Anisotropic displacement parameters U_{ij} / $\AA^2$ for the independent atoms in the structure of $Zn[AuCl_4]_2 \cdot (AuCl_3)_{1.114}$.

Atom	U_{11}	U_{22}	U_{33}	U_{23}	U_{13}	U_{12}
Au1	0.01598(9)	0.01256(10)	0.01735(10)	0	-0.00027(7)	0
Au2	0.01852(10)	0.01107(10)	0.01168(9)	0.00036(8)	0.00314(7)	-0.00079(8)

continued on next page

Atom	U_{11}	U_{22}	U_{33}	U_{23}	U_{13}	U_{12}
Zn1	0.0201(3)	0.0144(3)	0.0178(3)	0	0.0020(3)	0
Cl1	0.0247(5)	0.0183(5)	0.0341(7)	-0.0038(4)	0.0003(5)	0.0054(5)
Cl2	0.0167(4)	0.0159(5)	0.0279(5)	-0.0004(3)	0.0060(4)	-0.0004(4)
Cl3	0.0251(5)	0.0192(5)	0.0148(5)	0.0064(4)	0.0030(4)	-0.0025(4)
Cl4	0.0285(5)	0.0201(5)	0.0123(4)	0.0045(4)	0.0029(4)	-0.0016(4)
Au3	0.01504(10)	0.01574(11)	0.0577(2)	0	0.00787(11)	0
Cl5	0.0296(9)	0.0233(9)	0.0547(16)	0	0.0130(9)	0
Cl6	0.0335(7)	0.0227(7)	0.0722(14)	0.0004(5)	0.0183(7)	0.0071(8)

Table A.74: Coefficients of the i^{th} harmonic positional modulation wave for the independant atoms in the structure of $Zn[AuCl_4]_2 \cdot (AuCl_3)_{1.114}$.

Atom	i	$x$sin	$y$sin	$z$sin	$x$cos	$y$cos	$z$cos
Au1	1	0	-0.007008(12)	0	0.02119(3)	0	-0.00010(4)
	2	-0.00568(4)	0	-0.00569(6)	0	0.000126(16)	0
	3	0	-0.002051(17)	0	-0.00019(5)	0	0.00089(7)
	4	-0.00134(6)	0	0.00053(8)	0	0.00005(2)	0
Au2	1	0.03909(3)	-0.001871(12)	0.01561(4)	0	0	0
	2	0.00395(4)	0.000732(16)	0.00022(6)	0	0	0
	3	0.00040(5)	0.002056(17)	-0.00082(6)	0	0	0
	4	0.00009(6)	-0.00011(2)	-0.00023(8)	0	0	0
Zn1	1	0	-0.00778(4)	0	0.03993(11)	0	0.01558(14)
	2	-0.00389(13)	0	-0.00004(19)	0	-0.00002(5)	0
	3	0	-0.00180(5)	0	-0.00014(16)	0	0.0016(2)
	4	-0.00075(19)	0	0.0006(2)	0	0.00002(7)	0
Cl1	1	0.00564(15)	-0.00460(6)	-0.0088(2)	0.01135(16)	0.00503(6)	-0.0071(2)
	2	-0.00095(18)	0.00004(8)	0.0015(3)	0.00660(18)	0.00004(8)	0.0085(3)
	3	-0.0013(2)	0.00065(9)	-0.0012(3)	0.0006(2)	0.00188(9)	0.0012(3)
	4	0.0012(3)	0.00007(12)	-0.0006(4)	0.0004(3)	-0.00007(12)	-0.0013(4)
Cl2	1	-0.01749(15)	-0.00450(6)	-0.0067(2)	0.02610(15)	-0.00598(6)	0.0115(2)
	2	-0.00097(18)	-0.00006(7)	0.0022(3)	0.00457(18)	0.00021(7)	-0.0039(3)
	3	-0.0005(2)	0.00040(8)	-0.0029(3)	0.0003(2)	-0.00190(8)	-0.0010(3)
	4	0.0010(3)	-0.00001(11)	0.0007(4)	0.0011(3)	-0.00024(11)	0.0007(4)
Cl3	1	0.02017(17)	-0.00526(6)	0.0100(2)	0.03509(17)	0.00323(6)	0.0119(2)

continued on next page

Atom	i	$x$sin	$y$sin	$z$sin	$x$cos	$y$cos	$z$cos
	2	-0.00030(20)	0.00006(7)	-0.0001(3)	0.00235(20)	0.00013(8)	0.0012(3)
	3	0.0001(2)	-0.00080(8)	0.0018(3)	-0.0001(2)	0.00185(8)	-0.0003(3)
	4	0.0005(3)	0.00037(11)	-0.0003(3)	0.0000(3)	-0.00001(11)	-0.0003(4)
Cl4	1	0.02922(17)	-0.00479(6)	0.0136(2)	0.03181(17)	0.00630(6)	0.0066(2)
	2	-0.0003(2)	0.00007(8)	-0.0006(3)	0.00713(19)	0.00133(7)	-0.0003(3)
	3	-0.0021(2)	0.00047(9)	-0.0006(3)	0.0007(2)	0.00166(8)	-0.0007(3)
	4	-0.0002(3)	0.00010(11)	-0.0009(3)	0.0002(3)	0.00010(11)	0.0002(3)
Au3	1	0	-0.006489(14)	0	0.00746(4)	0	-0.07203(9)
	2	-0.00238(4)	0	0.04989(9)	0	0.001249(16)	0
	3	0	0.000939(19)	0	0.00140(5)	0	-0.00222(9)
	4	-0.00299(6)	0	-0.00745(11)	0	0.00036(2)	0
Cl5	1	0	-0.01812(10)	0	0	0.00154(10)	0
	2	0.0135(3)	0	-0.0375(6)	0.0051(3)	0	-0.0203(5)
	3	0	-0.00067(14)	0	0	0.00074(12)	0
	4	-0.0046(4)	0	-0.0059(7)	0.0029(4)	0	-0.0056(6)
Cl6	1	-0.0149(2)	-0.01879(8)	-0.1338(5)	0.0031(2)	0.00194(8)	-0.0337(4)
	2	-0.0071(2)	0.00217(8)	-0.0497(5)	0.0082(2)	-0.00186(8)	-0.0283(5)
	3	-0.0022(3)	-0.00078(10)	0.0006(5)	-0.0021(3)	0.00038(9)	-0.0005(5)
	4	-0.0025(3)	-0.00015(11)	-0.0046(5)	0.0011(3)	-0.00057(11)	-0.0096(6)

Table A.75: Tensor coefficients of the i^{th} harmonic ADP modulation wave for the independant atoms of structure of $Zn[AuCl_4]_2 \cdot (AuCl_3)_{1.114}$.

Atom	i	U_{11}sin U_{11}cos	U_{22}sin U_{22}cos	U_{33}sin U_{33}cos	U_{12}sin U_{12}cos	U_{13}sin U_{13}cos	U_{23}sin U_{23}cos
Au1	1	-0.00203(13)	0.00064(14)	0.00051(17)	0	-0.00172(12)	0
		0	0	0	0.00178(11)	0	-0.00144(13)
	2	0	0	0	-0.00053(12)	0	0.00032(15)
		-0.00009(16)	0.00154(18)	-0.0027(2)	0	0.00037(15)	0
Au2	1	0	0	0	0	0	0
		0.00075(14)	0.00006(13)	-0.00016(14)	0.00051(12)	0.00123(11)	0.00003(12)
	2	0	0	0	0	0	0
		0.00005(18)	-0.00114(17)	-0.0003(2)	0.00071(13)	0.00018(15)	0.00044(16)
Zn1	1	-0.0003(5)	-0.0009(4)	0.0011(5)	0	-0.0019(4)	0

continued on next page

Atom	i	U_{11}sin U_{11}cos	U_{22}sin U_{22}cos	U_{33}sin U_{33}cos	U_{12}sin U_{12}cos	U_{13}sin U_{13}cos	U_{23}sin U_{23}cos
		0	0	0	0.0003(4)	0	-0.0018(4)
	2	0	0	0	-0.0014(4)	0	0.0001(5)
		-0.0002(6)	0.0031(6)	0.0002(8)	0	0.0007(5)	0
Cl1	1	0.0012(7)	-0.0014(7)	-0.0003(9)	0.0000(5)	-0.0004(6)	-0.0006(6)
		0.0038(7)	0.0007(8)	-0.0016(9)	0.0033(6)	0.0057(6)	-0.0012(7)
	2	0.0001(8)	0.0015(9)	-0.0061(14)	-0.0003(7)	0.0024(8)	0.0005(9)
		0.0029(8)	0.0024(8)	-0.0009(13)	-0.0011(6)	0.0003(8)	-0.0005(8)
Cl2	1	0.0005(6)	-0.0001(7)	0.0008(9)	-0.0022(5)	-0.0002(6)	-0.0002(6)
		-0.0010(7)	0.0017(7)	-0.0028(9)	0.0000(5)	-0.0019(6)	0.0001(6)
	2	0.0002(8)	-0.0004(8)	-0.0009(12)	-0.0001(6)	0.0011(7)	0.0001(8)
		-0.0007(8)	0.0018(8)	0.0015(12)	-0.0029(6)	0.0013(7)	0.0014(8)
Cl3	1	-0.0012(8)	0.0013(7)	0.0007(8)	0.0014(6)	-0.0011(6)	-0.0012(6)
		0.0012(7)	-0.0024(7)	0.0004(8)	0.0024(6)	-0.0010(6)	0.0008(6)
	2	-0.0008(9)	0.0033(8)	-0.0006(11)	0.0005(7)	0.0010(8)	0.0010(8)
		-0.0020(9)	0.0015(9)	0.0012(11)	0.0010(7)	0.0008(8)	0.0008(7)
Cl4	1	-0.0012(8)	0.0014(7)	-0.0002(7)	0.0010(6)	-0.0014(6)	-0.0013(6)
		0.0021(8)	0.0029(8)	-0.0014(7)	0.0051(6)	0.0015(6)	0.0004(6)
	2	0.0002(10)	0.0061(9)	-0.0029(10)	0.0015(7)	-0.0001(8)	-0.0010(8)
		0.0009(9)	0.0023(8)	0.0007(9)	0.0020(7)	-0.0014(7)	0.0015(7)
Au3	1	-0.00047(14)	0.00100(16)	0.0055(3)	0	-0.00213(16)	0
		0	0	0	0.00009(12)	0	-0.0069(2)
	2	0	0	0	-0.00047(13)	0	-0.0005(2)
		-0.00106(15)	-0.00399(17)	0.0303(3)	0	-0.00312(18)	0
Cl5	1	0	0	0	-0.0012(9)	0	-0.0048(14)
		0	0	0	-0.0012(10)	0	-0.0052(12)
	2	0.0016(13)	-0.0001(13)	0.009(3)	0	-0.0030(15)	0
		0.0037(13)	0.0092(15)	-0.024(2)	0	0.0085(14)	0
Cl6	1	-0.0048(10)	-0.0002(9)	0.008(2)	-0.0006(7)	-0.0027(12)	-0.0051(11)
		-0.0012(10)	-0.0046(10)	-0.0117(18)	0.0039(8)	0.0101(11)	-0.0115(11)
	2	-0.0012(11)	-0.0016(10)	0.007(2)	-0.0014(8)	0.0027(13)	-0.0037(12)
		0.0023(10)	0.0063(11)	-0.016(2)	-0.0025(8)	-0.0002(12)	0.0073(12)

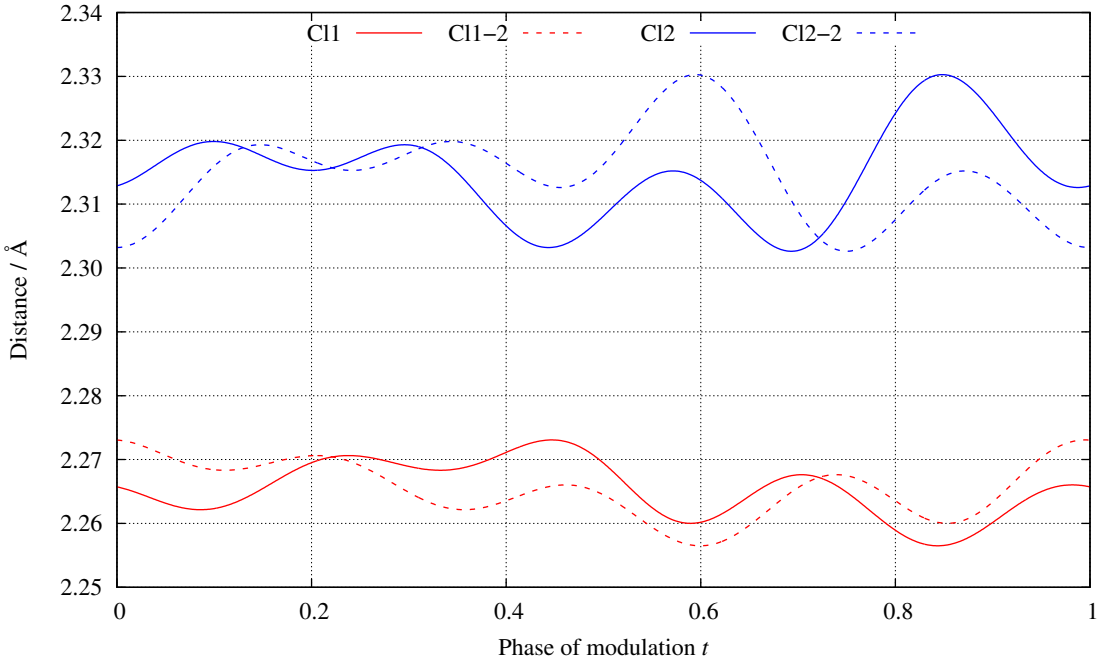

Figure A.1: *t*-Plot of the Au(1)–Cl(1/2) distances in the modulated crystal structure of $Zn[AuCl_4]_2 \cdot (AuCl_3)_{1.114}$

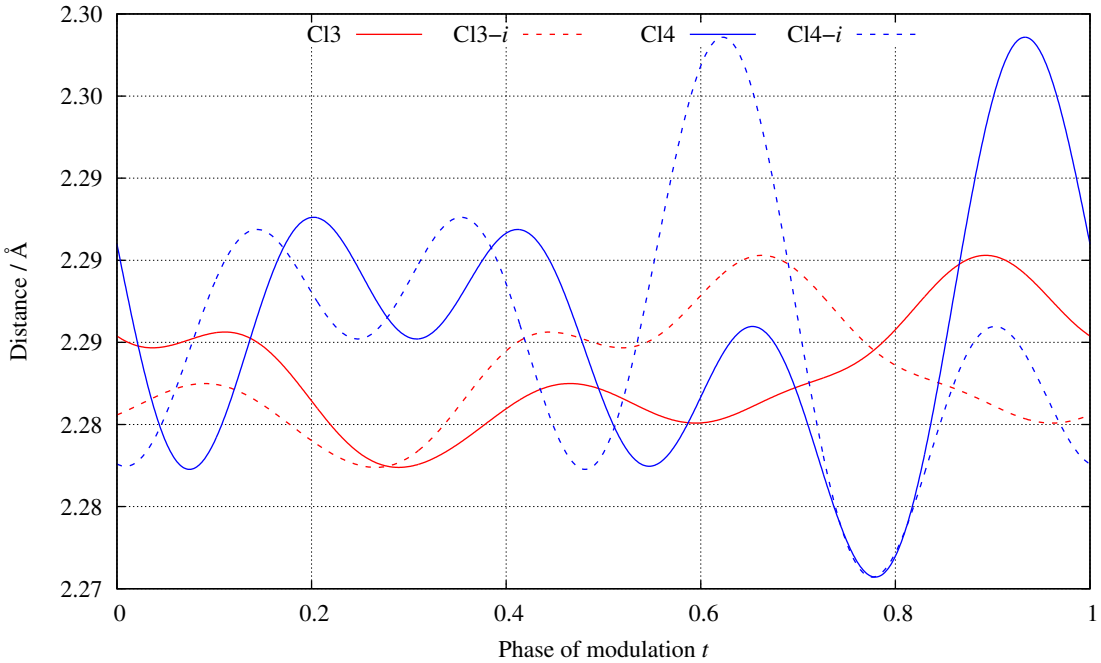

Figure A.2: *t*-Plot of the Au(2)–Cl(3/4) distances in the modulated crystal structure of $Zn[AuCl_4]_2 \cdot (AuCl_3)_{1.114}$

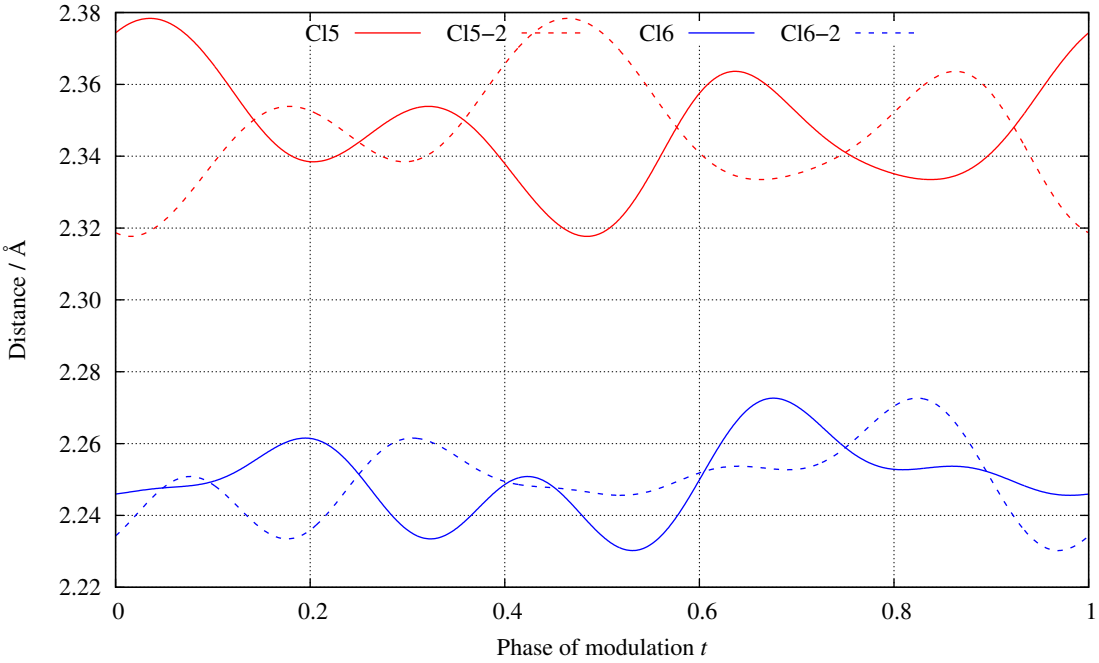

Figure A.3: *t*-Plot of the Au(3)–Cl(5/6) distances in the modulated crystal structure of $Zn[AuCl_4]_2 \cdot (AuCl_3)_{1.114}$

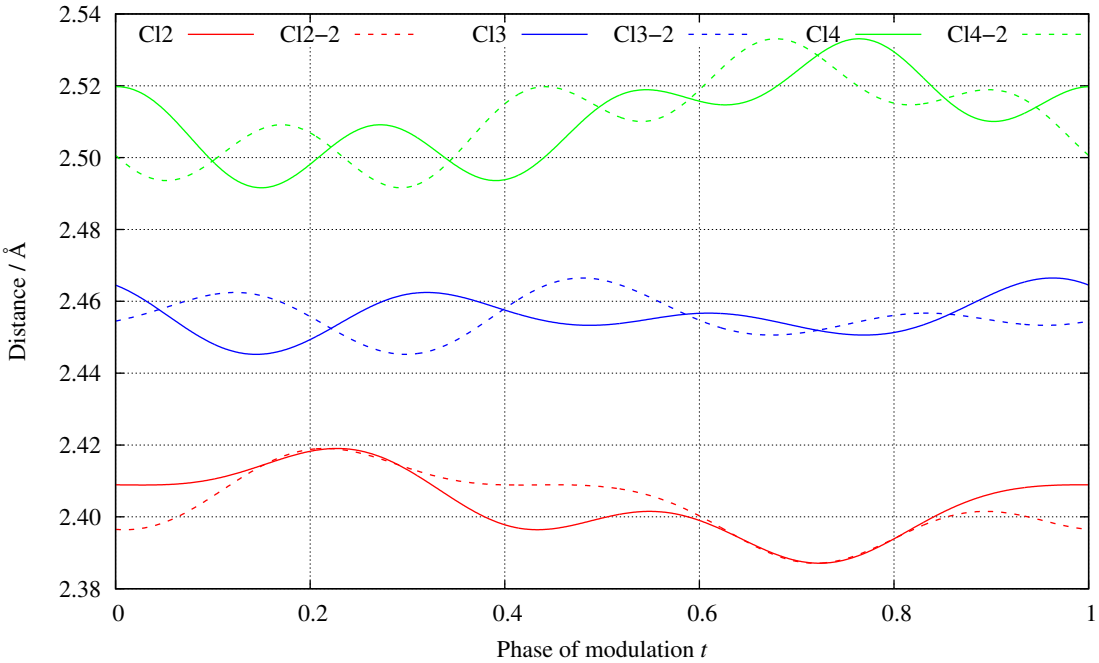

Figure A.4: *t*-Plot of the Zn(1)–Cl(2/3/4) distances in the modulated crystal structure of $Zn[AuCl_4]_2 \cdot (AuCl_3)_{1.114}$

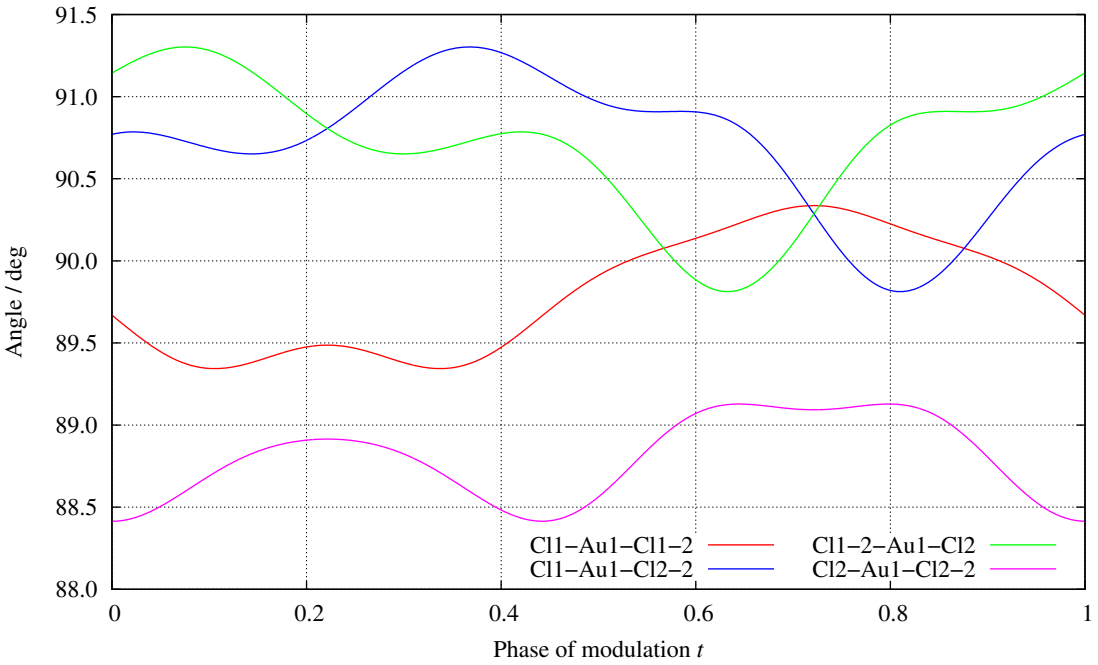

Figure A.5: *t*-Plot of the Cl–Au(1)–Cl bond angles in the modulated crystal structure of $Zn[AuCl_4]_2 \cdot (AuCl_3)_{1.114}$

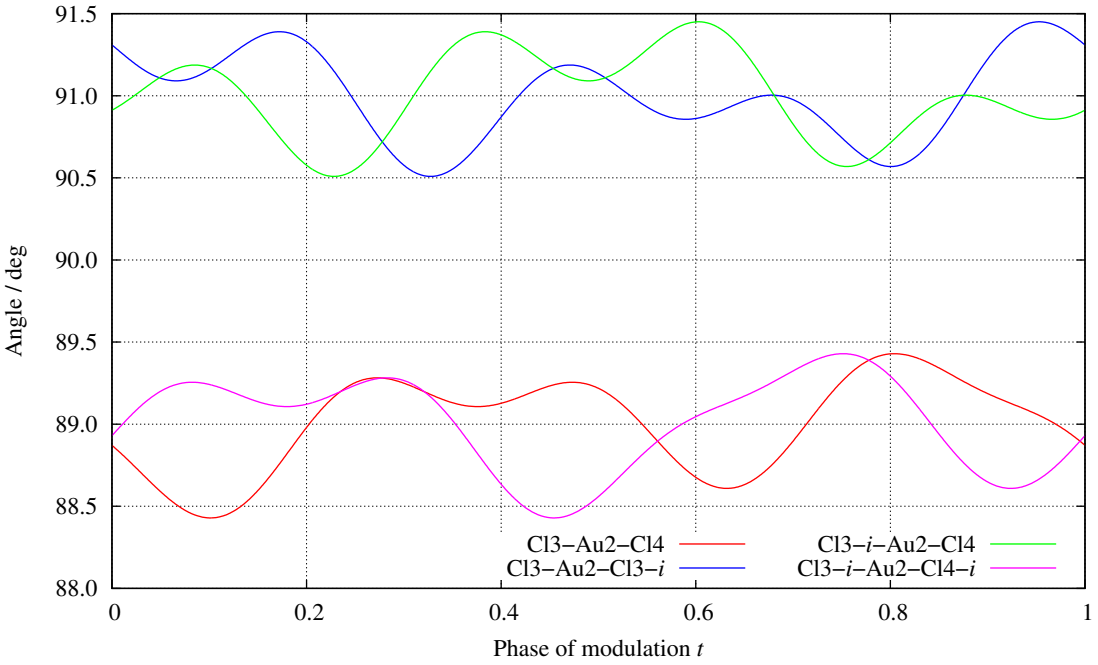

Figure A.6: *t*-Plot of the Cl–Au(2)–Cl bond angles in the modulated crystal structure of $Zn[AuCl_4]_2 \cdot (AuCl_3)_{1.114}$

A.1.17 $Cd[AuCl_4]_2$

Table A.76: Crystal data and structure refinement for $Cd[AuCl_4]_2$.

Empirical formula	$Au_2\,Cd\,Cl_8$
Formula weight / $g \cdot mol^{-1}$	789.93
Temperature / K	123(2)
Crystal system; space group	Monoclinic; $I2/a$
Lattice constants / $Å$	a = 12.2612(7)
	b = 7.3511(4); β = 95.403(5)°
	c = 12.8244(8)
Volume / $Å^3$	1150.77(12)
Z; F(000); calc. density / $g \cdot cm^{-3}$	4; 1368; 4.559
Wavelength	$Mo_{K\alpha}$ (λ = 0.71073 Å)
Crystal size / mm^3	0.088 × 0.058 × 0.002
Theta range for data collection / °	$3.191 \leq \theta \leq 27.547$
Limiting indices	$-21 \leq h \leq 21$; $-9 \leq k \leq 9$; $-15 \leq l \leq 15$
Reflections collected / unique	9785 / 1319
Completeness to θ = 25.242°	100.0 %
R_{int}; R_σ	0.1028; 0.0475
Absorption coefficient / mm^{-1}	29.060; Semi-empirical from equivalents
Max. / min. transmission	0.1822 / 0.0802
Refinement method	Full-matrix least-squares on F^2
Data / restraints / parameters	1319 / 0 / 51
R indices (all data) R_1; wR_2	0.0375; 0.0569
R indices [$I > 4\sigma(I)$] R_1; wR_2	0.0270; 0.0545; n = 1112 reflections
Goodness-of-fit for F^2	1.092
Largest diff. peak / $e^- \cdot Å^{-3}$	+1.329 (1.00 Å from Au)
	-1.731 (0.83 Å from Au)
Avg. diff. density / $e^- \cdot Å^{-3}$	0.282

Table A.77: Fractional coordinates and equivalent isotropic displacement parameter U_{eq} for the independent atoms in the structure of $Cd[AuCl_4]_2$.

Atom	Wyck.	Site	x / a	y / b	z / c	U_{eq} / $Å^2$
Au	$8f$	1	0.11606(2)	0.09115(4)	0.25426(2)	0.01899(11)
Cd	$4e$	2	0.2500	0.26178(10)	0.0000	0.02226(19)
Cl1	$8f$	1	-0.03920(17)	0.1859(3)	0.16083(13)	0.0261(4)
Cl2	$8f$	1	0.18154(17)	-0.0162(2)	0.10424(13)	0.0238(4)
Cl3	$8f$	1	0.27834(17)	0.0073(3)	0.34913(13)	0.0241(4)
Cl4	$8f$	1	0.05204(16)	0.1965(3)	0.40477(13)	0.0234(4)

Table A.78: Anisotropic displacement parameters U_{ij} / $Å^2$ for the independent atoms in the structure of $Cd[AuCl_4]_2$.

Atom	U_{11}	U_{22}	U_{33}	U_{23}	U_{13}	U_{12}
Au	0.01938(18)	0.01935(17)	0.01820(15)	-0.00006(10)	0.00144(11)	-0.00014(12)
Cd	0.0238(5)	0.0243(4)	0.0184(3)	0.000	0.0007(3)	0.000
Cl1	0.0244(11)	0.0285(10)	0.0243(9)	0.0002(7)	-0.0038(8)	0.0034(8)
Cl2	0.0287(12)	0.0235(10)	0.0198(8)	-0.0016(7)	0.0047(7)	-0.0010(8)
Cl3	0.0224(11)	0.0250(10)	0.0244(8)	-0.0021(7)	-0.0005(8)	0.0024(8)
Cl4	0.0206(10)	0.0282(10)	0.0215(8)	-0.0038(7)	0.0020(7)	0.0015(8)

Table A.79: Selected bond lengths for $Cd[AuCl_4]_2$. Symmetry transformations used to generate equivalent atoms: (i) $-x+\frac{1}{2}$, $-y+\frac{1}{2}$, $-z+\frac{1}{2}$; (ii) x, $-y+\frac{1}{2}$, $z-\frac{1}{2}$; (iii) $-x+\frac{1}{2}$, y, $-z$.

Atoms 1, 2	Distance / $Å$	Atoms 1, 2	Distance / $Å$
Au — Cl(1)	2.2616(19)	Cd — Cl(2)	2.6227(19)
Au — Cl(4)	2.2863(18)	Cd — $Cl(2)^{iii}$	2.6227(19)
Au — Cl(2)	2.2934(18)	Cd — $Cl(4)^{ii}$	2.6303(19)
Au — Cl(3)	2.3159(19)	Cd — $Cl(4)^{i}$	2.6303(19)
Cd — $Cl(3)^{i}$	2.6215(19)	Cl(3) — Cd^{i}	2.6215(19)
Cd — $Cl(3)^{ii}$	2.6215(19)	Cl(4) — Cd^{i}	2.6303(19)

Table A.80: Selected bond angles for $Cd[AuCl_4]_2$. Symmetry transformations used to generate equivalent atoms: (i) $-x+\frac{1}{2}$, $-y+\frac{1}{2}$, $-z+\frac{1}{2}$; (ii) x, $-y+\frac{1}{2}$, $z-\frac{1}{2}$; (iii) $-x+\frac{1}{2}$, y, $-z$.

Atoms 1, 2, 3	Angle / °	Atoms 1, 2, 3	Angle / °
Cl(1) — Au — Cl(4)	90.24(7)	$Cl(3)^{i}$ — Cd — $Cl(4)^{ii}$	94.97(6)
Cl(1) — Au — Cl(2)	90.30(7)	$Cl(3)^{ii}$ — Cd — $Cl(4)^{ii}$	76.26(6)
Cl(4) — Au — Cl(2)	179.44(7)	Cl(2) — Cd — $Cl(4)^{ii}$	90.11(6)
Cl(1) — Au — Cl(3)	177.38(7)	$Cl(2)^{iii}$ — Cd — $Cl(4)^{ii}$	100.36(6)
Cl(4) — Au — Cl(3)	89.60(7)	$Cl(3)^{i}$ — Cd — $Cl(4)^{i}$	76.26(6)
Cl(2) — Au — Cl(3)	89.87(7)	$Cl(3)^{ii}$ — Cd — $Cl(4)^{i}$	94.97(6)
$Cl(3)^{i}$ — Cd — $Cl(3)^{ii}$	99.29(9)	Cl(2) — Cd — $Cl(4)^{i}$	100.36(6)
$Cl(3)^{i}$ — Cd — Cl(2)	93.28(6)	$Cl(2)^{iii}$ — Cd — $Cl(4)^{i}$	90.11(6)
$Cl(3)^{ii}$ — Cd — Cl(2)	162.12(6)	$Cl(4)^{ii}$ — Cd — $Cl(4)^{i}$	166.61(9)
$Cl(3)^{i}$ — Cd — $Cl(2)^{iii}$	162.13(6)	Au — Cl(2) — Cd	108.28(7)
$Cl(3)^{ii}$ — Cd — $Cl(2)^{iii}$	93.28(6)	Au — Cl(3) — Cd^{i}	92.77(7)
Cl(2) — Cd — $Cl(2)^{iii}$	77.64(8)	Au — Cl(4) — Cd^{i}	93.23(7)

A.2 Atomic Distances and Angles

Table A.81: Summary of Au ·· Au distances for the cation of all discussed compounds.

Compound	Count	d(min) / Å	d(max) / Å	d(avg) / Å
$(Au_6Te_{18})[ZrCl_6]_3$	12	3.6710	3.8969	3.7946
$(Au_6Te_{18})[AlCl_4]_6$	6	3.7060	3.8457	3.7882
$(Au_6Te_{18})[AlBr_4]_6$	6	3.6770	3.8803	3.8040
$(Au_6Te_{18}Cl)[AlCl_4]_5$	12	3.7133	3.8676	3.7947
$(Au_6Te_{18}Cl)[GaCl_4]_5$	12	3.7123	3.8706	3.7956
$(Au_6Te_{18}Br)[AlCl_4]_5$	12	3.7252	3.8689	3.8034
$(Au_6Te_{18}Br)[AlBr_4]_5$	6	3.7211	3.8412	3.7705
$(Au_6Te_{18}Cl)[MoOCl_4]_5$	12	3.6677	3.9677	3.8208
$(Au_6Te_{18}Cl_2)[Mo_2O_2Cl_8]_2$	6	3.7757	3.8278	3.8102
$(Au_6Te_{18}Cl_2)[Bi_4Cl_{16}]$	12	3.7931	3.8441	3.8167
all		3.6677	3.9677	3.7998

Table A.82: Summary of Au – Te distances for the cation of all discussed compounds.

Compound	Count	d(min) / Å	d(max) / Å	d(avg) / Å
$(Au_6Te_{18})[ZrCl_6]_3$	24	2.6743	2.6990	2.6834
$(Au_6Te_{18})[AlCl_4]_6$	12	2.6705	2.6879	2.6789
$(Au_6Te_{18})[AlBr_4]_6$	12	2.6645	2.6893	2.6771
$(Au_6Te_{18}Cl)[AlCl_4]_5$	24	2.6692	2.6990	2.6843
$(Au_6Te_{18}Cl)[GaCl_4]_5$	24	2.6710	2.6992	2.6838
$(Au_6Te_{18}Br)[AlCl_4]_5$	24	2.6742	2.7064	2.6886
$(Au_6Te_{18}Br)[AlBr_4]_5$	8	2.6830	2.6947	2.6871
$(Au_6Te_{18}Cl)[MoOCl_4]_5$	24	2.6707	2.7062	2.6903
$(Au_6Te_{18}Cl_2)[Mo_2O_2Cl_8]_2$	12	2.6775	2.7039	2.6905
$(Au_6Te_{18}Cl_2)[Bi_4Cl_{16}]$	24	2.6764	2.7052	2.6902
all		2.6645	2.7064	2.6860

Table A.83: Summary of Te – Te distances for the cation of all discussed compounds.

Compound	Count	d(min) / *Å*	d(max) / *Å*	d(avg) / *Å*
$(Au_6Te_{18})[ZrCl_6]_3$	18	2.7140	3.1350	2.8862
$(Au_6Te_{18})[AlCl_4]_6$	9	2.7183	3.0948	2.8994
$(Au_6Te_{18})[AlBr_4]_6$	9	2.7236	3.1654	2.9153
$(Au_6Te_{18}Cl)[AlCl_4]_5$	12	2.7689	2.9958	2.8725
$(Au_6Te_{18}Cl)[GaCl_4]_5$	12	2.7693	2.9999	2.8718
$(Au_6Te_{18}Br)[AlCl_4]_5$	12	2.7746	2.9839	2.8766
$(Au_6Te_{18}Br)[AlBr_4]_5$	2	2.8530	2.8700	2.8615
$(Au_6Te_{18}Cl)[MoOCl_4]_5$	18	2.7363	3.0888	2.8848
$(Au_6Te_{18}Cl_2)[Mo_2O_2Cl_8]_2$	9	2.7632	3.0418	2.8930
$(Au_6Te_{18}Cl_2)[Bi_4Cl_{16}]$	6	2.8030	3.0282	2.8901
all		2.7140	3.1654	2.8852

A.3 Halide Tellurium Distance Histograms

A.3.1 $(Au_6Te_{18})[AlCl_4]_6$

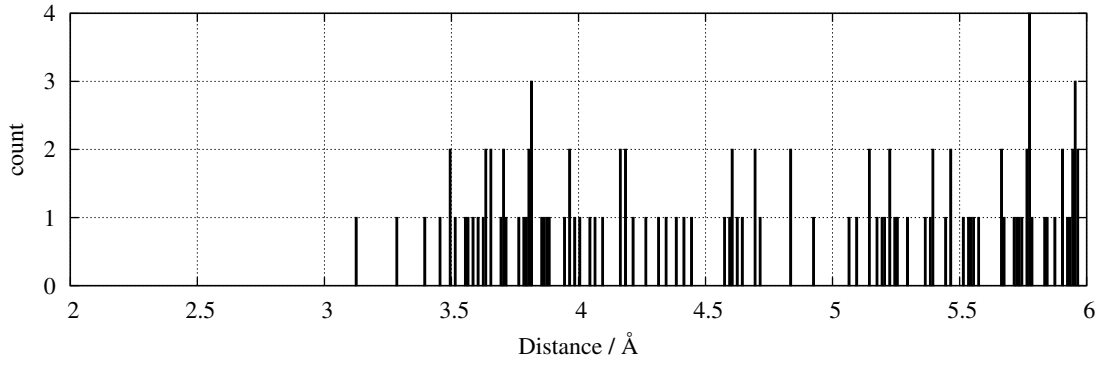

Figure A.7: Chlorine tellurium distance histogram for $(Au_6Te_{18})[AlCl_4]_6$.

A.3.2 $(Au_6Te_{18})[AlBr_4]_6$

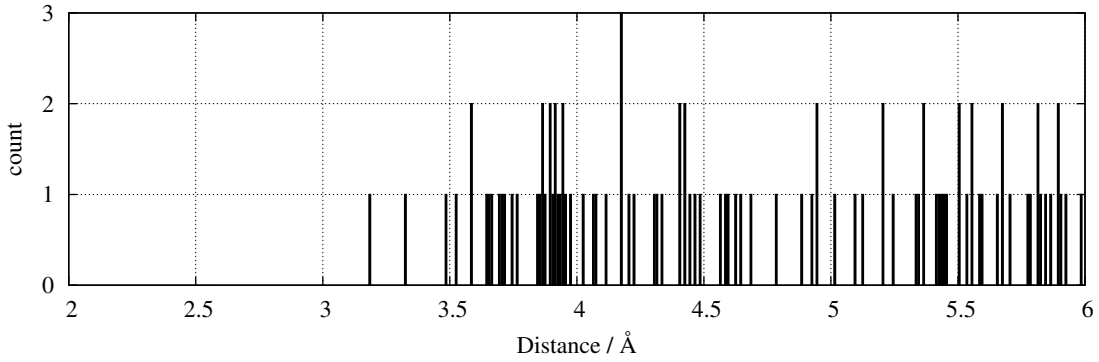

Figure A.8: Bromine tellurium distance histogram for $(Au_6Te_{18})[AlBr_4]_6$.

A.3.3 $(Au_6Te_{18})[ZrCl_6]_3$

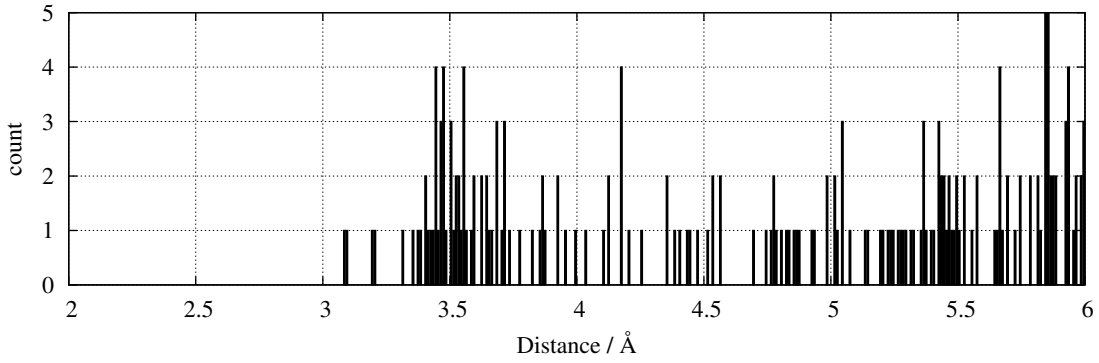

Figure A.9: Chlorine tellurium distance histogram for $(Au_6Te_{18})[ZrCl_6]_3$.

A.3.4 $(Au_6Te_{18}Cl)[AlCl_4]_5$

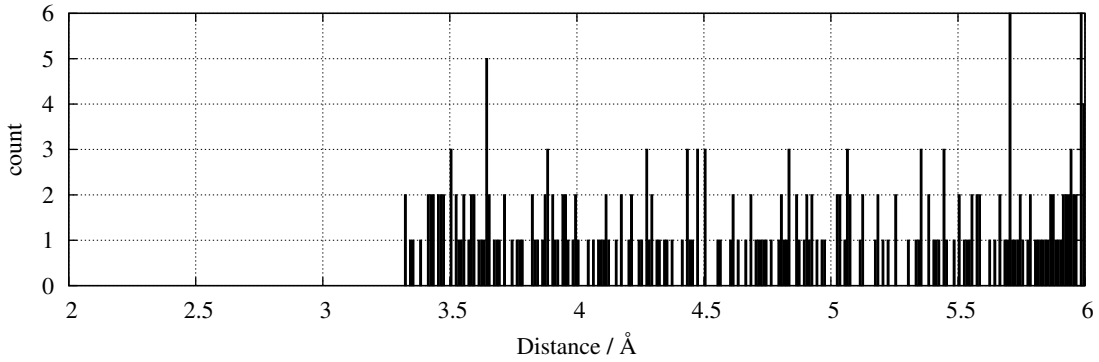

Figure A.10: Chlorine tellurium distance histogram for $(Au_6Te_{18}Cl)[AlCl_4]_5$.

A.3.5 $(Au_6Te_{18}Cl)[GaCl_4]_5$

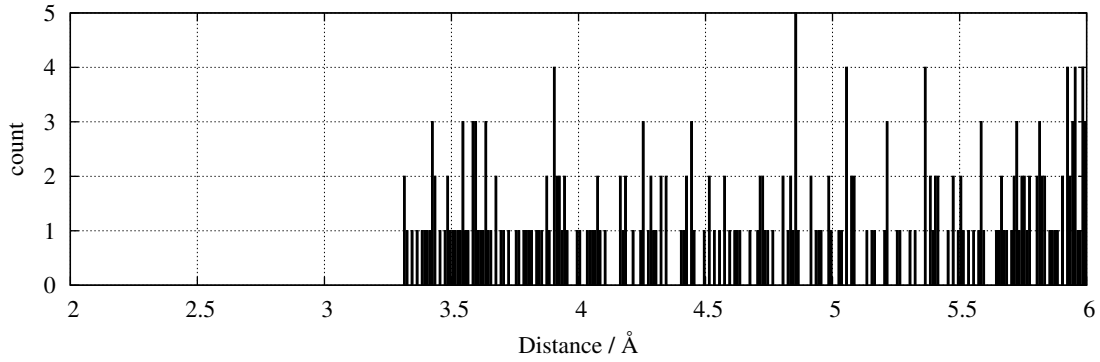

Figure A.11: Chlorine tellurium distance histogram for $(Au_6Te_{18}Cl)[GaCl_4]_5$.

A.3.6 $(Au_6Te_{18}Br)[AlCl_4]_5$

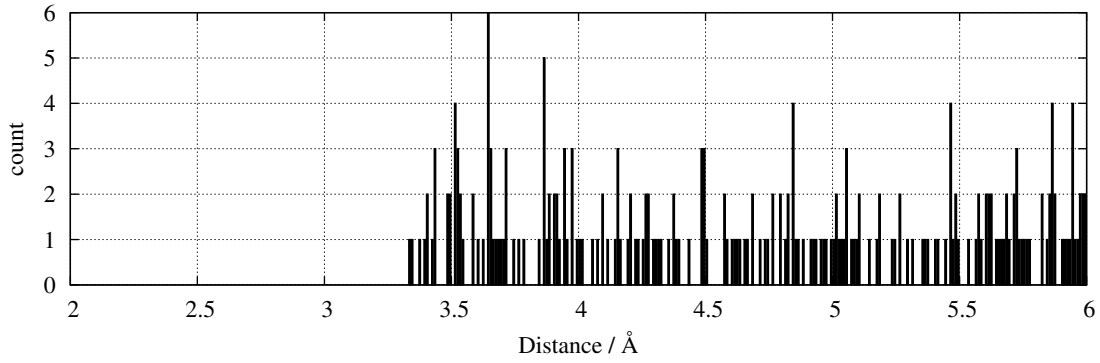

Figure A.12: Chlorine tellurium distance histogram for $(Au_6Te_{18}Br)[AlCl_4]_5$.

A.3.7 $(Au_6Te_{18}Br)[AlBr_4]_5$

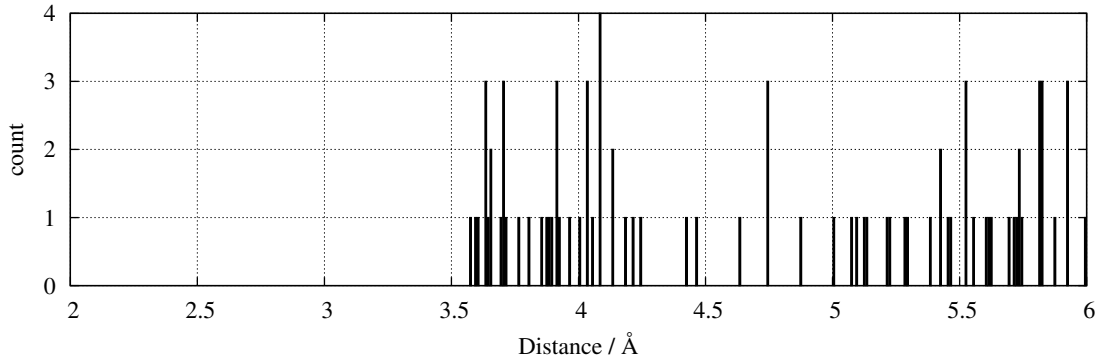

Figure A.13: Chlorine tellurium distance histogram for $(Au_6Te_{18}Br)[AlBr_4]_5$.

A.3.8 $(Au_6Te_{18}Cl)[MoOCl_4]_5$

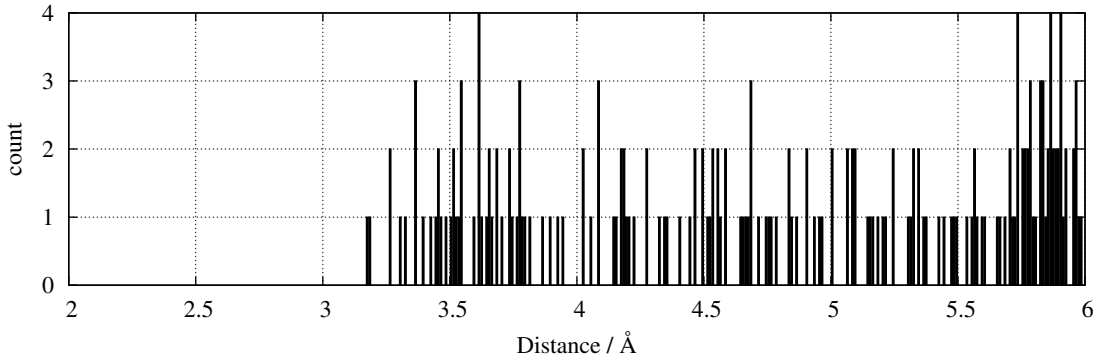

Figure A.14: Chlorine tellurium distance histogram for $(Au_6Te_{18}Cl)[MoOCl_4]_5$.

A.3.9 $(Au_6Te_{18}Cl_2)[Mo_2O_2Cl_8]_2$

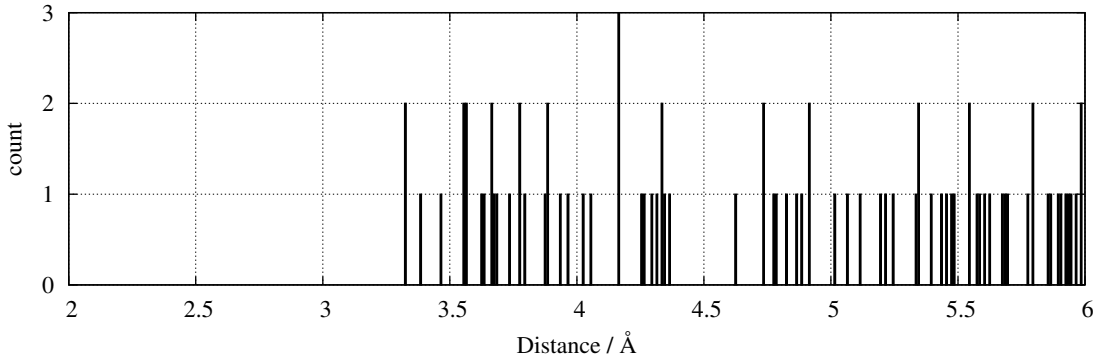

Figure A.15: Chlorine tellurium distance histogram for $(Au_6Te_{18}Cl_2)[Mo_2O_2Cl_8]_2$.

A.3.10 $(Au_6Te_{18}Cl_2)[Bi_4Cl_{16}]$

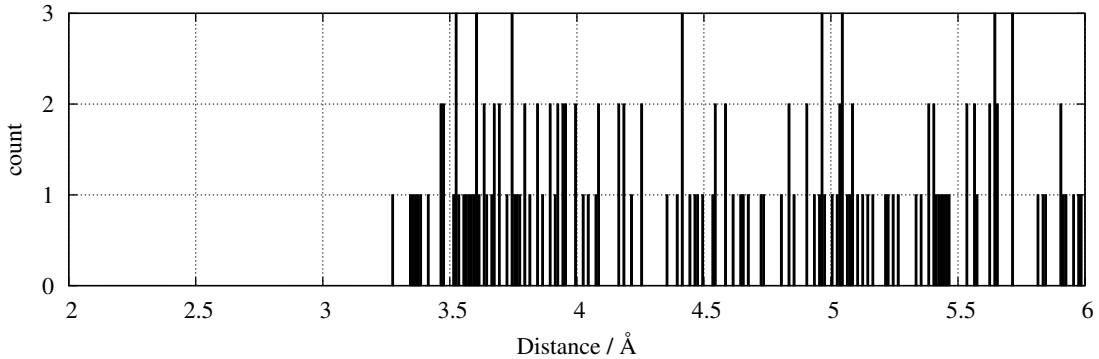

Figure A.16: Chlorine tellurium distance histogram for $(Au_6Te_{18}Cl_2)[Bi_4Cl_{16}]$.

A.4 Powder Diffraction Patterns

A.4.1 $AuTe_2Cl$

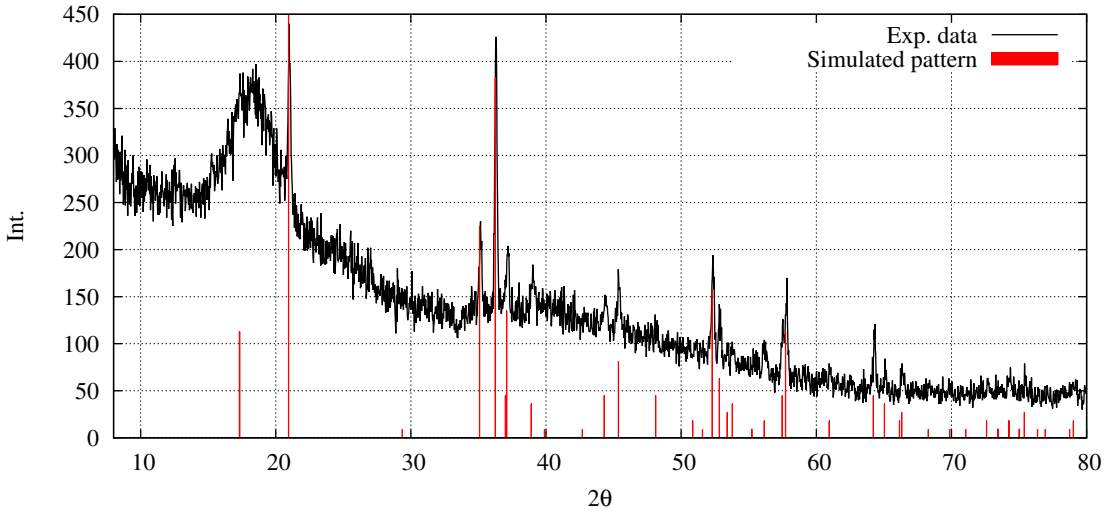

Figure A.17: Powder diffraction pattern of $AuTe_2Cl$. The experimental pattern is shown in black, theoretical peaks from single crystal structure are red.

A.4.2 $AuTe_2Br$

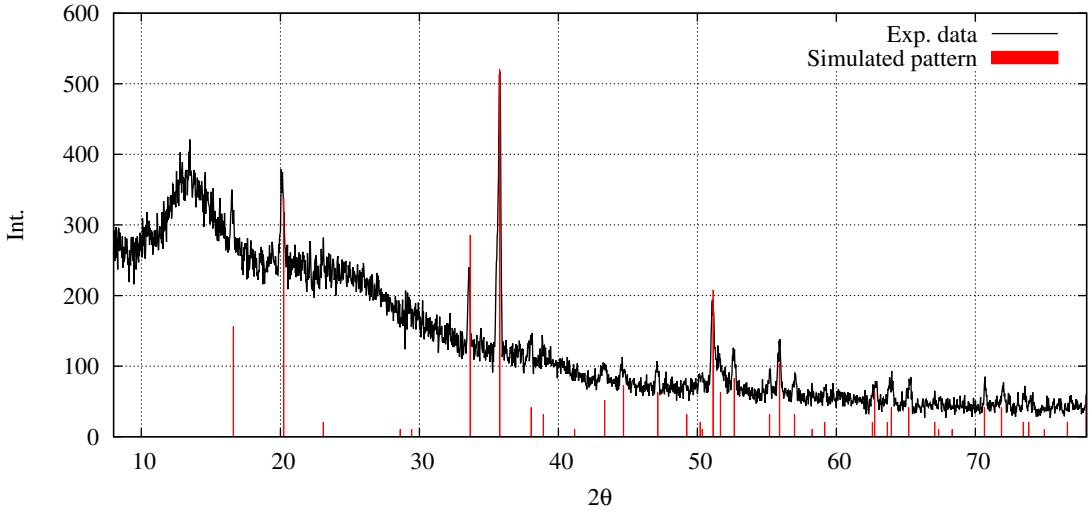

Figure A.18: Powder diffraction pattern of $AuTe_2Br$. The experimental pattern is shown in black, theoretical peaks from single crystal structure are red.

A.4.3 $Zn[AuCl_4]_2 \cdot (AuCl_3)_{1.114}$

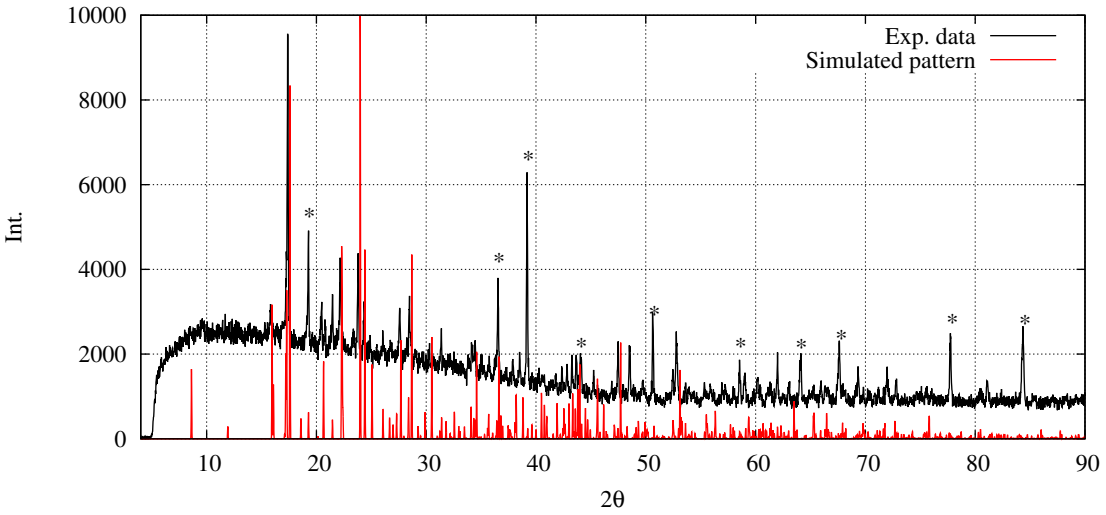

Figure A.19: Powder diffraction pattern of $Zn[AuCl_4]_2 \cdot (AuCl_3)_{1.115}$. The experimental pattern is shown in black, theoretical peaks from single crystal structure are red. Peaks marked with an asterisk belong to AuCl.

A.4.4 $Cd[AuCl_4]_2$

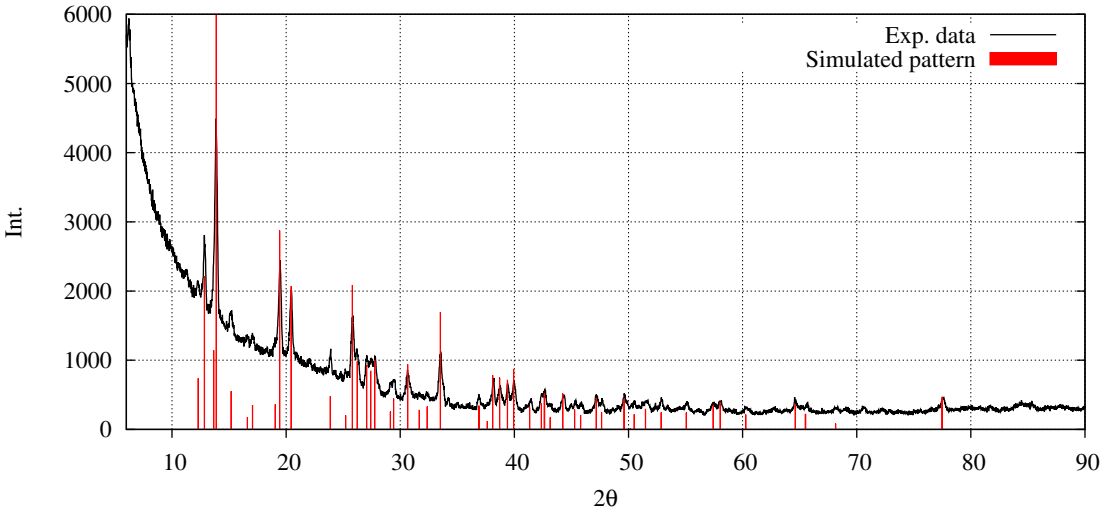

Figure A.20: Powder diffraction pattern of $Cd[AuCl_4]_2$. Experimental pattern recorded by S. Wagner [32] (black), theoretical peaks from single crystal structure (red) after refinement of the lattice constants to account for different data collection temperatures.

A.5 Basis Sets

Table A.84: Basis sets used for calculations performed by CRYSTAL14.

Element	Type	Literature
Al	8-311G	[99]
Au	ECP60MWB	[100, 101]
Br	TZVP	[102]
Cl	TZVP	[102]
O	TZVP	[102]
Mo	ECP28MWB	[100]
Te	ECP28MDF VDZ	[103]

A.5.1 Gold Basis Set

```
279 12        # MWB60
INPUT
19.0 0 2 2 2 2 0
  13.205100  426.846679 0
   6.602550   37.007083 0
  10.452020  261.199580 0
   5.226010   26.962496 0
   7.851100  124.790666 0
   3.925550   16.300726 0
   4.789820   30.490089 0
   2.394910    5.171074 0
0 0 3 2.0 1
  20.1152990  -0.1597614
  12.1934770   0.7893559
   6.0396260  -1.5714057
0 0 1 1.0 1
  1.3737210   1.0
0 0 1 0.0 1
  0.6500100   1.0
0 0 1 0.0 1
  0.1458160   1.0
0 2 2 6.0 1
  8.6096650   2.0982231
  7.3353260  -3.0458670
0 2 2 0.0 1
  1.9129700   0.3791452
  1.0576950   0.6456428
0 2 1 0.0 1
  0.4430600   1.0
0 2 1 0.0 1
  0.15        1.0
0 3 4 10.0 1
  4.1439490  -0.4058458
  3.5682570   0.4275070
  1.3443240   0.4755405
  0.5552890   0.5610972
0 3 1 0.0 1
  0.1896750   1.0
0 4 1 0.0 1
  1.4610000   1.0
0 4 1 0.0 1
  0.4980000   1.0
```

A.5.2 Tellurium Basis Set

```
252 10          # ECP28MDF
INPUT
24.0 0 2 4 4 2 0
 16.814473 281.045843 0
  8.793526  61.620656 0
```

```
 14.877801  67.449464 0
 14.269731 134.904304 0
  8.724435  14.689547 0
  8.291515  29.415063 0
 15.205008  35.432057 0
 15.225848  53.135687 0
  6.071769   9.069802 0
  5.804760  13.122304 0
 15.206168 -15.745450 0
 15.201702 -20.742448 0
0 0 8 2.0 1
 2111.19      0.000612
  311.691     0.003207
   13.8226    0.405512
    8.71748  -0.932588
    1.98303   0.919657
    0.970377  0.404671
    0.279765  0.012366
    0.106776 -0.001604
0 0 8 2.0 1
 2111.19      0.000251
  311.691     0.001457
   13.8226    0.163702
    8.71748  -0.398455
    1.98303   0.578074
    0.970377  0.327124
    0.279765 -0.784654
    0.106776 -0.499451
0 0 1 0.0 1
 0.279765 1
0 0 1 0.0 1
 0.146776 1
0 2 6 6.0 1
 17.0629    0.089340
 10.8306   -0.271168
  2.59380   0.662023
  1.12676   0.460744
  0.300176  0.028809
  0.097551 -0.003863
0 2 6 4.0 1
 17.0629  -0.026861
 10.8306   0.086304
  2.59380 -0.273502
  1.12676 -0.151390
  0.300176 0.583976
  0.097551 0.565014
0 2 1 0.0 1
 0.157551 1
0 3 6 10.0 1
 50.9106   0.003354
 18.4647  -0.003642
  4.27617  0.278080
  1.89770  0.516348
  0.786480 0.326571
  0.2638   0.045152
0 3 1 0.0 1
 0.2638 1
0 4 1 0.0 1
 0.75 1
```

A.5.3 Molybdenum Basis Set

```
242 11             # ECP28MWB
INPUT
14.0 0 2 2 2 2 0
 9.714594 180.103108 0
 4.680500  24.997228 0
 8.142137 123.772752 0
 4.625986  19.530228 0
 6.618415  48.375022 0
 3.248752   8.892053 0
 9.450000 -24.805177 0
 4.720000  -4.153782 0
0 0 3 2.0 1
 7.2033800 -0.8262973
 5.0522950  1.4675616
 2.9135330  0.3189549
0 0 1 2.0 1
 1.0289930 1.0
0 0 1 0.0 1
 0.4695340 1.0
0 0 1 0.0 1
 0.1100140 1.0
```

```
0 2 2 6.0 1
 3.1518660 -4.7381435
 2.4534820  5.0190400
0 2 2 0.0 1
 0.8787730 0.7493629
 0.4907910 0.2705697
0 2 1 0.0 1
 0.2847140 1.0
0 3 4 4.0 1
 5.0347700 -0.0239430
 1.8021490  0.2194576
 0.8072500  0.4611714
 0.3390050  0.4671210
0 3 1 0.0 1
 0.1283420 1.0
0 4 1 0.0 1
 1.2230000 1.0
0 4 1 0.0 1
 0.3380000 1.0
```

A.5.4 Bromine Basis Set

```
35 15          # Br_pob_TZVP_2012
0 0 8 2.0 1.0
 565073.25256     0.0002366031469
  84701.723179    0.0018348332508
  19276.271900    0.0095465849860
   5456.4284576   0.0388771421530
   1776.9503500   0.1271831423100
    639.19398276  0.3043766219100
    248.78823961  0.4449094049700
     98.678305494 0.2438164305800
0 0 4 2.0 1.0
 606.07824568  -0.0265271587090
 188.45598484  -0.1248458480900
  31.497144506  0.5646868355900
  13.736008320  0.5555526856400
0 0 2 2.0 1.0
 21.203212766  -0.2494092049300
  3.7616420178  0.7121311974300
0 0 1 2.0 1.0
 1.4940008700 1.0000000000000
0 0 1 0.0 1.0
 0.5908622600 1.0000000000000
0 0 1 0.0 1.0
 0.1454311300 1.0000000000000
0 2 6 6.0 1.0
 3019.6955723   0.0024971049798
  715.35481126  0.0204192675960
  229.98328751  0.0968971483090
   86.167844615 0.2805390125200
   34.667870802 0.4460639047300
   14.113870307 0.2441007392300
0 2 4 6.0 1.0
 57.085653082  -0.0218559507100
  8.8193845840  0.3270707532000
  3.9340302872  0.5785522952000
  1.7998830384  0.3357098769800
0 2 1 5.0 1.0
 1.5874541800 1.0000000000000
0 2 1 0.0 1.0
 0.4896365520 1.0000000000000
0 2 1 0.0 1.0
 0.150040570 1.0000000000000
0 3 5 10.0 1.0
 168.85370257  0.0089663981988
  49.977949919 0.0620620593160
  18.274913338 0.2147473238400
   7.2455694631 0.4033533674600
   2.8562315025 0.4220881308000
0 3 1 0.0 1.0
 1.0111406400 1.0000000000000
0 3 1 0.0 1.0
 0.4296930700 1.0000000000000
0 3 1 0.0 1.0
 0.2143006900 1.0000000000000
```

A.5.5 Chlorine Basis Set

```
17 10              # Cl_pob_TZVP_2012
0 0 7 2.0 1.0
 69507.990945      0.00054314897497
```

```
 10426.156880      0.00419904639610
  2373.2334061     0.02159214167900
   671.56420071    0.08459885009400
   218.41999790    0.24757249724000
    77.572249714   0.47016930228000
    28.888815277   0.37436370716000
0 0 3 2.0 1.0
   127.10527185    0.02518216660300
    39.339582961   0.10786112456000
     7.6740679989 -0.27408821574000
0 0 2 2.0 1.0
     3.8745627630  1.32138750140000
     1.8385832573  0.68636955368000
0 0 1 0.0 1.0
     0.4498594500  1.00000000000000
0 0 1 0.0 1.0
     0.1363703100  1.00000000000000
0 2 5 6.0 1.0
   666.50423284    0.00236326638360
   157.64241690    0.01887930037400
    50.262520978   0.08720634127300
    18.536078105   0.25285612970000
     7.2940532777  0.43507154820000
0 2 1 5.0 1.0
     2.80149164000 1.00000000000000
0 2 1 0.0 1.0
     0.73964278000 1.00000000000000
0 2 1 0.0 1.0
     0.21056105000 1.00000000000000
0 3 1 0.0 1.0
     0.23728440000 1.00000000000000
```

A.5.6 Aluminium Basis Set

```
13 5   # N. M. Harrison 8-311G
0 0 8 2.0 1.0
    59852.6     0.0004
     8507.9     0.0034
     1902.55    0.0173
      562.45    0.0617
      202.931   0.168
       77.6773  0.385
       31.1496  0.5224
       12.4308  0.2864
0 1 8 8.0 1.0
      565.087  -0.0004  0.0011
      144.448  -0.0059  0.0075
       50.1458 -0.0385  0.0339
       18.9981 -0.0964  0.116
        8.036   0.0204  0.2451
        3.5876  0.3772  0.3701
        1.5884  0.5164  0.3554
        0.7079  0.1783  0.1356
0 1 3 3.0 1.0
        1.9603 -0.0607  0.0514
        0.8551 -0.1183 -0.0938
        0.2477  0.2007 -1.0297
0 1 1 0.0 1.0
        0.140   1.0     1.0
0 3 1 0. 1.
       0.51      1.        1.
```

A.5.7 Oxygen Basis Set

```
8 8               # O_pob_TZVP_2012
0 0 6 2.0 1.0
 27032.382631     0.00021726302465
  4052.3871392    0.00168386621990
   922.32722710   0.00873956162650
   261.24070989   0.03523996880800
    85.354641351  0.11153519115000
    31.035035245  0.25588953961000
0 0 2 2.0 1.0
    12.260860728  0.39768730901000
     4.9987076005 0.24627849430000
0 0 1 0.0 1.0
     1.0987136000 1.00000000000000
0 0 1 0.0 1.0
     0.3565870100 1.00000000000000
0 2 4 4.0 1.0
    63.274954801  0.0060685103418
    14.627049379  0.0419125758240
```

```
     4.4501223456 0.1615384108800
     1.5275799647 0.3570695131100
0 2 1 0.0 1.0
     0.5489735000 1.0000000000000
0 2 1 0.0 1.0
     0.1858671100 1.0000000000000
0 3 1 0.0 1.0
     0.2534621300 1.0000000000000
```

Danksagung

Ich bedanke mich herzlich bei meinem Doktorvater Herrn Prof. Dr. Beck für die Betreuung meiner Arbeiten, die freie Themenstellung und das entgegen gebrachte Vertrauen, besonders auch im Bezug auf die Durchführung von meinen Lehrveranstaltungen.

Herrn Prof. Dr. Glaum danke ich für die freundliche Übernahme des Korreferats. Mein Dank geht auch die gesamte Prüfungskommission.

Ein besonders großer Dank geht an Dr. Jörg Daniels für die nicht durchgeführten Einkristallmessungen, da ich selbst Pilot des Einkristalldiffraktometers werden durfte `;-)`, aber auch an viele freundschaftliche Unterhaltungen abseits der Chemie. Weiterhin möchte ich ihm und Dr. Axel Pelka für viele interessante und lehrreiche Unterhaltungen über Kristallographie und Einkristallröntgenbeugung danken.

Weiterhin möchte ich mich bei Dr. Ralf Weisbarth für EDX- und DSC-Messungen, sowie natürlich auch für viele Unterhaltungen über Chemie, IT und alles andere bedanken. Ohne den Einstieg über die IT wäre ich vielleicht nie im AK Beck gelandet.

Mein Dank geht auch an Herrn Prof. Dr. Bredow für die großartige Unterstützung meines Ausflugs in die Theoretische Chemie. Hier möchte ich auch Dr. M. M. Islam und meiner Bürokollegin Vanessa Werth danken.

Mein Dank geht auch an Norbert Wagner, Volker Bendisch, Klaus Armbruster, Bärbel Knopp, Frank Forge, Andreas Eich und Simone Weisbarth für Unterstützung in chemischen Fragen, Bereitstellung von Chemikalien, Mikroskop-Bildern, Magnetismus- und Leitfähigkeitsmessungen, EDX-Messungen, DTA-Messungen, technische Unterstützung an Röntgengeräten aller Art und gute Unterhaltungen.

Natürlich möchte ich auch allen meinen Kollegen für ein gutes Arbeitskreisklima, besonders auch im 3. Stock, und einer unvergessenen Teerunde danken. Hier möchte ich auch explizit Dr. Ulrich Keßler danken, der mich immer bei Fragen über das D8, die Chlorierungsanlage und bei vielen anderen Themen unterstützt hat.

Vielen Dank an Jörg, Bettina, Sabine und Lisa für das Korrekturlesen der Arbeit.

Außerhalb meines Arbeitskreises möchte ich mich besonders bei der Montag-(Spiele?)Abend-Runde bedanken: Christian und Sarah, Christoph, Tobias und Tina, Yvonne und Tobi sowie Thomas und Maria (auch wenn ihr am Montag-Abend kaum anwesend seid). Das montägliche Treffen hat immer wieder für gute Unterhaltung, Spaß, fachliche Unterhaltungen aller Art und gute Freundschaft gesorgt.

Zum Schluss möchte ich mich bei meiner Familie und ganz besonders bei meiner Frau Lisa bedanken, die mich immer gut unterstützt und auch, wenn nötig, angetrieben hat. Ich hoffe auf noch viele weitere glückliche Jahre.

Eidesstattliche Erklärung

Hiermit erkläre ich an Eides statt,

- dass ich die Arbeit ohne fremde Hilfe angefertigt und keine anderen Hilfsmittel als die in der Dissertation angegebenen benutzt habe; insbesondere, dass wörtlich oder sinngemäß Veröffentlichungen entnommene Stellen als solche kenntlich gemacht worden sind,
- dass ich mich bis zu diesem Tage noch keiner Doktorprüfung unterzogen habe. Ebenso hat die von mir vorgelegte Dissertation noch keiner anderen Fakultät oder einem ihrer Mitglieder vorgelegen,
- dass ein Dienststraf- oder Ehrengerichtsverfahren gegen mich weder geschwebt hat noch gegenwärtig schwebt.

Bonn, _____ _____

(Datum) (Christian Landvogt)